Tailored Immunoassay and Molecular Methods for Viral and Fungal Pathogen Detection

Arabelle Cassedy, B.Sc. (Hons)

A thesis submitted for the degree of Ph.D.

Based on research carried out in the,
School of Biotechnology,
Dublin City University,
Dublin 9,
Ireland.

Under the supervision of Professor Richard O'Kennedy
and
Professor Anne Parle-McDermott

External Supervisor: Dr. Ewen Mullins (Teagasc)

August 2021

Declaration

I hereby certify that this material, which I now submit for assessment on the programme of study leading to the award of Ph.D. is entirely my own work, and that I have exercised reasonable care to ensure that the work is original, and does not to the best of my knowledge breach any law of copyright, and has not been taken from the work of others save and to the extent that such work has been cited and acknowledged within the text of my work.

Signed: _____ ID No.: _____ Date: _____

“It's the job that's never started as takes longest to finish.”

Samwise Gamgee

Acknowledgments

I would first like to thank Professor Richard O'Kennedy and Professor Anne Parle-McDermott, for their mentorship, advice, direction and support over the past years. A special thanks goes to Richard for providing me with the opportunity to undertake this research. Your constant enthusiasm and motivation helped to make this an invaluable experience for me.

Next, I wish to thank the past and present members of the applied biochemistry group (honorary members included!) for their help, but more importantly, for all the laughs and good memories! A special mention to Fay, your advice over the past years was so helpful, thank you. A further thanks to the postgrads of biotech, the chats and nights out were always a welcome distraction!

To Aoife, Jenny and Ciara, I count myself lucky to have made you as friends. Thank you for all the hilarity and great times, my experience would not have been the same without you. However, I do blame my current caffeine reliance on our routine coffees. A second thank you goes to Jenny and Aoife for your various science wisdoms and support over the years. Even when you were both busy you always seemed to have time to help – it was immensely appreciated, thank you so much.

To my closest friends Hollie, Sally and Aoife, the movie nights, trips, nights out, plant shopping expeditions (looking at you on that one, Hollie) and more recently, Zoom meetings, helped to contribute to wonderful memories over the last few years. Thank you for all the fun!

A special thanks goes to my parents, Rosaleen and Paul, and my brother, Stephen. Mam and Dad, you have always encouraged me in my endeavours. Thank you for showing interest and enthusiasm in my work throughout. It was a constant reassurance to know I had such support behind me.

Finally, to Kevin, you have endured first-hand all of the highs and lows over the past years and have always been a constant outpouring of optimism and positivity. Whether it be a silly joke, or a new variation on a seemingly endless list of nicknames, you always managed to make me laugh. You made everything easier and I cannot thank you enough.

List of Figures

List of Tables

Abbreviations

ABBREVIATION	*TERM*
Ab	Antibody
Ag	Antigen
AID	Activation-induced cytidine deaminase
ASC	Amber stop codon
bp	Base pairs
BSA	Bovine serum albumin
cDNA	Complementary deoxyribonucleic acid
CDR	Complementarity-determining region
C_H	Constant heavy chain (antibody)
C_L	Constant light chain (antibody)
CP	Coat protein
DMSO	Dimethyl sulfoxide
DNA	Deoxyribonucleic acid
dNTP	Deoxyribonucleotide triphosphate
E. coli	*Escherichia coli*
EDTA	Ethylenediaminetetraacetic acid
ELISA	Enzyme-linked immunosorbent assay
Fab	Antigen-binding fragment
Fc	Fragment, crystallisable
HA	Haemagglutinin
HPRA	Health Products Regulatory Authority
HRP	Horseradish peroxidase
Ig	Immunoglobulin
IgG	Immunoglobulin class G
IgY	Immunoglobulin class Y
IHC	Immunohistochemistry
IMAC	Immobilized metal affinity chromatography
IMS	Industrial methylated spirits
IPTG	Isopropyl-β-D-galactopyranoside
K_a	Association constant
K_d	Dissociation constant

K_D	Equilibrium dissociation constant
LFIA	Lateral flow immunoassay
mAb	Monoclonal antibody
MW	Molecular weight
NALFIA	Nucleic acid lateral flow immunoassay
NIP	Necrosis inducing protein
NTC	No template control
OD	Optical density
O/N	Overnight
pAb	Polyclonal antibody
PAGE	Polyacrylamide gel electrophoresis
PBS	Phosphate buffered saline
PBS-T	PBS Tween
PCR	Polymerase chain reaction
PEG	Polyethylene glycol
PD	Plasmodesmata
POC	Point-of-care
PTNRD	Potato tuber necrotic ringspot disease
POU	Point-of-use
PVY	Potato virus Y
$PVY^{O/N}$	Potato virus Y serotype O/N
rAb	Recombinant antibody
RAG	Recombination-activating gene
R. commune	*Rhynchosporium commune*
RNA	Ribonucleic acid
RPA	Recombinase polymerase amplification
RT	Room temperature
RT-RPA	Reverse-transcription RPA
SB	Super broth
ScAb	Single-chain antibody fragment
ScFv	Single-chain variable fragment
SD	Shine-Dalgarno
SDS	Sodium dodecyl sulphate

SHM	Somatic hypermutation
SOC	Super optimal catabolites
SOE	Splice-by-overlap-extension
SPR	Surface plasmon resonance
ssDNA	Single stranded DNA
TAE	Tris-acetate EDTA
TEMED	Tetramethylethylenediamine
TMB	Tetramethylbenzidine dihydrochloride
V_H	Variable heavy chain (antibody)
V_L	Variable light chain (antibody)
VRC	Viral replication complex
WB	Western blot(ting)

Units

UNITS	
Bp	Base pairs
x *g*	Centrifugal force expressed in units of gravity
°C	Degrees Celsius
µg	Microgram
µL	Microlitre
µM	Micromolar
kDa	KiloDalton
g	Gram
Kg	Kilogram
L	Litre
M	Molar
mg	Milligram
Min	Minute(s)
mL	Millilitre
ng	Nanogram
nM	Nanomolar
pM	Picomolar
rpm	Revolutions per minute
Sec	Second(s)
V	Volts
v/v	Volume per unit volume
w/v	Weight per unit volume

Publications and Presentations

Publications

Cassedy, A., Parle-McDermott, A. and O'Kennedy, R. (2021). Virus detection: A review of the current and emerging molecular and immunological methods. *Front. Mol. Biosci.*, 8, 637559.

Cassedy, A., Della Bartola, M., Parle-McDermott, A., Mullins, E. and O'Kennedy, R. (2021). A One-Step Reverse Transcription Recombinase Polymerase Amplification Assay for Lateral Flow-Based Visual Detection of PVY. Manuscript submitted.

Ma, H., **Cassedy, A.**, Fagan, C. and O'Kennedy, R. (2021). Generation, selection and modification of anti-cardiac troponin I antibodies with high affinity. Invited resubmission to *J. Immunol. Methods*.

Ma, H., **Cassedy, A.** and O'Kennedy, R. (2021). The role of antibody-based troponin detection in cardiovascular disease: A critical assessment. Accepted to *J. Immunol. Methods*, 113108.

Cassedy, A. and O'Kennedy, R. (2021). 'Antibody purification using affinity chromatography' in Ayyar, V., and Arora, S. (eds.) *Affinity Chromatography: Methods and Protocols,* New York, Springer. In press.

Cassedy, A., Mullins, E. and O'Kennedy, R. (2020). Sowing seeds for the future: The need for on-site plant diagnostics. *Biotechnol. Adv.,* 39, 107358.

Cassedy, A., Mullins, E. and O'Kennedy, R. (2019) 'Antibody-based sensors for the detection of pathogens of potato and barley' in O'Kennedy, R. (ed.) *Rapid Antibody-based Technologies in Food Analysis*. (London, RSC) Chapter 13.

O'Kennedy, R., Fitzgerald, J., **Cassedy, A.**, Crawley, A., Zhang, X. and Carrera, S. (2018). Applications of antibodies in microfluidics-based analytical systems: challenges and strategies for success. *J. Micromech. Microeng*., 28 (6), 063001.

Presentations

Cassedy, A., Ma, H., Murphy, C., Mullins, E., Della Bartola, M., O'Riordan, A., Diaz, F., Shao, H., Parle-McDermott, A. and O'Kennedy, R. (January 20th-24th, 2020) Improving Potato Virus Y Detection through the Use of Antibody Technology and Recombinant Protein Engineering. Peptalk, San Diego, USA.

Cassedy, A., Murphy, C., Della Bartola, M., Mullins, E., Diaz, F., O'Riordan, A. and O'Kennedy, R. (April 8th-12th, 2019). The Generation of a Sensitive Immunoassay for the Detection of Potato Virus Y. Protein Engineering Summit, Boston, Boston, USA.

Cassedy, A., Parle-McDermott, A. and O'Kennedy, R. (25th Jan, 2019). The Development and Screening of a Naïve Antibody Library for the Identification and Isolation of PVY Antibodies. Research Day, The School of Biotechnology, Dublin City University, Ireland.

Cassedy, A., Parle-McDermott, A. and O'Kennedy, R. (26th Jan, 2018). The Development of Recombinant Antibodies to Target Potato Virus Y and *Rhynchosporium commune.* Research Day, The School of Biotechnology, Dublin City University, Ireland.

Cassedy, A., Della Bartola, M., O'Riordan A., Mullins, E. and O'Kennedy, R. (28th June, 2017). Crop Disease Detection. Teagasc Open Day, Oak Park, Carlow, Ireland.

Cassedy, A., Mullins, E., O'Riordan, A. and O'Kennedy, R. (27th Jan, 2017). Utilising Recombinant Antibodies for the Improved Detection of Potato Virus Y and *Rhynchosporium commune*. Research Day, The School of Biotechnology, Dublin City University, Ireland.

Scholarships, Courses and Awards

Department of Agriculture, Food and the Marine's Competitive Research Funding Programme (Project Ref.15/S/618) PhD Scholarship Recipient, Dublin City University, Ireland (2016).

Allergan Innovation Award Winner, Dublin City University, Ireland (2017).

Laboratory Animal Science and Training (LAST) Animal Handling Training Course for Ireland and UK Licence. Trinity College Dublin, Ireland (2016).

BE516 Bioseparations, Dublin City University, Ireland (2017).

CS551 Advanced Laboratory Techniques, Dublin City University, Ireland (2017).

GxP Training Workshop as part of the Professional Skills for Scientists Module, Dublin City University, Ireland (2017).

BE550 Biosafety and Lab Standard Operating Procedures, Dublin City, University, Ireland (2018-2019).

Tailored Immunoassay and Molecular Methods for Viral and Fungal Pathogen Detection

Arabelle Cassedy

Abstract

The work described in this thesis involves the development of assays for the detection of two crop pathogens, potato virus Y (PVY) and *Rhynchosporium commune (R. commune)*. Infection of crops by these pathogens results in significant economic losses and reduced yields. Therefore, efficient control of their spread is paramount. It was proposed in this work to develop immunoassays and molecular techniques for PVY and *R. commune* to provide novel additional detection and control capabilities for these important pathogens.

An antibody library was generated in order to isolate PVY-specific scFv. The library was screened using a combination of ELISA, phage display, and biopanning approaches. From this screening, scFv were isolated and their PVY-binding abilities characterised in ELISA.

Anti-PVY mAbs were structurally engineered into recombinant scAb and scFv fragments. The performance characteristics of the parental antibodies and recombinant derivatives were determined through a combination of immunoblotting, ELISA and SPR. Subsequently, dot blots and SPR-based immunoassays were developed for the enhanced detection of PVY.

An isothermal nucleic acid amplification-based immunoassay for the detection of PVY-related nucleic acids was also generated. This method combines recombinase polymerase amplification with lateral flow immunoassay technology. The developed assay could detect PVY nucleic acids at high sensitivity from both DNA and RNA templates.

A recombinant scFv library was generated for the isolation of antibodies with *R. commune* specificity. Additionally, anti-*R. commune* avian pAbs were generated and characterised. This work led to the development of paper-based immunoassays for the detection of *R. commune*-associated antigens.

Both the immunoassay and molecular diagnostic approaches offer a means of early detection of the target pathogens such that their burden in the field can be ascertained and tailored treatment can be implemented at early stages of disease outbreaks.

Chapter 1

Introduction

1.1 Plant Pathogens

Plant pathogens are globally abundant, with their spread facilitated by factors including changing climate, cross-continental trade and genetic mutations which cause increased resistance to current chemical control methods (Scott et al., 2019). These plant pathogens, also termed biotic agents, can be viral, fungal, bacterial, oomycote or insect-borne and all can cause widespread plant disease. Plant diseases are a source of major economic losses due to the reduction of agricultural yields, with roughly 20-40% of crop losses being directly attributed to pathogens (Savary et al., 2012, 2019). Economic losses are further exacerbated by crop pathogens, with an additional estimated loss of 10% post-harvest as a result of continued pathogenic activity (Bebber and Gurr, 2015). There are two types of crop losses – primary and secondary. Primary losses are associated with yield losses directly resulting from the activity of a pathogen. Secondary losses are considered as those losses arising from residual pathogens surviving in fields where the initial infection occurred, causing a reoccurring infection in newly planted crops. Previously, secondary losses were largely negated by crop cycling/rotation, however, with increasing pressure to produce large quantities of cash crops, this has become a reduced practice and recurrent infection levels are high in certain crops. These repeated infections are now handled through chemical control means for the most-part (Cerda et al., 2017). However, the desire to explore alternative control measures in an effort to reduce the level of chemical use has driven research toward devising new strategies with which to control pathogens. Two sectors of agricultural interest which suffer from yield and economic losses are the potato and barley divisions. These crops are vulnerable to infection by numerous diseases, many of which cause a reduction in yield or quality of the produce. Potato and barley are cash crops of agricultural and economic importance worldwide, with an estimated 63,500 and 56,400 tonnes of barley and potatoes harvested, respectively, in Europe in 2019 (European Commission Statistical Office-Eurostat, 2021). Therefore, knowledge of their respective infective pathogens, and ways by which they are managed, is essential for overcoming yield reduction as a result of disease.

1.1.1 Importance of potato and barley

Potato (*Solanum tuberosum*) is a crop of major agricultural importance being the most widely produced non-cereal crop (Wijesinha-Bettoni and Mouillé, 2019). Many cultures are reliant upon the production of potatoes as both a staple food and an economic resource. Given the reliance on the production of the potato crop from both food-resource and

economic viewpoints, it is clear why investigations into diseases which can affect the yield and quality of the crop are of great interest. The occurrence of such disease is widespread and can arise from a number of sources, including being soil-borne or insect-borne. Losses as a result of disease occur both in-field and post-harvest, therefore, treatments must be provided at all stages to ensure the viability of the crop.

Barley (*Hordeum vulgare*) is another important crop grown in many regions. Barley was one of the founding crops grown for agricultural purposes by our ancestors (Jones et al., 2011). In terms of modern crop production, barley is the fourth most-produced cereal crop worldwide preceded by rice, wheat and maize (Langridge, 2018). This major cereal crop is grown during both winter and summer in temperate climates. The main usage of barley in present day agriculture is as feed grain for livestock, poultry and other animals, in addition to use in malting processes and for human consumption. Therefore, it is a necessity to ensure that the loss in yield of barley by pathogens is minimal. The potato and barley crops are affected by a range of pathogens. However, of primary interest in the research described in this thesis are a viral pathogen, potato virus Y (PVY) and a fungal pathogen, *Rhynchosporium commune* (*R. commune*), which infect potatoes and barley, respectively. Proliferation of these pathogens on their respective hosts is widespread and results in yearly losses, highlighting their importance and the need for control of these pathogens.

1.2 Important Pathogens of Potato and Barley

1.2.1 Potato virus Y

PVY, genus *Potyvirus*, is a viral pathogen which is a member of the *Potyviridae* family, the largest known plant virus family. It is considered the most important disease of the potato crop, worldwide. PVY is a filamentous, rod-shaped virus, roughly 730nm in length. The virus is composed of a positive sense, single-stranded RNA and a 3' poly-A tail, encapsulated in thousands of copies of a viral capsid, or coat, protein (CP) (Kežar et al., 2019). The genes and general structure of the PVY virus are depicted in *Figure 1.1*.

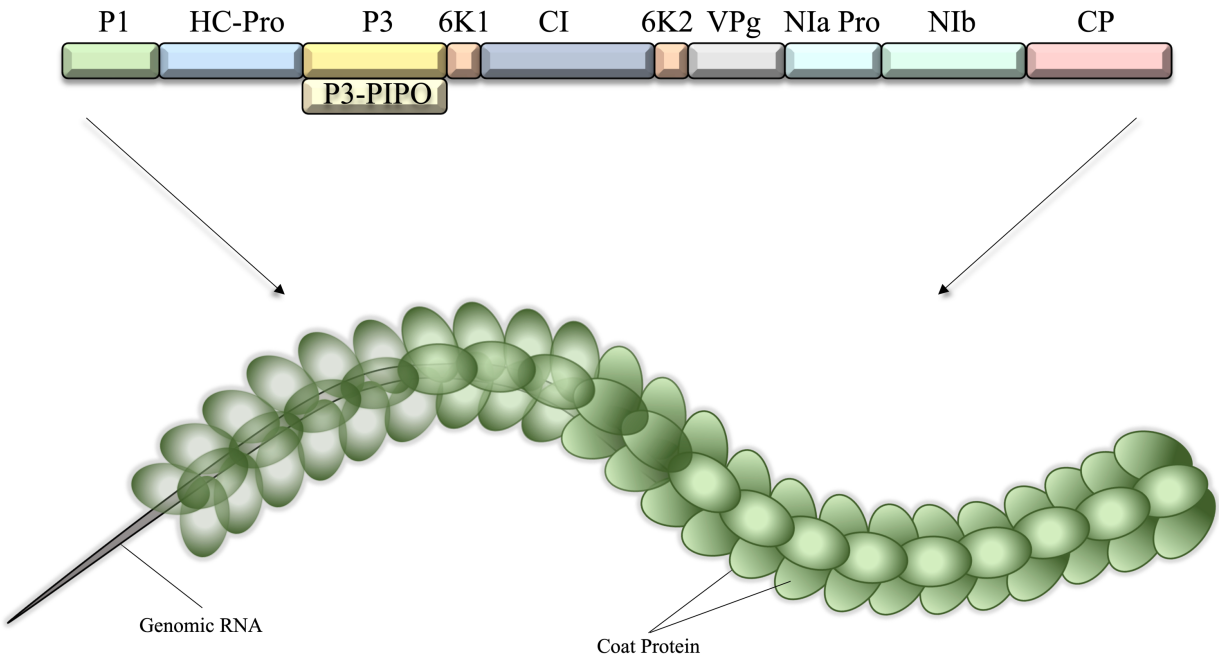

Figure 1.1 Depiction of the PVY genes and the assembled virion

The PVY polyprotein comprises of ten primary proteins, P1, HC-Pro, P3, 6K1, CI VPg, NIa Pro, NIb and the CP. An additional protein, P3-PIPO, is expressed through transcriptional slippage. When assembled, the viral RNA genome is encapsulated in thousands of copies of the coat protein.

Once the virus has entered a suitable host, the RNA is translated into a large polyprotein which is proteolytically cleaved by three viral proteases, NIa-Pro, P1-Pro and HC-Pro, into ten mature sub-unit proteins (Lacomme and Jacquot, 2017). Recently, it was revealed that translational slippage of the viral RNA polymerase results in the expression of an additional proteins, P3N-PIPO (Chung et al., 2008; Olspert, Carr, and Firth, 2016). *Table 1.1* provides a brief summary of the role of each viral protein. The largest of the viral sub-units is the ~30kDa CP, which packages the viral components.

Table 1.1 Summary of PVY proteins and their respective functions

Protein	**Function**	**Reference**
P1	Catalyses auto-proteolytic self-cleavage away from HC-Pro.	(Arbatova et al., 1998)
Helper Component Proteinase (HC-Pro)	Inhibits viral-induced gene silencing; important for virus transmission from aphid vector; involved in viral replication.	(Ivanov et al., 2014, 2016)
P3	Believed to be involved in replication, movement and pathogenesis.	(Luan et al., 2016)
6 kDa Protein 1 (6K1)	Not fully characterised but thought to be essential for viral replication at early stages.	(Cui and Wang, 2016)
Cylindrical Inclusion Helicase (C1)	Forms pinwheel shaped inclusion bodies; involved in viral replication; involved in aphid-plant transmission; aids cell-to-cell movement; involved in overcoming host-defences.	(Sorel, Garcia, and German-Retana, 2014)
6 kDa Protein 2 (6K2)	Associates with chloroplasts in cells and is essential for viral replication; interacts with several other viral proteins also involved in replication.	(Wei et al., 2010; Ivanov et al., 2014)
Viral Genome Linked Protein (VPg)	Interacts with host eukaryotic translation initiating factor 4E (eIF4E) to initiate the replication of the viral RNA.	(Tavert-Roudet et al., 2017)
Nuclear Inclusion Protein A (Nla-Pro)	Main protease involved in processing of initial viral polypeptide; induces vacuolar localisation of virus upon aphid feeding to aid in virus transmission.	(Bak et al., 2017; Tavert-Roudet et al., 2017)
Nuclear Inclusion Protein B (Nlb)	Involved in virus replication.	(Ivanov et al., 2014)
Coat Protein (CP)	Essential for virus transmission and vector interactions, virion assembly and cell-to-cell interaction.	(Quenouille, Vassilakos, and Moury, 2013)
Pretty Interesting Potyviridae ORF (P3N-PIPO)	Expressed by transcriptional slippage. Plays vital role in cell-to-cell movement of virus in plants .	(Wen and Hajimorad, 2010)

1.2.1.1 PVY transmission

PVY is spread through several means including mechanical transmission during harvest, progeny transmission from seed to crop, and the most predominant mode of transmission, through aphid vectors. PVY is spread by aphids in a non-circulative strategy, meaning that the virus is both acquired and transmitted by the aphid in a short space of time (seconds to minutes), with no latent period in between. Non-circulative viral spread may either be semi-persistent or non-persistent. PVY is categorised as non-persistent (Moreno et al., 2012). Non-persistent transmission dictates that the virus is acquired by the vector, in this case aphids, within seconds or minutes and is transferred to a new plant, also within seconds or minutes. The virus is taken up on the mouthparts, or stylet, through the feeding of the aphid on infected plant material. The aphid continues on to the next plant where the virus is deposited, permitting proliferation in a new host (Galimberti et al., 2020). In the transmission of potyviruses, it is thought that the virus is introduced to the plant through interactions between the aphid stylet, the HC-Pro protein and the viral coat protein. This specific interaction between the aphid components and viral proteins to allow transmission is termed bridge strategy (Brault et al., 2010; Whitfield, Falk, and Rotenberg, 2015). The species of aphid is a determining factor as to how rapidly PVY will spread through a population, with the species *Myzus persicae* being identified the most efficient vector of PVY. However, while the most efficient, *M. persicae* is not the sole carrier of PVY and many species of aphid can act as a viral vector, albeit generally with less efficiency (Fox et al., 2017). Multiple parental and recombinant strains of PVY exists, with the recombinant forms composed of various elements of the parental strains. The transmission rates between these PVY strains are usually comparable, however, some strains appear to have a competitive advantage in transmission rates, such as that seen in the strain $PVY^{EU\text{-}NTN}$ which presents with more rapid transmission when compared to PVY^{O} and $PVY^{NA\text{-}NTN}$. Furthermore, some recombinant versions of PVY appear to be more readily transmitted by the aphid vector than parental strains (Verbeek et al., 2010; Mello et al., 2011; Davie et al., 2017; Mondal and Gray, 2017).

1.2.1.2 PVY in-planta replication

PVY replication commences once the virus has gained access to the host cell. The CP is removed and viral RNA, which then acts as mRNA, is translated into a polypeptide. This polypeptide is processed and a viral replication complex (VRC) is formed. Within the VRC, the +ve sense single-stranded RNA is copied to create a -ve sense single strand. The host

cell-machinery is recruited, and this -ve strand is employed as a template to replicate many iterations of +ve sense RNA. These strands are encapsidated by many copies of the coat protein and new virions are formed. The newly formed virions relocate to pores in the plant cell membrane, termed plasmodesmata (PD) (Lacomme and Jacquot, 2017). *Figure 1.2* depicts an overview of this viral replication process. The virions traverse the PD and navigate to new cells through interactions between various viral and host proteins including the PD, HC-Pro, CI, CP and P3N-PIPO (Vijayapalani *et al.*, 2012; Olspert *et al.*, 2016). The virions move between plant cells in this manner until they reach the phloem. Upon accessing this region, the virus is free to travel to newly propagating tissues of the plant and replicate.

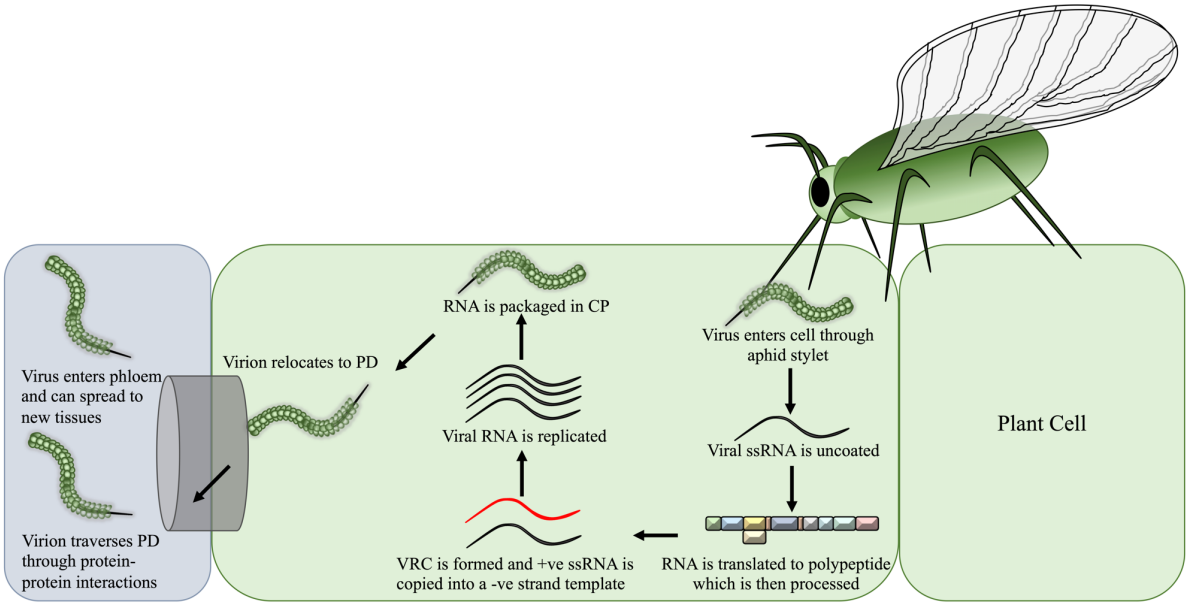

Figure 1.2 Simplified diagram of the replication cycle of PVY

The virus is delivered into the leaf tissue via the aphid mouthparts, where it uses host cell machinery to replicate and spread throughout the infected plant.

1.2.1.3 Symptoms of PVY infection

The symptoms of PVY infection range depending on factors such as the strain with which the crop is infected and the host cultivar. There are many strains of PVY, and these are categorised under five broad phylogroups, O, C, N, R1 and R2. Three of these phylogroups are the parental strains, PVY^{O}, PVY^{N} and PVY^{C}, while groups R1 and R2 are recombinant forms of these, mostly derived from recombination between PVY^{O} and PVY^{N} (Gibbs et al., 2017; Fuentes et al., 2019). Some strains of PVY, such as PVY^{C}, have adapted poorly to

potato crop infection, whereas others have adapted to be efficient in the process (Chikh-Ali et al., 2016). PVY^{O} infection may present as symptomless, as a mosaic pattern on the plant, or as systemic necrosis, depending on which cultivar the virus is propagating within (Nie et al., 2011). PVY^{O} transmits readily through a population and the risk of the development of systemic necrosis within the crop means that growers must be selective and vigilant for possible disease within the potato being cultivated. Infection with a different strain, PVY^{N}, results in a mild mosaic pattern across the crop. Infection with many of the isolates from the recombinant groups, R1 and R2, results in a severe, tissue-damaging disease denoted Potato Tuber Necrotic Ringspot Disease (PTNRD) (Fuentes et al., 2019). Recombinant strains of PVY are continuously discovered, with 36 known recombinants of PVY reported. Each recombinant may present different characteristics when compared to their parent strains, including mosaicking, necrosis, TNRD and canoe-shaped cracks in tubers (Benedict et al., 2015; Green, Brown, and Karasev, 2018). The number of identified recombinants is likely to rise in coming years, given the advent of rapid DNA-sequencing which allows more extensive analysis of PVY sequences. Furthermore, the fact that recombinant versions of PVY are more readily transmitted than some parental strains is likely driving population bias toward recombinant forms (Mondal and Gray, 2017). In addition, continued globalisation and international trade drives the mixing of crops from different geographic regions, providing more opportunity for recombination events.

Since the potato is one of the most widely produced crops worldwide, the ability to provide a healthy and stable, yearly output is essential for the economies of many developing and developed countries. PVY infection within crops poses a major risk to this production stability. In many cases, the disease can cause severe damage to the plant leaves, stem, and tuber. Infection may sometimes be symptomless, resulting in PVY spreading undetected in both fields and seed potatoes (Fuentes et al., 2019). The recurrent infection of potato crop with PVY results in stunted plant growth and unmarketable tubers, ultimately resulting in both yield and economic losses for the producers of the crop. Therefore, the development of targeted assays for the timely detection of PVY infection is considered pertinent. Alongside the targeted detection of PVY, another pathogen, *Rhynchosporium commune*, is of significant interest in crop disease management. This fungal pathogen infects both the foliage and seed of the barley crop.

1.2.2 Rhynchosporium commune

Rhynchosporium is a haploid fungus which infects a wide range of grasses. Thought to have arisen initially in northern Europe, the pathogen is now present in grasses globally. There are several host-specialized species of closely-related *Rhynchosporium* fungi such as *Rhynchosporium agropyri, Rhynchosporium orthosporum, Rhynchosporium lolii, Rhynchosporium commune* and *Rhynchosporium secalis* (McDonald, 2015). For the purpose of this research, the fungal pathogen *Rhynchosporium commune* (*R. commune*) will be discussed as this is the most relevant in the infection of barley and is the pathogen of focus within this work. Any cited literature which refers to *R. secalis* infection of barley will be referred to as *R. commune*, based on current species classification terminology.

1.2.2.1 Rhynchosporium commune transmission

Transmission is facilitated through several methods. In a field which had not previously presented with infection, the sudden proliferation of *R. commune* is likely as a result of sewing contaminated seed (Al-Shehadah, Al-Daoude, and Jawhar, 2018; Topp et al., 2019). Growing barley from contaminated seed gives rise to a high frequency of infection in the new plants. Asymptomatic infection of seed aids in the long-distance spread of disease as this seed often passes health inspections, which are typically visual. Once infected, continued fungal growth, predominantly on the plant foliage, eventually leads to the formation of asexual fungal spores, termed conidia, which are spread short distances through splash-dispersal to infect nearby plants. While *R. commune* reproduction is believed to be primarily asexual, there is some evidence that sexual reproduction may also occur, however, this mechanism has not yet been fully elucidated (King et al., 2015; Arzanlou, Karimi, and Mirabi, 2016). Transmission of *R. commune* is further facilitated by remnants of crop debris or stubble left behind post-harvest. The fungus may remain either on the debris in the field, or in the dust it forms, and is capable of re-infecting newly planted seed or crops (Lee, Tewari, and Turkington, 2001b; Avrova and Knogge, 2012). Once the fungus has successfully transferred to the crop, it will begin to propagate within the plant cells through a number of mechanisms.

1.2.2.2 Rhynchosporium commune mechanism of action

Germination of asexual spores occurs on leaves in the presence of moisture within 24 hours. These spores develop 1 to 2 germ tubes which enlarge to form cells that are capable of facilitating leaf cuticle access (Linsell et al., 2011). These cells are termed appressoria and

their access to the leaf cuticle is granted as a result of the physical pressure of their growth, this is also aided by enzymatic degradation of the leaf tissue (Ryder and Talbot, 2015). Post-cuticle penetration, fungal filamentous branches, termed hyphae, propagate on leaves between the cuticle and the outer epidermal layer of the plant cell wall, eventually travelling to the leaf base. The hyphae proceed to grow into the middle layer of the leaf, known as the mesophyll layer, further exacerbating plant damage, as illustrated in *Figure 1.3* (Linsell et al., 2011). In order to grow, the fungus relies on plant nutrients in the leaf as a food source. These are not always readily available, therefore, *R. commune* employs several proteins to aid in the degradation of plant cells which, in turn, releases nutrients for consumption. Three prominent proteins are involved in tissue destructed, Necrosis Inducing Proteins (NIP) 1, 2 and 3. NIP1 and NIP3 are thought to be associated with the formation of necrotic lesions on the barley leaf as a result of an undetermined indirect activation of the H^+-ATPase pathway (Stergiopoulos and de Wit, 2009). H^+-ATPases are pumps which establish potential across the plant cell membrane to control multiple basic processes including plant nutrient uptake and nutrient redistribution. NIP1, in particular, stimulates prolonged H^+-ATPase activity which, in turn, causes tissue necrosis from which the fungus sources the requisite nutrients for growth and proliferation (Elmore and Coaker, 2011). It was found that *R. commune* can tolerate deletion of NIP1 and maintain virulence, while NIP2 and NIP3 are present in nearly all populations of *R. commune*, indicating that they play a significant role in *R. commune* infectivity (Mohd-Assaad, McDonald, and Croll, 2019; Zhang, Ovenden, and Milgate, 2020). The hyphal growth continues throughout the plant cells, eventually causing the collapse of the mesophyll layer which results in characteristic blotched water-marks observed on the leaves of affected plants. Growth continues through the plant to form a mycelial network where conidia eventually form and facilitate fungal transmission through splash dispersal.

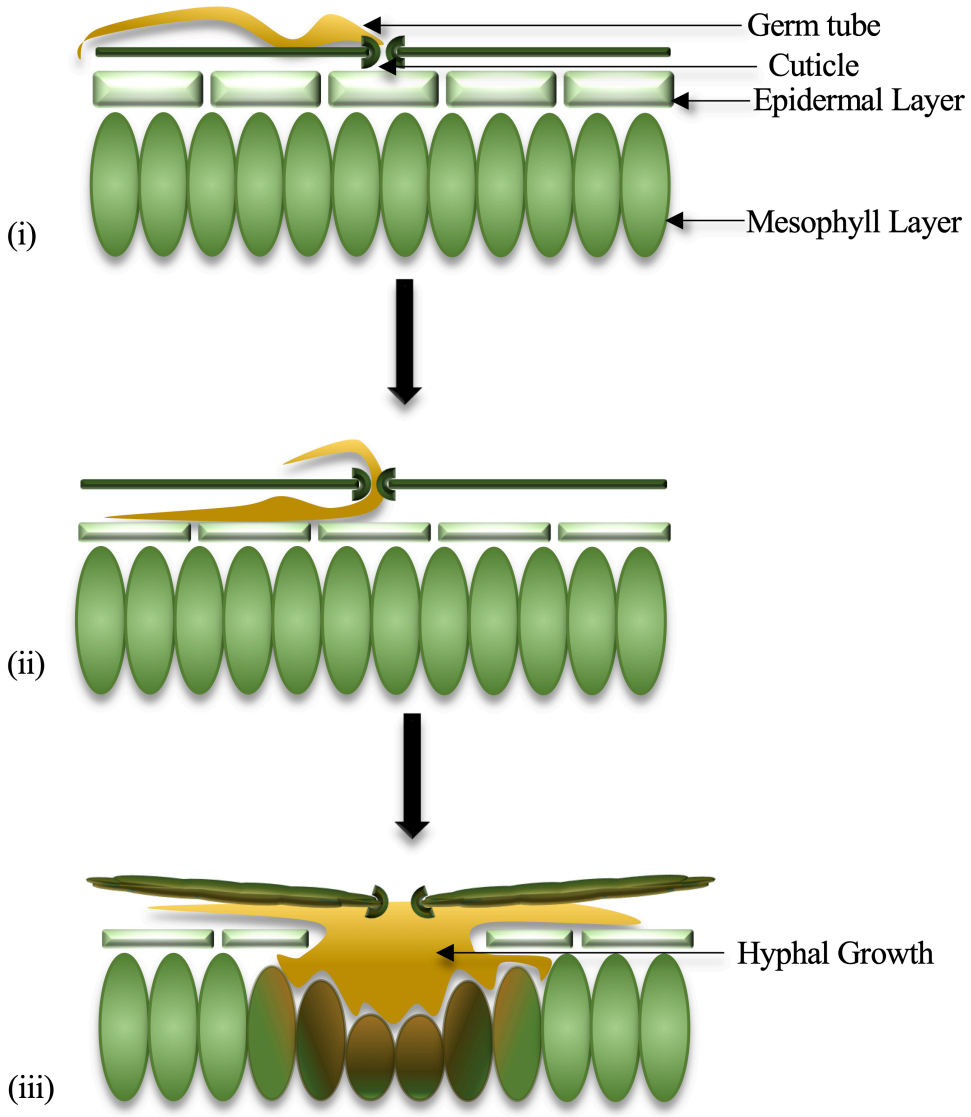

Figure 1.3 R. commune infection process

(i) *The germ tubes gain access to the leaf through the cuticle.* ***(ii)*** *The fungus begins to proliferate between the epidermal layer and the leaf surface.* ***(iii)*** *Continued growth results in invasion into the mesophyll layer. This causes degradation of the epidermal and mesophyll layers, leading to leaf necrosis and lesion formation.*

1.2.2.3 Symptoms of Rhynchosporium commune infection

Initial *R. commune* infection is characterised by a long asymptomatic stage prior to the point at which hyphal growth begins to break down the plant foliage. This leaf degradation results in irregularly shaped, grey or brown blotches on any part of the leaf belonging to the infected crop. These blotches further develop into large lesions, on account of the water retention which occurs due to fungal infection. Seed infection may be identified by browning at the

base of bristles around the seed, however, infection of seed may also be symptomless. This poses an issue when attempting to assess the crop health purely by visual means. The practice of grain assessment via visual inspection is still commonplace for the barley crop (Avrova and Knogge, 2012). Colonisation of barley by *R. commune* results in both yield and economic losses. Barley growth is stunted by *R. commune* proliferation due to the ongoing damage inflicted to the foliage due to *R. commune*-induced degradation. Furthermore, heavy infection of the grain reduces its suitability for purposes such as malting and human consumption, where high-quality grain is desired, meaning that it does not achieve as high a market price when sold. It is therefore important to improve the diagnostic accuracy for the detection of *R. commune* to prevent the spread of disease as a result of asymptomatic seed distribution and to prevent further yield and economic losses (Looseley et al., 2012).

1.3 Brief Overview of the Current Methods in Plant Pathogen Control

Currently, the spread of crop pathogens in controlled in the main through the seasonal spraying of various chemical treatments such as herbicides, fungicides and pesticides. However, the use of chemical agents is under reform in the EU, with strict legislative directives dictating the type of, and quantity, of chemical used in agriculture (Handford, Elliott, and Campbell, 2015). Traditionally, plant diseases were mainly diagnosed through visual inspection as pathogenic infections often result in characteristic marks, blotches or other identifying blemishes on the stem, leaves, grain or other plant components. Presently, the decision to spray crops is centred on workers' experience, visual methods to determine the presence of identifying symptoms, knowledge of the pathogen life-cycle and the burden of pathogen expected in each season (Lee, Tewari, and Turkington, 2001b; Geißinger et al., 2017). While this aids in the reduction of pathogen burden, it may not be a sustainable method given the push toward environmentally-friendly growing and the development of resistant pathogen strains. Furthermore, a dependence on a finite selection of chemical control agents could increase the likelihood of resistant pathogen emergence. In addition, visual inspection-based decisions to spray chemicals can be of limited value, or fail, in scenarios where pathogens proliferate asymptomatically or remnants of pathogens remain on crop debris, stubble or seed from previous fields or harvests.

In addition to chemical application, there are several other methods by which crop pathogens are controlled. These methods include cross breeding, crop cycling, correct storage and genetic engineering. Selective breeding is employed in the potato and barley sectors to

improve many aspects of the crop such as disease resistance, pest resistance, yield, appearance, taste, texture and, in general, to improve the ability of the crop to adapt to environments in which it is grown (Ullrich, 2010; Singh and Kaur, 2016). Classically, breeders choose resistance genes (R-genes) to perform genetic modifications to plant species (Gururani et al., 2012). Stacking of broad-spectrum R-genes and other quantitative trait loci (QTL) into a single genome has aided in the propagation of crops which harbour genomes resistant to a wide range of pathogens, thus overcoming some of the problems associated with the wide diversity observed in plant pathogens (Kim et al., 2012; Zhu et al., 2012; Boyd et al., 2013). Both the genomes of potato and barley are available which will assist in more in-depth study of resistant genomes and further the development of sturdier varieties of each crop (Sanderkar and Nielsen, 2011; Mayer et al., 2012). Crop rotation, the act of alternating crop species at set time-intervals, is also employed in the effort to prevent the proliferation of crop diseases. Ideally, the rotation crop will not act as an alternative host for any soil, insect or pest-borne disease which may be present in the field from the previous crop. Thus, rotation is important for disease management and reducing the spread of pathogens (Larkin, Griffin, and Honeycutt, 2010). Storage in specialised conditions is also utilised to ensure reduced pathogenic activity. Continued pathogen activity on post-harvest yields of fruits and vegetables results in further losses, therefore, the handling and storage of both crops is essential in maintenance of the integrity of the grain as factors such as tissue damage, temperature and humidity all affect the level of disease propagation (Woonton et al., 2005; Magan and Aldred, 2007; Nunes, 2012; Clasen et al., 2016). These non-chemical control means also aid in the overall reduction in chemical usage and minimising yield loss, however, as with chemical treatment, they do not provide a blanket solution to combating damage as a result of crop pathogens. The introduction of additional control measures, such as diagnostic sensing systems, could work in tandem with these established methods to offer an improved method of pathogen control.

This requirement for alternative control measures highlights the need for the design and deployment of systems that can quickly and accurately identify symptomatic fields which require focused treatments. The selection of treatments applied can be tailored based on the presence/absence of disease, as opposed to current programmes which are primarily based on growth stages of the crop. Such systems should be designed into user-friendly diagnostics assays which can be used in-field, or at whatever location that testing is deemed necessary (*Figure 1.4*). These assays could work in tandem with the growers' experience creating a

more sustainable method by which pathogens could be specifically identified, and a selective chemical treatment applied, rather than a broad-spectrum agent. Such assays would not require removal of samples from fields, and could be employed along the various checkpoints in the growing cycle, from sowing to harvest to sale. Methods used in the diagnostics of pathogens are broad, however, two of the primary and most rapid means are those which rely on nucleic acid detection or immunoassay methods.

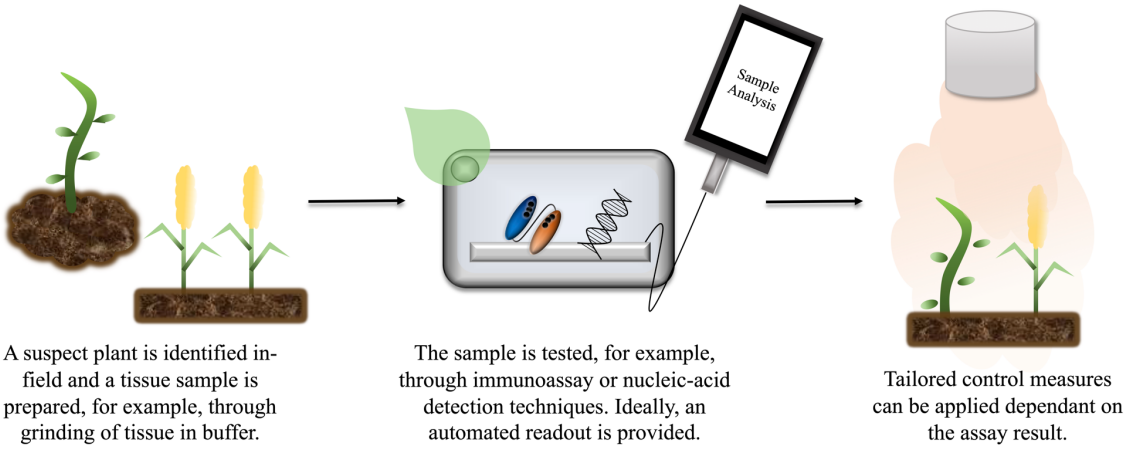

Figure 1.4 The potential of routine diagnostic assays in crop pathogen management
Immunoassays or nucleic acid-detection methods could be implemented for routine or site-specific crop testing. The result of the assay could provide added information on the pathogen burden in-field, allowing tailored treatment, where required.

1.4 Introduction to Diagnostic Methods for Pathogen Detection

1.4.1 Nucleic acid detection methods

1.4.1.1 Polymerase chain reaction

A key element of nucleic acid-based detection is polymerase chain reaction (PCR) which utilises multiple stepwise temperature cycles, and a polymerase, to amplify DNA strands (Mullis et al., 1986). The standard polymerase used in PCR can only transcribe from a DNA template, thus to amplify pathogens composed of RNA, for example PVY, the use of an enzyme with reverse transcription activity is required (Bustin, 2000). In standard PCR, the DNA products are generally visualised by gel electrophoresis, to check for the presence of expected DNA bands. Using this method, only semi-quantitative results can be achieved, facilitated by running known DNA standards alongside the unknown sample. The method can also fail when samples contain low concentrations of DNA. While high-sensitivity

detection can be achieved in some cases, sensitivity can vary greatly depending on the type of DNA stain used, and the type of system used to visualise the gel (Motohashi, 2019). Real time quantitative PCR (real time qPCR) measures the production of the target amplicon throughout the reaction. This is facilitated by DNA intercalating dyes, such as SYBR green, or fluorescently labelled probes. DNA dyes will bind to all double-stranded DNA. To use these dyes, the primers must be highly optimised and produce no non-specific amplicons as these non-specific products will also produce signal, skewing quantification. Fluorescently labelled probes are a more target-specific alternative. Many types of probe are employed in qPCR, however commonplace probes include those which must bind to a specific region on the target DNA in order for fluorescence to be achieved, for example, hydrolysis or hybridization probes (Navarro et al., 2015). An illustration of the use of fluorescent dyes and probes is depicted in *Figure 1.5*. The level of fluorescence in the PCR sample is measured and is directly proportional to the initial concentration of the target in the sample, thus, allowing rapid quantification.

While PCR-based methods are widely applied in pathogen detection, their use requires sophisticated equipment, for example thermocyclers and fluorimeters, which do not typically translate well to on-site diagnostics. To combat this, other nucleic acid detection methods are proposed, mainly those based on isothermal amplification. Isothermal amplification methods rely on singular temperature reactions, negating the need for the bulky and complex equipment needed for providing temperature controlled cycles in PCR, making them appealing for use in-field.

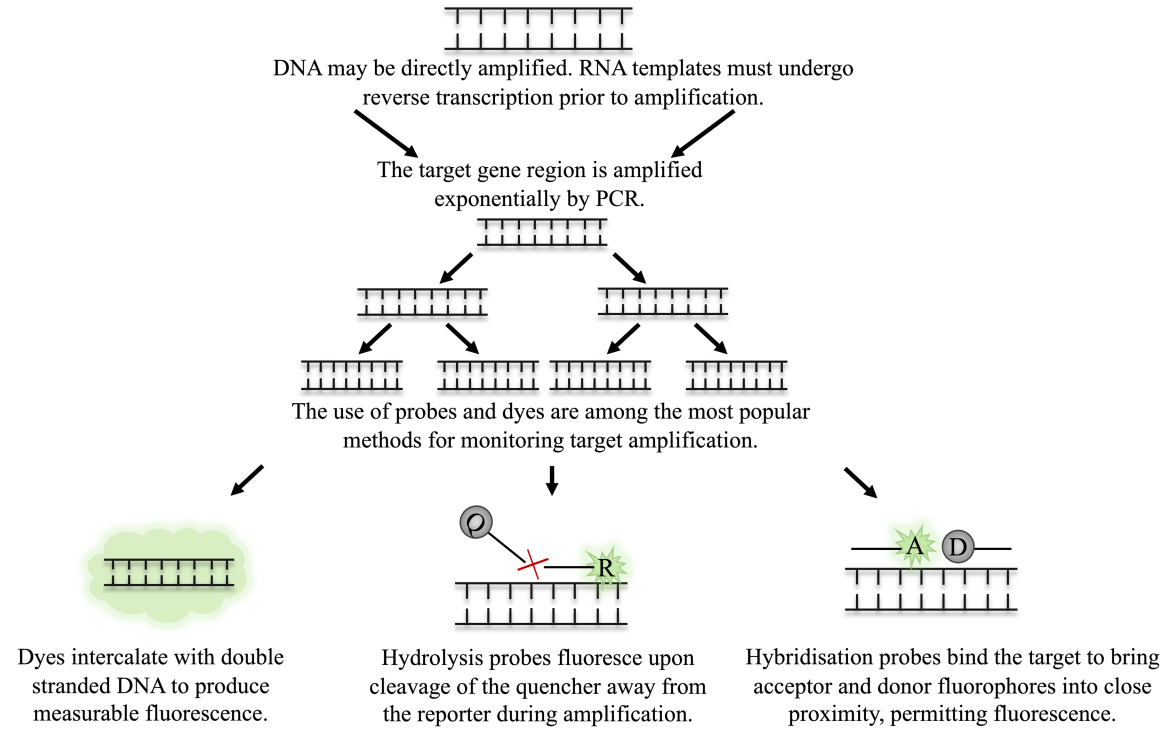

Figure 1.5 The detection of target amplicon in qPCR through dyes and probes

The target region is amplified by multiple rounds of PCR. During amplification, various methods are employed to monitor the real-time production of target DNA. Dyes intercalate indiscriminately with double stranded DNA, causing an increase in fluorescence as the level of double stranded DNA in the sample increases during amplification. Hydrolysis and hybridisation probes require binding to a specific sequence on the target amplicon to permit fluorescence. Fluorescence is achieved either by cleavage of the probe when employing hydrolysis probes, or through binding of the probes to the target region in close proximity to one another, as is the case for hybridisation probes.

1.4.1.2 Isothermal amplification methods

Many forms of isothermal amplification are proposed. Most can be used alongside either single stranded or double stranded DNA, making them applicable for detecting most pathogens. Some popular methods include loop-mediation isothermal amplification (LAMP), recombinase polymerase amplification (RPA), helicase-dependant amplification (HDA) and rolling circle amplification (RCA). LAMP, developed by Notomi *et al*. (2000), relies on the use of multiple primers, at minimum four, to initiate the polymerase-driven extension of the gene sequence (Notomi et al., 2000, 2015). The suggested reaction temperature for amplification is 65ºC, however, studies demonstrated successful amplification at temperatures ranging between 57ºC and 67ºC (Tomita et al., 2008; Francois

et al., 2011). The reaction time is rapid and typically ranges from 30-60 min, although with optimisation of the reaction conditions, such as reaction temperature and buffer composition, it was shown to be possible to reduce the time to result to 10 min (Tomita et al., 2008; Estrela et al., 2019). RPA was proposed by Piepenburg *et al*., in 2006, and since then has gained traction as a promising method for nucleic acid detection (Piepenburg et al., 2006). Recombinase polymerase amplification (RPA) uses a recombinase and a single-stranded DNA binding protein (SSBP), in the presence of other reagents such as a strand-displacing DNA polymerase and target-specific primers. The RPA reaction has an extremely flexible reaction temperature, typically between 22º-45ºC. Further to this, the reaction is usually complete within 20 min (Piepenburg et al., 2006; Daher et al., 2016; Lobato and O'Sullivan, 2018). Helicase-dependant amplification (HDA) functions by employing a DNA-helicase to unwind double stranded DNA. Flanking primers anneal to the strands, where a polymerase amplifies the target region. The reaction is performed at higher temperatures between 60ºC and 65ºC (Vincent, Xu, and Kong, 2004; An et al., 2005; Teo et al., 2015). Rolling circle amplification (RCA) mimics a natural process by which circular DNA is replicated (Kasamatsu and Vinograd, 1974; Mohsen and Kool, 2016). At its most basic, RCA requires only one primer, from which a strand displacing polymerase initiates replication. The resulting amplicon is a linear product, consisting of repeat sequences of the circular DNA (Schweitzer and Kingsmore, 2001; Mohsen and Kool, 2016). Alterations were made to the protocol to facilitate rapid, exponential amplification. These include the use of hyper-branched RCA and multiply-primed RCA, permitting exponential amplification of circular DNA. RCA incorporating padlock probes facilitates the amplification of linear sequences through RCA (Lizardi et al., 1998; Banér et al., 2001; Dean et al., 2001; Marincevic-Zuniga, Gustavsson, and Gyllensten, 2012; Mezger et al., 2014; Hamidi, Ghourchian, and Tavoosidana, 2015; Fux et al., 2018; Li et al., 2019). RCA can be performed at a range of temperatures between 30 and 65ºC (Marincevic-Zuniga, Gustavsson, and Gyllensten, 2012; Li et al., 2019).

Many of these isothermal amplification methods operate at relatively low temperatures, ranging from 22ºC - 65ºC. Operating temperatures in the range of 22ºC - 40ºC can be readily achieved using effectively no equipment, as demonstrated by successful amplification using ambient air temperatures or body heat (Crannell, Rohrman, and Richards-Kortum, 2014; Lillis et al., 2014). In addition, higher operating temperatures, or amplification in low ambient temperatures, can be achieved through the use of exothermal heaters, such as

reusable sodium acetate trihydrate (SAT) heaters (Lillis et al., 2014). Such chemical heating mechanisms are commonplace in hand-held heaters, making this technology widely available at relatively low cost. In addition, when using these isothermal amplification methods, qualitative results can be achieved on-site without the need for much additional equipment. For most assays, intercalating dyes such as SYBR green can be added. These dyes fluoresce upon binding double stranded DNA. This fluorescence can be observed by the naked eye in the presence of enough double stranded DNA product, permitting on-site detection without the need for any additional materials. A drawback to this method is that SYBR green will bind any double stranded DNA indiscriminately, causing fluorescence in the presence of primer dimers or non-specific amplification which can cause false positive results. Isothermal amplifications which operate at lower temperatures, such as RPA, can be prone to non-specific product generation, therefore, correct primer design is particularly important for such amplification techniques when using dye-based detection. The use of fluorescently labelled probes in the reaction can confer added specificity and reduce the level of false positives, however, additional equipment such as fluorimeters are generally required to monitor such reactions. For LAMP assays, the turbidity of the reaction can also be used for on-site qualitative analysis. LAMP produces large amounts of precipitated magnesium pyrophosphate as a by-product. Typically, the presence of precipitate is visible to the naked eye after a successful reaction, allowing a rapid qualitative answer (Zhang, Lowe, and Gooding, 2014). Turbidity within the assay can also be measured real-time via the employment of a turbidimeter, which facilitates quantitative analysis of target DNA by comparing an unknown sample to a standard curve (Parida et al., 2008; Wang et al., 2020a). However, as with the use of probes, this method requires additional equipment, limiting the usefulness for on-site applications. One of the most appealing methods by which isothermally amplified DNA products can be detected on-site is through lateral flow immunoassay. This method generally relies on the use of antibody-based detection of labelled amplicons and is a reliable and rapid visual method by which amplified target DNA can be detected. Lateral flow-based detection is generally qualitative but can be made semi-quantitative through the use of image analysis. The employment of antibodies in nucleic-acid detection is just one example of the many applications of immunoassay, a field which itself encompasses a huge number of assay formats and types.

1.4.2 Immunoassay

Immunoassays employ antibodies as the primary means by which a target pathogen is detected from a sample. Antibodies are available in polyclonal, monoclonal and recombinant formats (Ma and O'Kennedy, 2015). Polyclonal antibodies bind multiple different structures, termed epitopes, on the target organism/molecule i.e. they are polyspecific. In contrast, monoclonal antibodies, and certain recombinant forms of antibodies, present singular-epitope specificity, hence, they are monospecific. Monospecific antibodies are valued in diagnostics when highly specific detection is required as they offer the opportunity for the targeted detection of precise, distinct regions (Wu et al., 2015; Anjum et al., 2017; Seepiban et al., 2017; Zhang et al., 2018, 2020b). One of the most widely applied immunoassays is the enzyme-linked immunosorbent assay (ELISA). There are a number of formats in which the ELISA assay can be performed, namely direct, indirect, competitive and sandwich (*Figure 1.6)*. These formats are shared across the majority of immunoassays. Direct and indirect formats are similar. Initially, the target is coated to the surface of the ELISA well through passive adsorption, or it may be chemically linked. For direct detection, a labelled, anti-target antibody is applied to the well, and subsequently detected. For indirect detection, the primary antibody is unlabelled, and is detected by the addition of a labelled, secondary antibody. Another format, competitive ELISA, first involves the immobilisation of the target antigen to an ELISA well, followed by the simultaneous application of the antibody and the suspect sample to the same well. Free target antigen in the sample competes for antibody-binding, leaving less antibody available for binding to the immobilised antigen. The sample is washed away, and any remaining bound antibody is detected with a labelled, secondary antibody. Therefore, in this assay format, the signal is inversely proportional to the amount of analyte in the sample (He, 2013). Sandwich formats employ two antibodies, both specific for different regions on the target. The first of these is immobilised to the assay surface. Thereafter, the sample is applied, and is captured by the immobilised antibody. Unbound entities are washed away, and the second antibody is applied. This second antibody can be labelled directly or detected with a labelled-secondary antibody. This format offers high specificity as it requires the binding of two antibodies to produce a signal. It is also considered the most sensitive and robust ELISA format (Ecker et al., 2013; He, 2013).

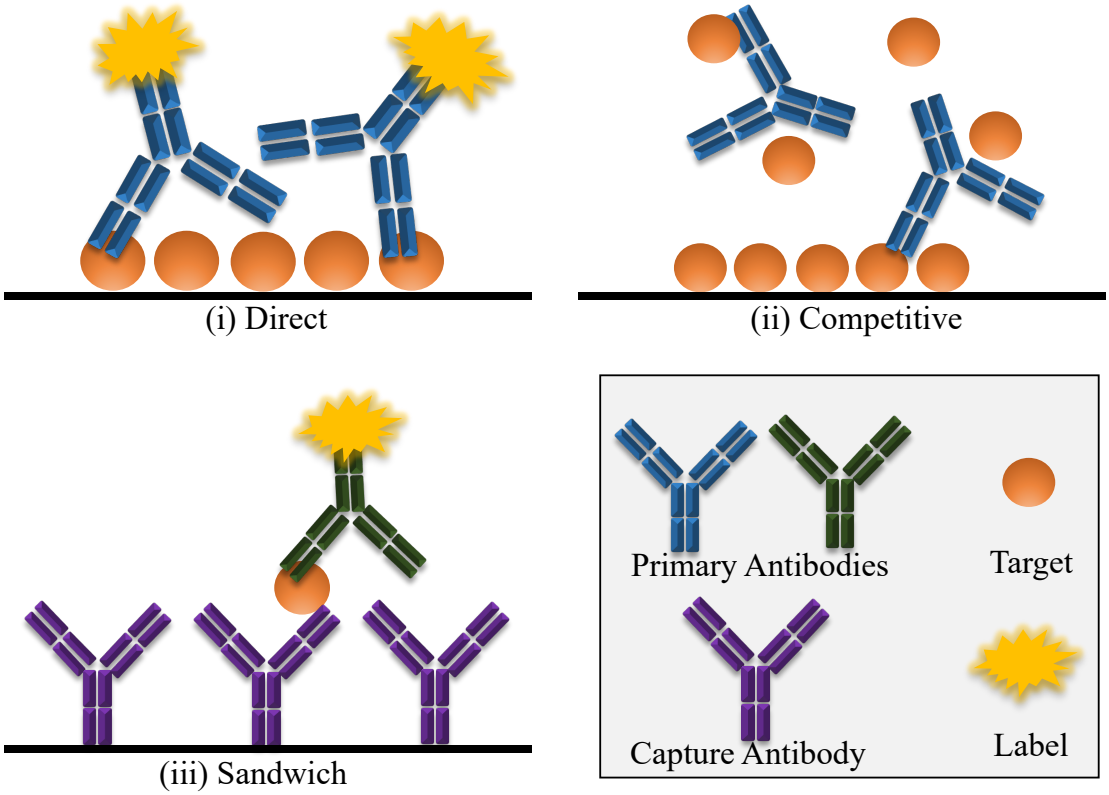

Figure 1.6 Examples of the various ELISA formats

(i) *Direct detection utilises a single, labelled antibody to detect the target coated to the assay surface.* ***(ii)*** *Competitive assays also employ one target-specific antibody. The target is initially immobilised to the assay surface. Thereafter, antigen is added in solution simultaneously alongside the antibody. The free target competes for antibody binding, reducing the level of antibody available to bind to the immobilised target. This makes the signal in competitive assays inversely proportional to antigen concentration.* ***(iii)*** *Sandwich assays use two target-specific antibodies. One antibody (immobilised on the assay surface) captures the target from the sample, while the second antibody binds to a different epitope on the target already captured by the immobilised antibody.*

ELISA is a well-used form of assay in plant pathogen detection due to its robustness and capability to be developed into a highly sensitive and specific assay (Balodi et al., 2017; Pagliaccia et al., 2017; Himananto et al., 2020; Bratsch, Olszewski, and Lockhart, 2021). Additional immunoassay methods involve paper based assays, such as dot blots and tissue blots which function through the pressing of suspect plant tissue into a membrane support and subsequent testing for the presence of the target using specific antibodies (Garzo et al.,

2011; Komor, 2011; Boukari et al., 2020). Lateral flow is another widespread example of a rapid paper-based immunoassay (Zeng et al., 2016; López-Soriano et al., 2017; Panferov et al., 2017; Safenkova et al., 2017). The lateral flow assay result is usually read by the way of a colour change at a test line. LFIA are used commonly in plant pathogen detection due to their rapid results turnaround, <15 min, and their robustness when using complex matrices such as leaf tissue. While there are many different immunoassay formats available, the key shared characteristic across all immunoassay platforms is the incorporation of antibody proteins as the biological sensing element. The ability of these proteins to recognise and bind specifically and sensitively to a target is exploited worldwide and has led to their employment in many diagnostics tests, examples of which include immunohistochemistry (IHC), Enzyme-linked immunosorbent assay (ELISA), Western blotting (WB), and lateral flow immunoassays (LFIA). Given the benefits of antibody-based diagnostics, one of the primary focuses of the work described in this thesis was the generation and isolation of antibodies, and subsequent development of immunoassays, for the targeted detection of *R. commune* and PVY targets.

1.5 Antibodies

Antibodies are naturally occurring proteins and are key components of the immune system. They are capable of highly sensitive and specific detection of a wide range of targets. The purpose of the natural immune system is to combat disease via the recognition of specific sequences, molecules or parts of molecules, termed antigens, associated with invading pathogens. The main proteins responsible for identifying these invading pathogens are known as immunoglobulins (Ig), or antibodies. B-cells, one of the key cells involved in the immune response, mediate the production of antibodies via activation through their B-cell receptor (BCR), a membrane-bound Ig receptor. Each B-cell presents a unique BCR which, when activated via the binding of its requisite antigen, triggers a series of responses. These responses ultimately lead to the differentiation of the antigen-specific B-cell into several cell types, including plasma cells, which secrete soluble Ig (Batista and Harwood, 2009). Antibodies are capable of binding to the invading foreign objects in the body, thus tagging them for destruction and neutralization by other immune components (Kenneth et al., 2016). *Table 1.2* provides a summary of some of the desirable properties of antibodies.

Table 1.2 Antibodies and their potential advantages

Characteristic	Description
Sensitive	Ability to detect antigen of interest at extremely low concentrations.
Specific	Unreactive with non-target antigens.
Stable	Capacity to remain viable for use in a range of conditions, e.g. range of pHs and buffers.
High Affinity	Strong antibody-antigen interaction. This is particularly useful in biosensor platforms.
Low Interference	Little or no interaction with other assay reagents e.g. buffers.
High Yields	High protein expression available in various systems e.g. *E. coli*, yeast, mammalian.
Engineering Potential	Recombinant antibodies may be engineered to improve various attributes e.g. sensitivity, stability, affinity.
Cost Effective	Recombinant antibodies can be produced at low cost in organisms such as *E. coli* or yeast.
Time Effective	Recombinant proteins are expressed rapidly due to the short growth time of expression organisms used.

1.5.1 Antibody diversity

There are many naturally occurring antibody forms, or isotypes, including Ig G, M, D, E, and A, with IgG being the most abundant mammalian isotype. IgY is the avian counterpart to IgG. Igs consist of two heavy and two light chains which form a Y-shaped molecule. Within each of these heavy and light chains lies variable regions which are vital in the determination of the antigen-binding properties of a given Ig. The observed diversity between Ig proteins is predominantly located within these variable regions. Theoretically, the antibody repertoire is capable of detecting an infinite number of invading pathogens or foreign molecules. However, given that a genome is of a finite size, in order for this to be feasible, two primary mechanisms evolved to permit diversity while utilising a limited number of genes. The first of these mechanisms is V(D)J recombination, followed by somatic hypermutation (SHM).

Antibody variable genes are encoded by three gene groups, the variable (V) gene segments, the diversity (D) gene segments and the joining (J) gene segments. Recombination events

between these genes segments are mediated by two recombinase enzymes, produced by recombination-activation gene (*RAG*) *1* and *RAG2* (Schatz, 2004). In heavy chain formation, one gene from each of the D and J segments are combined initially, followed by the addition of a V segment. Contrastingly, the light chain is formed by joining of V and J segments, with no joining of a D segment. A constant region is then added to the recombined genes to form the whole antibody mRNA which can then be translated into an antibody protein (Sadofsky, 2001; Jung et al., 2006). This concept is illustrated in *Figure 1.7*. This recombination mechanism is not uniform across all species, for example, in chickens, the V, D and J genes have much lower diversity, with only one V and J gene available for recombination, and a limited number of D genes available for the same. As such, recombination is not the main benefactor for the chicken's immune repertoire. Instead, in an act known as gene conversion, specific upstream pseudogenes act as sequence donors to introduce alterations to antibody genes. Pseudogene sequences are incorporated into the V segment, resulting in increased diversity and contributing to the wide repertoire observed in chickens (Leighton et al., 2018). In addition to recombination, somatic hypermutation (SHM) is utilised to introduce variation into antibody repertoires. SHM is a process mediated by activation-induced cytidine deaminase (AID) which incorporates point mutations into the V region of the antibodies. SHM can occur both before and after antigen-exposure to introduce either primary diversity or antigen-specific diversity, respectively (Teng and Papavasiliou, 2007; Maul and Gearhart, 2010).

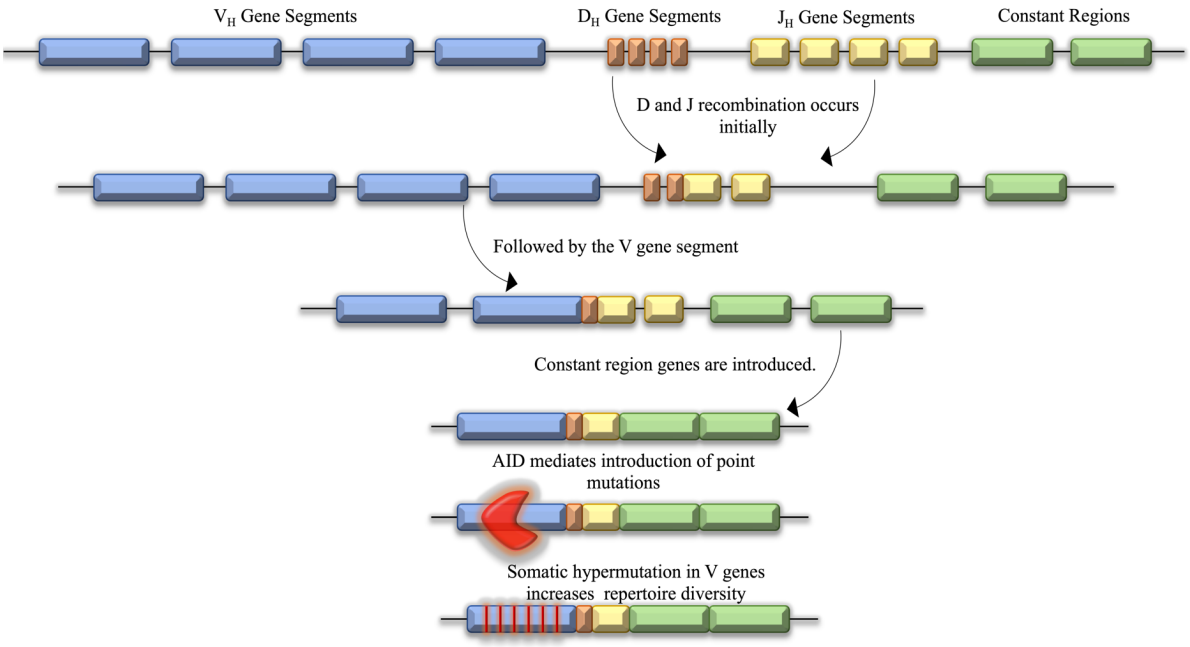

Figure 1.7 Simplistic overview of how V(D)J recombination and somatic hypermutation act to increase natural repertoire diversity

The diagram depicts the somatic recombination of antibody genes in order to create a diverse heavy chain repertoire. The light chain repertoire is generated in a similar manner, however, the light chain only comprises of V and J genes, making a VJ complex.

In addition to the primary diversification methods of V(D)J recombination and somatic hypermutation, other mechanisms for increasing antibody diversity are proposed. For example, one observation is the trans-chromosomal incorporation of functional, non-immunoglobulin proteins into the V regions of the antibody. In addition to this recombination-type diversification, it appears that the generation of amino acid inserts or deletions (indels) primarily within the variable regions also promotes diversification (Kanyavuz et al., 2019). However, it should be noted that diversification through these methods is not widely observed in B-cell populations, indicating that such mechanisms may be employed by the immune system in select circumstances whereby diversification and antibody selection through V(D)J and SHM are not suitable. Variation within the antibody structure and subsequent binding characteristics can also arise from other factors such as atypical glycosylation or recruitment of non-protein co-factors (Kanyavuz et al., 2019).

1.5.2 Structural characteristics of whole and recombinant antibodies

IgG and IgY are the most abundant antibody isotypes in mammalian and avian species, respectively. Therefore, the primary focus will be on the structure of these Igs and their sub-units. IgG/IgY structure is comprised of two heavy chains and two light chains. The antibody molecule can be further portioned into two distinct regions, known as the constant region (Fc) and the variable region (Fab). The variable region contains a binding site on each chain. Each of these binding sites features three complementarity determining regions (CDRs). The amino acid sequences located within the CDRs play a major role in defining the antigen which will be recognised. The CDRs are flanked by conserved regions of framework which assist in localisation of the antigen. Framework regions are also implicated in antigen binding (Klein et al., 2013; Murphy et al., 2018) The mammalian IgG and avian IgY share structural similarities in the sense that they each have two heavy and light chains which are, in turn, divided into variable and constant regions, however, there are dissimilarities between the two. The mammalian IgG contains a hinge joint, endowing flexibility to the variable "arms" of the protein. In contrast, the avian IgY lacks a hinge region, inferring that the molecule may have a more rigid structure (Spillner et al., 2012). There are also some differences in the glycosylation patterns observed in IgG when compared to IgY. Both antibodies feature a glycosylation site at the CH2 domain, while IgY has an additional glycosylation site at the CH3 domain. The extra glycosylation on IgY is not thought to confer added immunogenicity to the protein (Gilgunn et al., 2016).

Both IgG and IgY can be re-engineered into several functional sub-units, or fragments, of the whole molecule using recombinant protein engineering approaches. Depictions of the various structures of both naturally occurring, and recombinant mammalian and avian antibodies, can be seen in *Figure 1.8*. There are several formats of antibody fragment. The F(ab,)$_2$ fragment comprises of the entire variable portion of the antibody. The Fab is made up of a variable light domain, a variable heavy domain, a constant light domain, and a constant heavy domain. ScAbs contain a variable heavy domain, a variable light domain, and one constant domain, sourced from either the heavy or light chain. A scFv is a constant heavy domain and a constant light domain which are joined by a glycine/serine linker which provides flexibility to the antibody (Ma and O'Kennedy, 2015). SdAbs, or nanobodies, feature one domain, typically the variable heavy domain. These sdAbs are generally sourced from camelids or shark species as the antibody repertoires of these species naturally feature antibody classes devoid of light chains. As such, their variable heavy domains are usually

soluble, unlike some mammalian species such as mice. SdAbs sourced from such animals may be useful detection reagents *in vitro*, however, their associated immunogenicity means that humanization of these proteins is essential before considering them for in vivo applications (Holliger and Hudson, 2005; Vincke et al., 2009). If required, Fc portions can be appended to recombinant forms, e.g. scFv-Fc antibodies, to increase stability and half-life (Unverdorben et al., 2016).

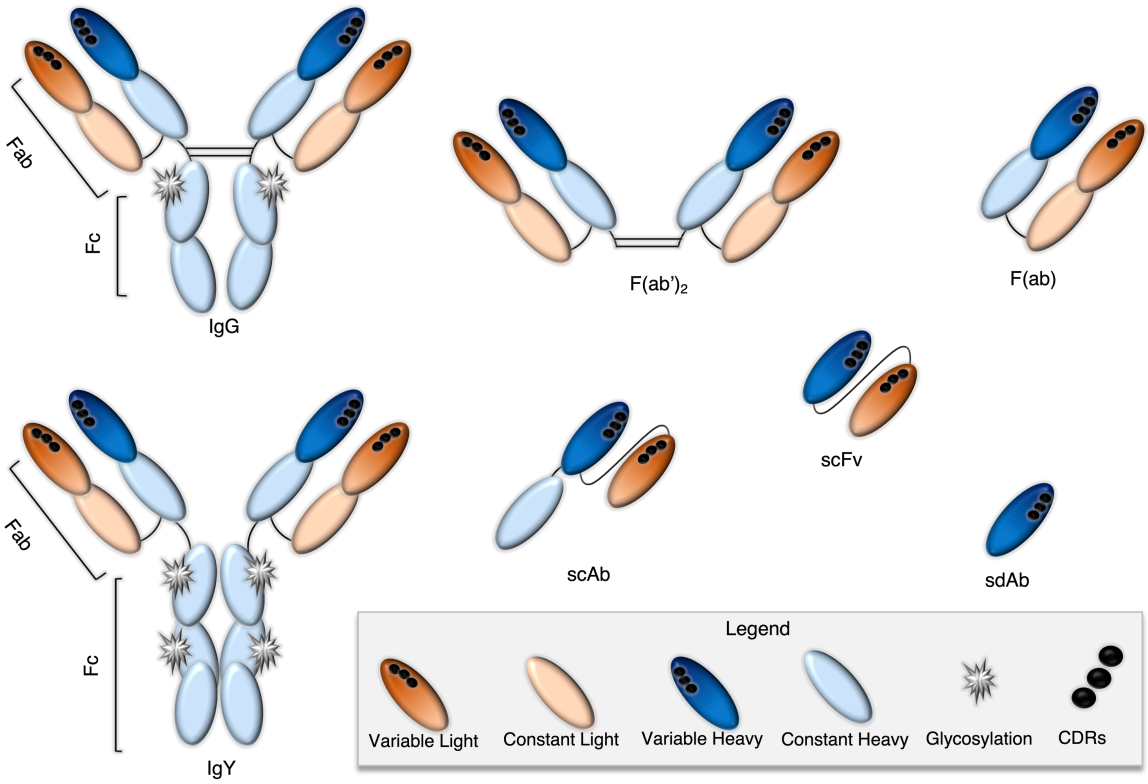

Figure 1.8 A depiction of the various antibody formats

The entire IgG (mammalian) and IgY (avian) molecules are illustrated alongside a selection of their potential recombinant forms. When compared to IgG, the IgY has an additional constant heavy domain, lacks a hinge region and features additional glycosylation sites on the CH3 domain. The recombinant forms of antibody are all smaller than their parent molecule and these range from large fragments such as the F(ab')$_2$, to the smallest antigen binding fragment, a sdAb.

The increased knowledge of antibody structure and function has facilitated the practice of genetic mutation to generate engineered, recombinant antibodies. Further to this, the understanding of the antigen binding mechanisms enables specific engineering to introduce improvements to a range of characteristics such as binding rates, stability, sensitivity and

specificity. The use of recombinant antibody technology offers major opportunities for improvement across all antibody attributes (Ma and O'Kennedy, 2017; Basu et al., 2019). Due to the plethora of advantages which recombinant protein expression offers, antibody fragments are evolving toward the forefront of sensing technology. In order to isolate recombinant antibodies against targets of interest, a specialised screening technique is employed. This technique, termed phage display, revolutionised the field of antibody discovery.

1.6 Isolation of Recombinant Antibodies through Phage Display

One of the most significant issues associated with recombinant antibody technology is the successful isolation of suitable antibodies from genetically engineered antibody repertoires, known as antibody libraries. Antibody libraries are a representation of the immune repertoire of the host from which they are derived. Given the enormous size of immune repertoires, difficulty lies within sheer number of antibody proteins which must be screened within these libraries. Phage display is proposed as a method by which these screening issues can be addressed. Phage display is a combinatorial screening method whereby functional proteins may be displayed on the surface of phage particles. These protein-displaying phage pools can then be employed for the investigation of biological interactions. With respect to the research herein, the phage display method will be discussed in relation to its application to recombinant antibody library screening as it has proved to be a highly efficient and powerful tool in the identification of antibodies with desirable binding characteristics.

1.6.1 Phage biology

Among the most studied filamentous phage are those which infect *E. coli*, Ff (f1, M13 and fd). These lysogenic, rod-shaped virions are composed of circular, single-stranded DNA (ssDNA). This ssDNA is enveloped by thousands of copies of a major coat protein, pVIII, which is capped by two minor protein pairs, pVII/pIX and pIII/pVI. The pIII and pVI proteins mediate entry and release from the host bacteria through host cell-receptor interactions, while pVII and pIX form a complex which is essential for virion assembly and secretion (Mai-Prochnow et al., 2015; Straus and Bo, 2018). Of these structural virus proteins, pIII is often chosen for phage display. Ff bacteriophage are deemed suitable for the display of antibodies as the pIII proteins are folded in the periplasm, an oxidative environment which allows for the formation of disulphide bonds. Display of antibodies, typically on the N-terminus of the pIII protein, results in up to five antibody-pIII fusions per

virion, making it a preferential expression partner for antibody screening. This is particularly useful in cases where the repertoire under investigation may contain only rare-binding antibodies. Antibodies may also be displayed on alternative proteins such as pVIII, pVII and pIX, however, for various reasons, these are not typically used. Display on the major coat protein, pVIII can cause steric hindrance due to the frequency of occurrence of the antibody-coat protein fusions on the virion. This hindrance can lead to limited binding of potential clones. With regards to display on the minor proteins, pVII and pIX, the copy number of fusion proteins is lower than that of pIII fusions. This is an unfavourable trait when selecting from a phage pool with limited numbers of binders (Zhao et al., 2016; Rakonjac et al., 2017). Therefore, display on pIII gives a balanced antibody representation whereby enough antibody-coat protein fusions exist on the virion to elicit sufficient binding, however not so many fusions occur that steric hindrance poses an issue.

1.6.2 Phage display

The combination of recombinant antibody library generation and screening through phage display is an efficient and useful method for the isolation of suitable antibodies. This approach negates the need to generate immortal monoclonal antibody cell lines, a time-consuming process. Instead, antibody libraries are generated through molecular techniques and screened rapidly on filamentous phage. Display of the antibody genes on the viral proteins in this manner is permitted as a result of a link that exists between the genotype and phenotype in filamentous bacteriophage particles which allows the co-expression of recombinant antibody and viral coat proteins (Smith, 1985). This genotype-phenotype link is exploited to facilitate the identification and isolation of antibodies with the desired binding characteristics from large libraries of recombinant clones. In addition, the antibody sequences can be recovered effectively from the antibody-displaying phage, permitting rapid identification and recording of the CDR sequences. In order to begin the process of phage display, antibody genes are isolated and cloned into a specific region of a phagemid vector, which results in the expression of a pIII-antibody fusion protein, as shown in *Figure 1.9.*

This vector is transformed into a suitable host, for example *E. coli*, and cyclic rounds of a process known as ‘biopanning’ are performed thereafter to enrich the phage pool for binding clones. The phagemid vectors often feature tags such as haemagglutinin (HA) or 6X Histidine (HIS) which are co-expressed with the antibody protein to aid in detection and purification. Another common feature in these vectors is an amber stop codon (TAG)

inserted between the antibody genes and the pIII gene. When the vector is harboured in suppressor strains of *E. coli*, for example XL1-Blue, the TAG codon is not read and the antibody-pIII fusion protein is expressed. However, when expressed in non-suppressor *E. coli* strains, the stop codon is read and the antibody protein is expressed in free, soluble form without PIII (Hammers and Stanley, 2014; Zhao et al., 2016).

Phagemid vectors, such as pComb3XSS, do not harbour all the requisite genes to assemble a full phage virion and require the introduction of helper-phage to aid assembly. Helper-phage are modified Ff phage. They contain an origin of replication and antibiotic resistance, however, they lack a key packaging signal. This packaging signal is provided by the phagemid vector, meaning that only when helper-phage are introduced to cells containing a phagemid, can virion replication and assembly commence (Ledsgaard et al., 2018). The helper-phage also contain a pIII gene. The phagemid pIII and helper-phage pIII proteins compete for incorporation into the virion. Therefore, the display proteins on the surface of the resulting virions is heterogenous, with antibody-pIII fusions and unfused pIII proteins existing simultaneously. Both the helper-phage and phagemid genomes may be replicated and packaged, however, the lack of a packaging signal in helper-phage greatly hinders its assembly and phagemid particles exist predominantly. The antibiotic resistance in helper-phage may also be utilised in the biopanning process in tandem with the phagemid antibiotic resistance, to select for bacteria which are infected with both phage particles (Ledsgaard et al., 2018). Once the antibody genes are linked to the phage-associated display genes, the antibody library may be screened for binding through a method termed biopanning.

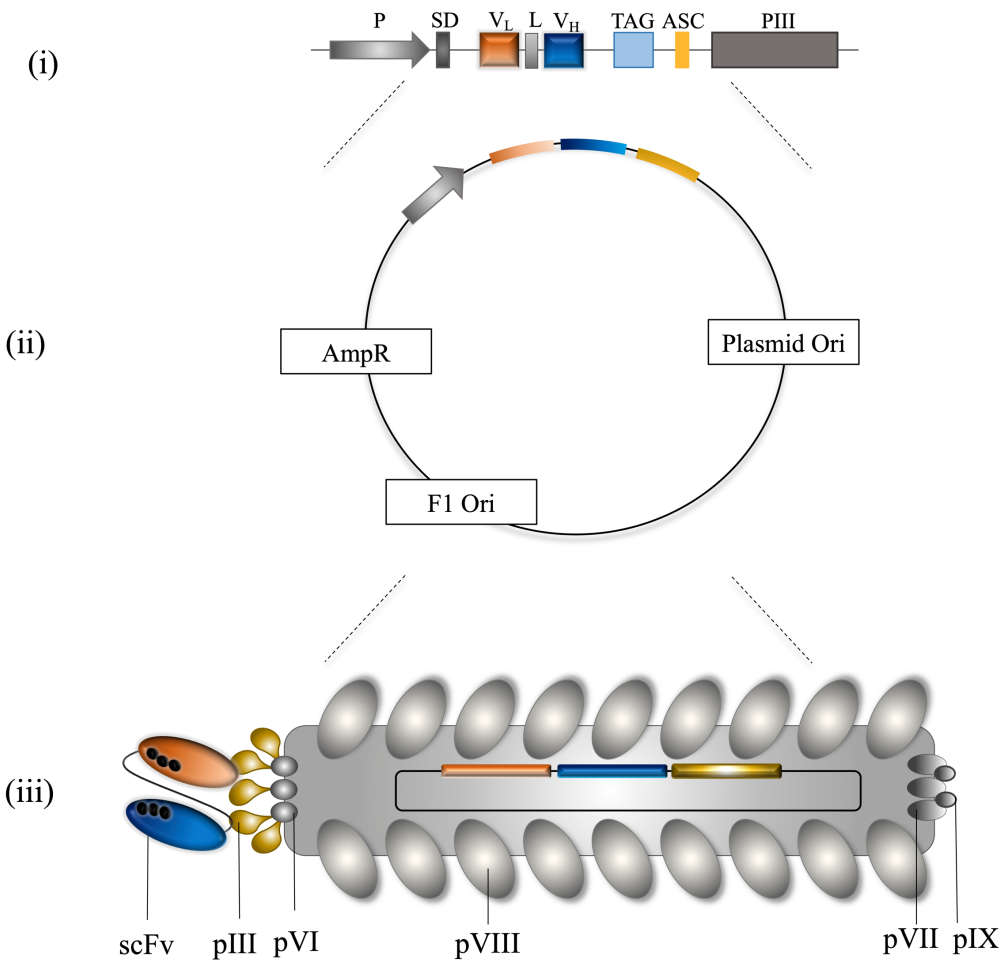

Figure 1.9 A depiction of gene order in an scFv-expressing phagemid vector, a phagemid vector, and a basic illustration of typical phage utilised in phage display

(i) *The promotor (P) controls gene expression. The pComb3XSS vector features the commonly used LacZ promoter which can be regulated via IPTG. The Shine Dalgarno (SD) sequence initiates protein synthesis. The light chain (V_L) and heavy chain (V_H) are joined by a glycine-serine linker (L). There are several tags (TAG) on the vector including a 6xHis tag and haemagglutinin (HA) tags. The amber stop codon (ASC) can be employed to allow soluble antibody expression, separate from pIII. Coat protein pIII (pIII) is expressed as a fusion protein alongside the scFv* (Barbas et al., 2001). ***(ii)*** *The pComb3XSS phagemid vector contains both a phagemid origin of replication and a bacterial origin of replication. This allows for the assembly of phage particles and recombinant protein expression in a bacterial host, respectively. The vector also contains ampicillin resistance to allow for antibiotic selection.* ***(iii)*** *The scFv protein is expressed as a fusion to the phage pIII minor coat protein where it retains its binding capacity. Other coat proteins illustrated are the major pVIII protein and the minor proteins pVI, pVII and pIX* (McCafferty et al., 1990).

1.6.3 Biopanning

Biopanning involves multiple iterations of screening rounds, the protocol of which is illustrated in *Figure 1.10*. Biopanning is a cyclic, affinity-based selection process during which phage pools are exposed to the antigen of interest, unbound and non-specifically bound phage are removed from the pool through washing steps while bound phage are eluted and subsequently re-infected into *E. coli*. After each iterative round, the phage pool should be enriched for antibodies specific to the target. In theory, one round of panning should yield phage pools with positive responses to the antigen, however, performing up to four rounds of panning will increase the likelihood of enriching for rare binders (Hammers and Stanley, 2014).

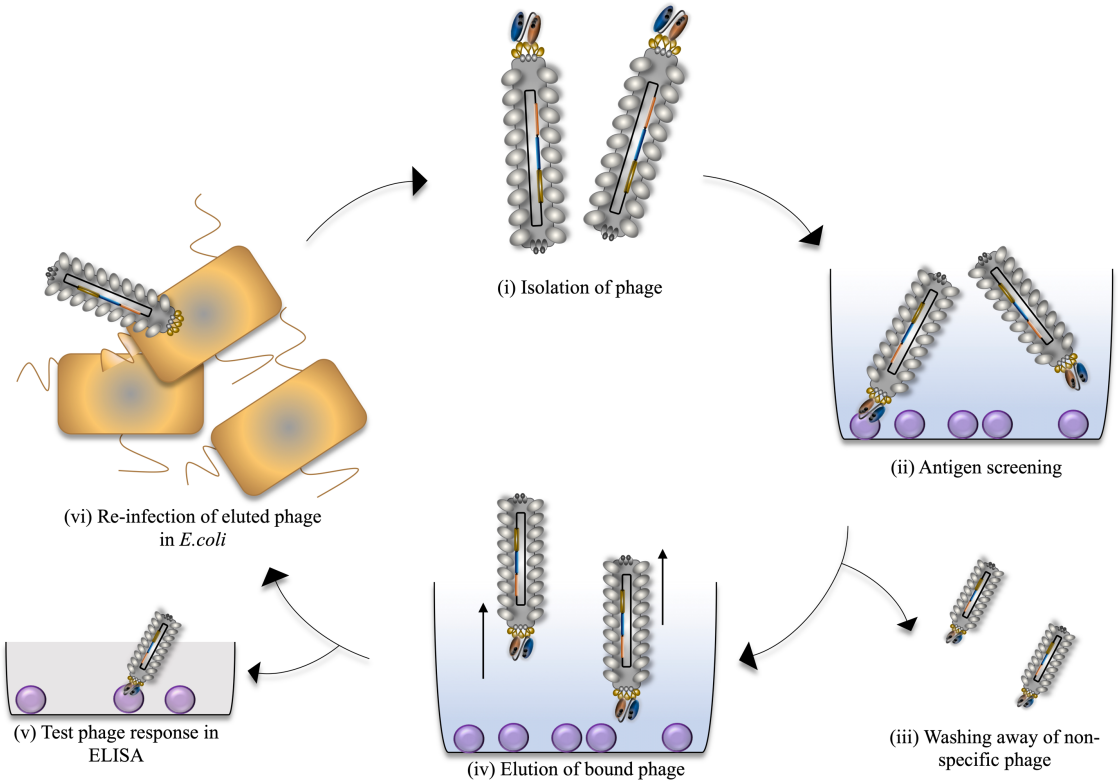

Figure 1.10 A simplified depiction of a single biopanning round

(i) *Phage are infected into an antibody library and the antibody-pIII fusion is expressed. The phage are then isolated.* ***(ii)*** *Phage pools are incubated alongside the antigen of interest, for example, in an immunotube.* ***(iii)*** *Unbound and non-specifically bound phage are washed away.* ***(iv)*** *Bound, antigen-specific phage are eluted from the immunotube.* ***(v)*** *The response of the phage pools against the antigen of interest can be tested concurrently in ELISA.* ***(vi)*** *The antigen-specific phage are re-infected into E. coli and amplified. The phage are isolated once more and the round begins again.*

The described screening methods are employed for the isolation of highly specific antibodies. After isolation, the recombinant antibody harbouring plasmids are conveniently placed in *E. coli* hosts, permitting rapid expression and purification. The isolated antibodies are then characterised through various methods including ELISA, immunoblotting and surface plasmon resonance (SPR).

1.7 Thesis Outline and Aims

The primary interest of this project is the development of diagnostic methods to facilitate the improved detection of PVY and *R. commune* through the design and application of immunoassays. This was performed in conjunction with molecular-based sensing in the form of isothermal amplification coupled with lateral flow immunoassay. The overarching goal of this research is to provide a means by which crops may be tested *in situ*, thereby providing an additional control measure, with the hope to curtail the spread of crop pathogens and reduce reliance on broad-spectrum chemical control measures.

Chapter three of the thesis describes the generation of a recombinant scFv library for the isolation of anti-PVY scFv. To screen this library, the PVY CP was recombinantly expressed in an *E. coli* system and subsequently purified. The generated anti-PVY library was then employed in a screening campaign against the CP antigen. From this screening, several scFv were isolated and characterised in ELISA.

Chapter four discusses the reformatting of multiple anti-PVY monoclonal antibodies into recombinant scFv and scAb formats. These recombinant forms were characterised in ELISA and suitable scFv and scAb candidates were identified. The expression characteristics of these recombinant forms were analysed prior to further characterisation and assay development in the form of immunoblot analysis, ELISA and kinetic analysis on SPR. In addition to this, an SPR-based immunosensor assay was developed.

In *chapter five*, a hybrid nucleic-acid lateral flow immunoassay was developed for the targeted detection of PVY nucleic acids. To facilitate this, PVY-specific probes and primers were designed and applied alongside an isothermal amplification system, recombinase polymerase amplification. Lateral flow immunoassay technology was then employed for the rapid visual detection of PVY-specific amplicons. The resulting assay was capable of

detecting PVY at low concentrations from both DNA and RNA samples in a short timeframe and with minimal equipment requirements.

Chapter six describes the generation of recombinant and polyclonal anti- *R. commune* antibodies. An anti-*R. commune* scFv library was constructed. This library was screened for *R. commune* binding antibodies using a total protein extract in conjunction with a combination of monoclonal analysis and subtractive and direct biopanning methods. Resulting scFv were purified and analysed in ELISA format. Additionally, anti- *R. commune* polyclonal antibodies were isolated and characterised using ELISA and immunoblot analysis.

Chapter 2

Materials and Methods

2.1 Equipment

Apparatus	Supplier
Mini-PROTEAN® Tetra Cell Micropulser™ Electroporator Gel Doc™ EZ Imager T100 Thermal Cycler Bio-Rad PowerPac™ Basic DNA Gel Apparatus Bio-Rad (Wide-Mini-Sub® Cell GT)	Bio-Rad Laboratories Inc., 1000 Alfred Nobel Drive, Hercules, California 9454, USA.
Biacore X100 CM5 sensor chip	Cytiva (formerly GE Healthcare), Amersham Place, Little Chalfont, Buckinghamshire, HP7 9NA, UK.
New Brunswick Scientific-Excella® E24 Incubator Eppendorf 5810R Benchtop Centrifuge	Mason Technologies, Greenville Hall, 228 South Circular Road, Dublin 8, Ireland.
Eppendorf 5804R Centrifuge Swing-Bucket Rotor (A-4-62); Fixed Angle Rotor (F-45-30-11)	Eppendorf UK Ltd., Endurance House, Vision Park Histon, Cambridge CB24 9ZR, UK.

Rotor (F-34-6-38)	
Branson Digital Sonifier®	ABG Scientific Ltd., Dublin Industrial Estate, Glasnevin, Dublin 9, Ireland.
Orion 3 star-pH meter Pierce™ G2 Fast Blotter Scrilogex MX-S Vortex Mixer Scrilogex D1008 Mini Centrifuge APW-200 Microplate Washer Airstream Class II Type A2 BSC (E-series)	Medical Supply Company Ltd., Damastown, Mulhuddart, Dublin 15, Ireland.
SSM4 See-Saw Rocker Binder CO_2 Incubator	Fisher Scientific Ireland, Suite 3, Plaza 212, Blanchardstown Corporate Park 2, Ballycoolin, Dublin 15, Ireland.
Tecan Safire^2 Plate Reader	Tecan Group Ltd., Seestrasse 103, CH-8708 Männedorf, Switzerland.
IKA® MTS 2/4 Plate Shaker STR6	Lennox,

Ohaus Pioneer 210g x 1mg Balance	John F. Kennedy Drive, Naas Road, Dublin 12, Ireland.
Biometra $T_{GRADIENT}$ Thermal Cycler	Biometra GmbH, Rudolf-Wissell-Str. 30, D-37079 Göttingen, Germany.
Homogeniser Ultra Turrax	Janke & Kunkel IKA-Werk Ultra-Turrax, Staufen, 79129, Germany.
Hermle Z233M-2 Air-Cooled Microcentrifuge	Hermle Labortechnik GmbH, 25 Siemensstrasse, Wehingen, 78564, Germany.
NanoDrop™ ND-1000 Spectrophotometer	NanoDrop Technologies, Inc., 3411 Silverside Rd 100BC, Wilmington, DE19810-4803, USA.
DCX-700 Dual Cool System	MyBio Ltd., Kilkenny Research and Innovation Centre, St. Kieran's College Road, Co. Kilkenny, Ireland.
Nikon Diaphot Inverted Tissue Culture Microscope	Nikon Instruments Inc., 1300 Whiteman Road,

	Melville, New York 11747-3064, USA.
Sigma Laborzentrifugen Model 2K15	SIGMA Laborzentrifugen GmbH, Osterode am Harz, Lower Saxony 37507, Germany.

2.2 Reagents

Note: Reagents were typically sourced from Sigma-Aldrich Ltd (Dublin, Ireland).

Reagent	Supplier
Bacteriological agar Tryptone Yeast extract	Cruinn Diagnostics Ltd., Hume Centre, Parkwest Business Park, Nangor Road, Dublin 12, Ireland.
PCR primers RPA primers RPA probe	Integrated DNA Technologies, Interleuvenlaan 12A, B-3001 Leuven, Belgium.
TriZol® SYBR® Safe RNAlater™ RNAzap Sodium acetate (3M) SOC media M13K07 helper phage TrackIt™ 100bp DNA Ladder	Bio-sciences, 3 Charlemont Terrace, Crofton Road, Dun Laoghaire, Co. Dublin, Ireland.

DMEM FBS	
HBS Ethanolamine-HCl	Cytiva (formerly GE Healthcare), Amersham Place, Little Chalfont, Buckinghamshire, HP7 9NA, UK.
Ni-NTA resin InstantBlue™	MyBio Ltd., Kilkenny Research and Innovation Centre, St. Kieran's College Road, Co. Kilkenny, Ireland.
HyperLadder™ 1kb HyperLadder™ 25bp	Medical Supply Co. Ltd., Damastown, Mulhuddart, Dublin 15, Ireland.
Pierce™ transfer buffer Molecular grade water Sodium chloride Tryptone Glycerol Agarose Carbenicillin Kanamycin PageRuler™ Plus pre-stained ladder HisPur Ni-NTA resin	Fisher Scientific Ireland, Suite 3, Plaza 212, Blanchardstown Corporate Park 2, Ballycoolin, Dublin 15, Ireland.

SureBlue™ TMB microwell peroxidase substrate	Insight Biotechnology Ltd., PO Box 520, Wembley, Middlesex, HA9 7YN, UK.
T4 DNA ligase Antarctic phosphatase Restriction enzymes Nfo (Endonuclease IV)	Brennan and Company, Unit 61, Birch Ave, Stillorgan Industrial Park, Stillorgan, Co. Dublin, Ireland.

2.3 DNA Polymerases, Reverse Transcriptases and RNAse Inhibitors

Polymerase	Supplier
MyTaq™ Red Mix	Medical Supply Co. Ltd., Damastown, Mulhuddart, Dublin 15, Ireland.
Maxima H Minus Reverse Transcriptase Ribolock RNAse Inhibitor	Fisher Scientific Ireland, Suite 3, Plaza 212, Blanchardstown Corporate Park 2, Ballycoolin, Dublin 15, Ireland.

2.4 Commercial Kits

Kit	Supplier
PCRD Nucleic Acid Lateral Flow Immunoassay Cassette	Abingdon Health Ltd, National Innovation Campus, Sand Hutton, York, UK.
SuperScript First-Strand Synthesis Kit	Bio-sciences, 3 Charlemont Terrace, Crofton Road, Dun Laoghaire, Co Dublin, Ireland.
NucleoSpin® Plasmid Purification Kit NucleoSpin® Gel and PCR Clean-up Kit	Fisher Scientific Ireland, Suite 3, Plaza 212, Blanchardstown Corporate Park 2, Ballycoolin, Dublin 15, Ireland.
Pierce™ BCA Assay Kit	Thermo Scientific, 12-16 Sedgeway Business Park, Witchford, Cambridgeshire CB6 2HY, UK.
TwistAmp® Basic Kit	TwistDx Limited, Abbott House Vanwall Business Park, Vanwall Road, Maidenhead SL6 4XE, UK.

2.5 Commercially Sourced Antibodies

Antibody	Supplier
Peroxidase-labelled rat anti-HA (cat. no. 12013819001) Peroxidase-labelled goat anti-rabbit IgG (cat. no. 1101M6251) Peroxidase-labelled goat anti-mouse IgG (whole molecule) (cat. no. A8924) Goat anti-mouse IgG Fc (cat. no. M4280)	Sigma-Aldrich Ireland Limited, Vale Road, Arklow, Wicklow, Ireland.
Peroxidase-labelled rabbit anti-mouse IgG (H+L) (cat. no. A16166)	Fisher Scientific Ireland, Suite 3, Plaza 212, Blanchardstown Corporate Park 2, Ballycoolin, Dublin 15, Ireland.
Peroxidase-labelled alpaca anti-chicken IgY (VHH) (cat. no. ab191865) Peroxidase-labelled goat anti-chicken IgY (H +L) (cat no. ab6877)	Abcam, 330 Cambridge Science Park, Cambridge, CB4 0FL, UK.
Rabbit anti-$PVY^{O/C/N}$ antibody (cat. no. 1130-01)	Neogen Europe, The Dairy School, Auchincruive, Ayr, KA6 5HU, Scotland, UK.

2.6 Media, Media Additives and Antibiotics

2.6.1 Media

Media	Component	Composition
Super Broth (SB) (1L)	MOPS Tryptone Yeast Extract	10g 30g 20g pH 7.0
Luria-Bertani Broth (LB) (1L)	Tryptone Yeast Extract NaCl	10g 5g 10g pH 7.0
LB Agar (1L)	LB Media Agar	1L 15g
Terrific Broth Salts (10X)	KH_2PO_4 K_2HPO_4	0.17M 0.72M
Terrific Broth Base (1L)	Tryptone Yeast Extract Glycerol	12g 24g 5mL
Terrific Broth (TB) (1L)	TB Base TB Salts	900mL 100mL

2.6.2 Media additives

Media Components	Component	Composition
$MgSO_4$	$MgSO_4$	1M
505 (100X)	Glycerol Glucose	50% (v/v) 5% (w/v)

IPTG	IPTG	1M

2.6.3 Antibiotics

Reagent	Composition
Carbenicillin	100mg/mL in mol. grade H_2O
Kanamycin	60mg/mL in mol. grade H_2O
Tetracycline	5mg/mL in 100% (v/v) EtOH

2.7 Buffers

2.7.1 General buffers

Buffer	Component	Composition
Phosphate Buffered Saline (PBS) (1L)	NaCl KCL Na_2HPO_4 KH_2PO_4	137mM 2.7mM 12mM 1.2mM pH 7.4
PBS Tween	PBS Tween20	1X 0.05% (v/v)
Milk Block	PBS Powdered milk	1X 5% (w/v)
BSA Block	PBS BSA	1X 3% (w/v)
Saturated ammonium sulphate solution	$(NH_4)_2SO_4$	4.06M at 20°C

2.7.2 Sodium dodecyl sulphate polyacrylamide gel electrophoresis (SDS-PAGE) and Western Blot (WB) buffers and gel recipes

Buffer	Component	Composition
10X Electrophoresis Buffer (1L)	Tris Glycine SDS	50mM 196mM 0.1% (w/v) pH 8.3
12.5% Separation Gel (2 Gels)	1M Tris HCl, pH 8.8 30% (v/v) Acrylagel 2% (v/v) Bis-Acrylagel Mol. Grade H_2O 10% (w/v) SDS 10% (w/v) APS TEMED	3ml 5ml 2ml 1.87ml 60µL 60µL 12µL
4.5% Stacking Gel (2 gels)	1M Tris HCl, pH 6.8 30% (v/v) Acrylagel 2% (v/v) Bis-Acrylagel Mol. Grade H_2O 10% (w/v) SDS 10% (w/v) APS TEMED	600µL 750µL 300µL 3.5ml 48µL 48µL 5µL
Commercial Running Buffer	MOPS 20X (Expedeon; Abcam)	1X
Commercial Pre-Cast Gels	Bis-Tris Precast Gels (12%; RunBlue™; Expendeon)	N/A

2.7.3 His-tagged protein purification buffers

Buffer	Component	Composition
Sonication/Equilibration Buffer (1L)	NaH_2PO_4 NaCl Imidazole	50mM 300mM 10mM pH 8.0
Wash Buffer 20mM Imidazole (1L)	NaH_2PO_4 NaCl Imidazole	50mM 300mM 20mM pH 8.0
Wash Buffer 30mM Imidazole (1L)	NaH_2PO_4 NaCl Imidazole	50mM 300mM 30mM pH 8.0
Wash Buffer 50mM Imidazole (1L)	NaH_2PO_4 NaCl Imidazole	50mM 300mM 50mM pH 8.0
Wash Buffer 80mM Imidazole (1L)	NaH_2PO_4 NaCl Imidazole	50mM 300mM 80mM pH 8.0
Elution Buffer – 300mM Imidazole (1L)	NaH_2PO_4 NaCl Imidazole	50mM 300mM 300mM pH 8.0

2.8 Bacterial Strains

Name	Supplier
XL1-Blue *E. coli*	Agilent Technologies Ireland Ltd., Euro House, Euro Business Park, Little Island, Cork, Ireland.
Top10F' *E. coli* BL21(DE3)	Biosciences Ltd., 3 Charlemont Terrace, Crofton Road, Dun Laoghaire, Dublin, Ireland.

2.9 Commercially Sourced Peptides and DNA Fragments

Protein/Peptide	Supplier
PVY-BSA Peptide (GNDTIDAGGSTKKDAKQEQGC) Genparts	GenScript Biotech(Netherlands)B.V. BioPartner Building 4, Robert Boyweleg 4 2333 CG, Leiden, Netherlands.

2.10 General Techniques

2.10.1 Agarose gel electrophoresis

Agarose was weighed out to give the required percentage agarose gel (e.g. 1%, w/v). The weighed agarose was added to an appropriate volume of 1X Tris Acetate-EDTA (TAE) buffer in a conical flask and microwaved until the agarose was dissolved. The dissolved agarose was allowed to cool before the addition of SYBR™ Safe stain at a 1:10,000 dilution.

The gel was mixed gently before being poured into a gel box. A comb was added, and the gel left to solidify. Once solidified, the comb was removed and the DNA samples and ladder were loaded. Electrophoresis was performed using a Bio-Rad PowerPac™ system. Samples were run in 1X TAE buffer at 90V-100V until the desired resolution was achieved. Gels were visualised using a Bio-Rad Gel Doc™ EZ Imager.

2.10.2 Ethanol-precipitation of DNA

Ethanol precipitation is used for the concentration of DNA samples or for exchange of the buffer in which the DNA is stored. Ethanol precipitation was achieved by the addition of sodium acetate (3M, pH 5.5) at $1/10^{th}$ the volume and 100% (v/v) ethanol at 2-3X the volume of the sample to be precipitated. DNA precipitation was performed either at -20°C overnight or -80°C for 2 h. After precipitating, DNA was centrifuged at 19,500 x *g* (Hermle Z233M-2) for 20-30 min at 4°C. The supernatant was poured off and cold 70% (v/v) ethanol was carefully added to the DNA pellet. This removes excess salts and chelators from the sample. The pellet was washed for 5-10 min by centrifugation at 4°C and 19,500 x *g* (Hermle Z233M-2). After this, the supernatant was removed, and the pellet allowed to air-dry. Once completely dry, the DNA pellet was re-suspended in the desired volume of mol. grade H_2O.

2.10.3 Purification of DNA

After resolving on an agarose gel, the desired DNA band was excised from the gel using a scalpel and weighed. Purification of DNA was performed using a NucleoSpin® Gel and PCR Clean-up kit as per the manufacturer's instructions. The DNA was eluted with mol. grade H_2O and quantified using the NanoDrop™ 1000.

2.10.4 NanoDrop™1000 DNA, RNA and protein quantification

The NanoDrop™ 1000 uses spectrophotometric methods to determine the concentration of protein, RNA or DNA in a given sample. The NanoDrop™ 1000 was initialised by first loading a sample of mol. grade H_2O onto the pedestal. The NanoDrop™ 1000 was then blanked using the relevant sample buffer. DNA and RNA are read at 260nm while protein is read at 280nm. The sample of interest was added to the pedestal and the concentration read at the correct wavelength. The pedestal was blotted clean between each sample reading.

2.10.5 Sodium dodecyl sulphate-polyacrylamide gel electrophoresis (SDS-PAGE)

SDS coats proteins in a negative charge and facilitates denaturation of secondary and non-disulphide type tertiary linkages. The quantity of SDS which binds to a protein is proportionate the molecular mass of the protein, causing different migration patterns of proteins based on molecular weight. Separation gels (12.5%) and stacking gels (4.5%) were prepared according to recipe in *Section 2.7.2*. The 12.5% gel was added to the glass plates first and isopropanol was carefully pipetted on top of this to remove any bubbles. Once the separation gel had polymerised, the stacking gel was added, and a comb inserted to form sample wells. Upon setting of the stacking gel, the glass plates were inserted into the electrophoresis chamber and the chamber filled with 1X electrophoresis buffer. The samples to be run on the gel were combined with 4X loading buffer and heated to 95°C for 5 min. Samples were allowed to cool prior to loading to the wells. One well was dedicated to PageRuler™ Plus pre-stained protein ladder. Alternatively, samples were loaded into commercially available pre-cast gels and the requisite pre-cast running buffer used. The samples were run at 120-130V until the tracking dye reached the bottom of the gels. The gels were removed from the apparatus and placed in Instant Blue™ stain for at least 1 h and up to O/N prior to visualisation using a Bio-Rad Gel Doc™ EZ imager. Background staining of the gel could be reduced by washing with H_2O.

2.10.6 Western blotting

Western blotting is a molecular technique which allows for the identification of specific protein(s) from a sample which may contain a mix of various proteins, e.g. plant, cellular, or tissue extract. Following the running of the sample of interest in SDS-PAGE, the gel was extracted from the glass plates and soaked in transfer buffer. A nitrocellulose membrane and two sheets of extra thick botting paper were soaked separately in transfer buffer. The gel was placed on top of the nitrocellulose membrane and these were sandwiched between the two sheets of blotting paper. A Pierce™ G2 Fast Blotter was run at the system pre-defined mixed range voltage setting to transfer proteins from the gel onto the nitrocellulose. Blocking, primary antibody and secondary antibody probing steps were performed either for 1 h on a rocker at room temperature (RT), or O/N at 4°C. The membranes were generally blocked with 5% (w/v) powdered milk. Thereafter, the membrane was washed 3X with PBS-T (0.05%, v/v) and 3X with PBS. An appropriate primary antibody was prepared at the required dilution in 1% (w/v) block and applied to the membrane. The membrane was

washed as previously described. If required, a secondary HRP-labelled antibody was prepared in the same manner as the primary antibody and applied to the membrane at the recommended dilution. The membrane was washed as before and subsequently the substrate, precipitating 3,3',5,5'- tetramethylbenzidine (TMB) was added. This forms an insoluble precipitate upon reacting with the HRP-label and allows clear visualisation of protein bands by means of a purple colour change on the membrane.

2.10.7 Bacterial stocks

Appropriate media (e.g. SB, LB) containing the relevant antibiotic (e.g. carbenicillin, kanamycin) was inoculated with either a single colony or bacterial glycerol stock of the clone to be stocked. This was grown O/N at 37°C at 220rpm. The following morning, the cells were pelleted by centrifugation at 3,220 x *g* (Eppendorf 5810R) for 10-15 min at 4°C. The supernatant was poured off and the pellet resuspended in media. Glycerol (80% v/v) was added to the cells and stocks were stored long-term at -80°C.

2.10.8 Sonication of bacterial cells

Bacterial cells were pelleted through centrifugation at 3,220 x *g* (Eppendorf 5810R) for 15-20 min at 4°C. The pellets were resuspended in ~10mL sonication buffer (*Section 2.7.3*) per 1-2g of pellet. Sonication was performed on ice under the following conditions; 40% amplitude, 3 sec on, 2 sec off for 2 min. Post sonication, the samples were centrifuged at 15,600 x *g* (Eppendorf 5804R) for 10-20 min at 4°C. The fractions were collected and stored appropriately for further use.

2.10.9 Freeze-thaw lysis of cells

Cells were resuspended in an appropriate buffer, e.g. PBS, and placed at -80°C until frozen. Following this, the cells were thawed rapidly at 37°C. This process was repeated a further two times to ensure thorough lysis. If necessary, sonication at 40% amplitude for 1 min (3 sec on, 2 sec off) was applied after freeze-thaw to shear released DNA. The cellular debris was pelleted by centrifugation at 11,000-15,600 x *g* (Eppendorf 5804R) for 10-20 min at 4°C and the requisite fractions reserved for use.

2.10.10 Optimisation of recombinant protein expression

The exact nature of the optimisation is dependent on the protein being expressed and is detailed in the relevant results chapters, however, some optimisations are considered standard routes of investigation. Isopropyl β-D-1-thiogalactopyranoside (IPTG), induction temperature, timepoint analysis or media composition are some of the main parameters assessed in expression optimisation. Media (5-10mL) containing the relevant antibiotic, was inoculated with a single colony or glycerol stock of the clone of interest. This was grown O/N at 37°C at 220rpm. The following morning, the cells were sub-cultured into a relevant media, containing the requisite antibiotic and 1x505 (50% glycerol (v/v) and 5% glucose (w/v)) and 1mM $MgSO_4$, if required. Cells were grown to an optical density $(O.D)_{600}$ of 0.4-0.8. To optimise IPTG concentration, IPTG was added at varying concentrations to induce individual cultures. If induction temperature was investigated, the concentration of IPTG was fixed and clones were induced O/N at 220rpm at varying temperatures (e.g. 25°C, 30°C). For timepoint analysis, cultures were pelleted for 10 min at 3,220 x *g* (Eppendorf 5810R) after given time of expression, e.g. 1 h, 2 h post-induction. For media optimisation, cells were subcultured into, and expressed in, the media to be investigated. The next day, samples were centrifuged at 3,220 x *g* (Eppendorf 5810R) for 10 min. The supernatant was discarded and the pellets resuspended in PBS. Cells were lysed through three rounds of freeze thaws, cycling from -80°C for 20 min to 37°C. The cellular debris was pelleted by centrifugation at 11,000 x *g* (Eppendorf 5804R) for 10-20 min at 4°C. The fractions, i.e. soluble supernatant and insoluble pellet, were collected and used for further analysis in SDS-PAGE, WB or ELISA.

2.10.11 Heat shock transformation

Chemically competent *E. coli* were thawed on ice prior to the addition of 1-5µL of ligation or 5-10ng of DNA to the cells. The two were mixed via gently tapping of the tube and then incubated on ice for 30 min. Heat shock transformation was achieved by the introduction of the cells to a 42°C water bath for 30 sec, followed by an immediate incubation on ice. Thereafter, 250µL of pre-warmed SOC media was added to the cells, and they were allowed to recover incubating at 37°C and 220rpm for 1 h. After this incubation, the cells were plated on agar plates, supplemented with the requisite selective antibiotic, and grown O/N at 37°C.

2.10.12 Concentration and buffer exchange

Vivaspin molecular weight cut-off (MWCO) columns were used to concentrate and buffer exchange samples. In general, a MWCO of one third to one half of the molecular weight of the target protein was used, e.g. for a 25kDa protein, a MWCO of not higher than 10kDa was appropriate. The MWCO column was typically rinsed with PBS three times prior to use. The sample to be concentrated/buffer exchanged was added to the column and centrifuged according to the manufacturers guidelines until the sample was reduced to the desired volume. The column was then topped up with sterile, filtered PBS and centrifuged until the volume was reduced again. This was performed 2-3 times to buffer exchange the samples. On the final concentration, the sample was reduced to the desired volume and was retrieved from the column by pipetting up and down prior to storage at the requisite temperature.

2.11 Construction of Recombinant Antibody Libraries

2.11.1 Generation of immune response

A group of three laying hens were immunised with PVY and *R. commune*-associated antigens, provided by collaborators in Teagasc, in order to generate a significant host immune response. The PVY antigen consisted of a PVY extract containing PVY coat protein (CP) and was prepared from PVY-infected plants. Additionally, a second PVY antigen was implemented, consisting of a PVY-BSA conjugate relating to a previously identified conserved region on the PVY CP (Tian et al., 2014). The *R. commune* antigens were total protein extracts prepared from two *R. commune* isolates, denoted 20.16 and 44.07, which were expected to have similar compositions. Immunisations were prepared with the requisite concentration of antigen in PBS and emulsified with an equal volume of TiterMax® Gold adjuvant. Immunisations were administered at minimum four weeks apart. One chicken was immunised with emulsifications prepared with 140µg PVY extract and 100µg PVY-BSA, followed by one boost prepared with 100µg PVY extract and 70µg PVY-BSA and two subsequent boosts prepared with 20µg PVY extract and 35µg PVY-BSA. A second chicken received an immunisation prepared with 100µg of the two *R. commune* isolate proteins, one following boost prepared with 50µg of each isolate and two subsequent boosts prepared with 25µg of each isolate. A third chicken received a combination of antigens. The first immunisation was prepared with 100µg of the previously described antigens, a following boost prepared with 50µg of each antigen and two further boosts prepared with 20µg PVY extract and 25µg of PVY-BSA and both *R. commune* isolates. The final boost for all

consisted of material prepared with 20µg PVY extract and 25µg of PVY-BSA and the *R. commune* isolates.

2.11.2 Assessment of response to antigens

Sera was used in ELISA analysis to determine the antibody response to the relevant antigens. Nunc MaxiSorp™ 96-well plates were coated with 2µg/mL of either PVY-BSA, PVY extract, *R. commune* 20.16 or *R. commune* 44.07 O/N at 4°C. The plates were blocked with 3% (w/v) BSA for 1 h at 37°C and subsequently washed 3X with PBST (0.05%, v/v) and 3X PBS. Serial dilutions of sera were applied to the appropriately coated wells and incubated at 37°C for 1 h. The plate was washed as before. HRP-labelled anti-chicken IgY (VHH) (100µL/well) was added to the wells and left to incubate at 37°C for 1 h. The plate was washed as before. TMB substrate was applied at 100µL/well and colour allowed to develop. HCL (10%, v/v) was added to the wells at 50µL/well to stop the reaction. The plate was then read using a Tecan Safire2™ plate reader at 450nm.

2.11.3 Extraction and isolation of RNA

In preparation for RNA extraction, tubes were soaked in Virkon™ for 24 h, followed by soaking in 'RNase-free' water and spraying with RnaseZap™ to ensure that no RNases remain. The probe of a homogeniser was subject to the same treatment. Ethanol (70%, v/v) was prepared using 'RNase-free' water in RNase free tubes. This was used to decontaminate a laminar flow hood. The hood was also sprayed down with RnaseZap™ to ensure no RNases remain in the hood. Separate RNA pools were generated from each avian spleen. Spleens were placed into RNase-free tubes and homogenised in 30mL of TriZol® reagent, using the previously sterilised homogeniser. TriZol® contains phenol and guanidine isothiocyanate which solubilises biological material and denatures proteins, without damaging DNA or RNA. TriZol® assists in the maintenance of RNA integrity while disrupting the tissue. The homogenate was then centrifuged at 1,575 x *g* (Sigma Laborzentrifugen Model 2K15) for 10 min at 4°C. The supernatant was removed and added to a fresh tube containing 6mL ice-cold chloroform. This was mixed and incubated at RT for 15 min. The mixture was centrifuged at 15,600 x *g* (Eppendorf 5804R) for 30 min at 4°C. After centrifugation, three phases were visible in the tube. These are protein in the bottom organic layer, DNA in the intermediary layer, and RNA in the upper layer. The upper aqueous phase (RNA) was carefully pipetted off. It is vital to ensure that none of the lipid/protein layer is pipetted

alongside the RNA layer. The aqueous phase was then added to a sterile 'RNase-free' tube containing 15mL of isopropanol, which causes the precipitation of the RNA. This was incubated for 10 min at RT before centrifugation at 15,600 x *g* (Eppendorf 5804R) for 30 min at 4°C. The supernatant was discarded and the RNA pellet was washed using 75% (v/v) ice-cold ethanol. This was centrifuged at 15,600 x *g* (Eppendorf 5804R) for 10 min at 4°C. The supernatant was discarded and the RNA pellet was allowed to air-dry completely before resuspension in molecular grade H_2O. The RNA was quantified on a Nanodrop™ 1000 and then carried forward for cDNA synthesis.

2.11.4 cDNA synthesis

A SuperScript (III) First Strand Synthesis SuperMix kit was used in the conversion of RNA to cDNA. Each RNA pool was treated in separate cDNA synthesis reactions. The components required for cDNA synthesis are detailed in *Table 2.1*.

Table 2.1 Required mastermix for cDNA synthesis from isolated RNA

Mastermix	In 8µL volume
RNA	5µg
Oligo (dT) 50 µM	1µL
Annealing Buffer	1µL
Mol. Grade H_2O	Up to 8µL

The strand synthesis reaction occurred in two stages. In stage 1, RNA is primed at the poly-A tail using Oligo (dT) in the RT mix under the parameters. After this stage, the reaction was paused and the tubes were cooled on ice for 1 min prior to introduction of 10µL of 2X First-Strand Reaction Mix, which contains SuperScript® Reverse Transcriptase (RT), and 2µL of a proprietary Enzyme Mix. The second stage of the reaction is then commenced. The parameters of each stage are listed in *Table 2.2*.

Table 2.2 cDNA synthesis PCR conditions

Stage	Temperature	Time (min)
1	65°C Pause	5
2	50°C 85°C 4°C	50 5 ∞

Upon completion of the reaction, the tubes were placed on ice to cool. Once cooled, the RNA yields were quantified on a NanoDrop™ 1000 and the cDNA aliquoted and stored at -20°C.

2.11.5 Amplification of variable heavy and light chains

CDNA, obtained from reverse transcription of RNA, was used as a template from which the avian heavy and light chain sequences were amplified. Relevant primer sequences for the amplification of avian antibody variable heavy (V_H) and variable light (V_L) chains are shown in *Table 2.3*. All primers used in the following recombinant library construction are also detailed in Barbas *et al.*, (2001).

Table 2.3 Primers for variable domain amplification

Primer		Sequence
V_H	CSCVHo-FL (sense)	5’ – GGT CAG TCC TCT AGA TCT TCC GGC GGT GGT GGC AGC TCC GGT GGT GGC GGT TCC GCC GTG ACG TTG GAC GAG – 3’
	CSCG-B (reverse)	5’ – CTG GCC GGC CTG GCC ACT AGT GGA GGA GAC GAT GAC TTC GGT CC– 3’
V_L	CSCVK (sense)	5’ – GTG GCC CAG GCG GCC CTG ACT CAG CCG TCC TCG GTG TC– 3’
	CKJo-B (reverse)	5’ – GGA AGA TCT AGA GGA CTG ACC TAG GAC GGT CAG G– 3’

The PCR reaction mix employed for the amplification of the antibody chains is described in *Table 2.4*. Deviation from the standard protocols will be cited in the relevant section.

Table 2.4 Variable domain PCR composition

Component	Concentration/Volume in 50µL Reaction
Forward Primer	60pM
Reverse Primer	60pM
MyTaq™ Polymerase Mastermix (2X)	25µL
Template and Mol. Grade H_2O	Up to 50µL

The PCR amplification of the variable heavy and light chains was performed under the parameters in *Table 2.5*.

Table 2.5 PCR conditions for variable domain amplifications

Step and Temperature	Time
Step 1: 94°C	5 min
Step 2: 94°C 56-62°C 72°C	15 sec 15 sec 90 sec } 30 cycles
Step 3: 72°C	10 min
Step 4: 4°C	∞

The success of the chain amplifications was determined by running a PCR sample on a 1% (w/v) agarose gel, alongside a 1kb Hyperladder™. The size of the amplicon was determined by visualisation of the gel in the Bio-Rad Gel Doc™ EZ imager. If the yield was satisfactory, multiple reactions were performed such that a sufficient yield of each chain was obtained for the next step of library construction. For purification of the chains, the DNA samples were run on a 1% (w/v) agarose gel. The chains were excised from the gel and purified thereafter using a NucleoSpin® PCR Clean-Up kit. The DNA was eluted with mol. grade H_2O and quantified on a NanoDrop™ 1000 at 260nm.

2.11.6 Splice by overlap extension-PCR

The purpose of the splice by overlap extension (SOE)-PCR to is anneal the heavy and light chains by the primer-mediated incorporation of a glycine-serine linker $(G_4S)_4$. The reaction primers are shown in *Table 2.6*.

Table 2.6 SOE-PCR primers

Primer	Sequence
CSC-F (sense)	5' – GAG GAG GAG GAG GAG GAG GTG GCC CAG GCG GCC CTG ACT CAG – 3'
CSC-B (reverse)	5' – GAG GAG GAG GAG GAG GAG GAG CTG GCC GGC CTG GCC ACT AGT GGA GG– 3'

Equal ratios of each variable domain were added to the PCR alongside 1.5mM $MgCl_2$. Further reaction components are described in *Table 2.7*. Any deviation is described in the relevant chapter. SOE amplification was performed under the cycle parameters in *Table 2.8.*

Table 2.7 SOE-PCR components

Component	Concentration/Volume in a 50µL Reaction
V_H	10ng
V_L	10ng
Forward Primer	60pM
Reverse Primer	60pM
MyTaq™ Polymerase Reaction Buffer (2x)	25µL
Mol. Grade H_2O	Up to 50µL

Table 2.8 SOE-PCR conditions

Step and Temperature	Time
Step 1: 94°C	5 min
Step 2: 94°C 60-62°C 72°C	15 sec 15 sec 120 sec } 25 cycles
Step 3: 72°C	10min
Step 4: 4°C	∞

SOE product formation was assessed by running a sample of the PCR on a 1% (w/v) agarose gel, alongside a 1kb Hyperladder™, prior to visualisation of the gel in the Bio-Rad Gel Doc™ EZ imager. Upon confirmation of a suitable product, multiple SOE-PCR reactions

were performed, pooled, run on a 1% (w/v) agarose gel and purified using a NucleoSpin® PCR Clean-Up kit until sufficient SOE yield was achieved for the following step in library building. The DNA was eluted in mol. grade H_2O and quantified using a NanoDrop™ 1000 at 260nm.

2.11.7 Restriction digest of the purified SOE-PCR product and pComb3XSS vector

The restriction digest was mediated by the *Sfi*I enzyme in the NEB CutSmart® Buffer, in which *Sfi*I has 100% activity. The restriction digest reaction components are described in *Table 2.9*.

Table 2.9 Composition for SfiI restriction digest of SOE and pComb3XSS vector

Component	Concentration/Volume in 200µL Reaction
SOE Product Digestion	
Purified SOE Product	10µg
*Sfi*I (36U/µg DNA)	360U
CutSmart® Buffer (10X)	20µL
Mol. Grade H_2O	Up to 200µL
pComb3XSS Vector Digestion	
Purified pComb3XSS Vector	20µg
*Sfi*I (6U/µg DNA)	120U
CutSmart® Buffer (10X)	20µL
Mol. Grade H_2O	Up to 200µL

Both restriction digests were incubated for 5 h at 50°C. Thereafter, pComb3XSS vector was treated with Antarctic Phosphatase for 15 min at 37°C prior to deactivation at 70°C for 5 min. Antarctic Phosphatase treatment results in de-phosphorylation at the digested 5' and 3' ends of the vector. This prevent re-circularisation of the plasmid which can interfere with the subsequent ligation of the SOE insert into the vector. The digested SOE and vector were run on 2% and 0.7% (w/v) agarose gels, respectively. The SOE and pComb3XSS were excised from the gels and purified using a NucleoSpin® Gel and PCR Clean-up kit. The purified products were quantified using the NanoDrop™ 1000 at 260nm.

2.11.8 Ligation of digested SOE-PCR product to digested pComb3XSS vector

T4 DNA ligase mediates the ligation of the purified, digested SOE-PCR product into the complementarily digested pComb3XSS phagemid vector. This ligase catalyses the generation of phosphodiester bonds between the juxtaposed 5' phosphate ends and 3' hydroxyl termini, also termed "sticky ends". The reaction mixture (*Table 2.10*) was incubated O/N at RT and subsequently ethanol precipitated (*Section 2.10.2)*. The DNA pellet was resuspended in mol. grade H_2O prior to electroporation into XL1-Blue *E. coli*.

Table 2.10 Composition of SOE and pComb3XSS ligation reaction

Component	Concentration/Volume per 200µL
Digested SOE-PCR Product	700ng
Digestion pComb3XSS Product	1.4µg
T4 Ligase Buffer (10X)	20µL
T4 Ligase	10µL
Mol. Grade H_2O	Up to 200µL

2.11.9 Electroporation of SOE-harbouring pComb3XSS vector into XL1-Blue E. coli

Electroporation cuvettes were chilled at -20°C and subsequently placed on ice. SOC media was warmed to 37°C prior to electroporation. The ligation reaction and XL1-Blue electrocompetent *E. coli* cells were thawed on ice. The ligation reaction was added to an aliquot of XL1-Blue *E. coli* (150µL) and mixed by gentle tapping. The mixture was incubated for 1 min on ice before transferral to the pre-chilled cuvette. Electroporation was performed in a Bio-Rad Micropulser™ Electroporator at 2.5kV. Once electroporation was complete, the cuvette was immediately flushed with 1mL SOC media into a 50mL tube containing 1mL of pre-warmed SOC media. This was performed one further time to make a total of 3mL in the 50mL tube. The cells were allowed to rescue while shaking for 1 h at 37°C and 220rpm. The library size was estimated through titration of the transformed cells. After the incubation, 25µL of rescued cells was added to 225µL of SOC media and serial dilutions were performed. Dilutions were plated on agar plates (100µL/plate) containing 100µg/mL carbenicillin. This allowed for the selection of cells harbouring the pComb3XSS plasmid. The plates were inverted and incubated O/N at 37°C.

The remainder of the rescued cells were centrifuged for 15 min at 3,220 x *g* (Eppendorf 5810R) at 4°C. The supernatant was discarded and the pellet was resuspended in SB. The resuspended cells were subsequently plated onto agar plates (100µL/plate), supplemented with 100µg/mL carbenicillin, to prepare stock plates of the library. Following incubation of the stock plates O/N at 37°C, the cells were scraped into SB using a rubber policeman. These scrapings were combined in a sterile 50mL tube and centrifuged at 3,220 x *g* (Eppendorf 5810R) for 15 min at 4°C. The supernatant was discarded, the pellet resuspended in SB and glycerol (80%, v/v) was added to the bacteria. This was stored at -80°C as an "unpanned" library stock.

2.11.10 Colony-pick PCR

A colony-pick PCR is carried out on single colonies sourced from transformation plates to determine whether the clones selected harboured the scFv insert. The employed primers are the SOE primers i.e. CSC-F and CSC-B. The PCR is performed in a similar manner to the SOE-PCR (Section *2.11.6*).

2.12 Phage-Display and Biopanning of Recombinant Antibody Libraries

2.12.1 Rescue and precipitation of scFv-displaying phage

For round one of screening the prepared antibody library stock (*Section 2.11.9*) was inoculated into 200mL SB media containing 100µg/mL carbenicillin and 10µg/mL tetracycline. This was grown at 37°C and 220rpm until the bacteria achieved logarithmic phase growth, typically when the $O.D_{600}$ reached between 0.4 and 0.7. Helper phage M13K07 (2mL) was added to the culture and incubated statically at 37°C for 20 min. This was followed by a 2 h incubation at 37°C and 220rpm. After this, kanamycin was added to a final concentration of 70µg/mL and the culture was left to incubate overnight at 37°C and 220rpm. An immunotube was coated with 500µL of the appropriate antigen, detailed in the relevant chapter's results. The tube was sealed with parafilm and was stored upright O/N at 4°C. Additionally, XL1-Blue *E. coli* cells were prepared by inoculation of colonies into SB containing 10µg/mL tetracycline. These were grown at 37°C at 220rpm O/N.

The following morning, the O/N XL1-Blue *E. coli* cells were subcultured into fresh SB media, supplemented with 10µg/mL tetracycline. These were left growing at 37°C and 220rpm until an $O.D_{600}$ of 0.4-0.6 was achieved. Concurrently to this, the 200mL phage-

culture from the previous day was pelleted by centrifugation for 10 min at 15,600 x *g* (Eppendorf 5804R) and 4°C. The supernatant was poured into fresh, sterile tubes. Polyethylene Glycol 8000 (PEG 8000) and sodium chloride (NaCl) were added to final concentrations of 4% (w/v) and 3% (w/v), respectively. When the PEG and NaCl were fully dissolved, the tubes were placed at 4°C on ice for 1 h to allow precipitation of the phage particles. After this incubation, the tubes were centrifuged at 15,600 x *g* (Eppendorf 5804R) for 20 min at 4°C, brake off. The supernatant was discarded and the precipitated phage pellets air-dried for at least 5 min prior to resuspension in 1mL sterile filtered PBS. This was labelled as "input phage" and stored at 4°C. For longer term storage, the input phage pool was filtered through a 0.2µm filter and kept at 4°C.

2.12.2 Enrichment of the phage library via biopanning against immobilised antigens

Antigen prepared in the immunotube (*Section 2.12.1*) was poured off and the tube was filled with 5% (w/v) powdered milk block. The tube was sealed with parafilm and incubated at 37°C for 1 h. The block was poured off and the immunotube was washed once with PBS-T (0.05%, v/v) and once with PBS. The "input phage" (500µL), *Section 2.12.1*, was added to the immunotube, which was then sealed tightly with parafilm. This was incubated for 2 h on a roller at RT. After incubation, non-specifically bound phage were washed off through a number of wash steps, with an increased in stringency with each iterative round. Washes are detailed in their relevant results chapters. Elution of antigen-specific phage was achieved through the addition of 500µL of freshly prepared 10mg/mL (w/v) trypsin in PBS to the immunotube. The tube was incubated for 30 min at 37°C. The eluted phage were subject to vigorous pipetting to ensure that all bound phage were removed from the tube. These were stored at 4°C and labelled as "output phage".

2.12.3 Re-infection of phage into XL1-Blue E. coli and library titre

The subcultured XL1-Blue *E. coli* (*Section 2.12.1*), once at an $O.D_{600}$ of 0.4 – 0.6, were used in the re-infection and dilution of the "input" and "output" phage pools. Serial dilutions of the phage-infected *E. coli* were prepared to determine phage input and output values. The remaining output phage pool (~400µL) was re-infected into 4mL of the XL1-Blue *E. coli* in a separate, 50mL tube. This ~4mL culture, the input titre, and the output titres were incubated stationary at 37°C for 30 min. The input/output titres were plated on agar plates containing 100µg/mL carbenicillin. Non-infected XL1-Blue *E. coli* was plated in the same fashion, as

a control. These were incubated O/N at 37°C. The ~4mL infected culture was centrifuged at 3,220 x g (Eppendorf 5810R) for 10 min at 4°C and the pellet resuspended in 400µL SB. This was plated across agar plates (100µL/plate) to act as library stock plates. These were grown O/N at 37°C. The following day, the stock plates were scraped into SB using a rubber policeman and pelleted by centrifuging for 15 min at 3,220 x g (Eppendorf 5810R) and 4°C. The pellet was resuspended in SB and acted as a new "panned" library stock. Panning protocols outlined in *Sections 2.12.1 - 2.12.3*, inclusive, were repeated several times, with subsequent rounds being performed using a smaller phage culture volume of 100mL.

2.12.4 Polyclonal phage ELISA

In order to monitor enrichment for antigen-positive scFv in the biopanning process, a polyclonal-phage ELISA was performed. This assay investigates the binding of the polyclonal input phage pools, sourced from each round of panning, to the antigen of interest. A Nunc MaxiSorp™ 96-well plate was coated O/N at 4°C with 100µL/well of antigen at a concentration specified in the results. The following morning, the antigen was discarded and the plate blocked with 200µL/well of 5% (w/v) powdered milk for 1 h at 37°C. The wells were washed 3X with PBS-T (0.05%, v/v) and 3X with PBS. Phage input pools were added to wells at 100µL/well. This was incubated for 1 h at 37°C and washed as before. A HRP-labelled anti-HA secondary antibody was prepared in 1% (w/v) block and 100µL/well was added. The plate was then incubated for 1 h at 37°C. Washing was performed as before. TMB substrate (100µL/well) was added and colour allowed to develop, after which the reaction was stopped using 50µL/well of 10% (v/v) HCl. The absorbance was read at 450nm on a Tecan Safire2™ plate reader.

2.13 Screening for Antigen-Binding Clones

2.13.1 Soluble monoclonal ELISA analysis

Monoclonal ELISA was used to determine the antibody response of single clones against the antigen of interest. SB media (150µL), supplemented with 100µg/mL carbenicillin, was added to wells of a sterile 96-well plate. Single colonies sourced from agar plates, e.g. rounds of panning or transformation plates, were picked and placed into the individual wells of the 96-well plate. The single colonies were grown O/N at 37°C and 220rpm. The following morning, the clones were subcultured into new sterile 96-well plates containing 150µL/well fresh SB media, supplemented with 100µg/mL carbenicillin, 1X 505 and 1mM $MgSO_4$.

Glycerol (80%, v/v) was added to the wells of the original O/N plate to prepare stocks, this plate was stored at -80°C. The subcultured plate was grown at 37°C and 220rpm for 4-6 h, after which, IPTG was added to a final concentration of 1mM and the plate incubated shaking at 220rpm and 30°C O/N. The following day, cells were subjected to three rounds of freeze thaws; freezing at -80°C followed by thawing at 37°C. Cell debris was pelleted via centrifugation at 2,750 x *g* (Eppendorf 5810R) for 10 min at 4°C and the lysate used in monoclonal ELISA analysis.

Antigen (100µL/well) was coated to a Nunc MaxiSorp™ 96-well plate O/N at 4°C. The antigen, specified in the results, was discarded and the wells were blocked with 200µL/well of 5% (w/v) powdered milk for 1 h at 37°C. The wells were then washed 3X with PBS-T (0.05%, v/v) and 3X with PBS. Lysates (100µL/well) were added and the plate was incubated for 1 h at 37°C. The plate was washed as before. Thereafter, 100µL/well of anti-HA HRP-labelled secondary antibody in 1% (w/v) block was added and incubated for 1 h at 37°C. The plate was washed as before. To develop the plate, 100µL/well of TMB substrate was added and colour allowed to develop out of sunlight prior to the addition of 50µL/well of 10% (v/v) HCl to stop the reaction. The plate well absorbance was then determined at 450nm using a Tecan Safire2™ plate reader.

2.13.2 Lysate titre of responsive clones

ScFv which showed positive binding to the antigen of interest in monoclonal ELISA analysis were subjected to a lysate titre to further assess antigen specificity. The clones of interest were grown O/N in 5-10mL SB supplemented with 100µg/mL carbenicillin and at 37°C and 220rpm. The following morning, the clones were subcultured into 5-10ml SB, supplemented with 100 ug/mL carbenicillin, 1X 505 and 1mM $MgSO_4$. They were grown for 4-6 h, after which, IPTG was added at a final concentration of 1mM. The clones were left to grow O/N at 30°C, 220rpm. The following morning, the cultures were centrifuged for 10-15 min at 3,220 x *g* (Eppendorf 5810R) at 4°C. The supernatant was discarded and the pellets were resuspended in PBS. The cells were subjected to three rounds of freeze-thaws: freezing at -80°C following by thawing at 37°C. Post freeze-thaw, the cells were spun at 11,000 x *g* (Eppendorf 5804R) for 10 min to pellet debris. The resulting lysates were analysed in a titration to determine binding.

Antigen (100µL/well) was coated to a Nunc MaxiSorp™ 96-well plate O/N at 4°C. The antigen was discarded and the wells blocked with 200µL/well of 5% (w/v) powdered milk for 1 h at 37°C. The wells were then washed 3X with PBS-T (0.05%, v/v) and 3X with PBS. Dilutions were performed on the lysates and 100µL/well of each dilution was added and incubated for 1 h at 37°C. The plate was washed as before. Thereafter, an anti- HA HRP-labelled antibody was added (100µL/well) in 1% (w/v) block and incubated for 1 h at 37°C. The plate was washed as before. Subsequently, 100µL/well of TMB substrate was added and allowed to develop out of sunlight and with gentle agitation. This was followed by the addition of 50µL/well of 10% (v/v) HCl to stop the reaction. The absorbance of the plate wells was analysed at 450nm using a Tecan Safire2™ plate reader.

2.13.3 Competitive ELISA analysis of lysate

ScFv-enriched lysates were prepared as per *Section 2.13.2*. Antigen (100µL/well) was coated onto a Nunc MaxiSorp™ 96-well plate O/N at 4°C. The antigen was discarded and the wells were blocked with 200µL/well of 5% (w/v) powdered milk for 1 h at 37°C. The wells were washed 3X with PBS-T (0.05%, v/v) and 3X with PBS. Free antigen was prepared at various concentrations, specified in the results chapters. This was combined with an equal volume of scFv-enriched lysate, prepared at a fixed dilution, to a combined final volume of 100µL/well. These were added to the wells and incubated for 1 h at 37°C. The plate was washed as before. Secondary antibody probing and subsequent analysis was performed as per *Section 2.13.2*.

2.14 Construction, Expression and Purification of Recombinant PVY Coat Protein

2.14.1 Amplification of coat protein genes

Initial coat protein (CP) cloning was performed as described in Folwarczna *et al.*, (2008) and Jeevalatha *et al.*, (2013), however, the resulting inserts were found to be out of frame and unsuited to expression from the pET-26b(+) vector. New primers were designed and used to amplify the CP gene from cDNA and plasmids. This workflow is described below. Primers to amplify the PVY CP genes of PVY^{O} and PVY^{NTN} strains were designed based on the sequence of Irish isolates of the strains (Della Bartola, Byrne, and Mullins, 2020). The primers, shown in *Table 2.11*, were designed to incorporate *Nco*I and *Hind*III restriction sites for future cloning experiments.

Table 2.11 CP amplification primers

Primer	Sequence
O- Forward	5’ – GAATCCATGGGAAACGATACAATTGATGCAGG– 3’
O- Reverse	5’ – GAATAAGCTTCATGTTCTTCACTCCAAGTAGAGT– 3’
N- Forward	5’ – GAATCCATGGGAAATGATACAATTGATGCAGG– 3’
N- Reverse	5’ – GAATAAGCTTCATGTTCTTAACTCCAAGTAGAGT– 3’

The genes were amplified as per the composition and reaction conditions shown in *Tables 2.12 and 2.13,* respectively.

Table 2.12 PCR composition for CP amplification

Component	Concentration/Volume in a 50µL Reaction
Forward Primer	60pM
Reverse Primer	60pM
MyTaq™ Polymerase Reaction Buffer (2x)	25µL
Mol. Grade H_2O	Up to 50µL

Table 2.13 Reaction conditions for CP amplification

Step and Temperature	Time
Step 1: 94°C	5 min
Step 2: 94°C 56°C 72°C	30 sec 30 sec 60 sec } 30 cycles
Step 3: 72°C	10 min
Step 4: 4°C	∞

The results of the amplification were analysed by running a PCR sample on agarose gels, alongside a 1kb Hyperladder™. The size of the amplicon was determined by visualisation of the gel in the Bio-Rad Gel Doc™ EZ imager. The PVY^{O} and PVY^{NTN} amplicons were gel purified separately. This was achieved by excising the PCR products from the gel using a scalpel and performing subsequent gel purification using a NucleoSpin® PCR Clean-Up kit. The DNA was eluted in mol. grade H_2O and quantified using a NanoDrop™ 1000 at 260nm.

2.14.2 Restriction digest of CP and pET-26b(+) vector

Both the CPs and the pET-26b(+) vector were subjected to double digests using *Nco*I (NEB) and *Hind*III (NEB) restriction enzymes, as per the manufacturer's instructions. Digests were performed in the NEB CutSmart® buffer, in which both enzymes have 100% activity. The digested CPs and vector were run on agarose gels, excised from the gels and purified separately using a NucleoSpin® Gel and PCR Clean-up kit. Elution of DNA products was performed in mol. grade H_2O. The purified products were quantified using the NanoDrop™ 1000 at 260nm.

2.14.3 Ligation of digested CP and pET-26b(+)

T4 DNA ligase (NEB) was employed to facilitate the joining of the complementarily digested CPs and pET-26b(+) vector, as per the manufacturer's instructions. The enzyme was inactivated at 65°C for 10 min before the reaction was transformed into chemically competent cells. Ligated plasmids were transformed by heat shock as per *Section 2.10.11* and expressed in BL21(DE3) *E. coli* cells.

2.14.4 Optimisation of CP expression

Timepoint and IPTG optimisations were performed as per *Section 2.10.10*. Expression of the CPs was performed in LB media supplemented with 60µg/mL kanamycin.

2.14.5 Large-scale CP expression

Cultures of CP were grown O/N in LB supplemented with 60µg/mL kanamycin at 37°C and 220rpm. The following morning, flasks containing 400mL LB media and 60µg/mL kanamycin were inoculated with the overnight culture and grown at 37°C and 220rpm until an $O.D_{600}$ of around 0.6-0.8 was achieved. Thereafter, IPTG, at the optimised concentration, was added and the culture left to express O/N at 25°C and 220rpm. The following day, the cells were harvested via centrifugation at 3,220 x *g* (Eppendorf 5810R) for 15 min. For IMAC purification, the resulting pellets were resuspended in lysis/sonication buffer (*Section 2.7.3)* and sonicated as described in *Section 2.10.8*, or subjected to freeze-thaw lysis and one minute sonication at 40% (3 sec on/2 sec off) as per *Section 2.10.9*. The lysed cells were centrifuged at 15,600 x *g* (Eppendorf 5804R) for 15 min at 4°C. The resulting lysate was filtered through a 0.2µm filter and used for purification.

2.14.6 Immobilised metal affinity chromatography (IMAC) purification of CP

IMAC purification buffers are detailed in *Section 2.7.3.* Approximately 2mL Ni^2-NTA resin slurry was applied to the column, allowed to settle and the storage buffer drained. Thereafter, the resin was equilibrated by flowing through 10mL of equilibration buffer. The lysate was applied to the column and flowed through twice. The column was then washed several times with 10mL of IMAC wash buffers containing either 30mM, 50mM, or 80mM imidazole. Elution was performed with ~6mL of a 300mM imidazole-containing elution buffer. The elution was concentrated and buffer-exchanged against sterile filtered PBS as per *Section 2.10.12*. The purified protein sample was aliquoted and stored at -20°C. Purified protein was quantified via densitometry in ImageJ. The 'flow-through', wash and elution fractions were analysed via SDS-PAGE and Western blot as described in *Sections 2.10.5* and *2.10.6*.

2.15 Recombinant Antibody Fragment Expression and Purification

2.15.1 Large-scale recombinant antibody expression

Optimisation of scFv expression was carried out as per *Section 2.10.10.* Once identified, the optimum conditions were utilised for subsequent antibody expression experiments. An O/N culture of the antibody to be expressed was prepared via the inoculation of the clone of interest into SB media, containing 100µg/mL carbenicillin. This was grown O/N at 37°C and 220rpm. The following day, flasks containing 200-400mL SB, 100µg/mL carbenicillin, 1mM $MgSO_4$, and any additional required supplements, e.g. 1X 505, were inoculated with the O/N culture. This was grown at 37°C and 220rpm until an $O.D_{600}$ of 0.4-0.8 was achieved. The culture was then induced with the pre-determined optimum concentration of IPTG and grown O/N at the optimum induction temperature at 220rpm. The following morning, the culture was centrifuged at 3,220 x *g* (Eppendorf 5810R). The cell pellet was resuspended in sonication buffer, ~20-30mL, and sonicated as described in *Section 2.10.8* or subjected to freeze-thaw lysis and one min sonication at 40% (3 sec on 2 sec off) as per *2.10.9*. Once lysed, the cells were centrifuged at 15,600 x *g* (Eppendorf 5804R) for 15-20 min at 4°C. The lysate (supernatant) was then filtered through a 0.2µm filter and used in purification protocols.

2.15.2 Purification of His-tagged recombinant antibodies by IMAC

IMAC purification buffers are detailed in *Section 2.7.3.* Ni^2-NTA resin slurry (~2mL) was applied to the column and allowed to settle before the storage buffer was allowed to flow

through. The column was equilibrated with 10mL of equilibration buffer. Once equilibrated, the lysate was applied to the column and flowed through. This flow-through was re-applied to the column a further time. The column was first washed with 10mL of 20mM imidazole buffer. Thereafter, a second wash consisting of 10mL of 30mM imidazole buffer was applied to the column. Elution was performed with 6mL of elution buffer containing 300mM imidazole. The elution was concentrated and buffer-exchanged against sterile filtered PBS (*Section 2.10.12*). The purified protein sample was aliquoted and stored at -20°C. The purification fractions were analysed via SDS-PAGE and Western blot as described in *Sections 2.10.5* and *2.10.6*.

2.16 Monoclonal Antibody Expression and Purification

2.16.1 Hybridoma cell culture

Anti-PVY hybridomas were generated and provided by Dr. Hui Ma (DCU). Cell lines were retrieved from LN_2 and thawed at 37°C. The cells were added to 20-30mL pre-warmed DMEM supplemented with Briclone, 4500mg/L glucose and 10% (v/v) FBS and centrifuged at 230 x *g* (Sigma Laborzentrifugen Model 2K15) for 5 min. The media was poured off and the cell pellet resuspended in pre-warmed media. The resuspended cells were then added to flasks containing additional pre-warmed media to a final volume of 25mL. Hybridomas were grown until roughly 80-90% confluency was achieved, at which stage, the cells were scraped from the flask into the media using a rubber policeman. An equal volume of fresh media, composition as previously described, was added directly to the resuspended cells and the resulting cell suspension split across fresh flasks. Hybridoma lines were propagated in this manner until purification, at which stage the IgG-enriched media was retrieved and any hybridoma cells present in the media were pelleted by centrifugation at 3,220 x *g* (Eppendorf 5810R) for 15 min. The supernatant (media) was decanted into Vivaspin MWCO concentrating columns and concentrated to a workable volume for gravity-flow column purification (e.g. 25-50mL).

2.16.2 Protein G affinity purification

Protein G resin (~2mL slurry) was equilibrated with 10mL PBS. Thereafter, the resin was removed from the column and incubated with the IgG-enriched media on a roller for 1 h at RT. The resin and bound IgG was reapplied to the column after this incubation and the resin allowed to settle. The media was flowed through and subsequent wash steps consisting of

two washes with 10mL PBS each were performed. Finally, bound IgG was eluted with 10mL of 100mM glycine buffer (pH 2.7) into a tube containing 1mL of 1M tris-HCl (pH 8.5) to permit immediate neutralisation of the elution fraction and return the purified IgG to physiological pH. The flow through, washes and elution were retained for analysis in SDS-PAGE and WB (*Sections 2.10.5* and *2.10.6*). The elution fraction was concentrated and buffer exchanged into PBS as per *Section 2.10.12.*

2.17 Characterisation of Purified Antibodies in ELISA

2.17.1 Indirect ELISA

Antigen (100µL/well) was coated to the wells of a Nunc MaxiSorp™ 96-well plate O/N at 4°C. The antigen is detailed in the relevant section. The antigen was discarded and the plate blocked with 5% (w/v) powdered milk (200µL/well) for 1 h at 37°C. The wells were washed 3X with PBS-T (0.05%, v/v) and 3X with PBS. Purified antibody (100µL/well) was prepared in 1% (w/v) block and added to the wells. The plate was washed as before. For secondary antibody detection, the antibody used was dependant on the purified antibody tested. For example, HA-tagged recombinant clones could be detected with a HRP-labelled anti-HA secondary antibody, while monoclonal or polyclonal antibodies could be detected with a HRP-labelled anti-species antibody. The employed secondary antibody is detailed in the relevant results section. The secondary antibody was applied to the wells (100µL/well) in 1% (w/v) block and incubated at 37°C for 1 h. The plate was washed as before. Subsequently, 100µL/well of TMB substrate was added and allowed to develop out of sunlight under gentle agitation. This was followed by the addition of 50µL/well of 10% (v/v) HCl to stop the reaction. The plate wells were then analysed using a Tecan Safire2™ plate reader at 450nm.

2.17.2 Competitive ELISA

Antigen (100µL/well) was coated to the wells of a Nunc MaxiSorp™ 96-well plate O/N at 4 °C. The antigen is detailed in the relevant section. The antigen was discarded and the plate blocked with 200µL/well of 5% (w/v) powdered milk for 1 h at 37°C before washing 3X with PBS-T (0.05%, v/v) and 3X with PBS. Free antigen was prepared in PBS at a range of concentrations, the concentration range of the antigen is detailed in the relevant results section. Purified antibody was prepared in 1% (w/v) block at a fixed dilution. The chosen dilution factor is typically determined by the results of an antibody titre. If feasible, the dilution which results in an absorbance@450nm of ~1.0 is typically chosen. Antigen (50µL)

and antibody (50µL) were mixed in a 1:1 ratio and applied to the wells for a final volume of 100µL/well. Subsequent secondary antibody probing and analysis was performed as per *Section 2.17.1.*

2.18 Surface Plasmon Resonance Kinetic Analysis of Antibodies

HBS was employed as the running buffer for all Biacore kinetics analysis.

2.18.1 Functionalisation of CM5 sensor chip

Amine coupling was performed to immobilise biomolecules, e.g. capture antibody, to the surface of the CM5 sensor chip. An underivatized chip was docked to a Biacore X100 system. Functionalisation of the chip was performed at a flow rate of 10µL/min. A 1:1 ratio of 0.4M EDC and 0.1M NHS was mixed directly prior to functionalisation. The EDC/NHS mixture was passed over the chip surface for 240 sec, activating the surface. Thereafter, the biomolecule to be immobilised, diluted in 10mM sodium acetate (pH 5), was passed over the chip until the desired response units (RUs) were immobilised. For a capture antibody chip, a response of ~5,000RUs was considered satisfactory. After immobilisation, active sites on the chip were capped by flowing over 1M ethanolamine-HCl (pH 8.5) for 240 sec. After capping, three 12 sec washes of 20mM NaOH were performed. The chip was then functionalised and ready for use.

2.18.2 Kinetic analysis of 11B2 mAb

Multicycle kinetics on a Biacore X100 were utilised for the kinetic characterisation of the 11B2 mAb. In this form of kinetics, the mAb was captured, antigen (CP) flowed over the surface, binding measured and the chip regenerated, stripping away any bound 11B2 mAb or antigen. This process was performed for each concentration assessed in the kinetics run. The analysis was performed using a capture approach. To permit this, both flow cells of a CM5 sensor chip were functionalised with an anti-mouse Fc antibody (*Section 2.18.1*). Flow cell 2 acted as the assay surface while flow cell 1 acted as a reference cell. The 11B2 mAb was diluted 1 in 2,000 in running buffer (HBS). Antigen was prepared in HBS at a range of concentrations, specified in the relevant results section. The mAb was passed over flow cell 2 of the sensor the chip for 50 sec and allowed stabilise for 480 sec. Thereafter, antigen was passed over the surface of both flow cells and allowed to associate for 180 sec at a flow rate of 30µL/min. Dissociation was monitored for 700 sec. Then the entire surface was

regenerated for 40 sec with 20mM NaOH with a following stabilisation period of 30 sec. A 0µg/mL CP concentration (HBS) was included as a blank reference and any response from this concentration was subtracted from the dataset. Any signal arising from the reference flow cell was also subtracted from the dataset. The data obtained was globally fit to a 1:1 Langmuir binding model.

2.18.3 Kinetic analysis of 11B2 scAb

Multicycle kinetics on a Biacore X100 were utilised for kinetic characterisation of the 11B2 scAb in a similar manner to the mAb, described in *Section 2.18.2*. Both flow cells of a CM5 sensor chip were functionalised with an anti-chicken Fab region antibody (*Section 2.18.1*). Flow cell 2 acted as the assay surface while flow cell 1 acted as a reference cell. The 11B2 scAb was diluted 1 in 10 in running buffer (HBS). Antigen was prepared in HBS at a range of concentrations, specified in the relevant results section. The scAb was passed over flow cell 2 of the sensor the chip for 90 sec and allowed stabilise for 480 sec. The remainder of the protocol was as per *Section 2.18.2*.

2.19 Characterisation of mAbs and scAbs in Dot Blot

Samples were spotted onto a nitrocellulose membrane in 2µL volumes and allowed to dry for 1 h at RT. Both recombinantly expressed CP and crude plant extracts (provided by Teagasc) were used as samples. Details of sample concentration is described in the relevant results chapter. After drying, the blots were blocked O/N at 4°C in 5% (w/v) powdered milk. The following day, blots were washed 3X with PBS-T (0.05%, v/v) and 3X with PBS. For mAb analysis, the mAb was applied at a final dilution of 1 in 20,000 in 1% (w/v) block in PBS-T (0.05%, v/v) and incubated with the membrane for 1 h at RT on a rocker. For scAb analysis the scAb was diluted 1 in 100 in 1% (w/v) block in PBS and applied for 1 h at RT. The mAb control blot was incubated with 1% (w/v) block in PBS-T (0.05%, v/v) while the scAb control blot was incubated with 1% (w/v) block in PBS. The blots were washed as before, prior to the application of an anti-mouse H+L HRP-labelled secondary antibody in 1% (w/v) block in PBS-T (0.05%, v/v) for 1 h at RT on a rocker for mAb detection, or anti-HA-HRP in 1% (w/v) block for 1 h at RT for scAb detection. After a final wash, the blots were developed using precipitating TMB substrate.

2.20 Biacore-Based Immunosensor Development

Analysis was performed on a Biacore X100 system. HBS was the employed running buffer for all Biacore sensing assays. The entire surface of a CM5 sensor chip was functionalised with an anti-mouse Fc antibody as per *Section 2.18.1*. Flow cell 2 acted as the assay surface while flow cell 1 acted as a reference cell. For binding analysis, the 11B2 mAb was diluted 1 in 2,000 in HBS and injected over the chip surface for 25 sec and stabilised for 60 sec. Various antigen concentrations were prepared in HBS, detailed in the relevant results section. Each concentration was injected over the chip surface for 180 sec and allowed a dissociation period of 60 sec. Binding of the antigen to the antibody was measured. The chip surface was regenerated in between each concentration tested with a 30 sec wash of 20mM NaOH and a following stabilisation of 30 sec. The values obtained from the reference flow cell and from a 0µg/mL CP antigen concentration (HBS) were subtracted from the dataset. RU values were recorded based on the stability reading, i.e. antigen remaining captured after injection, to account for any potential sample-buffer induced systemic effects.

2.21 Generation of a Recombinase Polymerase Amplification Assay

2.21.1 Primer and template design

Recombinase polymerase amplification (RPA) primers were designed by aligning the CP sequences (Genbank Accessions: MT264731, MT264732, MT264733, MT264734, MT264735, MT264736, MT264737, MT264738) from various Irish PVY isolates in Clustal. Preliminary sequence data was provided by colleagues in Teagasc (Oak Park) and was later published in Bartola, Byrne and Mullins, (2020). The alignment was manually scanned for regions roughly 30 nucleotides in length which contained high sequence similarity across all strains. The selections were further restricted to pairs of regions which would produce amplicons of ~150bp as this is suggested as an optimal amplicon size for later application to lateral flow analysis (Safenkova et al., 2020). The selected primers were assessed in BLAST for any potential cross-reactivity with other potato viruses, including potato virus X, potato virus A, potato virus S and potato leaf roll virus. Ultimately, three primers sets were chosen, shown in *Table 2.14*.

Table 2.14 PVY-specific RPA primers

Primer	Sequence
RPA1 - Forward	5’ – GTTTGGTGCATTGAAAATGGAACCTCGCCAAA– 3’
RPA1 - Reverse	5’ – AACATCTGAGAAATGTGCCATGATTTGCCTAA– 3’
RPA2 - Forward	5’ – TGAGGTCACATCACGAACACCAGTGAGGGCTA– 3’
RPA2 - Reverse	5’ – TCCTCGGTGGTGTGCCTCTCTGTGTTCTCCTC– 3’
RPA3 - Forward	5’ – CCAAACATCAACGGAGTTTGGGTTATGATGGA– 3’
RPA3 - Reverse	5’ – GTTGCGCATTTCTATATACGCTTCTGCAACAT– 3’

Gene fragments, corresponding to CP regions of common potato viruses PVY (communication with Teagasc, Oak Park), PVA (accession no. KF152953) and PVX (accession no. D00344) were synthesised by Genscript to act as DNA templates in RPA reactions. The sequences of each are displayed in *Table 2.15*. In addition to these templates, primers suitable for the amplification of PVA and PVX were identified in the literature and acquired, these sequences are shown in *Table 2.16*.

Table 2.15 CP gene templates

Virus	Sequence
PVY	GGAAACGATACAATTGATGCAGGAGGAAGCAGCAAGAAAGATGCAAGAC CAGAGCAAGGCAGCATCCAGTCAAACCCGAACAAAGGCAAAGATAAGGA TGTTAATGCTGGCACATCTGGGACACATACTGTGCCGAGAATCAAGGCTA TCACGTCCAAGATGAGAATGCCCAAAAGCAAGGGAGCAACCGTGCTAAA CTTAGAACATTTGCTTGAGTATGCTCCACAACAAATTGATATTTCAAATAC TCGGGCAACTCAATCACAGTTTGATACGTGGTATGAGGCAGTGCGGATGG CATACGACATAGGAGAAACTGAGATGCCAACTGTGATGAATGGGCTTATG GTTTGGTGCATTGAAAATGGAACCTCGCCAAATGTCAACGGAGTTTGGGT TATGATGGATGGGAATGAACAAGTTGAGTACCCGTTGAAACCAATCGTTG AGAATGCAAAACCAACCCTTAGGCAAATCATGGCACATTTCTCAGATGTT GCAGAAGCGTATATAGAAATGCGCAACAAAAAGGAACCATATATGCCAC GATATGGTTTAATTCGAAATCTGCGGGATGTGGGTTTAGCGCGTTATGCCT TTGACTTTTATGAGGTCACATCACGAACACCAGTGAGGGCTAGGGAAGCG CACATTCAAATGAAGGCCGCAGCATTGAAATCAGCCCAACCTCGACTTTT CGGGTTGGACGGTGGCATCAGTACACAAGAGGAGAACACAGAGAGGCAC ACCACCGAGGATGTCTCTCCAAGTATGCATACTCTACTTGGAGTGAAGAA CATG
PVX	ATGTCAGCACCAGCTAGCACAACACAGGCCACAGGGTCAACTACCTCAAC TACCACGAAAACTGCAGGCGCAACTCCTGCCACAGCTTCAGGCCTGTTCA CCATCCCGGATGGGGATTTCTTTAGTACAGCTCGTGCCATAGTAGCCAGC AATGCTGTCGCAACAAATGAGGACCTCAGCAAGATTGAGGCTATTTGGAA GGACATGAAGGTGCCCACAGACACTATGGCACAGGCTGCTTGGGACTTAG TCAGACACTGTGCTGATGTGGGATCATCTGCTCAAACAGAAATGATAGAT ACAGGTCCTTATTCCAACGGCATCAGCAGAGCTAGACTGGCAGCAGCAAT CAAAGAGGTGTGCACACTTAGGCAATTTTGCATGAAGTATGCTCCAGTGG TATGGAACTGGATGTTAACTAACAACAGTCCACCTGCTAACTGGCAAGCA CAAGGTTTCAAGCCTGAGCACAAATTCGCTGCATTCGACTTCTTCAATGG AGTCACCAACCCAGCTGCCATCATGCCCAAAGAGGGGCTCATCCGGCCAC CGTCTGAAGCTGAAATGAATGCTGCCCAAACTGCTGCTTTTGTGAAGATT ACAAAGGCCAGGGCACAATCCAACGACTTTGCCAGCCTAGATGCAGCTGT CACTCGAGGTCGTATCACTGGAACAACAACCGCTGAGGCTGTTGTCACTC TACCACCACCATAA
PVA	GCCGGAACTCTTGATGCAAGCGAAACACTAGCGCAGAAATCTGAAGGTA GGAAGAAAGAAGGAGAAAGCAACAGTAGCAAAGCTGTAGCCGTGAAGG ACAAAGATGTCGATTTAGGTACTGCTGGGACTCATTCAGTACCACGCTTA AAATCAATGACATCAAAACTGACACTACCAATGCTCAAAGGTAAGAGTGT CGTTAACCTAGATCACTTGCTATCTTACAAACCAAAGCAAGTAGACTTGT CAAATGCTAGAGCCACCCACGAACAATTCCAAAACTGGTATGATGGCGTT ATGGCAAGTTATGAGTTAGAGGAATCAAGCATGGAGATCATTCTAAATGG TTTCATGGTATGGTGCATTGAGAATGGAACCTCTCCAGACATTAATGGAG TTTGGACCATGATGGATAATGAGGAACAAGTGTCATATCCATTAAAACCC ATGCTTGACCATGCAAAGCCTTCTTTAAGGCAAATTATGAGACATTTCAG CGCACTCGCAGAGGCGTACATTGAGATGAGAAGTCGTGAGAAACCATAC ATGCCCAGGTATGGTCTTCAACGCAACCTGAGAGATCAAAGTTTGGCAAG GTATGCTTTTGATTTCTATGAGATCACTGCAACCACTCCGATCAGAGCCAA AGAGGCGCATCTGCAGATGAAAGCAGCAGCGCTGAAGAATTCGAACACT AATATGTTTGGACTGGACGGAAATGTCACAACTTCAGAAGAGGACACAG AAAGGCACACAGCAACGGATGTTAATCGCAACATGCATCACCTTTTAGGC GTGAAGGGGGTGTGA

Table 2.16 Primers for PVX and PVA virus-specific detection

Primer	Sequence	Ref.
PVX – Forward	5' – AAGCCTGAGCACAAATTCGC– 3'	(Agindotan, Shiel, and Berger, 2007)
PVX – Reverse	5' – GCTTCAGACGGTGGCCG– 3'	
PVA – Forward	5' – TGTCGATTTAGGTACTGCTGGGAC– 3'	
PVA – Reverse	5' – TGCTTTGGTTTGTAAGATAGCAAGTG– 3'	

2.21.2 Assessment of template and primer functionality in conventional PCR

A standard PCR was performed to ensure that all primer sets were functional with their corresponding gene fragment template. The composition of the PCRs are described in *Table 2.17*. The reactions were prepared and 10^6 copies DNA template added prior to PCR being performed as per the conditions listed in *Table 2.18*. Gene copy numbers were calculated using online resource Science Primer (http://www.scienceprimer.com/copy-number-calculator-for-realtime-pcr).

Table 2.17 Reaction composition for PVY, PVA and PVX amplifications

Component	Concentration/Volume in a 50µL Reaction
Forward Primer	0.2µM
Reverse Primer	0.2µM
MyTaq™ Red Mix (2x)	25µL
$MgCl_2$	1.5mM
Template and Mol. Grade H_2O	Up to 50µL

Table 2.18 Conditions for the amplification of the PVY, PVA and PVX templates

Step and Temperature	Time
Step 1: 94°C	5 min
Step 2: 94°C 52°C;68°C (PVA and PVX;PVY) 72°C	30 sec 30 sec 30 sec } 25 cycles
Step 3: 72°C	10 min
Step 4: 4°C	∞

2.21.3 Analysis of primer-specificity in conventional PCR

In order to confirm that the primers were specific to PVY, they were used alongside the PVX and PVA templates in conventional PCR. The reaction composition is shown in *Table 2.19*. The reactions were prepared and 10^6 copies DNA template added prior to PCR being performed, as per the conditions listed in *Table 2.20*.

Table 2.19 Composition of RPA primer specificity analysis in PCR

Component	Concentration/Volume in a 50µL Reaction
Forward Primer	0.2µM
Reverse Primer	0.2µM
MyTaq™ Red Mix (2x)	25µL
$MgCl_2$	1.5mM
Template and Mol. Grade H_2O	Up to 50µL

Table 2.20 Conditions for specificity analysis of RPA primers in PCR

Step and Temperature	Time
Step 1: 94°C	5 min
Step 2: 94°C 68°C 72°C	30 sec 30 sec 30 sec } 25 cycles
Step 3: 72°C	10 min
Step 4: 4°C	∞

2.21.4 Recombinase polymerase assay

RPA reactions were performed using the TwistAmp® Basic RPA kit. The reaction components are outlined in *Table 2.21*. This is the recommended reaction composition and conditions provided by TwistDx, and any deviation from this is described in the relevant results section. The mixture in *Table 2.21* was then added to a lyophilised TwistAmp® Basic reaction pellet to dissolve the pellet. Thereafter, 2.5µL of 280mM magnesium acetate (MgOAc) was pipetted into the lid of the tube and 1µL template added. The RPA reaction was initiated through brief centrifugation of the tubes in a microcentrifuge to facilitate introduction of the MgOAc. The reaction mixture was incubated for 20 min at 39°C.

Typically, reactions were manually mixed 4 min into the 20 min incubation. After incubation, the RPA reactions were either cleaned-up using a NucleoSpin® Gel and PCR Clean-up kit or by heating the products to 65°C for 10 min. After RPA, samples were run on agarose gels for analysis.

Table 2.21 Composition of RPA reagents

Component	Concentration/Volume in a 46.5µL Reaction
Forward Primer	480nM
Reverse Primer	480nM
'Primer-free' Rehydration Buffer	29.5µL
Mol. Grade H_2O	Up to 46.5µL

2.22 Development of a Nucleic Acid Lateral Flow Immunoassay

2.22.1 Primer screening in NALFIA format

To facilitate the development of a nucleic acid lateral flow immunoassay (NALFIA), primers were labelled with Biotin and FITC (FAM). As the target DNA is amplified, it is dual-labelled by Biotin and FAM. The labels on the amplicon then act as antigens to be captured in lateral flow, permitting visual detection of nucleic acids.

Table 2.22 Dual-labelled NALFIA primers

Primer	Sequence
RPA2LF-F	5' – 6-FAM/ TGAGGTCACATCACGAACACCAGTGAGGGCTA– 3'
RPA2LF-R	5' – Biotin/ TCCTCGGTGGTGTGCCTCTCTGTGTTCTCCTC– 3'
RPA3LF-F	5' – 6-FAM/CCAAACATCAACGGAGTTTGGGTTATGATGGA – 3'
RPA3LF-R	5' – Biotin/GTTGCGCATTTCTATATACGCTTCTGCAACAT -3'

The initial RPA reaction for NALFIA detection was performed as per *Section 2.21.4*. After incubation, the RPA products were analysed using a PCRD™ nucleic acid lateral flow-based detection cassette, as per the manufacturer's instructions, Briefly, 6µL of the RPA product was mixed with 84µL of the PCRD extraction buffer and 75µL of this sample was then loaded to the sample application well of the lateral flow cassette. The results were recorded after 10 min and any result after 10 min was not counted. A positive result was considered one in which both the test line and control line presented colour development. A negative

result was one where only the control line showed colour development. Any tests in which no colour formation was observed at the control line were discounted.

2.22.2 Optimisation of primer concentration in dual-labelled primer NALFIA

To optimise the primer concentration, RPA and lateral flow analyses were performed as per *Section 2.22.1*, with the deviation that primer concentrations were varied between 100nM-360nM.

2.22.3 Design of RPA probe

The RPA probe was designed as per the TwistDx recommendations and the sequence selected based on a regions of homology across PVY strains located internally on the relevant amplicon. Furthermore, the probe was designed to have no overlap with either the forward or reverse primers. The sequence of the probe is detailed below in *Table 2.23*. This oligonucleotide features a 5' 6-FAM antigenic label (FITC), an internal tetrahydrofuran residue (THF; abasic site) and a 3' C-3 spacer. Also detailed in *Table 2.23* are the RPA3 primer pairs. The primary alteration to these primers was the removal of the antigenic label from the forward primer. The reverse primer remained unchanged.

Table 2.23 Summary of RPA primers and probe

Primer/Probe	Sequence
RPA3LF-Forward	5'– CCAAACATCAACGGAGTTTGGGTTATGATGGA – 3'
RPA3LF-Reverse	5'– Biotin/GTTGCGCATTTCTATATACGCTTCTGCAACAT -3'
RPA Probe	5' – 6-FAM/ TGAAACCAATCGTTGAGAATGCAAAACCAAC /THF/ CTTAGGCAAATCATG /C-3 Spacer – 3'

2.22.4 Primer and probe-based RPA and NALFIA

RPA utilising the probe was performed as per the manufacturer's recommendations. The reaction components for probe-based RPA are listed in *Table 2.24*. The remaining amplification protocol and lateral flow analysis was performed as previously described per *Section 2.22.1*.

Table 2.24 Composition of primer and probe RPA of PVY

Component	Concentration/Volume in a 46.5µL Reaction
Forward Primer	420nM
Reverse Primer	420nM
Probe	120nM
Nfo	10U
'Primer-free' Rehydration Buffer	29.5µL
Mol. Grade H_2O	Up to 46.5µL

2.22.5 Specificity of primer and probe-based RPA and NALFIA

Specificity analysis was as per *Section 2.22.4* using DNA from PVA, PVLR and healthy plants as template in lieu of PVY.

2.22.6 Sensitivity of primer and probe-based RPA and NALFIA

To determine the sensitivity of the assay, a series of dilutions were performed on the PVY DNA template. The dilutions series consisted of gene copies ranging from 10^4 gene copies to 1 gene copy. The RPA reactions for each dilution were performed as per *Section 2.22.4*.

2.23 Design of a One-Step Reverse Transcription-NALFIA

2.23.1 Reverse-transcription RPA and NALFIA

PVY is a single stranded RNA virus, therefore, transcription of viral RNA into double stranded cDNA is required for RPA functionality. To facilitate this, reverse-transcription RPA (RT-RPA) was employed. The reaction components for the RT-RPA are shown in *Table 2.25*. The template consisted of total RNA extracted from a PVY-infected plant or total RNA prepared from a healthy plant (provided by Teagasc, Oak Park). The procedures for amplification and lateral flow analysis remain otherwise unchanged from *Section 2.22.4*.

Table 2.25 Composition of RT-RPA reaction

Component	Concentration/Volume in a 46.5µL Reaction
Forward primer	420nM
Reverse Primer	420nM
Probe	120nM
Nfo	10U
Maxima H Minus RT	200U
RiboLock RNAse Inhibitor	20U
'Primer-free' Rehydration Buffer	29.5µL
Mol. Grade H_2O	Up to 46.5µL

2.23.2 Sensitivity of RT- RPA and NALFIA

The sensitivity of the assay was determined by performing a series of dilutions on the RNA template, and specific concentrations are provided in the relevant results. The RT-RPA and NALFIA analyses for each dilution tested were performed in as per *Section 2.23.1*.

2.24 Isolation of Polyclonal Antibody

IgY (polyclonal antibody; pAb) was isolated from serum by ammonium sulphate precipitation. Ammonium sulphate solution 80% (w/v) was prepared fresh from a saturated ammonium sulphate solution. This was added dropwise to the serum to a final concentration of 40% under gentle mixing. This solution was incubated at RT for 3 h and subsequently centrifuged at 3,220 x *g* (Eppendorf 5810R) for 30 min at 4°C. The resulting pellet was resuspended in mol. grade H_2O in a volume equal to that of the original sample. Similar precipitations were performed twice more. Thereafter, the sample was desalted and buffer exchanged into PBS using a MWCO column (*Section 2.10.12)*. The resulting pAb concentration was quantified using a Pierce™ BCA kit, as per the manufacturer's instructions.

2.25 Analysis of pAb Binding in ELISA

2.25.1 Checkerboard analysis of pAb by indirect ELISA

A range of antigen concentrations (1-10µg/mL; 100µL/well) were coated to the wells of a Nunc MaxiSorp™ 96-well plate O/N at 4°C. The antigen was discarded and the plate blocked with 200µL/well of 5% (w/v) powdered milk for 1 h at 37°C. The wells were washed

3X with PBS-T (0.05%, v/v) and 3X with PBS. Serial dilutions of the pAb in 1% (w/v) block were applied to the wells (100µL/well) and incubated for 1 h at 37°C. The wells were washed as before. Bound pAb was detected via an anti-IgY (VHH) antibody diluted in 1% (w/v) block. The wells were washed as before and the substrate TMB added (100µL/well). This was allowed develop out of sunlight under gentle agitation. The reaction was stopped by the addition of 50µL/well of 10% (v/v) HCl and the well absorbances read at 450nM on a Tecan Safire2™ plate reader.

2.25.2 Analysis of pAb by indirect ELISA

Indirect analysis of pAb binding was performed as per *Section 2.25.1,* with the exception that the antigen and antibody concentrations were fixed. Additionally, a HRP-labelled anti-IgY H+L was alternatively employed as the secondary antibody.

2.26 Dot Blot Analysis of an Anti-*R. commune* pAb

Various concentrations of antigen, specified in the relevant results section, were blotted in 2µL spots onto a nitrocellulose membrane. These were allowed to dry for 1 h at RT prior to blocking of the membrane in 5% (w/v) powdered milk O/N at 4°C. The following morning, the blots were washed 3X with PBS-T (0.05%, v/v) and 3X with PBS. Thereafter, the pAb was applied in 1% (w/v) block and incubated with the membrane for 1 h at RT under gentle agitation. The blot was washed as before and a secondary HRP-labelled anti-IgY H+L antibody was applied in 1% (w/v) block for 1 h at RT under gentle agitation. The blot was washed once more as previously described and colour development permitted via the addition of TMB.

Chapter 3

Generation and Screening of a Recombinant Antibody Library for the Development of Anti-PVY ScFv

3.1 Introduction

Recombinant antibody fragments offer numerous advantages over traditional "whole antibodies". These include their rapid generation times, low cost of production and their amenability to genetic engineering which allows tailoring of the antibody for specific attributes. Recombinant antibodies are generated through genetic manipulation and cloning of the various antibody genes, with the variable regions being of paramount relevance for retention of antigen-binding. Following this, the requisite genes are cloned into suitable expression vectors prior to production in host organisms (Hoogenboom, 2005). Overall, this means that recombinant antibodies, once generated, can be produced continuously, rapidly, at high yields and in economic hosts. Furthermore, the act of recombinant expression from vectors permits tagging of the expressed protein, facilitating rapid purification on affinity purification columns and subsequent detection of the relevant tag in various assays such as ELISA or immunoblotting. There are multiple formats of recombinant antibody, for example dAb, scFv, scAb, Fab, with each having their own benefits. ScAb and Fab formats contain constant regions which can provide additional stability *in vivo* while scFvs are quicker to generate due to their comparatively smaller size. Furthermore, scFv antibodies consist of a single polypeptide, suggesting that they are suited to expression in *E. coli* as they do not require the folding of two separate proteins (Frenzel, Hust, and Schirrmann, 2013). For these reasons, it was decided to commence with the generation of a recombinant scFv library for the purpose of isolating anti-PVY antibodies.

A recombinant scFv antibody library is constructed by first cloning the heavy and light chains of the antibody from a suitable source, for example a cDNA pool. The two chains are then annealed via a splice-overlap extension (SOE)-PCR which also incorporates a glycine-serine linker to endow flexibility to the resulting antibody construct once expressed in the designated host. Upon generation and isolation of the requisite SOE product, it is cloned into a phagemid vector. In this work the employed vector was pComb3XSS (Andris-Widhopf et al., 2000). The pComb3XSS vector supports both the soluble expression of the scFv proteins and the assembly of the scFv-displaying phage particles. These antibody-displaying phage particles play an intrinsic role in the method by which antigen-specific antibodies are isolated from recombinant antibody libraries, termed biopanning (Winter et al., 1994). The scFv-containing vector is then transformed into a suitable host, for example *E. coli*, and the library is considered assembled at this stage. In this work, aves (chickens) were selected as hosts from which to generate recombinant antibody libraries. Aves are a suitable source from

which to isolate antibody genes as avian immunoglobulin diversity is generated primarily through gene conversion, rather than multiple recombination events, as is the case for murine and leporine repertoire diversification (Dias da Silva and Tambourgi, 2010). As a result of this reduced avian germ-line diversity, fewer primer pairs are required in order to facilitate equal amplification of all heavy chain and light chain antibody genes. This can lead to better overall immune repertoire representation in the subsequent avian recombinant antibody library when compared to murine- or leporine-based libraries where representation of the full repertoire is often limited by failed, biased or incomplete chain amplifications (Lee et al., 2017). The construction of such recombinant libraries yields a pool of thousands to millions of antibody clones, each with various antigen specificities. In order to develop, isolate and characterise pathogen-specific antibodies from these libraries, and to develop related immunoassays, a target is required.

The requisite target is often a distinct protein, but may be a lipid, sugar, chemical or other molecule. Regardless of origin, of key importance is that the target is produced by, or is specifically associated with, the pathogen to be detected. The selected antigen should allow accurate and confident detection and quantification of the pathogen of interest. With regards to PVY, the coat protein (CP) offers a promising target for several reasons. Firstly, it permits broad-spectrum PVY detection due to the presence of several regions of conserved amino acid (AA) homology in the polypeptide sequence across both parental and recombinant strains of PVY. This is highlighted by the alignment of several coat protein sequences in *Figure 3.1* which illustrates extensive regions of conserved AAs. This alignment was generated from CP-coding regions of Irish PVY isolates, sequenced by Bartola, Byrne and Mullins (2020). The observed conservation across several CP regions permits the opportunity for a wide-reaching detection approach which should allow the indiscriminate detection of the PVY serotypes, N and O, using a single antibody (Van der Vlugt, Leunissen, and Goldbach, 1993; Crosslin, 2013; Glais, Bellstedt, and Lacomme, 2017). This manner of broad-spectrum detection is applicable for PVY as the presence of any strain of the virus is deemed unfavourable by growers, importers, and exporters of potatoes and seed potatoes. The ability to detect the presence of multiple strains within one assay reduces testing duration, data analysis and other associated costs, making it a favourable approach in immunodiagnostics. Finally, during the packaging of the virus, thousands of copies of the CP are produced, making this an essential and abundant target protein as the virus begins

replication (Kežar et al., 2019). For these reasons, the CP was employed as the antigen of interest when attempting to develop immunoassays for the detection of PVY.

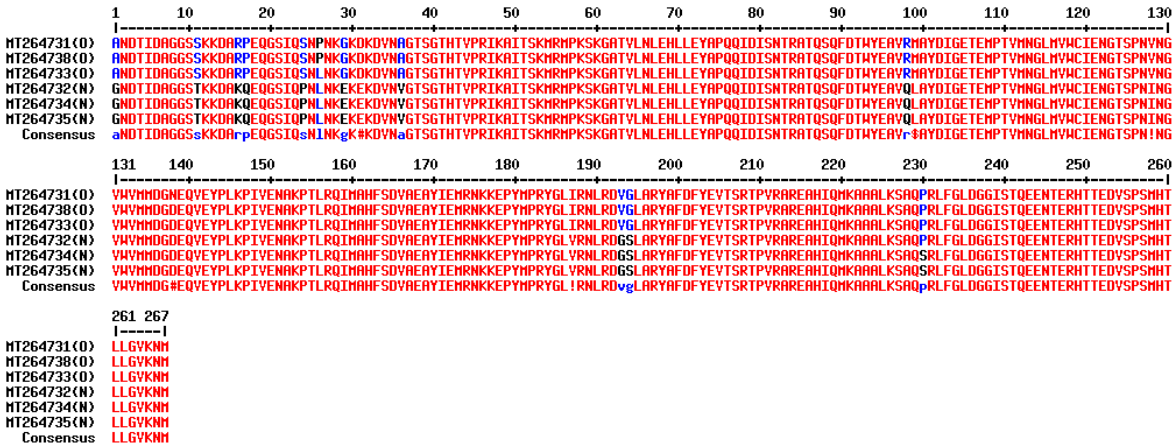

Figure 3.1 Alignment of the amino acid sequence from the CPs of PVY strains

Amino acid sequences were sourced from their denoted Genbank ID and aligned in Multalin. The relevant serotype for the strain is listed after each accession number. It should be noted that serotype O may also be described as serotype O/C.

Ideally, a relatively high concentration of antigen should be readily available throughout the library screening and characterisation processes. Recombinant protein technology is a widely used technique which facilitates the rapid production of proteins through DNA cloning methods. These proteins may be expressed from a range of hosts, where the host organism does not necessarily need to be associated with the recombinant protein. For example, many eukaryotic proteins are recombinantly expressed in prokaryotic cells (Rosano and Ceccarelli, 2014b). *E.coli* is one of the most popular host cells for the production of small proteins. This expression host can rapidly produce high yields of the desired protein. This fact, in addition to the low costs and fast turnaround times associated with expression in *E. coli*, makes it an appealing organism for use in recombinant technology (Demain and Vaishnav, 2009). The general workflow of cloning a gene into an expression vector is illustrated in *Figure 3.2*. In this, work, the pET-26b(+) vector was employed for the recombinant expression of the CP. This vector system was selected due to features such as a T7 polymerase and hexahistidine tag. The T7 system is extremely effective at expressing recombinant proteins, with up to 50% of the total cellular protein being comprised of the target protein with a few hours post-induction (Francis and Page, 2010). Additionally, the

6X histidine tag, which is co-expressed attached to the target protein, facilitates rapid protein purification through immobilised metal affinity chromatography.

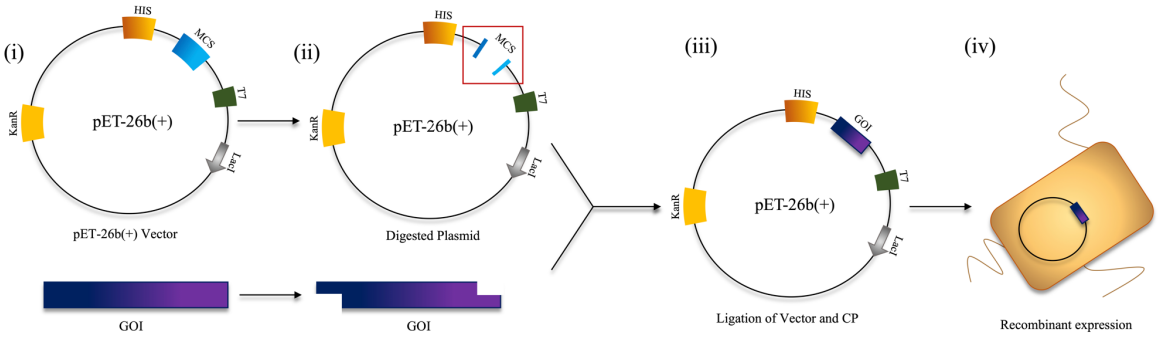

Figure 3.2 Overview of the recombinant protein cloning and expression workflow

(i) *The expression vector and gene of interest (GOI) are selected and isolated.* ***(ii)*** *Restriction enzymes, can be used to digest complementary regions on both the plasmid and the GOI. This leaves 'sticky end' overhangs on both products.* ***(iii)*** *Joining of the plasmids and the GOI is mediated by a ligase which facilitates the incorporation of the gene into the appropriate location on the vector.* ***(iv)*** *The ligated product is transformed into a suitable host, e.g. E. coli, in which the recombinant protein can be expressed (HIS = 6X histidine tag, MCS = multiple cloning site, T7 = T7 promoter, LacI = lac repressor, KanR = kanamycin resistance, GOI = gene of interest).*

It was proposed to utilise the recombinantly expressed form of the CP in a screening campaign with which PVY-specific antibodies could be isolated from a scFv library. The intention was also to employ the CP antigen alongside any anti-PVY scFv candidates resulting from library screening to develop immunoassays for the detection of PVY.

3.2 Results

3.2.1 Generation of a recombinant scFv library

3.2.1.1 Serum response to antigens

A serum antibody titre was employed to monitor the immune response against PVY antigens, a PVY extract and a PVY-associated peptide, which were administered as immunogens to a hen (*Section 2.11.1*). The PVY antigens were coated onto the wells of an ELISA plate and probed with sera prepared in a series of dilutions (*Section 2.11.2*). A "pre-bleed" sample was incorporated in order to act as a comparison against the post-immunisation response. From *Figure 3.3*, it was observed that there was an initial response against the PVY antigens in

the pre-bleed serum at lower dilutions. This response was attributed to background interference caused by the complexity of the serum matrix leading to non-specific signal. The titre points of roughly 1:100 to 1:1,000 for the pre-bleeds act as a further indication that this signal arose from non-specific binding, as opposed to a specific response. An adequate immune response was observed against the PVY extract, with a titre of between 1:100,000 and 1:1,000,000 achieved (*Figure 3.3*). The response of the chicken to the PVY-BSA peptide was lower, with the titre point of between 1:1,000 and 1:10,000 identified. This suggests that the antigen was not as immunogenic as the PVY extract, possibly as a result of the peptides comparatively small size and consequently lower epitope availability. This peptide was not considered a suitable target due to the observed low response.

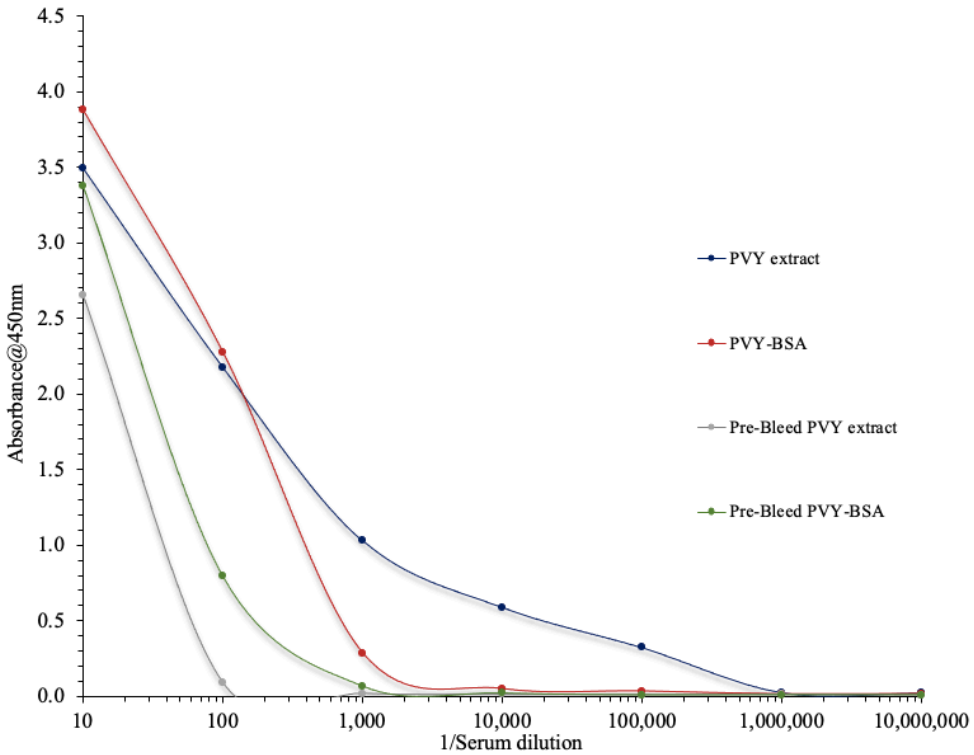

Figure 3.3 Titration of serum antibodies against PVY antigens

Sera were applied in a series of dilutions to the wells of an ELISA plate coated with 2µg/mL PVY extract or PVY-BSA. Bound serum antibodies were detected using a HRP-labelled anti-chicken VHH antibody. The absorbance was then read at 450nm.

3.2.1.2 Isolation and reverse transcription of RNA to cDNA

The spleen from the immunised chicken was homogenised in TriZol® reagent, as per *Section 2.11.3.* The total RNA phase was carefully extracted, ensuring no cross-contamination with

the lipid or protein phases. The resulting RNA-pool was quantified on a Nanodrop™ 1000. A cDNA template was generated from the isolated RNA through the employment of first-strand synthesis reactions, wherein RNA may be converted to cDNA (*Section 2.11.4*). The resulting cDNA pool acts as a template in subsequent PCRs for recombinant library building as Ig heavy and light chains may be isolated from this source.

3.2.1.3 Amplification of variable domains from cDNA

Variable domain-specific PCR primers are employed in order to isolate the requisite variable heavy (V_H) and variable light (V_L) genes. Amplification of these genes is the primary step in the commencement of recombinant antibody library construction. These reactions were performed as per *Section 2.11.5*. From this analysis, it appeared that the V_L genes amplified successfully, as demonstrated by strong bands at the expected size of ~350bp (*Figure 3.4 (i)*). Contrastingly, the V_H genes failed to amplify, evidenced by the lack of signal at the expected product size of ~400bp (*Figure 3.4 (ii)*).

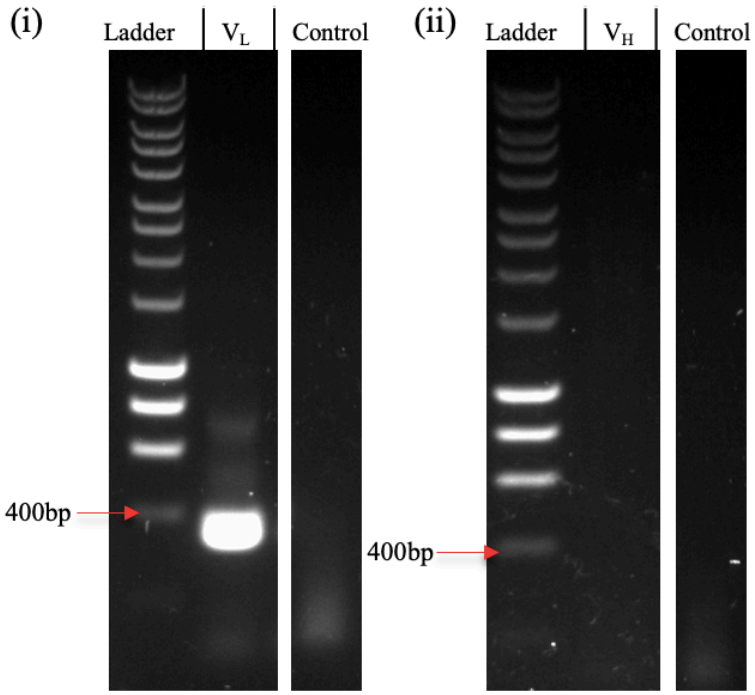

Figure 3.4 Amplification of V_L and V_H domains

(i) *Amplification procedures resulted in the successful amplification of the V_L, as evidenced by a DNA band ~350bp.* ***(ii)*** *No such amplification was observed in the V_H amplification. (Ladder = Hyperladder™ 1 kb, V_L = variable light chain, V_H = variable heavy chain, control = PCR without cDNA template).*

In an attempt to improve the amplification efficiency of the V_H chain, various optimisations were performed. The first optimisation undertaken was to increase the annealing temperature implemented in the reaction from 56°C to 62°C as this affects the binding of the primers to the DNA template. If the annealing temperature is too low, binding will be inefficient, and amplification may be hindered. Based on the result (*Figure 3.5*), the increase in annealing temperature appeared to aid in the amplification of the heavy chain, as a band was now observable at ~400bp. However, the yield was still lower than desired for continuation to the future steps of the scFv library building.

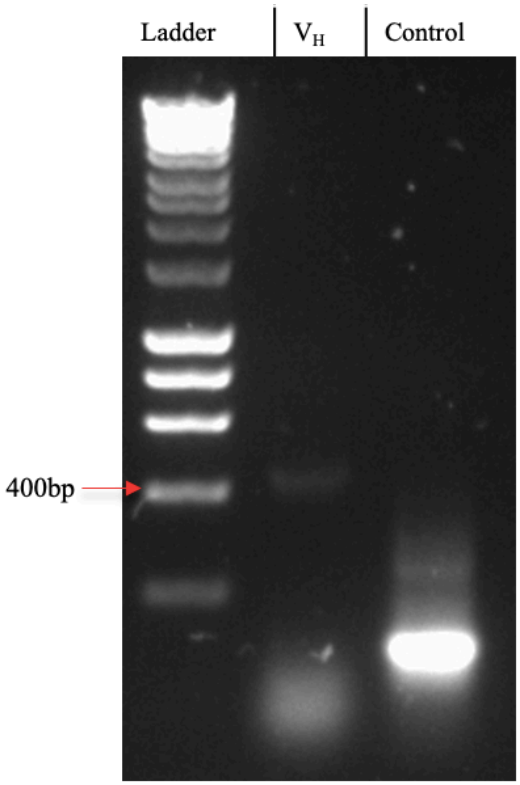

Figure 3.5 Optimisation of annealing temperature for V_H amplification

The increase of annealing temperature from 56℃ to 62℃ yielded improved amplification of the V_H genes (Ladder = Hyperladder™ 1 kb, V_H = variable heavy chain, control = PCR without cDNA template).

In a continued effort to optimise the efficiency of the reaction, the use of a PCR additive, DMSO, was investigated. DMSO assists in the denaturation of double-stranded DNA and can also result in the lowering the T_M of the reaction primers (Lorenz, 2012). The addition of DMSO at a 3% (v/v) concentration proved effective in improving the amplification of the V_H from the cDNA pool (*Figure 3.6 (i)*). In a final optimisation, the reactions were

performed with a fixed concentration of 3% (v/v) DMSO while the concentration of $MgCl_2$ was altered in the range of 0.5mM to 4mM (*Figure 3.6 (ii)*). The supplementation of $MgCl_2$ alters the action of the polymerase to aid in the addition of nucleotides to the template strands which can improve product synthesis rates (Yang et al., 2004; Batra et al., 2006). A concentration of 0.5mM $MgCl_2$ was found to be optimal, producing a specific amplicon at the correct ~400bp size.

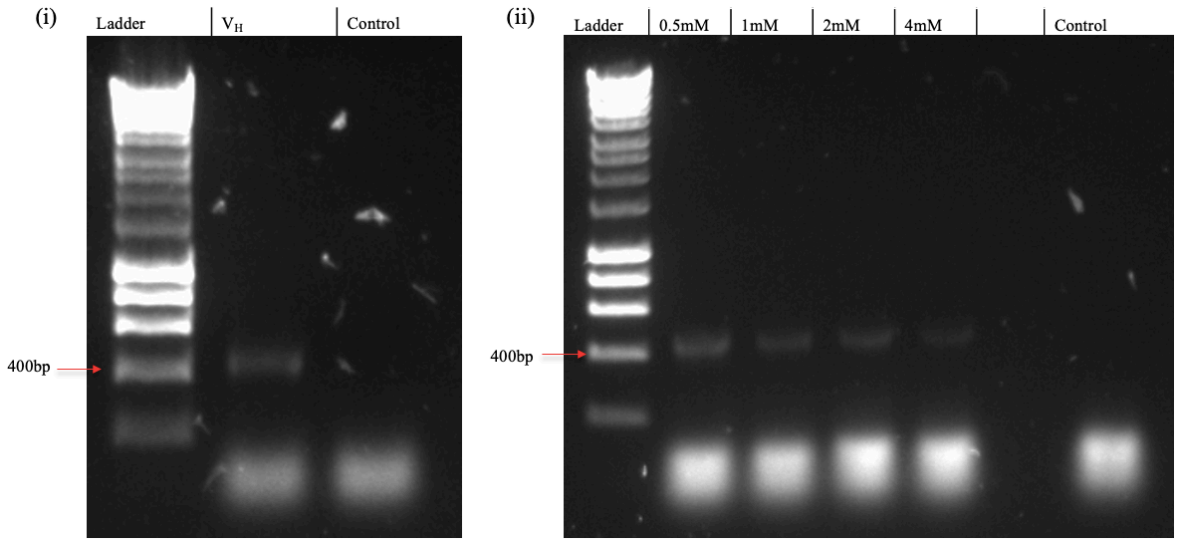

Figure 3.6 DMSO and $MgCl_2$ optimisation of V_H amplification

(i) *The V_H amplification reaction performed in the presence of 3%* (v/v) *DMSO. This yielded improved amplification.* ***(ii)*** *$MgCl_2$ concentration optimisation ranging from 0.5mM to 4mM. This analysis revealed that 0.5mM $MgCl_2$ was the optimal concentration in the PCR reaction (Ladder = Hyperladder™ 1 kb, V_H = variable heavy chain, control = PCR without cDNA template).*

At this stage, the amplification of the V_H from the PVY cDNA pool was considered adequate and no further optimisations were performed. After chain amplification, the next step in the library building process was to employ these purified chains in the generation of a splice overlap extension (SOE)-product. To permit this, both the V_L and V_H genes were amplified, run on agarose gels and purified and quantified on a Nanodrop™ 1000. The purified chains were then carried forward for SOE-PCR.

3.2.1.4 Generation of splice by overlap extension product

The SOE-PCR mediates the linkage of the heavy and light antibody chains through the incorporation of a glycine-serine $(G_4S)_4$ linker. The addition of the linker endows the scFv with the requisite flexibility for antigen binding and aids in correct folding of the scFv. In SOE-PCR, the V_L and V_H chains are combined at random, producing a final pool of highly diverse pairs of each chain.

The purified V_L and V_H chains were employed at equal concentrations to act as template DNA in the SOE-PCR. The reaction parameters for this PCR are described in *Section 2.11.6*. The SOE product has an estimated size of ~750-800bp, comprising of the 400bp V_H, 350bp V_L and the linker. From the result, shown in *Figure 3.7*, it was clear that the SOE product was preferentially amplified in the reaction, demonstrated by strong band formation at ~750bp. Hence, no optimisation of this reaction was required. Any further SOE-PCRs were performed under these conditions. The resulting amplification products were run on gels and the specific SOE bands excised, purified and quantified on a Nanodrop™ 1000.

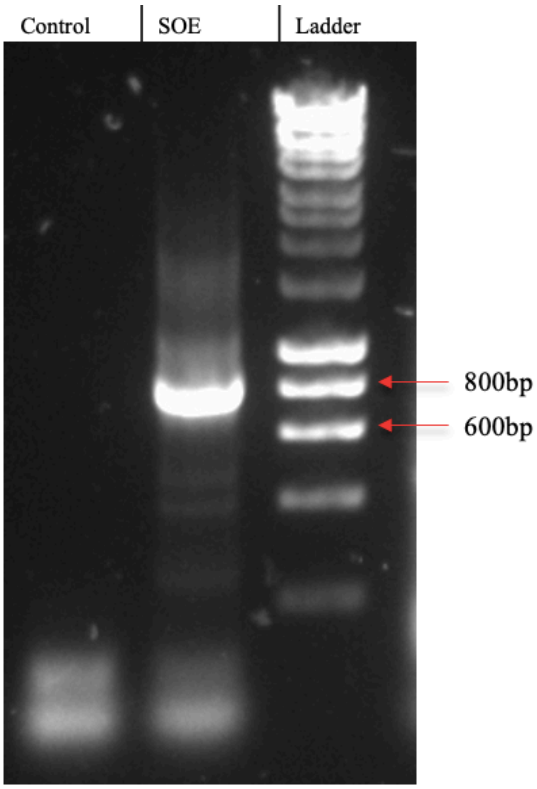

Figure 3.7 Splice by overlap extension-PCR to anneal V_L and V_H chains

The SOE-PCR permits the joining of the ~350bp V_L and ~400bp V_H. These, in conjunction with the linker, produce a product of a final size around 800bp (Ladder = Hyperladder™ 1 kb, Control = PCR without template).

3.2.1.5 Library assembly

The isolated SOE products and a phagemid vector, pComb3XSS, are employed for the final library assembly. Single colonies containing the pComb3XSS phagemid were grown overnight. From these overnight cultures, plasmid was isolated and purified prior to quantification on a Nanodrop™1000. The restriction enzyme *Sfi*I was used to digest both the pComb3XSS vector and the SOE products in separate reactions (*Section 2.11.7*). Digestion of these products with *Sfi*I yields juxtaposed 'sticky ends' which can be ligated together to form a complete vector containing the scFv insert. The digested vector and SOE were resolved on agarose gels, shown in *Figure 3.8 (i)* and *(ii)*, respectively. The pComb3XSS digestion yields multiple products. The size of the undigested vector is ~4900bp, however, *Sfi*I digestion results in the excision of a stuffer fragment of ~1600bp from the phagemid. The remaining ~3300bp product is the required vector with which library construction is performed. Care is taken to extract only this product, as carry-over of the stuffer fragment can result in inefficient library assembly. The main bands observed after

the restriction digest of the pComb3XSS vector were the ~3300bp target phagemid and the stuffer fragment. The size of the digested SOE remains relatively unchanged as the digestion of this product is primarily to introduce complementary 'sticky-ends'. This does not yield a major size difference between the digested and undigested SOE product. The resolved fragments were excised from their respective gels, purified and quantified on a Nanodrop™ 1000. Thereafter, the two products were joined via the action of a T4 DNA ligase, as described in *Section 2.11.8,* to form an assembled recombinant scFv library.

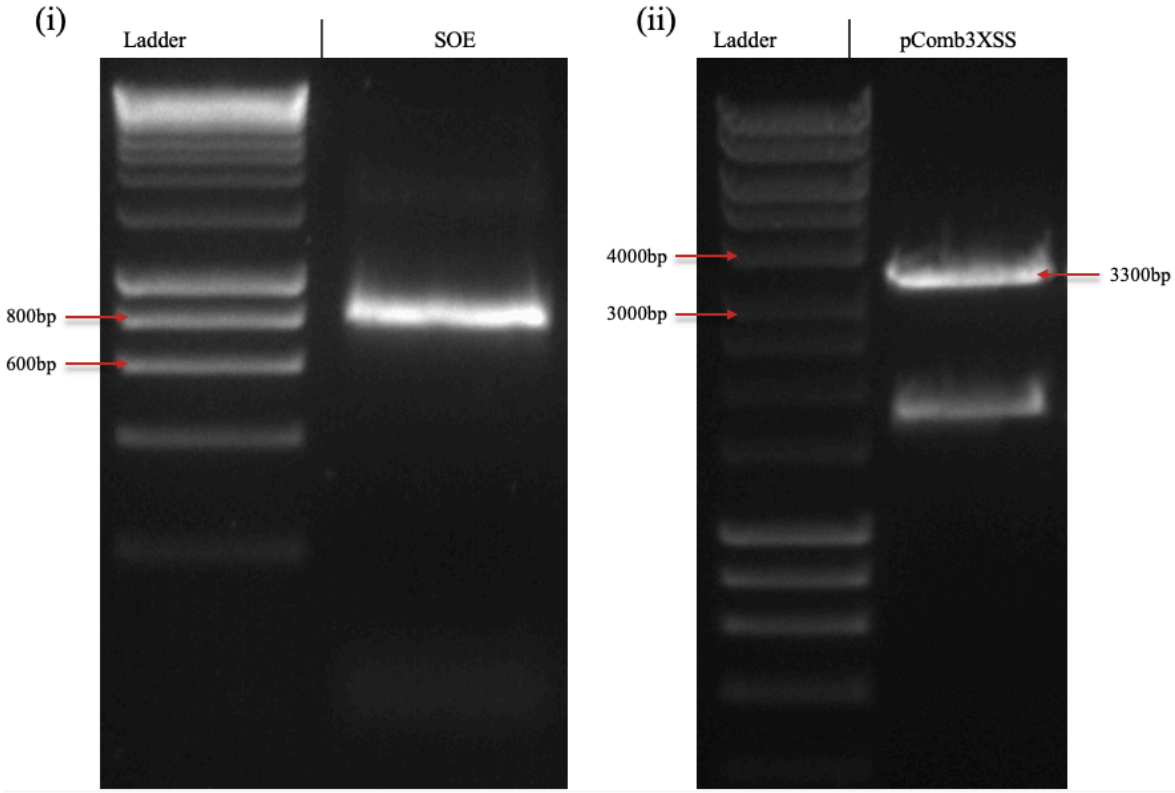

Figure 3.8 SfiI digestion of the SOE product and pComb3XSS phagemid

(i) *Analysis of the digested SOE product on a 2% agarose gel. The digested SOE presents as a ~800bp product.* ***(ii)*** *Analysis of the digested pComb3XSS vector. The digestion of the vector resulted in two primary products, the stuffer fragment of ~1600bp while the product of interest is located at 3300bp (Ladder = Hyperladder™ 1 kb).*

3.2.1.6 Transformation into electrocompetent E. coli

The constructed anti-PVY scFv library was transformed into electrocompetent XL1-Blue *E. coli* cells by electroporation, as described in *Section 2.11.9*. After the transformation, a colony-pick PCR was performed to determine the efficiency with which the vector, harbouring an scFv sequence, was both ligated into the pComb3XSS vector and

subsequently transformed into the cells (*Section 2.11.10*). To achieve this analysis, ten colonies were selected at random from the transformation plates and the SOE was selectively amplified through PCR. The efficiency was determined by running the resulting products on an agarose gel to determine how many of the selected colonies harboured the expected 750bp-800bp insert. In *Figure 3.9*, inserts can be observed in each of the ten colonies, indicating an insert efficiency of 100% in the library building. This was deemed sufficient to proceed to screening of the library for anti-PVY scFv.

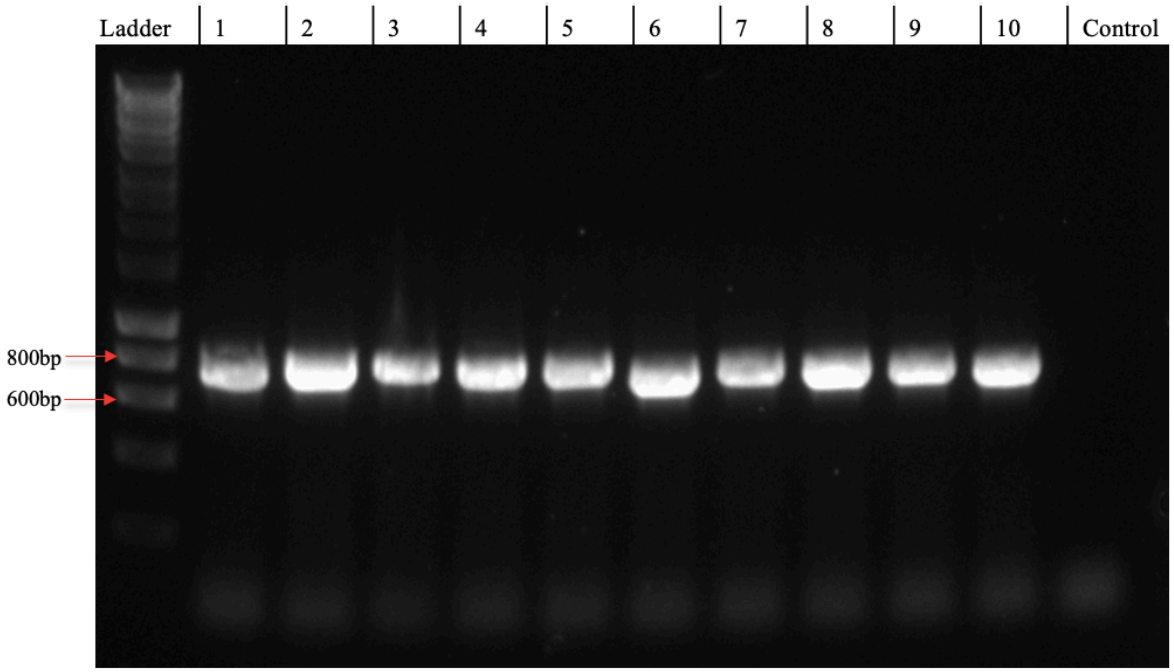

Figure 3.9 Analysis of the colony-pick PCR performed on transformed colonies

Ten colonies were selected at random and subjected to a colony-pick PCR to determine the level of insert efficiency (Ladder = Hyperladder™ 1 kb, 1-10 = ten random colonies, control = PCR with no colony).

This assembled library concluded the work with respect to construction of a recombinant scFv library. However, in order to screen the library and identify PVY-binding scFv, a suitable antigen was required. Isolation of natural PVY antigens would require infection and propagation of PVY *in-planta* followed by the subsequent isolation of the CP from the leaf tissue. This approach would be relatively time consuming and was not considered sustainable given the continuous and relatively high supply of CP required for onward screening and characterisation. As such, a recombinant protein expression approach was taken as this provides a reliable and rapid method with which to express target proteins.

3.2.2 Construction of recombinant PVY coat protein vectors

3.2.2.1 Amplification of the coat protein genes

PVY^{O} and PVY^{NTN} strains were employed for the generation of recombinant CP vectors. These PVY strains represent each of the two PVY serotypes, O and N. Serotype-specific primers were designed to amplify the CP gene for each serotype. Additionally, the primers incorporated 5'-*Nco*I and 3'-*Hind*III restriction sites in order to facilitate directional cloning of the amplified gene into the desired vector, pET-26b(+). Details of the primers and the amplification conditions are described in *Section 2.14.1*. The CP products will be referred to as O (PVY^{O}) and N (PVY^{NTN}) henceforth in order to reflect their serological categorisation. Successful amplification of the CP genes is depicted in *Figure 3.10*, wherein products of the expected size of ~801bp can be observed for both the N (*Figure 3.10 (i)*) and O (*Figure 3.10 (ii)*) serotypes.

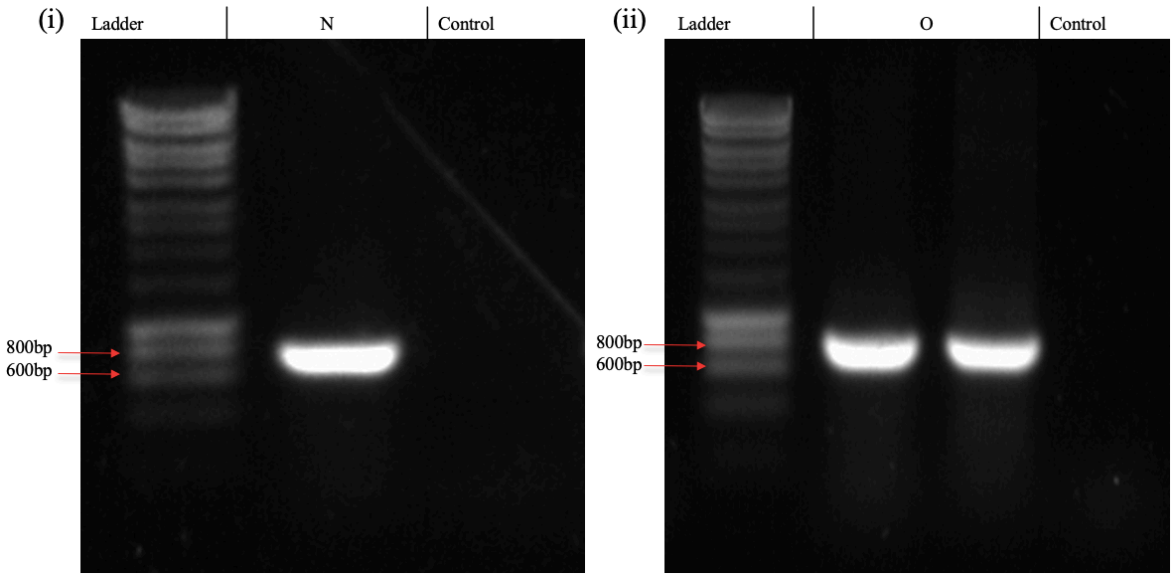

Figure 3.10 PCR-mediated amplification of CP genes

(i) *Amplification of the N serotype CP.* ***(ii)*** *Analysis of the amplification of the O serotype CP. Both CP genes amplified successfully with products observed at the expected size of 801bp (Ladder = Hyperladder™ 1 kb, Control = PCR without DNA template).*

3.2.2.2 Construction of O- and N-harbouring vectors

In order the generate a recombinant plasmid capable of expressing the CP gene with good efficiency, the pET-26b(+) vector was selected. This vector was grown and purified prior to quantification on the Nanodrop™ 1000. The plasmid then underwent double-digestion by the action of *Nco*I and *Hind*III. The O and N CP genes, amplified in *Section 3.2.2.1*, were

also subjected to similar *Nco*I and *Hind*III double-digestion protocols. These are described under *Section 2.14.2*. Results of the digestion of both the pET-26b(+) vector and the CP genes are shown in *Figure 3.11 (i)* and *(ii),* respectively. Successful digestion of the vector was confirmed by the apparent linearisation of pET-26b(+) when compared to that of the undigested plasmid control. No major size difference can be observed for the digested CP genes as the purpose of the double-digestion of these products was only to generate sticky-ends, making the change in length effectively unobservable on the gels. The digested products were excised from their respective gels, purified and quantified on the Nanodrop™ 1000. Thereafter, in separate reactions, the two CP genes were ligated into pET-26b(+), as described in *Section 2.14.3*.

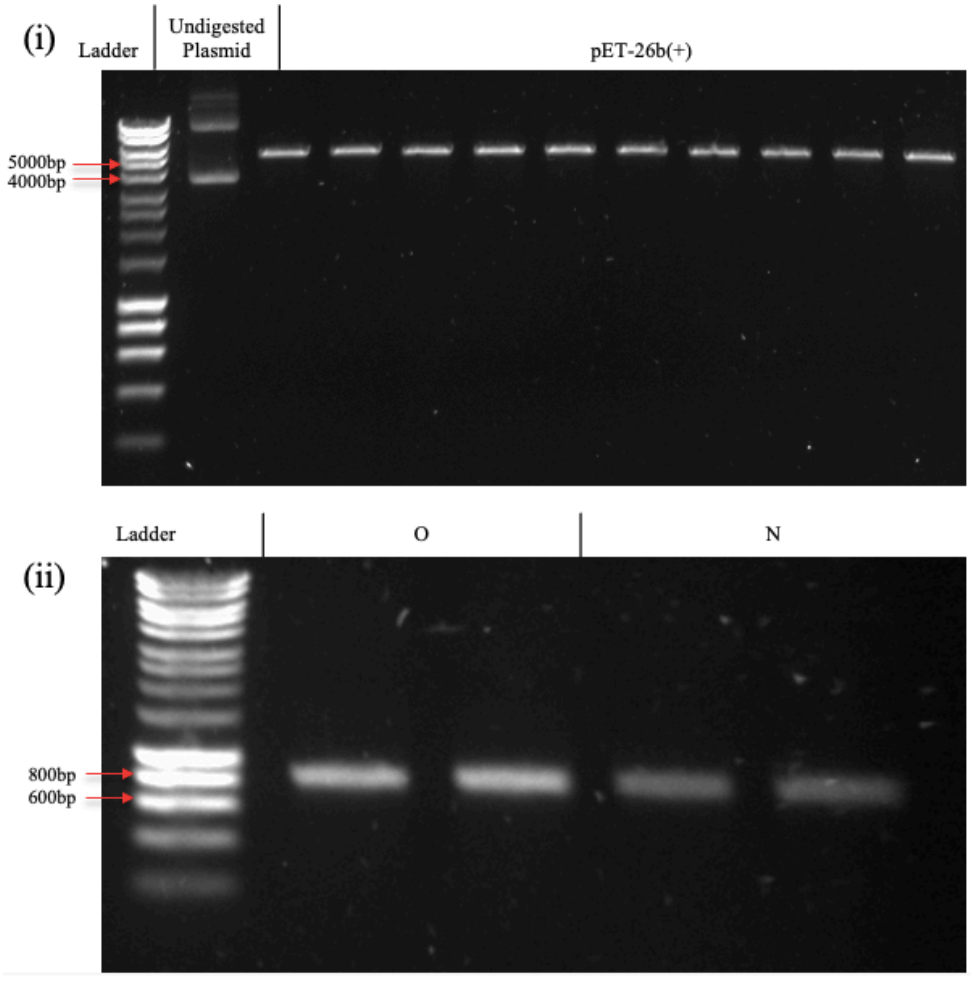

Figure 3.11 Double digest of the pET-26b(+) vector and CP serotypes

(i) *Analysis of the pET-26b(+) vector digestion. Double digestion of pET-26b(+) linearises the plasmid. This linearised vector can be observed as a single band while the undigested vector presents as multiple bands.* ***(ii)*** *Analysis of digested O and N CP genes (Ladder = Hyperladder™ 1 kb).*

In order to facilitate the recombinant expression of the CPs, the assembled CP-harbouring vectors were transformed into BL21(DE3) chemically competent cells via heat shock, as per *Section 2.10.11*. The transformants were plated onto LB agar, supplemented with kanamycin to enable selective growth of colonies containing the pET-26b(+) vector.

3.2.2.3 Analysis of CP sequences

Colonies sourced from the transformation plates were grown, their plasmids extracted, and these plasmids sent for sequencing by Source Biosciences. The sequence data returned for the O and N CPs was translated into AA form in Expasy Translate and analysed in Blastp in order to compare the retrieved cloned CP sequences against other published PVY CP sequences. The gene insert for each strain was found to have suitable similarity to CP sequences. The O serotype CP insert was revealed to be a 100% sequence match to previously identified and sequenced O CP genes. The sequences were aligned to demonstrate homology, shown in *Figure 3.12*.

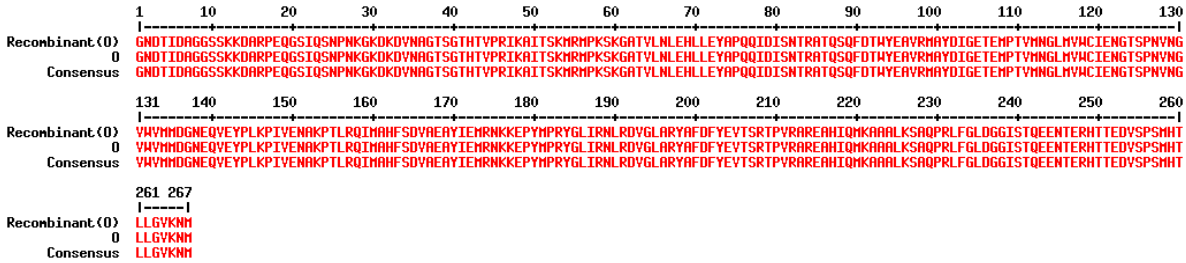

Figure 3.12 Alignment of cloned O CP sequence and published O CP sequences

The cloned O CP sequence, termed recombinant (O), was inputted into Blastp and compared against similar PVY sequences. A sample of a 100% match sequence was chosen (accession no. ACZ26395) to demonstrate the alignment between the cloned insert and other published O-type sequences.

With respect to the N serotype, sequences with the highest homology were found under accession numbers ABO15899, BAN58743, ACZ26381 and BAM15282, with a 99.63% percentage identity match observed between the cloned gene AA sequence and the sequences under each of the listed accession numbers. A sample alignment between the cloned N gene and a published CP gene are shown in *Figure 3.13*. There was one consistent AA variation present between the cloned gene and the published PVY sequences with 99.63% matches, an alanine (A) in lieu of a threonine (T) at position 206, shown in blue in

Figure 3.13. From analysis of other CP sequences, it was posited that the T206A variation was unexpected as the threonine at this position appeared conserved based on its frequency of occurrence with the PVY CP sequence data. The variation of this residue from the expected, alongside its seemingly conserved nature, indicated that the difference at this position may have been caused by error during the PCR process, typically introduced by infidelity on the part of the DNA polymerase.

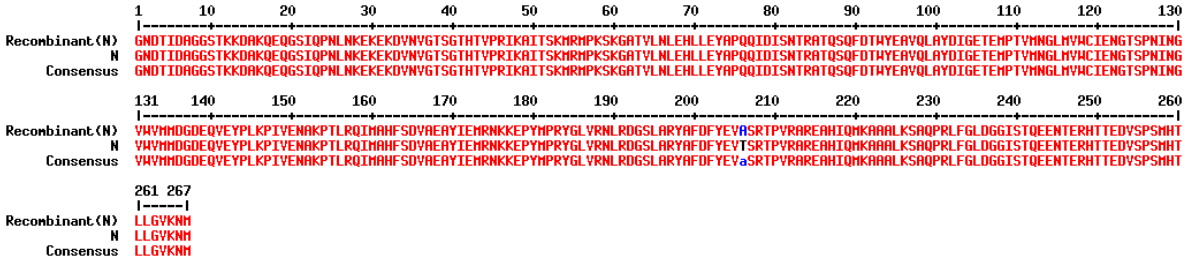

Figure 3.13 Recombinant N CP sequence aligned to a published N CP sequence

The cloned N CP sequence, denoted as recombinant (N), was analysed against other PVY sequences in Blastp. A sample of a 99.63% match sequence was chosen (accession no. ABO15899) to demonstrate the alignment between the cloned gene and other known N-type sequences.

Site directed mutagenesis or re-cloning of the gene could be employed to alter this residue, however, considering the high similarity between the O and N serotype AA sequences it was decided to proceed to protein purification and subsequent antibody library screening using only the O CP. This was performed with the proposal that scFv reactive with the O strain would likely also be reactive with the N serotype. The O CP is referred to as "CP" for the remainder of this work, unless specified otherwise.

3.2.3 Expression and purification of recombinant CP

3.2.3.1 Optimisation of expression of the CP

The CP clone was grown and subjected to optimisation of expression studies, as per *Section 2.14.4*. The first optimisation performed was the variation of IPTG concentration used for induction in the range of 0.2mM - 1mM. The chosen concentration of IPTG can impact the solubility of the protein. All expression was performed at a fixed temperature of 25ºC to encourage expression of soluble protein as lower temperatures are generally favoured for this purpose. The soluble fractions from the various expression conditions were isolated and

run in SDS-PAGE (*Section 2.10.5)* and WB (*Section 2.10.6)*. The results of the SDS-PAGE and WB analysis are shown in *Figures 3.14 (i)* and *(ii),* respectively. Little information can be ascertained from the SDS-PAGE due to the quantity of cellular proteins present in the lysates, however, WB analysis using a CP-specific pAb confirms the presence of the PVY CP around 30-35kDa. The predicted molecular weight of the CP is 30kDa, however, the CP band appears to migrate as ~35kDa in this SDS-PAGE and WB analysis. It was noted through WB that in hand-cast gels the CP typically migrated to ~30kDa, however, in the pre-cast gel system it was generally found at ~35kDa. The disparity in migration pattern was attributed to the different buffering systems used for each. Observation of the thickest bands in WB, and thus the highest level of expressed protein, revealed that optimal IPTG concentration was 0.2mM IPTG.

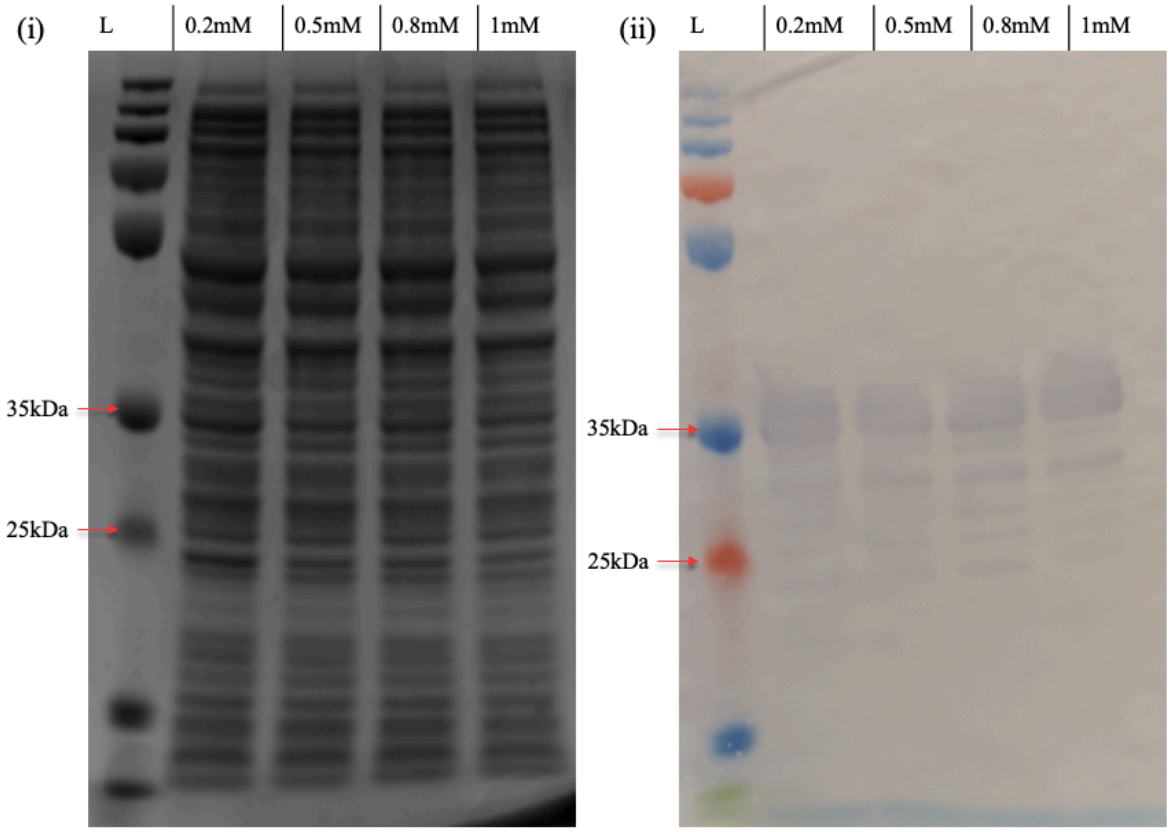

Figure 3.14 Optimisation of IPTG concentration for the expression of the CP

(i) *SDS-PAGE analysis of each IPTG variation, ranging from 0.2mM to 1mM.* ***(ii)*** *WB analysis of cultures induced with differing IPTG concentrations, ranging from 0.2mM to 1mM. The WB was probed with a primary anti-PVY polyclonal antibody (pAb) which was subsequently detected with a secondary HRP-labelled anti-rabbit antibody (L = PageRuler plus prestained protein ladder).*

Following IPTG concentration investigations, the duration of the induction time was optimised to determine the timepoint at which the highest level of protein was expressed. This is a useful parameter to investigate to account for the case that the expressed protein may not stable or may be prone to proteolytic degradation under prolonged induction. To determine the optimal timepoint for cell-harvesting, the cultures were induced with a fixed concentration of 0.2mM IPTG at 25ºC and samples of the expressed protein were collected 1 h, 2 h and 3 h post-induction. A final sample of the CP was left to induce O/N. The expression levels at the given timepoints were analysed in SDS-PAGE (*Figure 3.15 (i)*) and WB (*Figure 3.15 (ii)*). This investigation revealed that expression of the CP O/N yielded the highest quantity of protein, as evidence by the strongest reactive bands in the WB found at this timepoint. However, it was noted that expression of the protein appeared very quickly, with low levels of CP noted at the 1hr timepoint. An O/N incubation was selected for any subsequent expression of this protein.

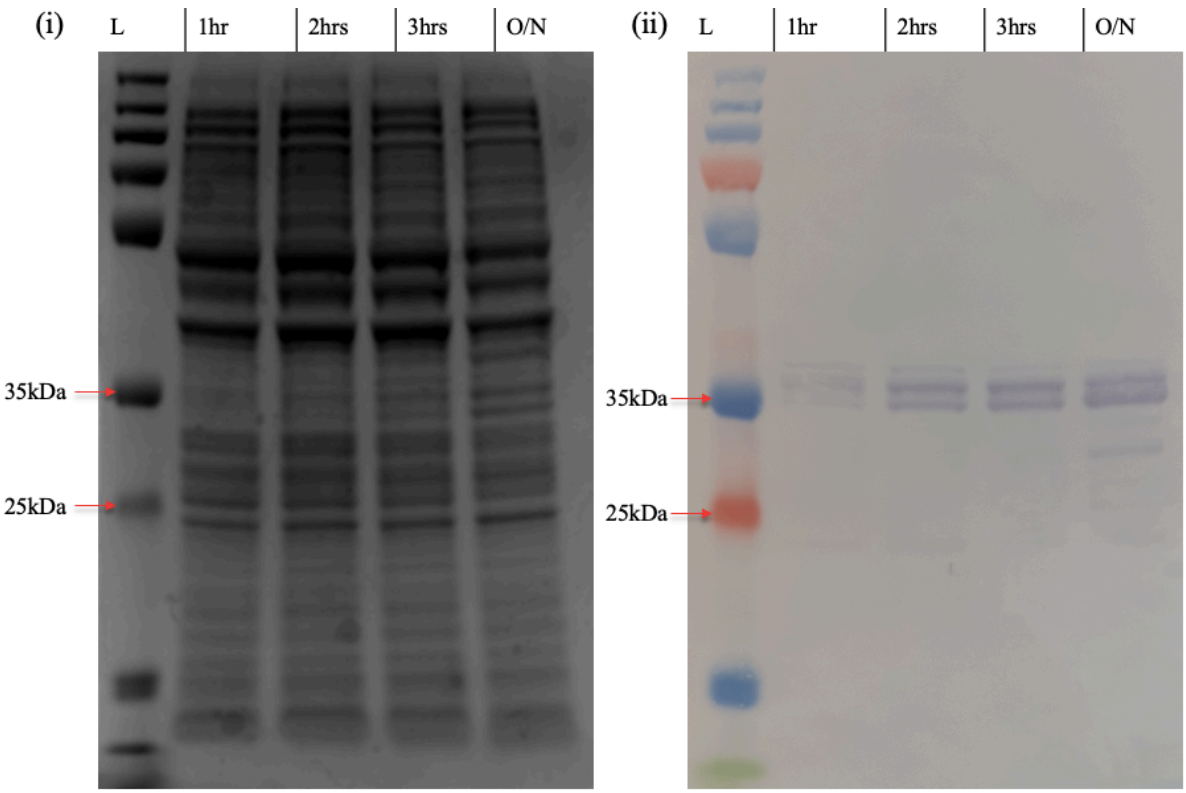

Figure 3.15 Timepoint analysis of the CP expression

(i) *SDS-PAGE analysis of each induction timepoint.* ***(ii)*** *WB analysis of 1 h, 2 h, 3 h and O/N induction timepoints. The WB was probed with a primary anti-PVY pAb which was subsequently detected with a secondary HRP-labelled anti-rabbit antibody (L = PageRuler™ plus prestained protein ladder).*

3.2.3.2 Large-scale expression and Ni-NTA purification of the CP

Having optimised the IPTG concentration and expression timepoint, work was progressed to producing the CP in larger volumes such that the protein could be isolated in purified form through IMAC. The CP was expressed in large-scale cultures as per the defined optimal conditions identified in *Section 3.2.3.1.* From these large-scale cultures, lysates were isolated as per *Section 2.14.5*. This lysate was then subjected to IMAC purification protocols as described in *Section 2.14.6*. This purification protocol included a series of wash steps, each containing gradually increasing concentrations of imidazole. These imidazole washes help to remove non-specifically bound proteins which may harbour some level of binding to the nickel resin used in IMAC. These generally include endogenous bacterial proteins which naturally contain histidine residues. Gradually increasing concentrations of imidazole in wash buffers should permit the competitive elution of these loosely-bound proteins. Contrastingly, at such concentrations, the recombinant protein should remain attached to the resin, as the co-expressed hexahistidine tag will present much stronger binding to nickel and requires high concentrations of free imidazole to competitively elute.

From the purification, the flow-through and wash fractions were collected for analysis. The resultant elution fraction was concentrated and buffer exchanged into PBS. Each of the purification fractions, and the isolated CP sample, were analysed through SDS-PAGE and WB, as outlined in *Sections 2.10.5* and *2.10.6*, respectively. The analysis of the IMAC purification of the CP is shown in SDS-PAGE (*Figure 3.16 (i))* and WB *Figure 3.16 (ii)).* The presence of protein bands at ~30kDa in both the SDS-PAGE result and in the WB is indicative of a successful purification. Thin bands at the ~30kDa size in washes 4 and 5 indicate there may have been minimal premature elution of the CP, however, this did not appear to negatively affect the overall purification, with an acceptable quantity apparent in the final concentrated CP sample. This method was applied for all required purifications of the CP.

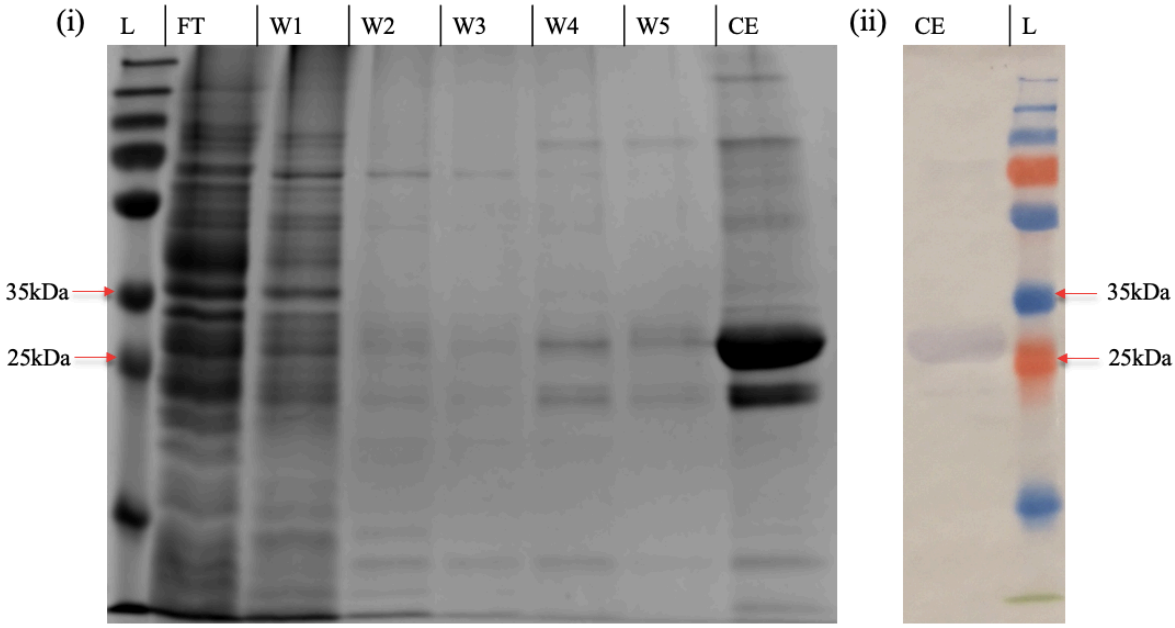

Figure 3.16 SDS-PAGE and WB analysis of purification of CP through IMAC

(i) *SDS-PAGE analysis of the CP purification.* ***(ii)*** *WB analysis of the concentrated CP sample. The blot was probed with a primary anti-PVY pAb, which was subsequently detected with a secondary HRP-labelled anti-rabbit antibody (Ladder= PageRuler™ plus prestained protein ladder, W1 = 30mM imidazole wash, W2/W3 = 50mM imidazole washes, W4/W5 = 80mM imidazole washes, CE = concentrated and buffer exchanged elution fraction).*

Having successfully isolated the CP in this manner, purified CP was employed as the requisite antigen in the screening process for the isolation of anti-PVY scFv from the previously constructed recombinant antibody library.

3.2.4 Screening of a recombinant antibody library for anti-PVY scFv

3.2.4.1 Pre-panning library screening

The transformed library (*Section 3.2.1.6*) was used alongside the isolated CP antigen in a pre-panning screening approach to determine the level of PVY-binding clones in the library prior to enrichment. For this analysis, 192 clones were selected from the plates of the transformed library and grown individually. Soluble scFv expression was induced in each clone, as described under *Section 2.13.1*. The lysates for the individual clones were obtained via freeze-thaw lysis and were subsequently carried forward into ELISA analysis to assess their CP-binding capacity. The results of these investigations are depicted in *Figure 3.17* and *Figure 3.18*. From this, several clones demonstrated a high in-assay signal against the CP when compared to other clones selected and assayed in the same manner. An elevated

signal in this analysis indicates the presence of PVY-binding scFv in the library. Of the clones tested, two clones in particular presented the best signal, these were 10A and 12D.

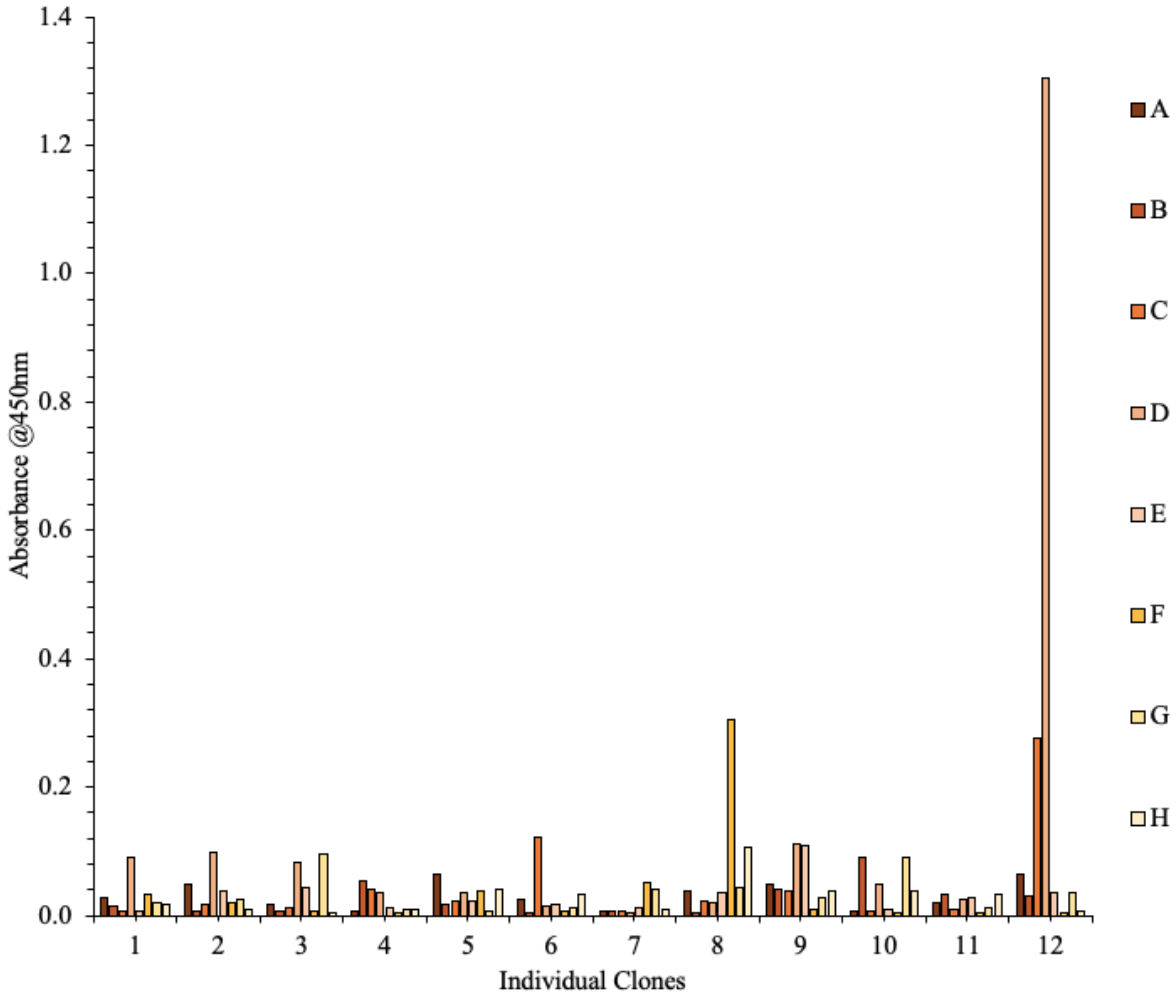

Figure 3.17 Pre-panning monoclonal ELISA against the CP

Lysates of single colonies (1-12; A-H) from transformation plates were applied to ELISA wells coated with 1µg/mL CP. Bound scFv were detected using a HRP-labelled anti-HA antibody. The absorbance was read at 450nm.

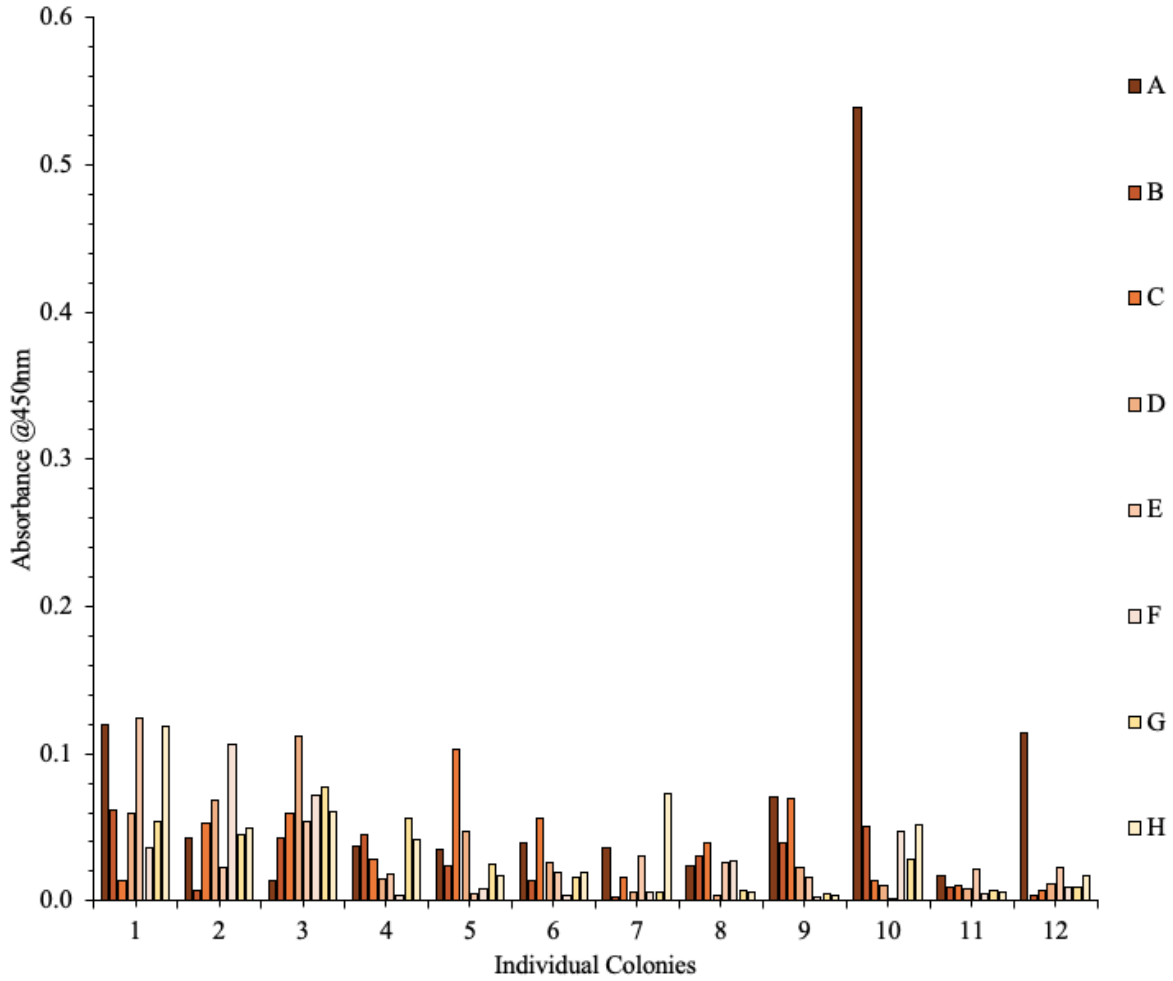

Figure 3.18 Pre-panning monoclonal ELISA against the CP

Lysates of single colonies (1-12; A-H) from transformation plates were applied to ELISA wells coated with 1µg/mL CP. Bound scFv were detected using a HRP-labelled anti-HA antibody. The absorbance was read at 450nm.

3.2.4.2 Indirect ELISA analysis of binding clones

To permit further analysis of the two clones of interest, 12D and 10A, they were re-grown, expression was induced, and the lysate was obtained, as per *Section 2.13.2*. The resulting scFv-enriched lysate was applied in doubling dilutions to an ELISA plate coated with the CP in order to determine if their in-assay response persisted, and, if so, to what extent. The titre, shown in *Figure 3.19*, indicated that both clones titred against the CP antigen, as demonstrated by a decrease in absorbance value correlating to an increase in lysate dilution factor. It was also noted that a more extensive series of dilutions was required to fully titre both clones, particularly the 12D clone, as both failed to achieve a final titre point in this analysis.

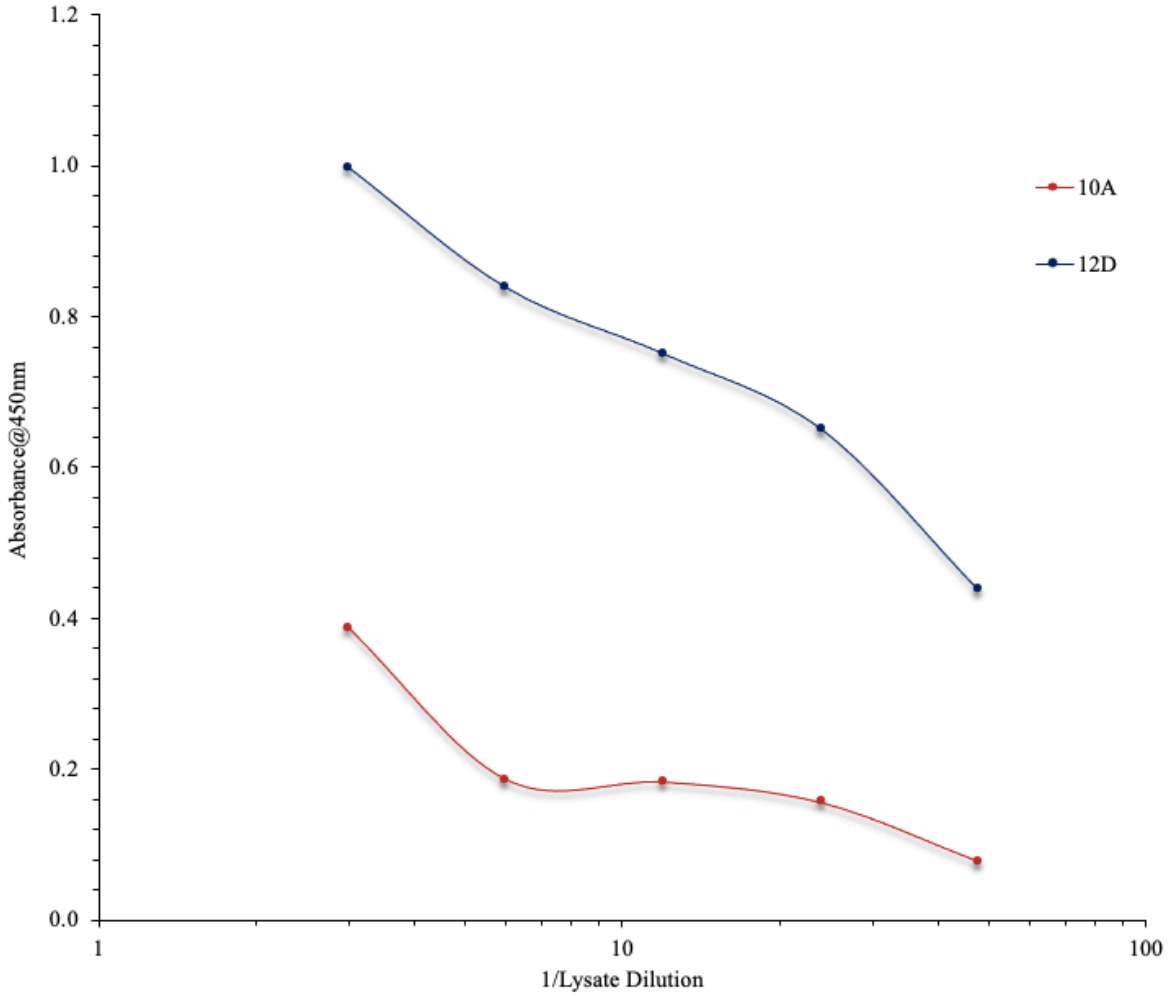

Figure 3.19 Titration of scFv-enriched lysates against CP

ScFv-containing lysates from 10A and 12D were applied in a series of dilutions to the wells of an ELISA plate coated with 1μg/ml CP. Any bound scFv protein was detected using a HRP-labelled anti-HA antibody. The absorbance was then read at 450nm.

In addition to the clones identified from the pre-screening, isolation of clones was also attempted through the employment of an advanced screening and enrichment method termed biopanning. This method allows the mass-screening of antibody clones derived from recombinant antibody libraries through display of the antibody proteins, in this case scFv clones, on the surface of filamentous phage particles. This method utilises multiple rounds of screening to enrich the antibody repertoire for antigen-specific pools of scFv. The method is also recruited to aid in the identification of high-affinity clones through the use of parameters such as reduced antigen coating concentrations and increased washing stringency throughout the screening campaign.

3.2.4.3 Enrichment of the phage library for PVY-positive clones via biopanning

While, in theory, enrichment for antigen-specific scFv occurs from the first round, it is advised to proceed with at least three rounds of panning in order to ensure strong enrichment for the most sensitive and specific scFv (Pande, Szewczyk, and Grover, 2010; Hammers and Stanley, 2014). In order to achieve this, the constructed scFv library was screened against the CP antigen for four rounds of biopanning. These were performed as described in *Section 2.12* and under the conditions shown in *Table 3.1.* The parameters listed in *Table 3.1* illustrate the approach in biopanning whereby stringency is increased in each round to select for high-affinity scFv, for example, the reduction in antigen coating concentration and the more extensive washing performed at later rounds.

Table 3.1 Parameters for biopanning of the scFv library for PVY-positive clones

The antigen coating concentration and washing stringency was altered in each round to apply selective pressure for the isolation of high sensitivity and specificity clones.

Round	Antigen Coating Concentration	Wash Steps
1	20µg/mL	3X PBS-T (0.05%, v/v), 3X PBS
2	2µg/mL	3X PBS-T (0.05%, v/v), 3X PBS
3	0.2µg/mL	5X PBS-T (0.05%, v/v), 5X PBS
4	0.1µg/mL	8X PBS-T (0.05%, v/v), 8X PBS

During panning, it was noted that in round four, the output titre decreased to the point where no colonies were present on the titration plates and only single colonies were present on the stock plates. The reduction in the output titre indicated the loss of anti-CP scFv in this final round, potentially due to the increased stringency employed. However, given that even one round provides substantial enrichment against the target antigen it was decided to proceed with analysis of the antibody clones sourced from the other rounds of biopanning. To achieve this, single colonies were selected from each of the rounds of biopanning and assessed for their CP-binding capacity.

3.2.5 Monoclonal and indirect ELISA analysis of clones from biopanning

3.2.5.1 Monoclonal ELISA analysis of CP-binding

Individual clones were selected, grown and soluble scFv protein expression induced. Subsequently, their lysates were isolated and screened for their ability to bind the CP antigen

in indirect ELISA format, as per *Section 2.13.1*. The results of the screening against the recombinant CP are shown in *Figure 3.20* and *Figure 3.21*. Elevated signals were observed in several clones across the screening, indicating the presence of anti-PVY antibodies. Of these clones, nine with the highest observed signals were selected for further analysis.

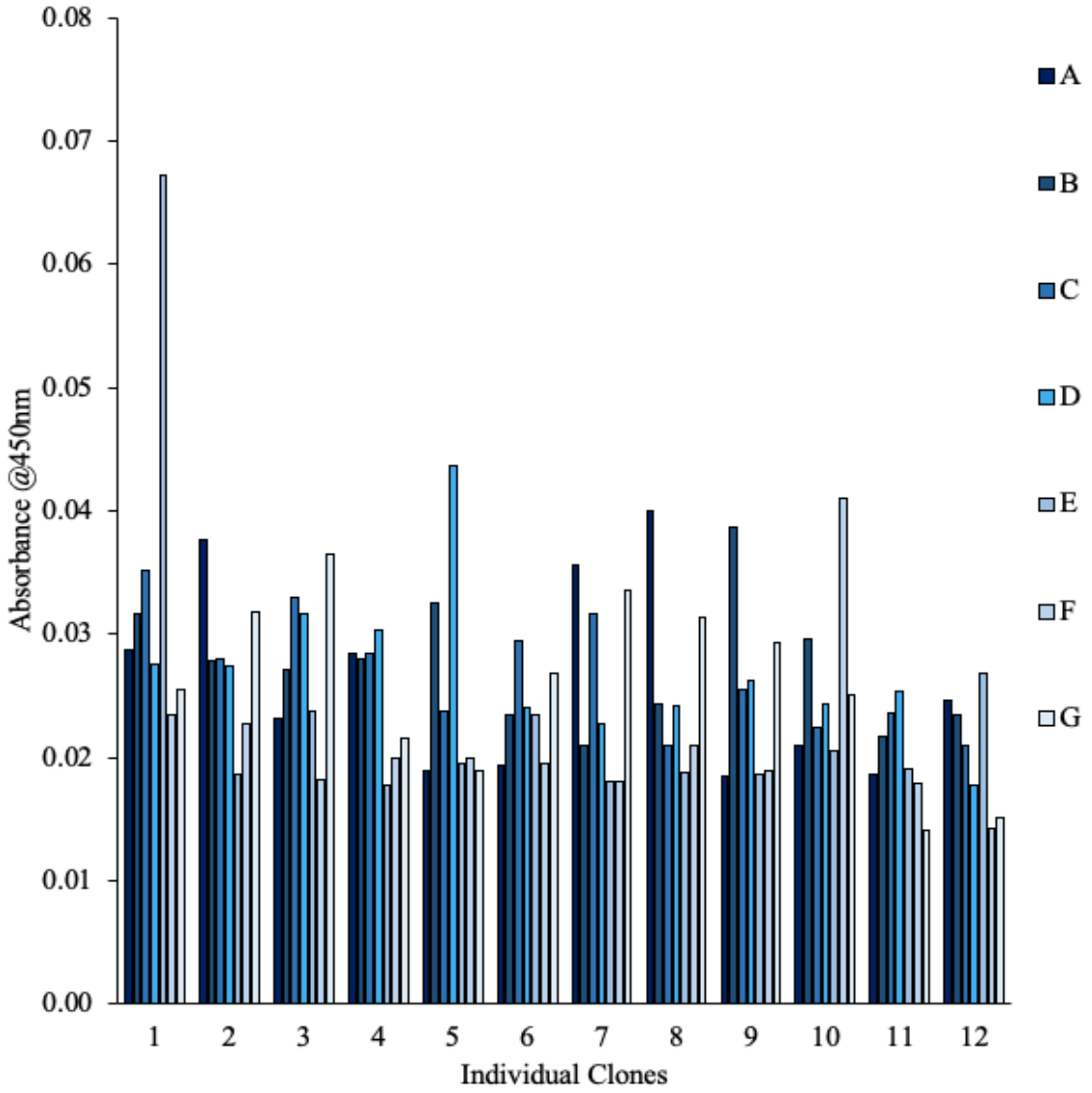

Figure 3.20 Monoclonal ELISA against the CP to identify positively binding clones

ScFv-enriched lysates sourced from individual clones (1-12; A-G) were acquired and applied to ELISA wells coated with 1µg/mL CP. Bound scFv were detected using a HRP-labelled anti-HA antibody. The absorbance was then read at 450nm.

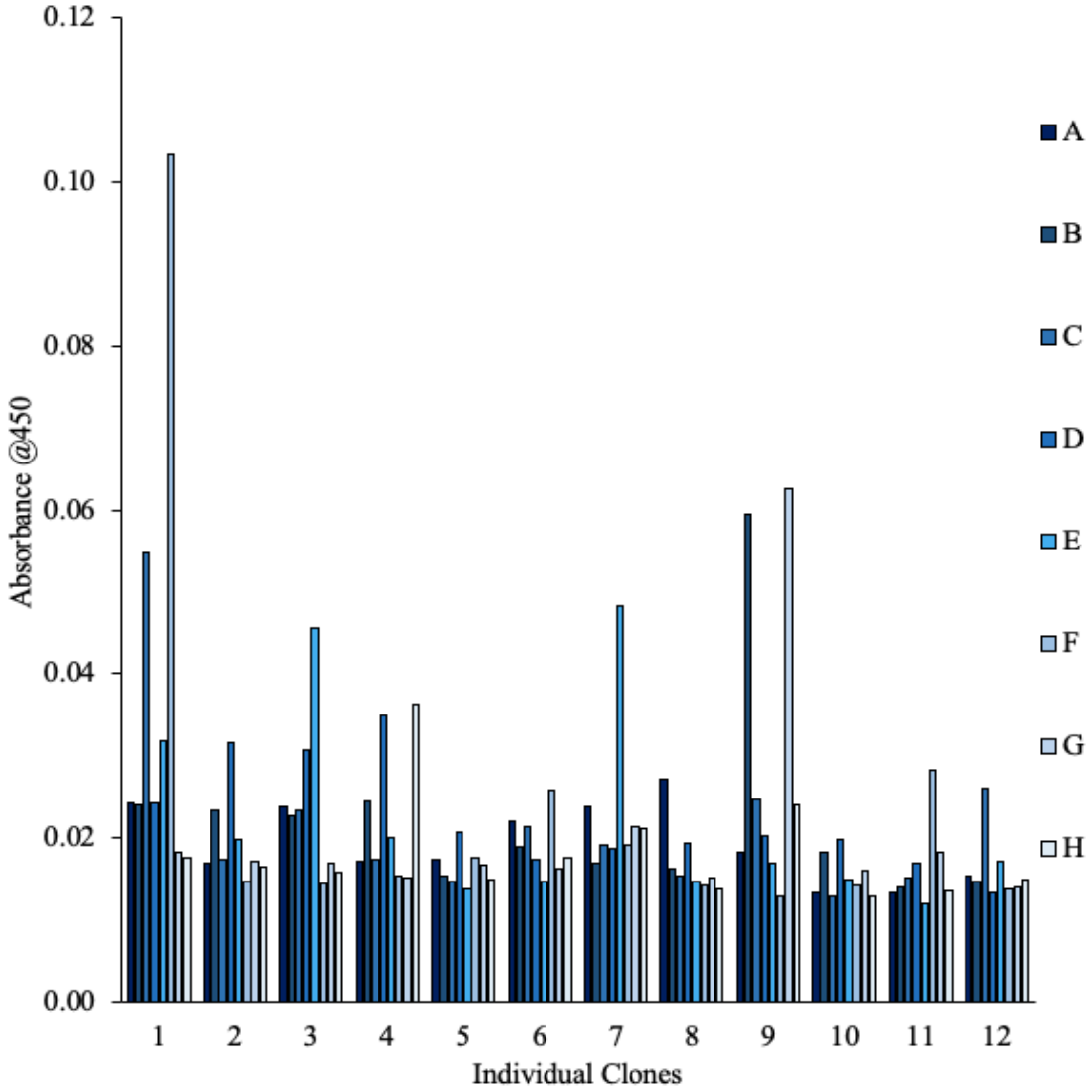

Figure 3.21 Monoclonal ELISA against the CP to identify positively binding clones

ScFv-enriched lysates were obtained for individual clones (1-12; A-H) and applied to ELISA wells coated with 1μg/mL CP. Bound scFv were detected using a HRP-labelled anti-HA antibody. The absorbance was read at 450nm.

3.2.5.2 Indirect ELISA analysis of clones of interest

The nine clones of interest from post-panning analysis were grown individually and soluble expression of the scFv was induced. Lysates were obtained for each of the clones to be analysed and this scFv-enriched lysate was used in an indirect ELISA to monitor CP binding, as per *Section 2.13.2*. The lysate was applied in doubling dilutions to an ELISA plate coated with the CP. The analysis, shown in *Figure 3.22*, revealed several of the clones continued to present a signal against the CP. An unexpected signal at lower dilutions was observed for clone 5D. This was attributed to some non-specific binding occurring in the well at this

dilution point as the signal for this clone was relatively low otherwise. The clones 1C and 1F were carried forward for further investigation in conjunction with the other previously identified clones of interest, 10A and 12D, due to the observed elevated signal of the clones and the fact that they appeared to demonstrate a suitable titration curve.

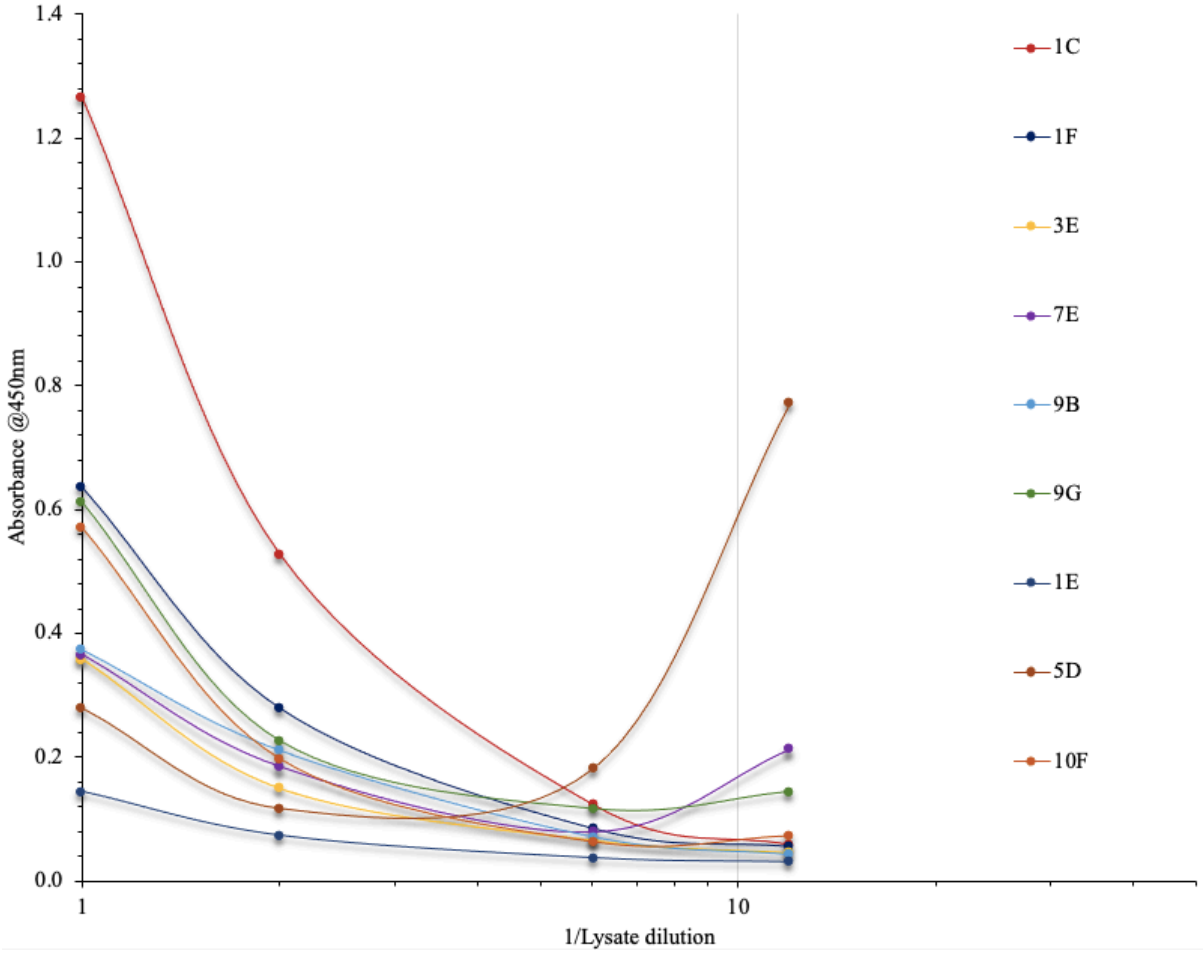

Figure 3.22 Indirect ELISA analysis of clones of interest

ScFv-containing lysates from several clones (1C, 1F, 3E, 7E, 9B, 9G, 1E, 5D and 10F) were applied in a series of dilutions to the wells of an ELISA plate coated with 1µg/ml CP. Any bound scFv protein was detected using a HRP-labelled anti-HA antibody. The absorbance was then read at 450nm.

3.2.6 Competitive analysis of clones of interest

The 12D, 10A, 1C and 1F clones were used in further characterisations in an attempt to elucidate their binding properties. Analysis was performed in order to determine detection abilities of the clones using competitive ELISA. Competitiveness of clones indicates whether the scFv have the ability to detect the requisite antigen from solution when

challenged with immobilised antigen and free antigen in the same assay well. To permit such an investigation, the lysates of each of the clones of interest were obtained as per *Section 2.13.3*. To assess the competitive capability of the clones, two different concentrations of free CP antigen were added to separate wells, alongside the scFv-containing lysate. Additionally, a well containing a zero concentration of free antigen was included as a reference for each clone. If the scFv bound to the antigen in solution, the signal in free antigen-containing wells should be lower than that of the wells which contained no free antigen. The assay signal is reported as A/A0, where the absorbance values of the samples containing free antigen (A) are expressed as a function of the blank which contains no free antigen (A0). The results, shown in *Figure 3.23*, indicate that only two of the clones presented the characteristic trend of lower signal in both wells containing free antigen. These were clones 10A and 12D. It was noted that clone 12D showed a greater reduction in A/A0 at the 5μg/mL free antigen concentration than the 10A clone, suggesting that 12D had better competitive binding. Nonetheless, both 12D and 10A were brought forward for further analysis

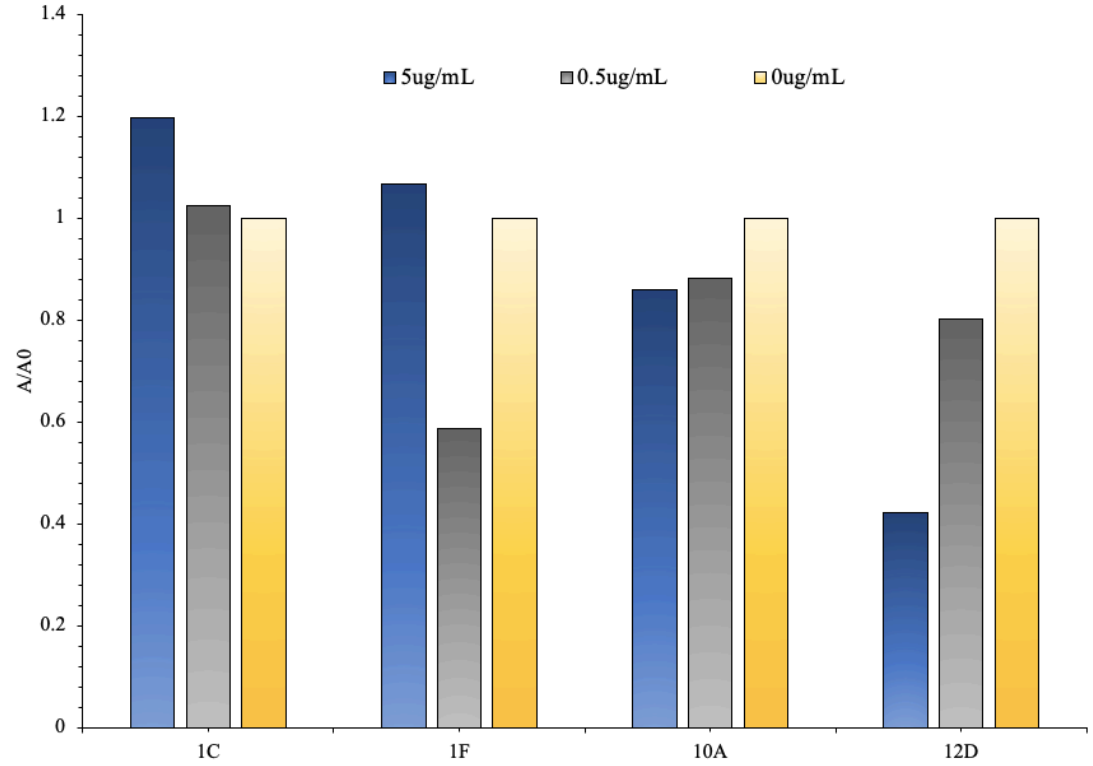

Figure 3.23 Preliminary competitive analysis of scFv clones

For competitive analysis, free CP was applied at concentrations of either 5µg/mL, 0.5µg/mL or 0µg/mL alongside the scFv-enriched lysate. The zero-concentration acted as reference with which to compare signal in the competitive wells. Any bound scFv protein was detected using a HRP-labelled anti-HA antibody. The absorbance was read at 450nm.

3.2.7 Assessment of 12D and 10A CP binding

3.2.7.1 Indirect ELISA titre of 12D and 10A

Clones 10A and 12D were subjected to a titre against the CP using a broad dilution range, from 1 in 10 to 1 in 1,280, in order to elucidate each clone's titre point and working dilution requirement. This was performed as described in *Section 2.13.2*. From the titre, *Figure 3.24*, it was determined that clone 12D presented a higher titre and overall signal when compared to that achieved when using 10A. Based on this result, working dilution factors of 1 in 50 for 12D and 1 in 20 for 10A were chosen for more extensive competitive analysis.

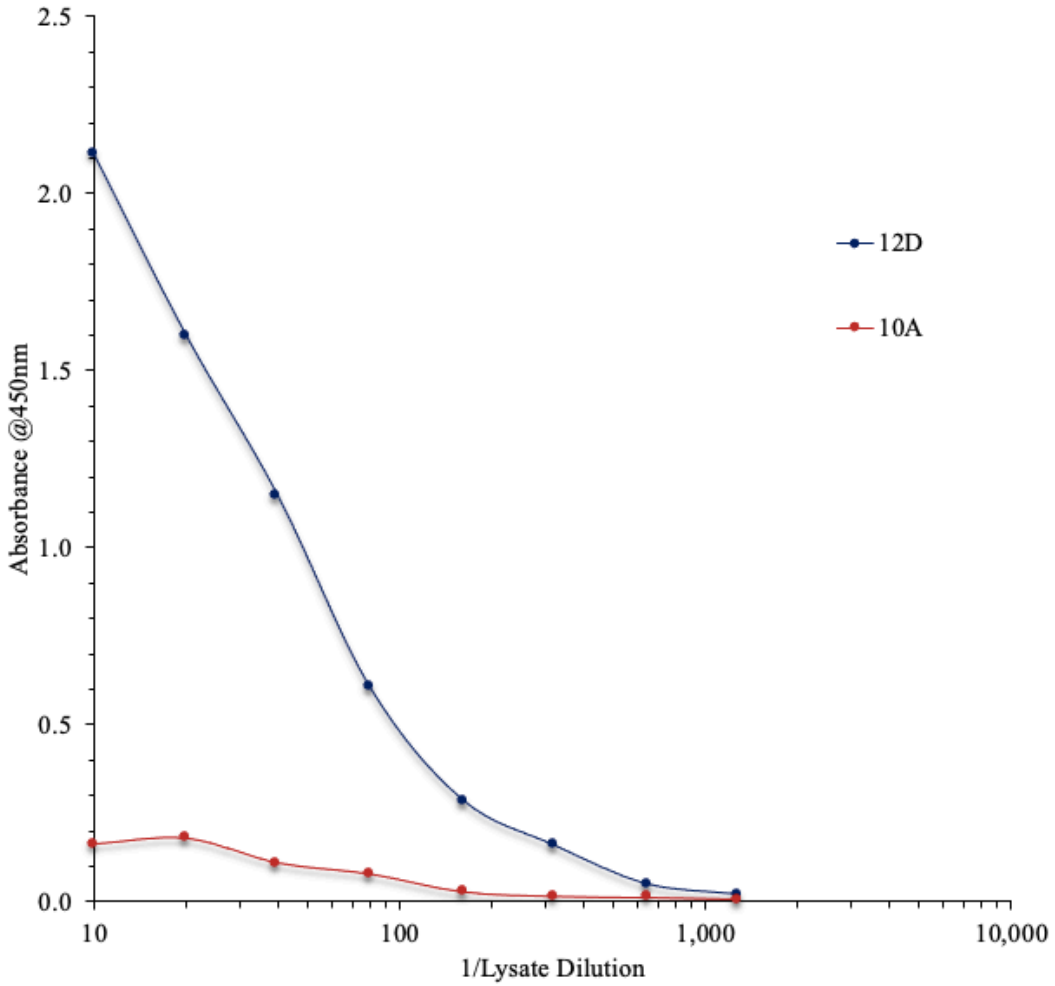

Figure 3.24 Titration of 12D and 10A lysates against the CP

Lysates from clones 10A and 12D were applied in a series of dilution to the wells of an ELISA plate coated with 1μg/ml CP. Any bound scFv protein was detected using a HRP-labelled anti-HA antibody. The absorbance was then read at 450nm.

3.2.7.2 Competitive analysis of 12D and 10A

Having elucidated suitable dilution factors for each, both clones were employed in a competitive ELISA analysis (*Section 2.13.3*) wherein a broad free antigen range (5,000ng/mL - 19.5ng/mL) was employed. The results, presented in *Figure 3.25*, indicate that 12D showed clear competition for the antigen in solution, as evidenced by a decreasing A/A0 in the presence of higher concentrations of free antigen. No such trend was observed for the 10A scFv, suggesting that this clone lacked competitive detection capacity.

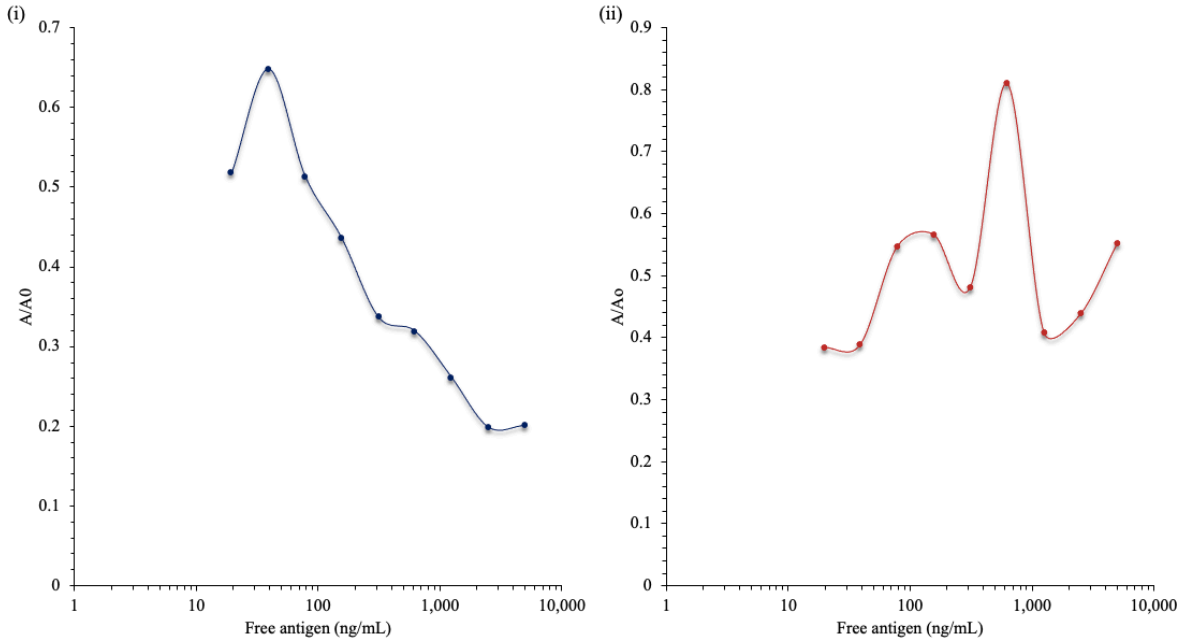

Figure 3.25 Competitive analysis of 12D and 10A lysates

Lysates from ***(i)*** *12D and* ***(ii)*** *10A were applied to the wells of an ELISA plate coated with 1μg/ml CP alongside free CP ranging in concentration from 5000-19.5ng/mL. Bound scFv protein was detected using a HRP-labelled anti-HA antibody. The absorbance was then read at 450nm.*

3.2.8 Sequence analysis of 12D and 10A

Plasmids were isolated from 12D and 10A and sent for sequencing by Source Biosciences Ltd. The resulting nucleotide sequences were translated in Expasy Translate and the CDR regions identified according to the Kabat scheme. The AA sequences were aligned in Multalin, with the CDR alignments shown in *Table 3.2*. Sequence analysis revealed that the CDRs of 12A and 10A contain high variation, as demonstrated by the minimal homology between these regions. Both 12D and 10A feature cysteines in their heavy chain repertoires, and these residues are known to occur more frequently in aves than in other species. It was also noted that the CDR-H3 of the clones, particularly 12D, had a high number of smaller residues, such as alanine (A), threonine (T), glycine (G) and serine (S). It is established that in avian heavy chain repertoires, small residues are present at a higher abundance (54%) than in murine (35%) or human (36%) repertoires. It is suggested that hydrogen bonding via these smaller residues may drive antigen recognition in avian species, while antigen recognition in murine and human antibodies is driven by hydrophobic interactions, mediated through residues such as tryptophan (W), tyrosine (Y), or charged interactions due to AAs

such as arginine (R) (Wu et al., 2012). Although it should be noted that such residues do also appear in avian heavy chain regions, as exemplified by the presence of W, Y and R residues in the CDR-H3 of 12D.

Table 3.2 Comparative sequence analysis of 12D and 10A

CDR regions from the light and heavy chains are displayed for 12D and 10A. Nucleotide sequences were translated in Expasy, the CDRs identified, and the resulting sequences aligned in Multalin.

	CDR-L1	***CDR-L2***	***CDR-L3***
12D	SGGGSSYYG	DNNKRPS	GSFD--SSINSGL
10A	SGSSGSH-G	WDDERPS	GSEDYSSAADSGI

	CDR-H1	***CDR-H2***	***CDR-H3***
12D	FDFSSYGMG	IGNTGGSTGYGPAVQG	CAYGGSWSSYTADRIDA
10A	FAFRNYGVN	SISSDGSRATYGAAVKG	AVS----CCGGPDEIDA

While both clones contained scFv sequences and showed reactivity with the CP in indirect ELISA, 12D was the only clone to show the necessary competitive detection capabilities. Additionally, this clone produced good in-assay signals and had a higher titre point in ELISA compared to 10A. These factors indicated that 12D was the most suitable scFv candidate for use in further assay development, and this clone was carried forward for more in-depth characterisation.

3.2.9 WB analysis of 12D lysate

To confirm scFv expression, lysate sourced from 12D was employed in WB analysis (*Section 2.10.6*) to ensure that a HA-tagged protein of the correct size was present, indicating expression of scFv. The results of the WB are depicted in *Figure 3.26*. A purple-coloured band can be observed at ~30kDa. The molecular weight of the scFv protein alone is roughly 27kDa, however, when expressed from pComb3XSS in XL1-Blue *E. coli*, the scFv is produced alongside a phage coat protein, rendering a scFv-pIII fusion. Therefore, when the molecular weight is analysed, for example in WB, the apparent size is typically higher than

that of the standalone scFv. Based on the reactivity with the HA-tag, which is linked to the scFv, it was confirmed that the 12D clone was producing soluble antibody protein.

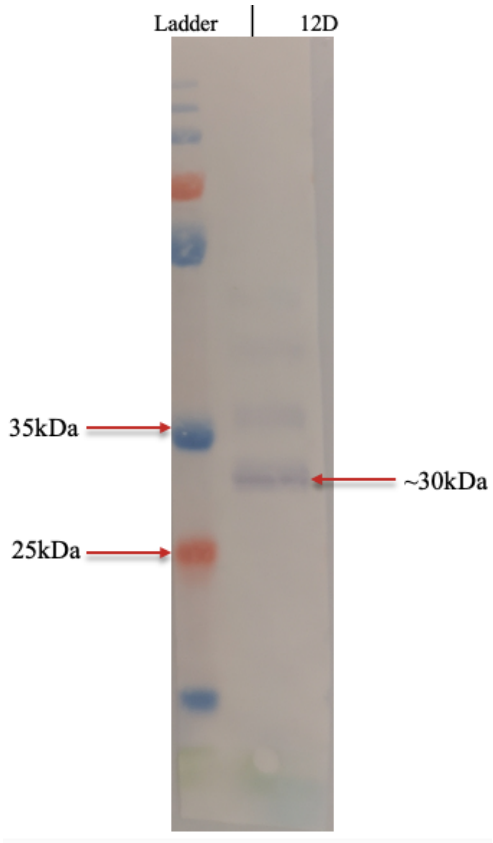

Figure 3.26 WB Analysis of 12D

Lysate enriched with the 12D scFv was run in SDS-PAGE and subsequently transferred to a nitrocellulose membrane in WB. The blot was probed with a HRP-labelled anti-HA antibody. Colour development at ~30kDa indicates the presence of the scFv protein fused to the phage-derived pIII protein (Ladder = PageRuler prestained plus).

3.2.10 Optimisation of expression of 12D

To this point, the scFv sourced from the recombinant antibody library used in biopanning were expressed in the suppressor *E. coli* strain XL1-Blue for the purposes of biopanning and preliminary screening. This strain is chosen for use in phage display as it suppresses an amber stop codon positioned after the scFv and prior to the phage pIII protein. This permits expression of the scFv as a fusion to the pIII phage protein which is essential for the display of scFv in biopanning (Winter et al., 1994; Barderas et al., 2006). Transformation of the scFv-harbouring pComb3XSS plasmid into non-suppressor strains, such as Top10F', facilitates reading of the amber stop codon after the scFv, preventing expression of the pIII

fusion protein. While initial characterisation in XL1-Blue is useful as the fusion protein should not hinder scFv-binding, soluble expression in Top10F' is generally deemed more appropriate for further characterisation of scFv as often the expression level is observed to increase in non-suppressor strains.

To optimise scFv expression, the 12D plasmid was transformed into Top10F' *E. coli,* as per *Section 2.10.11,* and two expression parameters were investigated i.e. the IPTG level and overnight induction temperature. IPTG plays a key role in inducing the lac promoter for protein expression. Using a non-optimised concentration of IPTG can lead to under-induction which results in low yields, or over-induction which can lead to potential aggregation, insolubility and inclusion body formation (Tolia and Joshua-Tor, 2006; Gutiérrez-González et al., 2019). With respect to induction temperature, lower temperatures are often favoured as they can reduce the level of aggregation in the expressed protein by slowing protein synthesis rates (Tolia and Joshua-Tor, 2006). To determine which conditions yield the highest level of scFv expression, cultures were induced with a range of IPTG concentrations (0.1mM – 1mM) and left to express at either 30°C or 25°C overnight. Lysates were obtained for these conditions and tested in ELISA against the CP, as per *Section 2.13.2*. Based on the result (*Figure 3.27*), the IPTG concentration did not appear to play a major role in the expression level of the scFv as no large increase or decrease was observed when varying the concentration, however, the overnight induction temperature was noted to have a greater effect. Cultures of 12D induced at 25°C overnight gave higher absorbance values than those incubated 30°C. This observation was true for all cultures at this temperature, regardless of IPTG concentration. Overall, from the analysis it was decided that 1mM IPTG and an overnight induction temperature of 25°C provided the most suitable expression conditions, as demonstrated by the comparatively increased absorbance in ELISA under these conditions, indicating the highest concentration of scFv achieved.

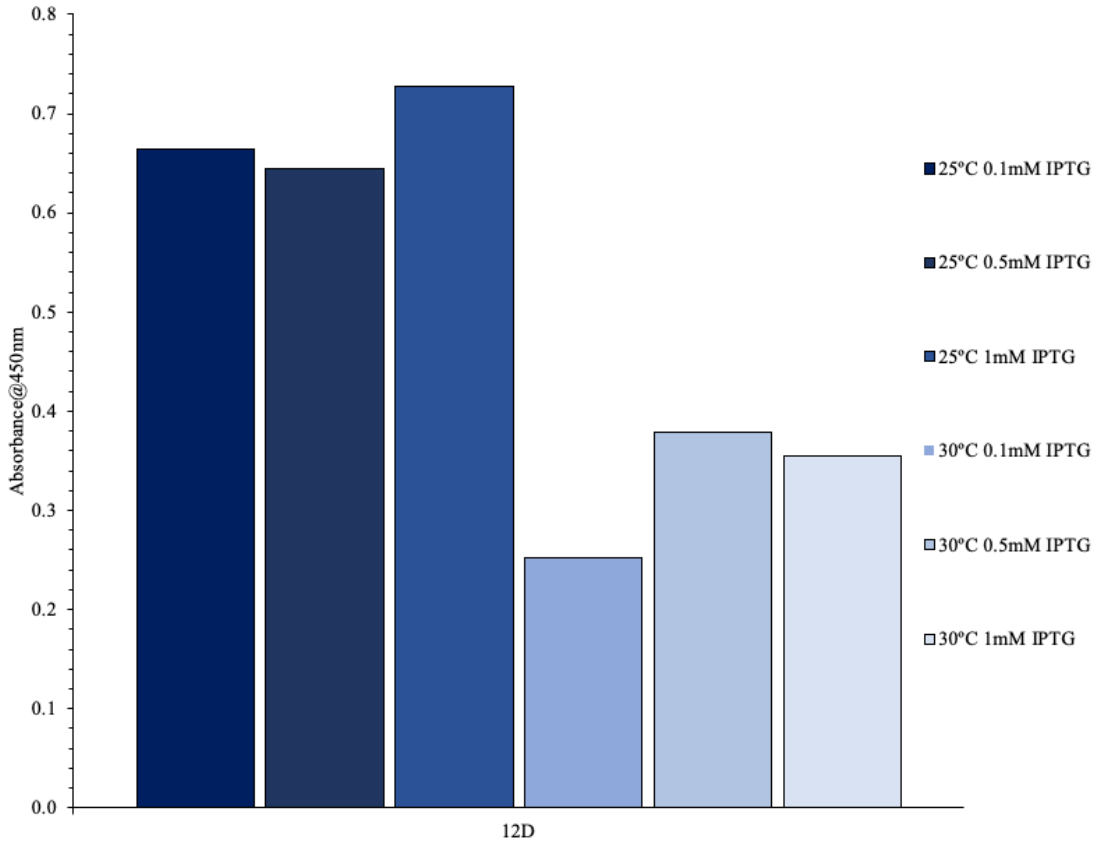

Figure 3.27 Optimisation of expression for the 12D scFv

Cultures of 12D were induced with a range of IPTG, 0.1mM ,0.5mM and 1mM and left to express overnight at either 30°C or 25°C. Lysates from each condition were applied to the wells of an ELISA plate coated with 1μg/mL CP. Bound scFv was detected using a HRP-labelled anti-HA antibody. The absorbance was then read at 450nm.

3.2.11 Further investigation of 12D expression and ELISA parameters

During the process of scaling up and re-expressing 12D for further characterisation, it was noted that the signal arising from the clone in ELISA was inconsistent. From the previous analyses, it could not be determined whether this source of inconsistency arose from poor expression conditions of the clone, or from non-optimised ELISA parameters. In an attempt to investigate this, the 12D clone was expressed under a range of different condition, including varying glucose supplementation and temperature. Additionally, in order to assess the effect of the ELISA parameters, the lysates resulting from each of these expression parameters were employed in an ELISA blocking buffer optimisation to determine the effect of this on the generated assay signal.

To examine scFv expression levels, 12D was first grown in overnight cultures that contained either 1% (v/v) glucose or no glucose. This was to assess whether premature leaky expression of the scFv was resulting in poor cell viability in the overnight starters used for subculturing. To further assess the media composition used for expression, subcultures were prepared from each of these overnights in media supplemented with either 1X 505 or no 505. All cultures were induced with a fixed 1mM IPTG concentration. Two identical sets of these cultures were established. One set was incubated at the previously identified suitable induction temperature of 25°C (*Figure 3.27*), while the other set was incubated at RT O/N to further investigate induction temperature. Alongside the optimisation of expression parameters, the impact of blocking buffer utilisation on the signal generated in ELISA was investigated. This was achieved by applying the lysates from each of the various culture optimisations to ELISA wells under a series of blocking of conditions. Two primary blocking systems were investigated, BSA and powdered milk. For the BSA-block analysis, 12D lysates were diluted in 1% (w/v) BSA and applied to wells blocked with 3% (w/v) BSA. For milk-block analysis, the lysates were diluted in 1% (w/v) powdered milk and applied to wells blocked with 5% (w/v) powdered milk. One further assessment was included whereby the lysates were diluted in 1X PBS and applied to wells blocked with 5% (w/v) powdered milk.

The results of these investigations are depicted in *Figure 3.28*. With respect to the expression analysis, it appeared that clones which were subcultured for expression from O/N starter cultures grown in the absence of glucose expressed the most scFv, demonstrated by higher signal in these tests. Furthermore, the clones which were expressed in media containing no 505 also expressed optimally, with elevated signal arising in these wells when compared to wells containing lysates from the other expression conditions. Furthermore, it was determined that the lower induction temperature, RT, was favoured as lysates from these cultures demonstrated higher signal than those expressed at 25°C.

Regarding the ELISA blocking conditions optimisation, it was found that the blocking buffer played a major role in dictating the signal produced in the assay. The 12D lysates diluted in 1% (w/v) powdered milk had greatly reduced signal when compared to those diluted in 1% (w/v) BSA or 1X PBS, regardless of the culture expression condition. Lysates applied in the BSA-block system presented a relatively high signal in the assay, however, the lysates diluted in 1X PBS had the highest signal. Based on these findings, it was determined that

the chosen blocking buffer and diluent buffer appeared to play a pivotal role in determining the signal produced in the assay and could be the source of the previously observed assay inconsistency.

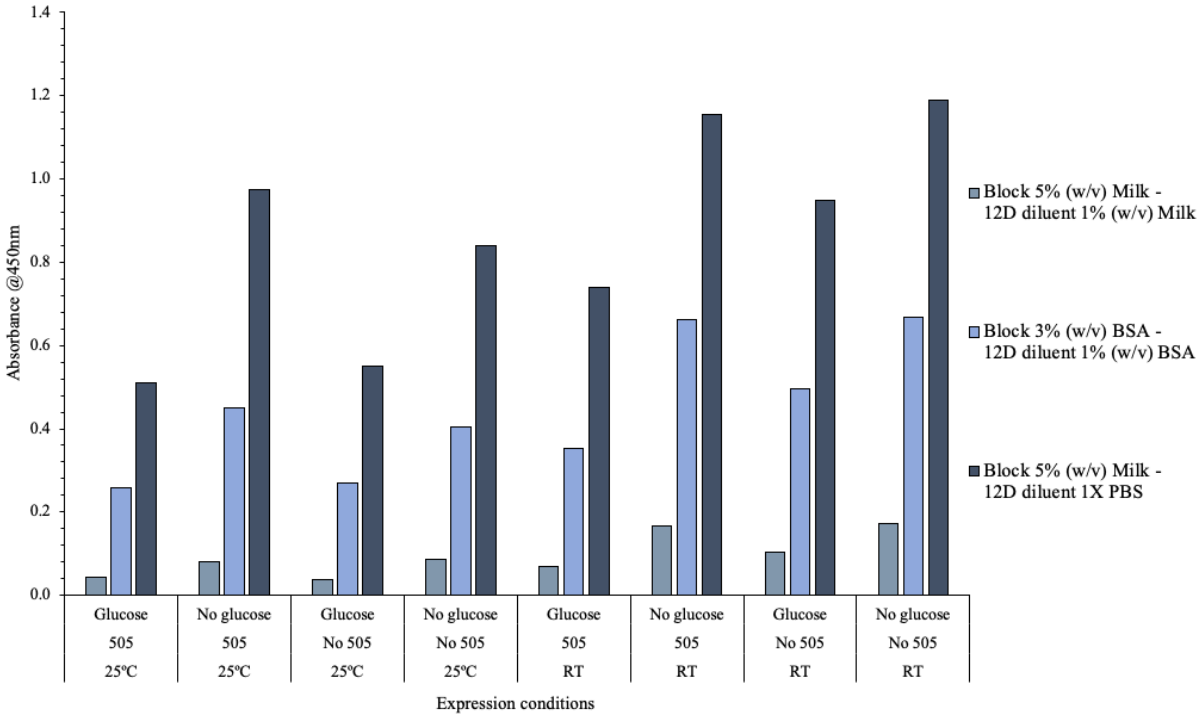

Figure 3.28 Optimisation of expression conditions and blocking buffer for the 12D ELISA *Overnight cultures of 12D were set up either with 1% (v/v) glucose or no glucose. These were subcultured into fresh cultures the next day containing either 1X 505 or no 505. The induced cultures were incubated at either 25°C or RT. Lysates from each condition were diluted 1 in 4 in either 1% (w/v) BSA, 1% (w/v) powdered milk or 1X PBS and applied to the wells of an ELISA plate coated with 1µg/mL CP. Bound scFv was detected using a HRP-labelled anti-HA antibody. The absorbance was then read at 450nm.*

To further investigate the impact of blocking buffers on the 12D binding characteristics, a small-scale competitive assay was established using BSA or powdered milk block systems. ScFv-enriched lysates were diluted in either 1% (w/v) BSA, 1% (w/v) powdered milk or 1X PBS and applied, alongside free CP antigen, to wells blocked with either 3% (w/v) BSA or 5% (w/v) powdered milk. As described in *Section 3.2.6*, this assay was in competitive format, therefore, a lower absorbance value is expected in the wells containing free antigen. The results in this analysis were reported in absorbance, as opposed to the typical 'A/A0' used for competitive assays, in order to reflect the signal achieved under each block

condition. The results are shown in *Figure 3.29.* In three of the four analyses, the signal was seen to reduce with high antigen concentrations (20µg/mL), suggesting that there was still binding occurring between 12D and the CP antigen. However, it was still apparent that the employed diluent buffer was playing a key role in the binding of 12D to the CP.

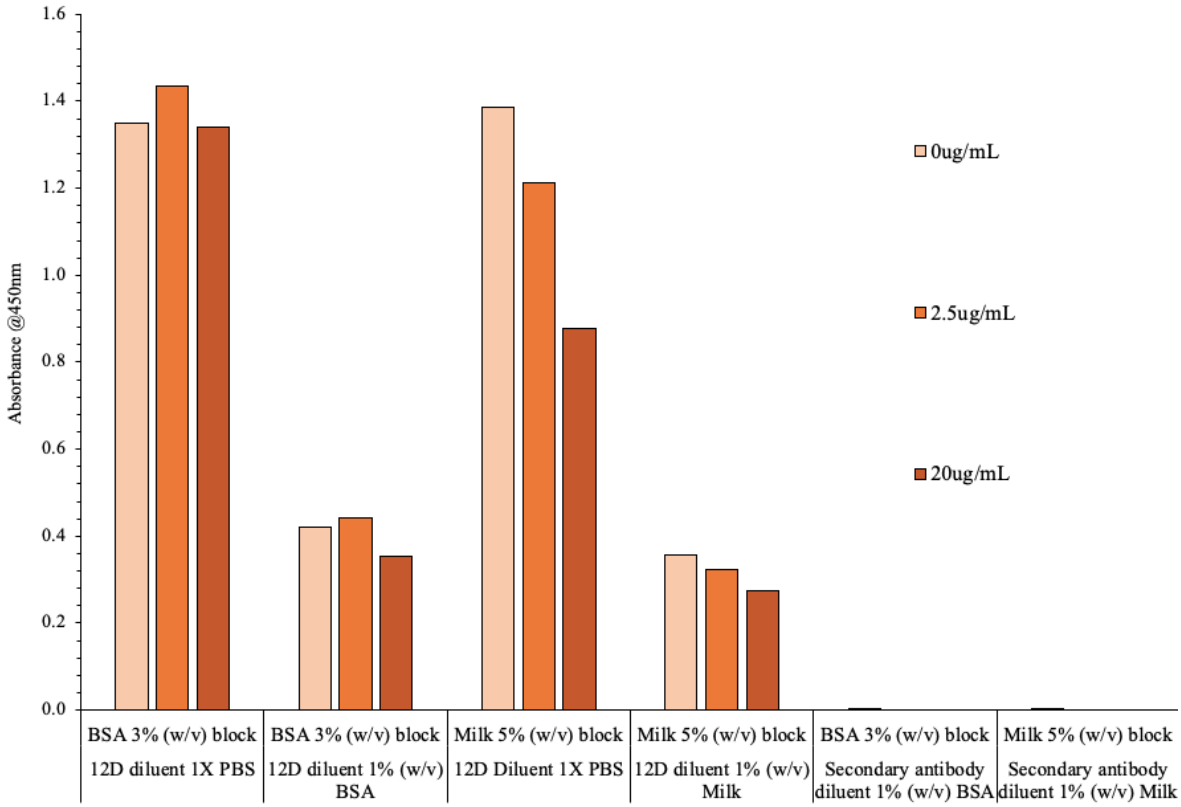

Figure 3.29 Optimisation of blocking for competitive ELISA

The wells of an ELISA plate coated with 1µg/mL CP. The wells were then blocked with either 3% (w/v) BSA or 5% (w/v) powdered milk. Free CP antigen was applied at various concentrations (20µg/mL, 2.5µg/mL and 0µg/mL) alongside 12D lysate diluted 1 in 8 in either 1% (w/v) BSA, 1% (w/v) powdered milk or 1X PBS. Bound scFv was detected using a HRP-labelled anti-HA antibody. Control reactions are shown for the secondary antibody whereby PBS was applied in lieu of 12D lysate and the anti-HA secondary antibody was applied in the described diluent thereafter. The absorbance was then read at 450nm.

3.2.12 Large-scale expression and purification of 12D

The 12D scFv was expressed under the conditions identified in *Section 3.2.10.* Expression and purification in IMAC via the scFvs hexahistidine tag was performed as described in Sections *2.15.1* and *2.15.2*. The purification fractions were run in SDS-PAGE and WB to

assess the purification of the protein. Successful purification is evidenced by the ~27kDa band present in the elution lanes of the SDS-PAGE (*Figure 3.30 (i)*) and by the purple colour development at the same size in the WB (*Figure 3.30 (ii)*). A slightly smaller band, ~25kDa, and a larger band, ~50kDa-55kDa, was also recognised to be reactive with the HRP-labelled anti-HA secondary in the WB. The smaller band may be attributed to slight degradation of the scFv, either throughout expression, purification or storage of the scFv, while the larger band could be attributed to a dimerised form the of scFv given that its weight is roughly double that of an scFv monomer. The resulting elution fractions were concentrated, and buffer exchanged into PBS.

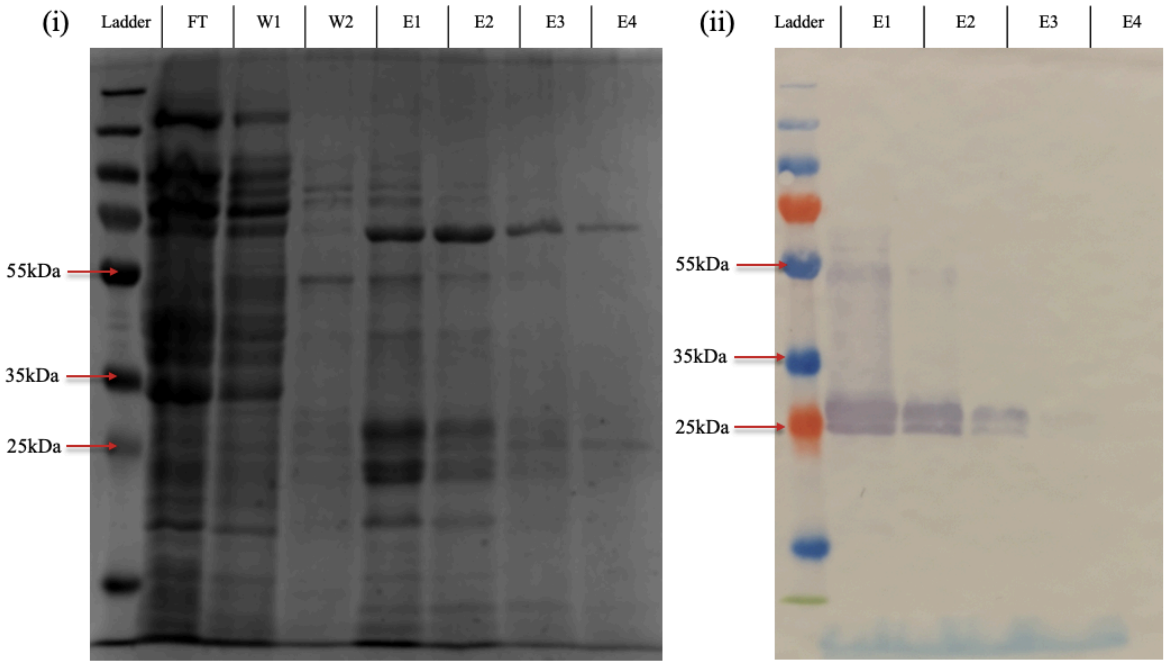

Figure 3.30 Ni-NTA chromatography purification of the 12D scFv

(i) *SDS-PAGE gel depicting each fraction of the purification process.* ***(ii)*** *Elution fractions probed with a HRP-labelled anti-HA antibody (Ladder = PageRuler prestained plus, FT = flow through (1:2), W1 = 20mm imidazole wash buffer, W2 = 30mM imidazole wash buffer, E1-E4 = elution fractions 1 to 4).*

3.2.13 Purified antibody titre and competitive analysis

The purified 12D scFv was titred against the CP antigen in indirect ELISA. This was achieved by preparing a series of dilutions of 12D in 1% (w/v) powdered milk and applying them to wells coated with CP as described in *Section 2.17.1*. In addition to a titre, a competitive analysis was performed whereby the CP in a range of concentrations was

applied to CP-coated wells alongside the 12D scFv. The results of the titre and competitive analyses are depicted in *Figure 3.31 (i)* and *(ii)*. The results indicate that the purified 12D antibody retained binding to the antigen in indirect ELISA. However, only minimal competition was observed for the free antigen, with a slight reduction in A/A0 achieved toward free CP concentrations of 5µg/mL. This analysis confirmed that the 12D antibody could be successfully purified through IMAC. Further assay optimisation using a purified form of the scFv would be preferred to the continued use of lysates as a purified sample should yield less non-specific signal.

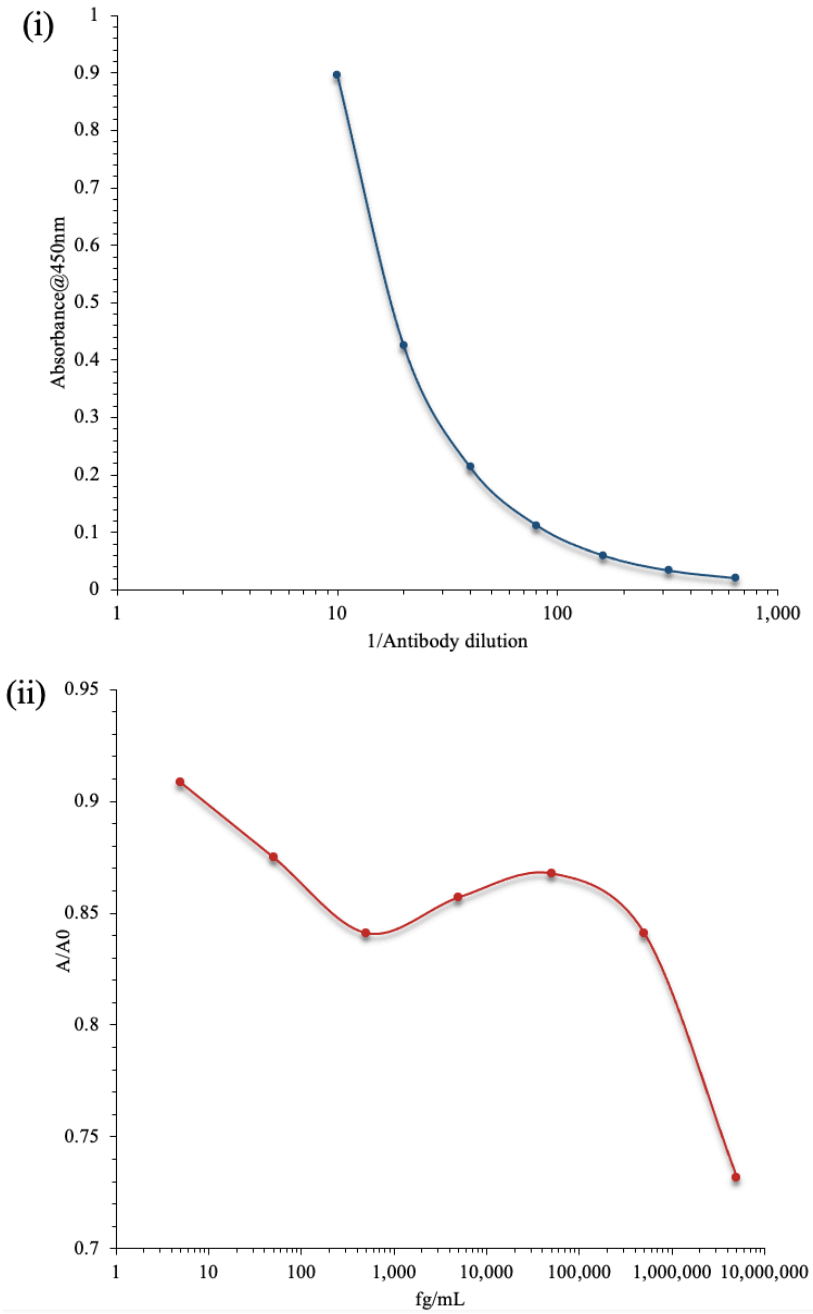

Figure 3.31 Titration and competitive analysis of purified 12D

(i) *The 12D scFv was prepared in a series of dilutions prior to application to the wells of an ELISA plate coated with 1μg/mL CP.* ***(ii)*** *Competitive analysis whereby 12D was applied to wells alongside free antigen concentrations ranging from 50fg/mL - 5,000,000,000fg/mL. Bound scFv was detected using a HRP-labelled anti-HA antibody. The absorbance was then read at 450nm.*

3.3 Discussion

The work in this chapter aimed to generate recombinant antibody candidates to aid in the improved detection of PVY, a damaging and economically important virus of potato. It was proposed to achieve this using a combination of recombinant protein expression in conjunction with immunoassay development as such assays exhibit good sensitivity and may eventually be developed into user-friendly formats.

To this end, a recombinant anti-PVY scFv library was successfully constructed. To perform screening of this library and subsequent characterisations of PVY-binding clones, a reliable supply of PVY-specific antigen was required. Presently, no commercial PVY antigen is available, therefore, it was proposed to generate an antigen with which the library could be screened. For this, the PVY CP was chosen. This structural protein is expressed in high abundance and is an essential viral protein, involved in both the transmission and packaging of PVY (Kežar et al., 2019). Furthermore, the CP was shown to harbour regions of highly conserved AA sequences which would facilitate 'broad-spectrum' detection of PVY (Vuento *et al*, 1993). This was considered advantageous with respect to assay development as, at minimum, only one antibody would be necessary to detect many strains of the same virus. In this work, the CP gene was successfully cloned into a vector and expressed in an *E. coli* system. From this, the CP could be rapidly produced in soluble form and purified through IMAC. Overall, this provided a reliable and convenient method through which a PVY-specific antigen could be expressed for multiple applications, including screening campaigns, assay characterisations, standard curve generation, or for incorporation as a positive control in future field-trials.

Upon successful isolation of the CP antigen, it was employed in the screening of the recombinant scFv library. From this screening, one primary clone of interest was isolated, denoted 12D. This clone displayed the capacity to detect the CP antigen in indirect ELISA and in soluble form in competitive ELISA. However, during additional preliminary analysis and scaling-up of 12D it was noted that the apparent binding pattern of the antibody was irregular. To investigate this, a series of optimisations were performed with respect to both the growth conditions of the cultures and the employed ELISA blocking and dilution buffers. The results revealed that while expression conditions did not appear to play a major role in the generated signal, the employment of specific blocking buffers dictated the in-assay signal to a large extent. Of specific note in the research was the effective blocking of signal in

indirect ELISA when using a complicated blocking reagent such as powdered milk when compared to a more homogenous block such as BSA. Based on these findings, it is clear that extensive optimisation of the employed ELISA conditions is necessary if future assay development with 12D is to be considered. This could involve the further investigation and application of alternative blocking buffers including powdered milk, BSA, serum, fish gelatin and also the addition of detergents such as SDS, Tween or Triton-X-100 to buffers, all of which can reduce the level of non-specific binding occurring in immunoassay (Crowther, 1995).

The impact of complicated blocking buffers with antibody binding was previously observed. One study identified scFv antibodies which demonstrated binding to the target antigen in basic diluents, however, struggled to detect antigen in a more complex diluent solution, PBS with 1% (w/v) milk, in addition to displaying some off-target binding (Tiller et al., 2017). In the study, the non-specific binding was attributed to the presence of charged residues, primarily arginine, in the more hydrophilic regions within the antibody CDRs. Furthermore, other investigations into antibody interactions have confirmed the potential negative impact that the arginine residues in the binding regions may impart, particularly with respect to non-specific binding (Birtalan et al., 2008; Tiller et al., 2017; Rabia et al., 2018; Zhang et al., 2020c). Based on this, it could be hypothesised that some residues in 12D polypeptide sequence may be contributing to polyspecificity, permitting CP binding in simpler block buffers, but causing inhibition of binding in more complex block solutions. The presence of any non-specific binding to components of the assay matrix is unfavourable given that 12D is destined to be used for plant pathogen detection, and would be required to detect antigen from highly complex matrices. As such, it is paramount that off target binding is abrogated to the greatest extent possible.

While alteration of blocking buffers may be of use, it is likely that more permanent alteration of the scFv would be required for future immunoassay development. For this purpose, it would be of interest to explore the potential enhancement of 12D through alteration of its arginine residues, of which there are two identified within the CDR regions, one in the CDR-L2 and one in the CDR-H3. Of primary utility would be alteration of the CDR-H3 region as this binding site is well regarded as one of the most important regions in antigen-binding and specificity determination (Xu and Davis, 2000). To facilitate site-specific alteration of the proposed arginine residue, site-directed mutagenesis could be used. Conversely, random

mutagenesis or CDR shuffling could be employed for a more uncontrolled diversification of the CDR-H3 (Borrebaeck, 2000; Kennedy et al., 2017). The application of mutagenesis methods within this region may yield an antibody with altered antigen-binding characteristics and potentially enhanced specificity or sensitivity for the CP.

In conclusion, this chapter discusses the generation of a recombinant scFv library against the prevalent crop pathogen PVY. Additionally described is the generation, expression and purification of a PVY-specific antigen. This CP target may serve multiple purposes including use as both an antigen for screening and for future assay characterisation. The screening of the scFv library with the CP yielded one clone in particular, 12D, which initially presented high assay signal and competition for the CP antigen. However, based on the observed interference of the employed blocking buffer on the functionality of 12D, it is a necessity to further investigate the specificity of this clone. Mutagenesis of certain residues within the binding regions, particularly the CDR-H3, of 12D could improve the binding characteristics, particularly with respect to specificity. However, thorough investigation of the qualities of any resultant scFv derivative would be required to ensure that the antibody possessed the requisite fidelity for the CP antigen, in the absence of non-specific interactions with sample matrices.

Chapter 4

Characterisation of Monoclonal Antibodies and their Engineered Recombinant ScFv and ScAb Derivatives

4.1 Introduction

One of the desirable traits of recombinant antibodies is that the characteristics of a given antibody can be altered and enhanced. This is achieved through a number of methods. Three commonly used engineering approaches for *in vitro* optimisation of antibody characteristics are site-directed mutagenesis, random mutagenesis and chain-shuffling (Igawa et al., 2011). Mutagenesis methods can be used to target the highly variable regions, i.e. the CDRs, or to target the more conserved framework regions flanking the CDRs in the variable heavy and variable light chains. Site-directed mutagenesis of amino acids can be achieved by using tailor-made primers to introduce specific point mutations to the antibody sequence, while random mutagenesis can be performed using error-prone PCR (Fujii, 2004). More recently, *in-silico* methods are employed to aid in the identification of amino acids which are proposed to be involved in traits such as antigen binding or stability. This facilitates exact targeting of hypothetical binding sites or framework regions and can be used in conjunction with site-directed mutagenesis approaches for an increased confidence that the targeted residues are implicated in the characteristic to be altered (Baran et al., 2017; Zhao et al., 2018). Mutagenesis is performed with the ultimate goal of altering certain residues within the binding pocket, or framework regions, in an attempt to enhance a particular quality such as specificity, sensitivity or stability. Chain shuffling is another approach used for antibody enhancement, whereby, one variable chain is fixed, while the other is 'shuffled' (Wark and Hudson, 2006). This leads to a new repertoire of recombinant antibodies sharing one homologous variable chain while presenting a large number of variations on the second, 'shuffled' chain. This can have marked improvements on antibody binding properties (Fitzgerald et al., 2011; Rangnoi et al., 2018). While these engineering methods are useful and relatively rapid, they are largely restricted to recombinant antibody technology whereby the antibody proteins are expressed from vectors. This limits their capacity to be applied to other classical means of antibody production such as hybridoma technology. To overcome this, additional antibody engineering approaches in the form of restructuring of full-length antibodies into their recombinant forms may be undertaken. This permits expression of the Ig genes in soluble, fragmented form from recombinant vectors. Restructuring of full-length antibodies into their various recombinant derivatives can play a role in many factors including effector function, solubility, stability, avidity or sensitivity (Reader et al., 2019). Some of the primary methods by which antibodies can be altered are summarised diagrammatically in *Figure 4.1*.

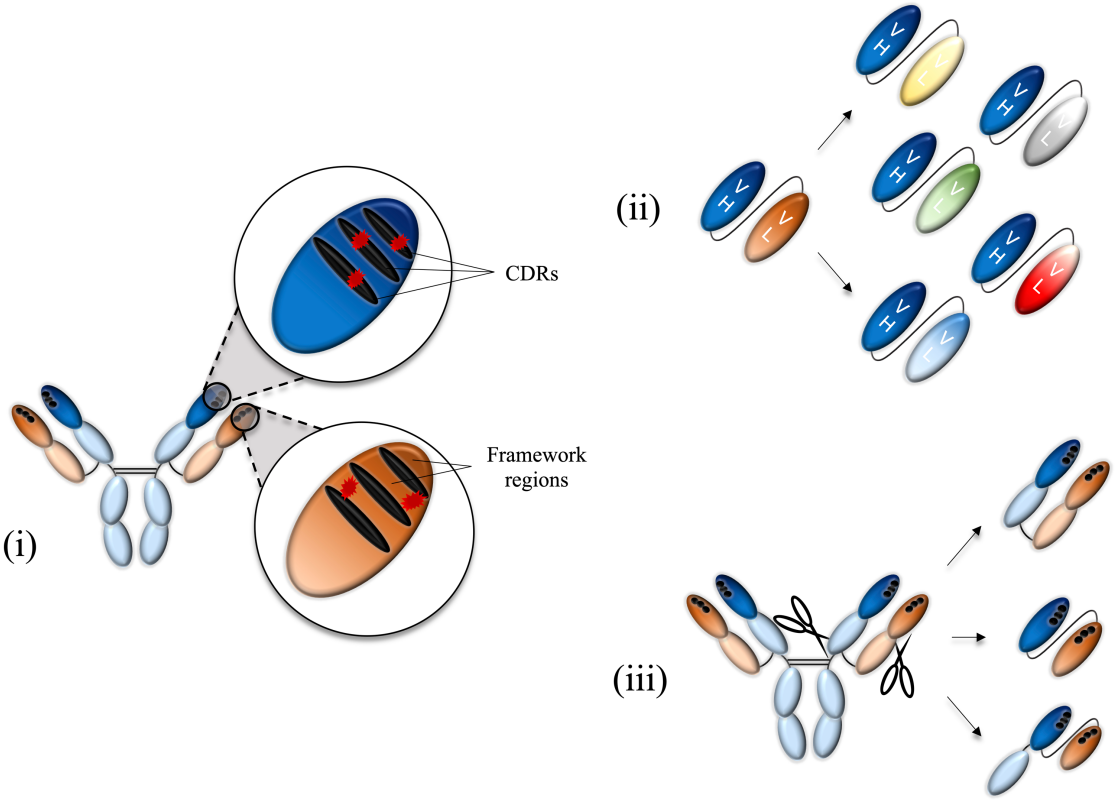

Figure 4.1 Simplistic representation of various antibody engineering methods

(i) Mutagenesis can be performed on both the CDRs and framework regions, causing alteration (represented in red) of certain residues. The altered amino acids can be specifically targeted through site-directed mutagenesis, or randomly introduced through methods such as error-prone PCR. (ii) Chain shuffling fixes one chain, for example the heavy chain, while the other chain is interchanged, or "shuffled". (iii) Genes can be isolated from full-length antibodies and engineered into recombinant formats consisting of various constant and variable domain combinations.

Hybridoma technology is the traditional means by which full-length antibodies, typically IgG, are isolated. Hybridoma lines are generated via the immortalisation of B-cells, most commonly murine-derived, through fusion with an immortal myeloma cell line, typically in the presence of polyethylene glycol (PEG). As fusion efficiency is generally low, a specific media, termed HAT (Hypoxanthine, Aminopterin and Thymidine), is used to select for fused cells. The immortal myeloma cells lack the requisite gene for survival on this media. Contrastingly, B-cells contain the necessary gene for survival, however, lack the ability to survive independently for long durations in the absence of an immortal fusion partner. Therefore, the fusion between B-cell and myeloma endows the fused hybrid cell, the hybridoma, with both immortality and the genes needed to survive on the selective media

(Köhler and Milstein, 1975; Liu, 2014). Fused hybridomas are grown to such a point where a limiting dilution method can be employed. This facilitates the isolation of single hybridoma lines, thereby making the line "monoclonal" (Parray et al., 2020). Hybridomas generally secrete monospecific antibodies, termed monoclonal antibodies (mAbs). The secreted antibody can be harvested directly from the surrounding culture media and the media used for preliminary antigen-binding analysis, permitting screening of the clones prior to cell line expansion or further antibody purification. Upon confirmation of antigen binding, the expressed antibody can be grown and purified through various methods, with some of the most common being a combination of protein precipitation and affinity chromatography using resin conjugates such as Protein A, G, A/G or L (Arora, Saxena, and Ayyar, 2017). While the full-length antibody is often desirable when there is a requirement for low immunogenicity, effector functionality or when a longer half-life is necessary, traits typically valued in therapeutic endeavours, the full-length molecule is generally not a prerequisite for immunodiagnostic applications. Given that fragments of the full-length antibody can be expressed at high yields with a fast rate in hosts such as *E. coli* or yeast, as opposed to the mammalian cell culture conditions required for mAbs, it is useful to investigate the binding properties of the recombinant forms of the parental whole mAb when developing diagnostic platforms.

Previously, reformatting of mAbs into their respective fragments was facilitated through digestion of full-length antibodies by enzymes such as papain or pepsin. Proteolytic cleavage by papain cuts above the IgG disulphide bond at the hinge region, yielding two monovalent Fab fragments. Pepsin acts below the disulphide bond, producing a single $F(ab')_2$ fragment (Lipman et al., 2005). Partial antibody fragments could be isolated in this manner, however, this method requires constant production of the whole antibody in cell culture followed by the need for subsequent digestion and further purification, making it a relatively arduous means to isolate fragmented forms of antibodies. Recombinant technology has overcome these challenges by introducing the capability to clone the antibody genes of interest and place them in expression vectors from which recombinant homologues of the antibody can be continuously produced in short time frames (Basu et al., 2019). This method maintains the fidelity of the CDRs designated to the full-length antibody, while providing a means to express the binding regions in inexpensive hosts. Restructuring of a full-length antibody into its fragments offers the immediate benefit of quick protein production when compared to mammalian culture, which is required to express full-length, glycosylated IgG. However,

characterisation of the binding and expression of the recombinant forms is necessary to ensure functionality and applicability of the antibody fragments. Of the recombinant forms of antibody, scFv and scAbs are the second and third smallest in size, respectively. They can be expressed in *E. coli* and purified rapidly and at low-cost through the use of chromatographic methods such as IMAC or other affinity chromatography procedures. Due to the advantages of the quick and economic production of these recombinant forms for application to diagnostic method development, this chapter focuses on the investigation of restructuring full length anti-PVY mAbs into their fragmented forms, namely the scFv and scAb derivates, and the subsequent characterisation of these antibodies.

In addition to the characterisation of mAbs, scAbs and scFvs, the work described in this chapter endeavoured to create a 'proof-of-concept' biosensor in the form of a surface plasmon resonance (SPR)-based bioassay. SPR is a sensitive means of monitoring biomolecular interactions between various entities such as enzymes and substrates, receptors and drugs, viruses and cells or, for the purposes of this work, antibodies and antigens. The SPR phenomenon occurs upon projection of polarized light, 'incident' light, through a prism at a particular angle, the resonance angle, onto a metallic sensor surface, typically made of gold. The incident light is absorbed by electrons at this gold interface, yielding surface plasmon waves which oscillate along the gold surface. The gold surface reflects the incident light, now termed reflected light, and this is detected by a light sensor. The angle at which this light is reflected is dictated by the refractive index of the sensor surface. It is this concept of refractive index which permits the measurement of biomolecular processes. Interactions between molecules immobilised on the gold surface and molecules flowing through the system in solution bring about changes in the mass to charge ratio at the sensor surface. The mass to charge ratio impacts the refractive index of the surface, and thereby the angle at which the incident light is reflected. The changes in the angle of the reflected light can be measured to determine binding characteristics (Mariani and Minunni, 2014; Nguyen et al., 2015; Zhou et al., 2019). A simplified diagram of the principle of SPR sensing when using antibodies and antigens is depicted in *Figure 4.2*.

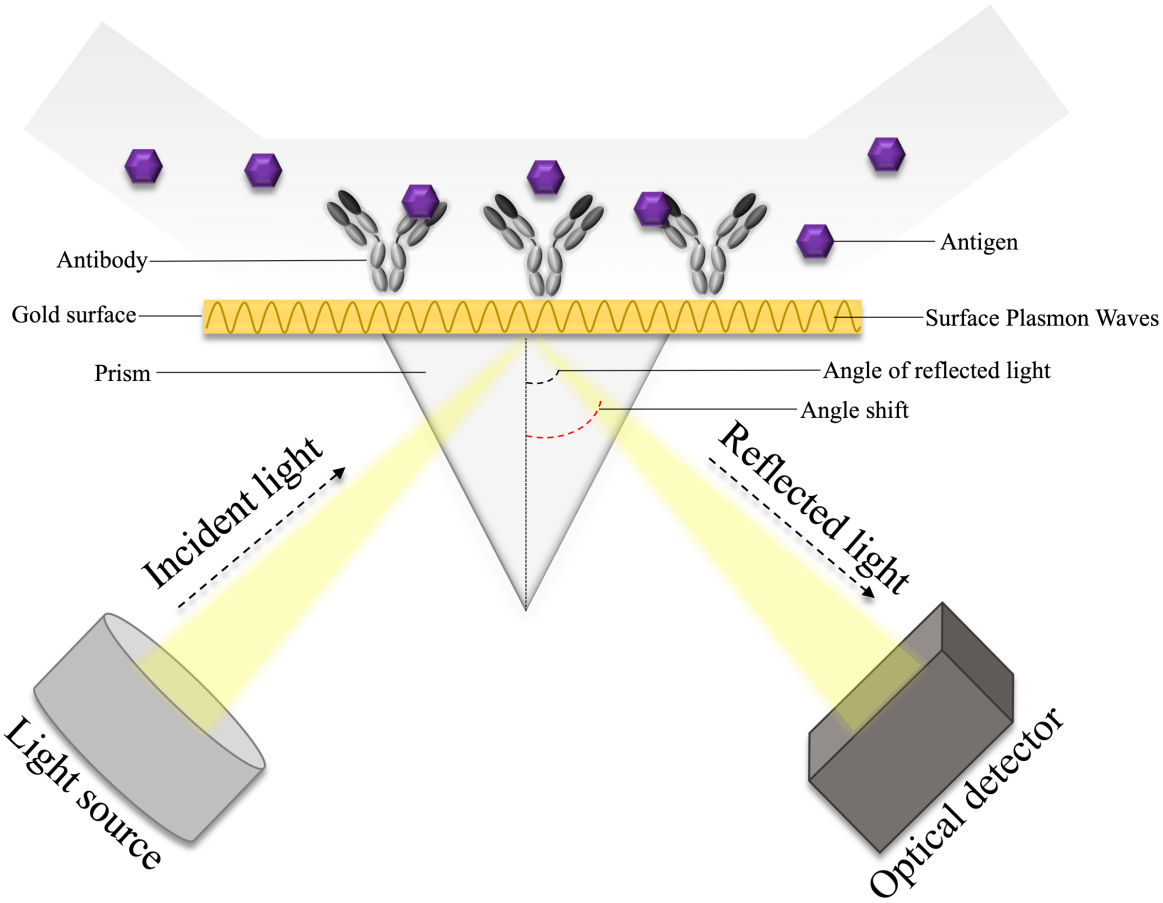

Figure 4.2 Simplified schematic of SPR-based systems

The gold surface is functionalised with a biomolecule, for example an antibody, also known as the ligand. Thereafter, the interaction partner, in this case an antigen, also known as the analyte, is passed over the surface. Binding between the antibody and antigen causes a change in refractive index of the sensor surface, which in turn shifts the angle of the reflected light. The changes in the angle of reflected light are measured, allowing the elucidation of biomolecular interaction characteristics.

It was proposed to employ SPR within this work both to characterise the binding of the generated antibodies to their antigens, and to also develop an immunosensor-based platform whereby PVY antigens could be detected from solution in a 'real-time', 'label-free' system.

4.2 Results

4.2.1 Generation of recombinant antibody forms from monoclonal antibodies

Four mAbs, derived from anti-CP IgG-secreting hybridomas lines, were chosen for reformatting, namely 9A1, 41B, 11B2 and 20D. These mAbs were previously sequenced

and their CDRs and framework regions identified by Absolute Antibody, providing a means of generating recombinant versions of the antibodies. The CDRs of each of the selected antibodies are aligned in *Figure 4.3*. For scFv reformatting, the variable heavy and light chain sequences were joined by a glycine serine linker in V_L - V_H format. ScAb homologues of the hybridomas were generated similarly, with the exception of the addition of an avian constant light region following the V_H. Gene inserts, codon optimised for *E. coli* expression, for the scFv and scAbs were generated and cloned into the pComb3XSS vector by Eurofins. The antibody-harbouring plasmids were transformed into Top10F' *E. coli* by heat shock (*Section 2.10.11*). From the transformation plates, single colonies were selected and plasmids isolated. These plasmids were sent for sequencing by Source Biosciences Ltd in order to verify correct insert sequence and orientation. Upon confirmation of correct inserts for all clones, small-scale expression analysis was commenced using the scFv formats for each.

Table 4.1 CDR alignment of anti-PVY antibodies

The CDRs, denoted according to the Kabat number scheme, were aligned in Multalin.

Antibody	***CDR-L1***	***CDR-L2***	***CDR-L3***
9A1	RSSQSIVHSNGNTYLE	KVSNRFS	FQGSHVPWT
41B	RSSQSIVHSNGNTYLE	KVSNRFY	FQGSRVPPT
11B2	RASENIYSY-----LA	NAKTLGE	QHHYGTPFT
20D	RSSQSIVHSNGNTYLE	KVSNRFS	FQGSHVPRT
	CDR-H1	***CDR-H2***	***CDR-H3***
9A1	TSGMGVG	HIW-WDDVKRYNPALKS	IRTDHDAAMDY
41B	DTYMH	RIDPANGNTKYDPKFQG	IAYGSSYAMDY
11B2	SDYAWN	YIS-YSGITSYNPSLKS	F--DGFDGFPY
20D	DYEMH	AYHPGSGGTAYNQKFKG	ASY--------

4.2.2 Preliminary binding analysis of reformatted scFv

4.2.2.1 Lysate titre

Initial analysis was performed using the scFv format of all four clones, 9A1, 41B, 11B2 and 20D. The clones were expressed small-scale using 1mM IPTG and an O/N induction

temperature of 30°C. After expression, lysates for each clone were obtained and titred against the CP antigen as per *Section 2.13.2*. Results of the titre are shown in *Figure 4.3*. The initial titre showed that three of the four clones produced signal in the assay, namely, 11B2, 41B and 20D. Of these, 41B generated the highest signal of all the clones. Clone 9A1 did not exhibit any signal in the assay.

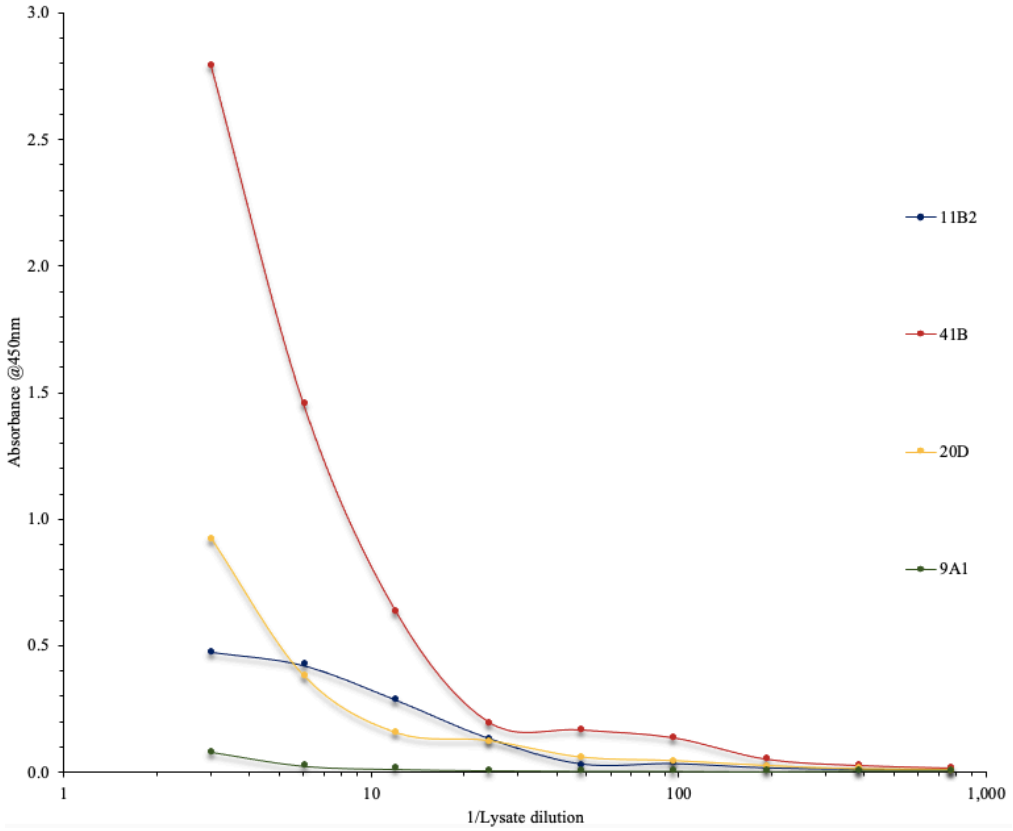

Figure 4.3 Lysate titre of reformatted scFv clones

Lysates were obtained and applied in doubling dilutions to the wells of an ELISA plate coated with 1µg/mL CP. Bound scFv was detected with a HRP-labelled anti-HA antibody and the absorbance was read at 450nm on a Tecan Safire™ plate reader.

4.2.2.2 Competitive analysis of lysate

In addition to the titre, a small-scale competitive analysis was performed using these lysates, as per *Section 2.13.3*, whereby free CP antigen was added to the wells at concentrations of 5µg/mL or 0.5µg/mL. In competitive analysis, wells containing higher concentrations of free antigen in solution should present with lower signal as less antibody is available to bind to the immobilised antigen. Results are depicted in *Figure 4.4*. Of the clones, 11B2, 41B and 9A1 exhibited the competitive characteristic of lower absorbance in the wells containing free

antigen. As observed previously in the antibody titre, 9A1 displayed a low in-assay signal. The results of the competitive analysis are reported as absorbance to reflect this.

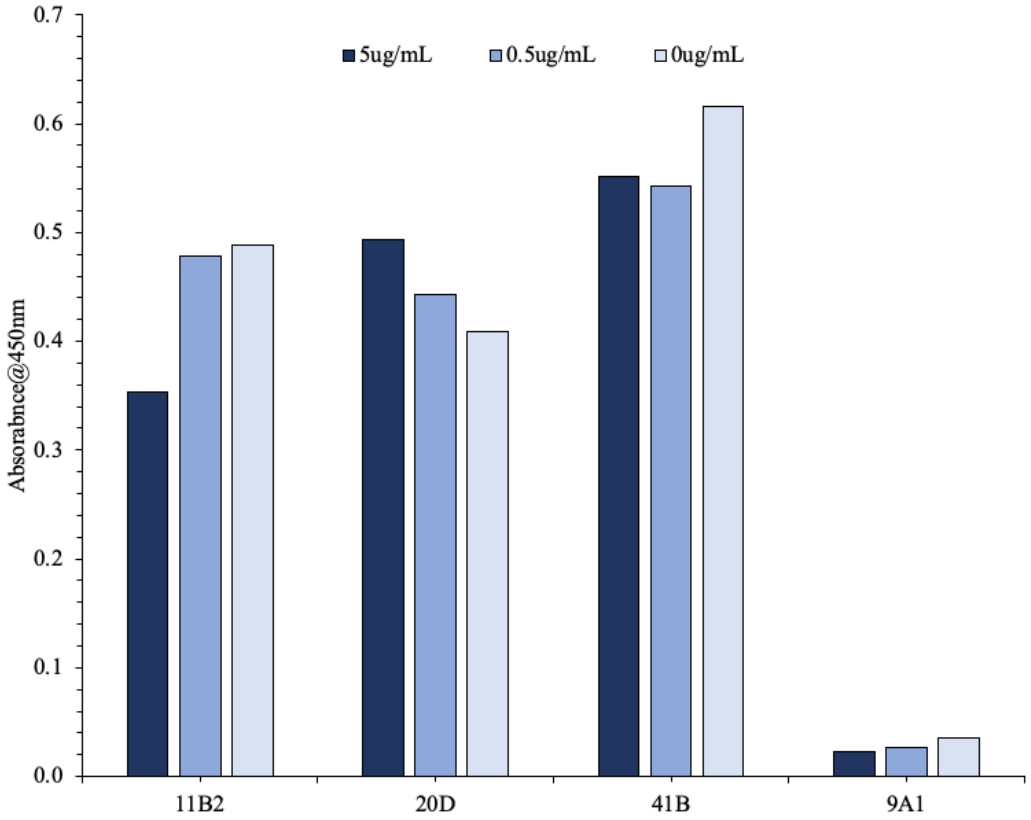

Figure 4.4 Competitive analysis of reformatted scFv clones

Lysates were obtained and applied to the wells of an ELISA plate coated with 1μg/mL CP alongside free CP antigen concentrations of 5μg/mL, 0.5μg/mL or 0μg/mL. Bound scFv was detected with a HRP-labelled anti-HA antibody and the absorbance was read at 450nm.

Given that it was previously established that clone 9A1 had the capacity to bind the CP in its full-length IgG format, it was decided to investigate whether alternative expression parameters would affect the observed binding. Parameters such as IPTG and induction temperature play a significant role in the expression level of the protein, with unfavourable conditions often resulting in low yields and, therefore, low in-assay signal. To investigate whether this was the case for 9A1, it was decided to re-express each clone under altered expression parameters and monitor the subsequent binding.

4.2.2.3 Expression of clones under alternative conditions

The clones were re-expressed using a lower IPTG concentration, 0.1mM, and a lower O/N induction temperature, 25°C. Lower temperatures and reduced IPTG concentrations are linked to slower *E. coli* metabolism and reduced rates of recombinant protein expression induction, respectively. These can aid in the production of correctly folded and functional proteins, which in turn can increase the in-assay signal. The new titre under these conditions is shown in *Figure 4.5*. On this occasion, it appeared that all clones titred, indicating that the reduced absorbance in the previous analysis could be attributed to unfavourable expression conditions for some clones.

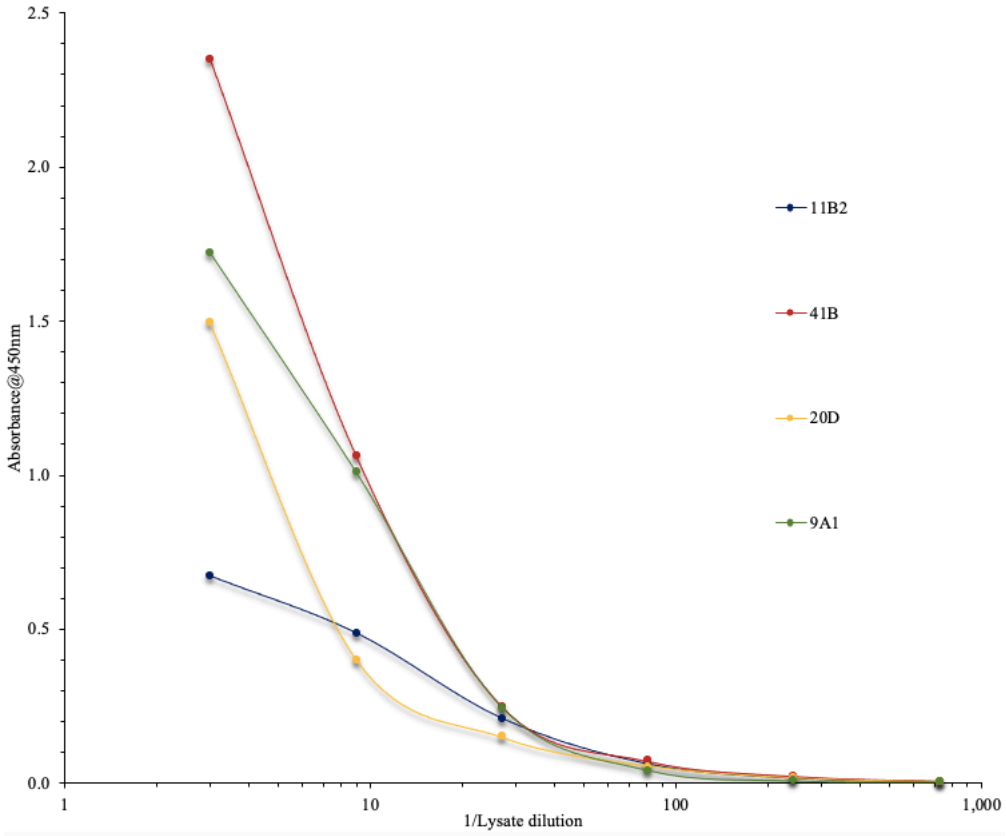

Figure 4.5 Lysate titre of scFv clones expressed under alternative conditions

Lysates were obtained and applied in a series of dilutions to the wells of an ELISA plate coated with 1µg/mL CP. Bound scFv was detected with a HRP-labelled anti-HA antibody and the absorbance was read at 450nm.

Having observed an increase in signal from all the tested clones when using these new expression parameters, it was decided to re-assess the competitiveness of the clones of interest.

4.2.2.4 Competitive analysis of clones expressed under alternative conditions

The competitive described in *Section 4.2.2.2* was repeated once more using lysates from these new expression conditions. From the results (*Figure 4.6*), it appeared that 11B2 and 41B persisted with a competitive signal, this is in contrast to 9A1 which, on this occasion, did not appear to present any competition for the free antigen. Clone 20D also failed to present competition for the free CP.

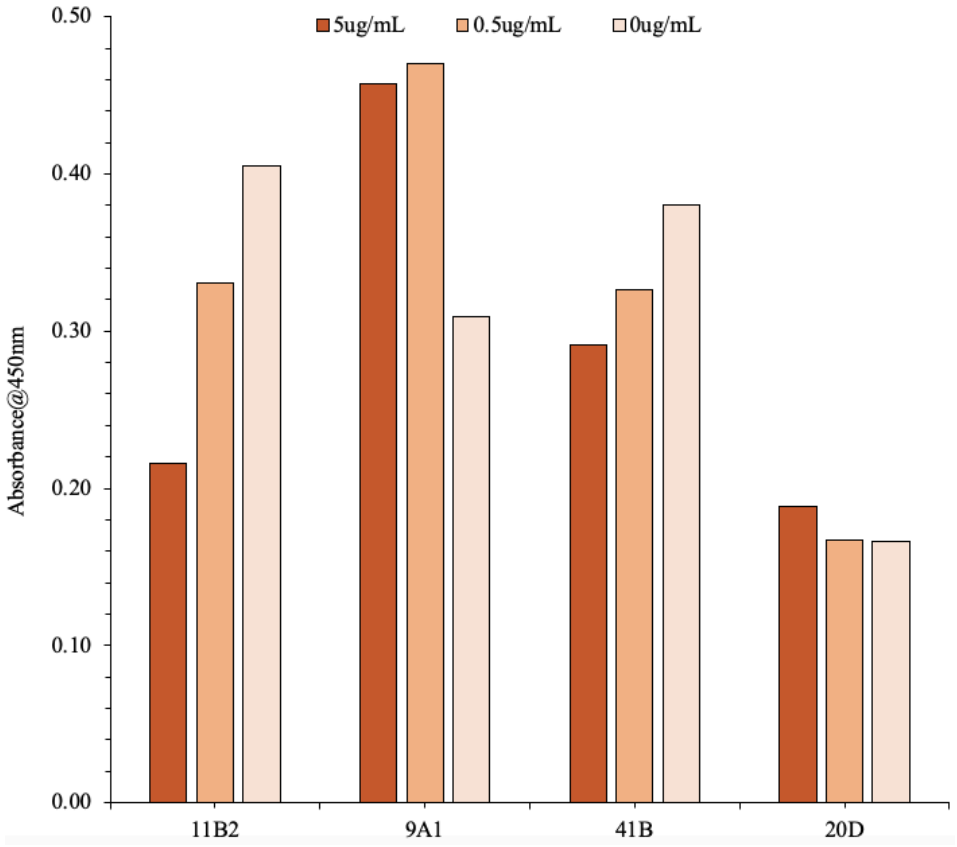

Figure 4.6 Competitive analysis of scFv expressed under alternative conditions

Lysates were obtained and applied to the wells of an ELISA plate coated with 1μg/mL CP alongside free antigen concentrations of 5μg/mL, 0.5μg/mL or 0μg/mL. Bound scFv was detected with a HRP-labelled anti-HA antibody and the absorbance was read at 450nm.

Based on the results observed from the lysate titres and competitive analyses, it appeared that the clones 11B2 and 41B presented themselves as the most suitable candidates as both displayed binding to the CP antigen in indirect ELISA and also demonstrated the capacity for soluble-antigen detection in competitive format. As such, it was decided to progress with characterisation of these two clones in mAb, scAb and scFv formats.

4.2.3 Expression and purification of monoclonal antibodies

4.2.3.1 Expression of monoclonal antibody in hybridoma cell culture

The original hybridoma lines of the selected recombinants were propagated in cell culture in order to express and isolate the parental IgG molecule. The 41B hybridoma line was recovered from LN_2 and grown in cell culture (*Section 2.16.1*). MAbs in hybridoma culture are expressed by the cells directly into the culture media. When sufficient volumes of IgG-enriched media were obtained, ~300mL, the media was concentrated and used in Protein-G affinity chromatography purification procedures (*Section 2.16.2*). The resulting purified antibody samples were run in SDS-PAGE and WB, *Figure 4.7 (i)* and *(ii)*, respectively. The purification was deemed successful, with bands present on the SDS-PAGE elution fractions at roughly ~55kDa and ~25kDa, representing the IgG heavy and light chains, respectively. The staining of a band around ~55kDa, corresponding to the heavy chain, in the WB analysis confirms the presence of IgG.

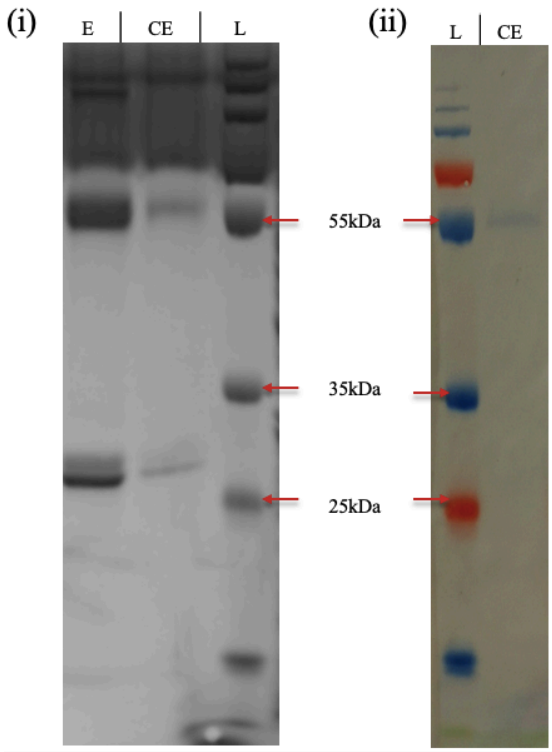

Figure 4.7 Affinity purification of the 41B mAb

(i) *SDS-PAGE analysis of the eluted and concentrated elution fractions the heavy and light chains are observable at ~55kDa and ~25kDa, respectively.* ***(ii)*** *WB analysis of the 41B concentrated elution probed with an anti-mouse IgG HRP-labelled antibody. Reactivity with the heavy chain is apparent at ~55kDa (Ladder = PageRuler Plus prestained, E = unconcentrated elution (neat), CE = concentrated and buffer exchanged elution run at a 1:50 dilution).*

The 11B2 mAb was already available in purified form. A sample of this mAb was run in SDS-PAGE and WB to ensure its integrity was acceptable to commence with further characterisation. The results of the SDS-PAGE and WB analysis are shown in *Figure 4.8 (i)* and *(ii)*, respectively. Heavy chains at ~55kDa and light chains at ~25kDa are apparent in the SDS-PAGE. Additionally, heavy chains at ~55kDa can also be seen in WB analysis, confirming the presence of 11B2. A doublet band was observed for the heavy and light chains in SDS-PAGE and for heavy chains in WB, potentially arising from incomplete reduction of the mAb, or perhaps due to minor degradation during storage. Additionally, a higher band located in the range of 130kD to 250kDa is observed in the SDS-PAGE gel. The also suggests incomplete reduction of the mAb as the whole antibody protein has a molecular weight of ~150kDa.

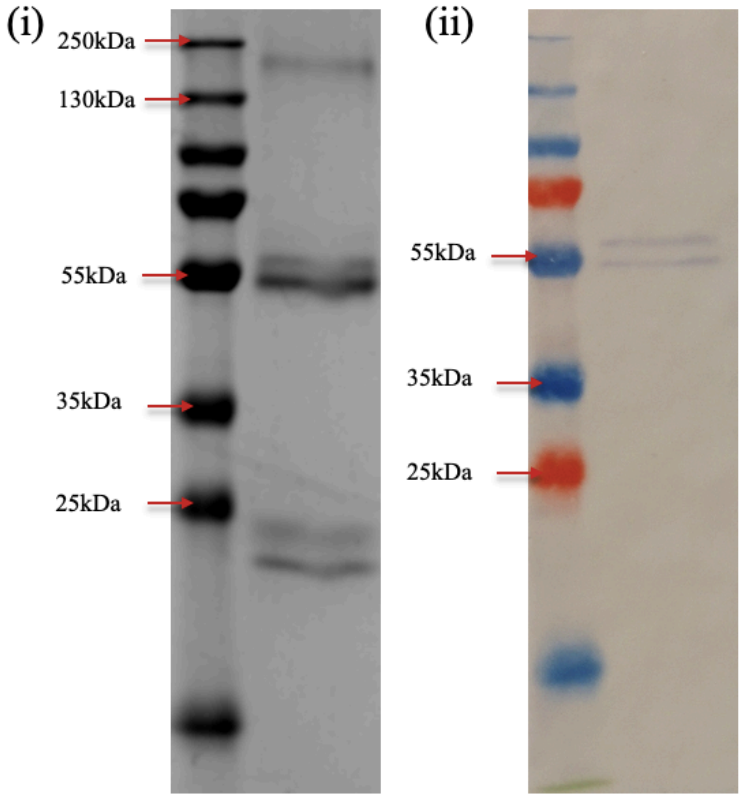

Figure 4.8 11B2 mAb sample analysis

(i) *In SDS-PAGE analysis, the heavy and light chains are observable at ~55kDa and 25kDa, respectively.* ***(ii)*** *Reactivity with the heavy chain is apparent around 55kDa in the WB when probed with anti-mouse IgG HRP-labelled antibody (Ladder = PageRuler Plus prestained).*

4.2.3.2 Titration of purified monoclonal antibodies 41B and 11B2

To determine a suitable working dilution for 41B and 11B2, the two mAbs were used in an antibody titre whereby the purified antibody sample was serially diluted and the response against the CP antigen tested in ELISA as per *Section 2.17.1*. The results in *Figure 4.9* indicate that both antibodies successfully titred against the antigen and working ranges of 1 in 10,000 – 1 in 50,000 and 1 in 100 - 1 in 200 were chosen for 11B2 and 41B, respectively.

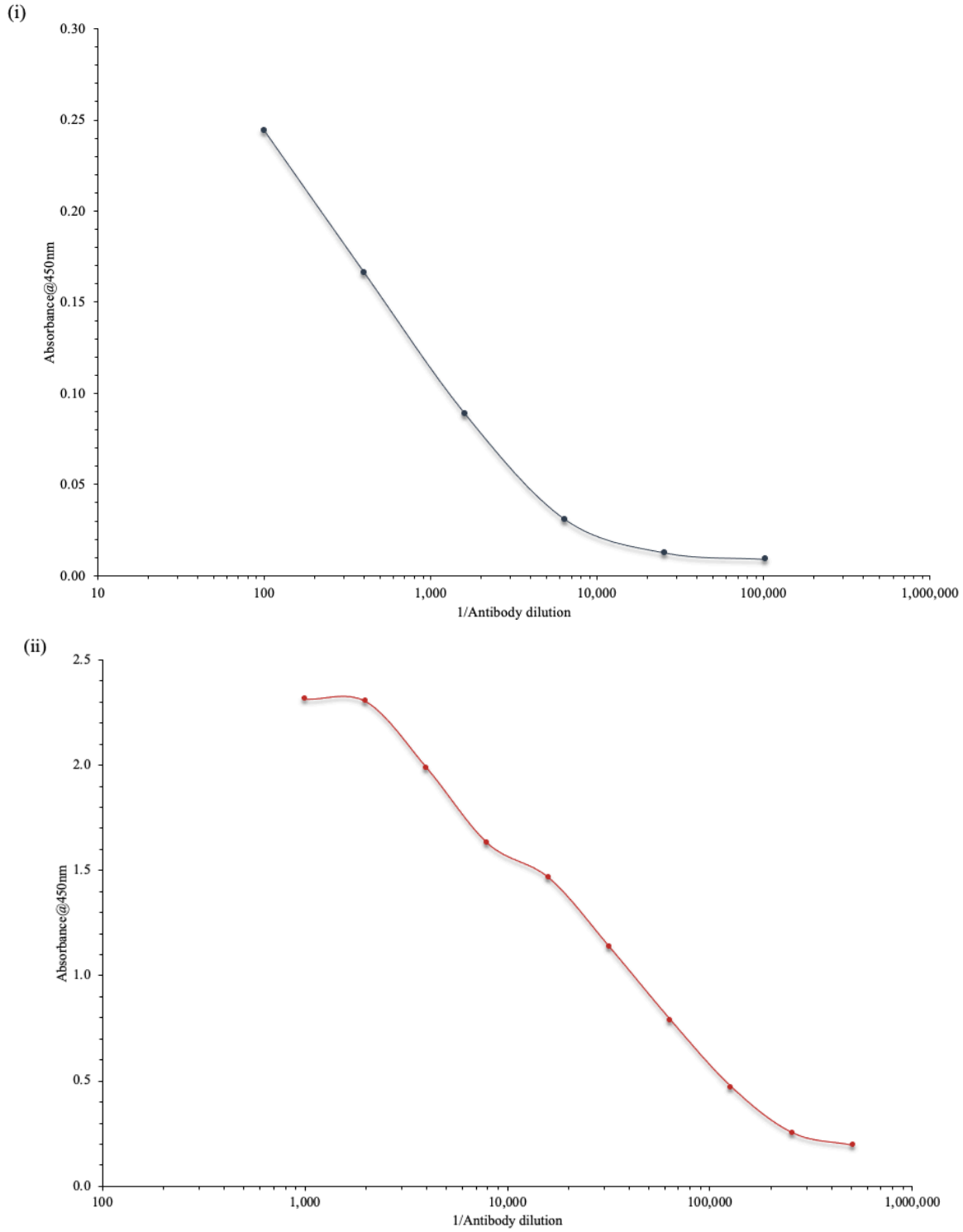

Figure 4.9 Titration of 41B and 11B2 mAbs

Purified mAb was applied in a series of dilutions to the wells of an ELISA plate coated with 1μg/ml CP. ***(i)*** *Bound 41B mAb was detected with an anti-mouse IgG (whole molecule) HRP-labelled antibody.* ***(ii)*** *11B2 mAb was detected by a HRP-labelled anti-mouse IgG (H+L) antibody. The absorbance for both was read at 450nm.*

Having isolated and confirmed binding of the parental mAbs for the 41B and 11B2 antibodies, the work toward the characterisation of these antibodies in their recombinant forms was progressed. This involved optimisation and large-scale expression of the recombinant forms of the mAbs, of which there were two, a scAb and scFv form.

4.2.4 Expression of 11B2 and 41B scFv and scAb recombinant forms

4.2.4.1 Optimisation of expression conditions

Prior to large-scale expression of the recombinant clones, optimisation of their expression conditions was performed as per *Section 2.10.10*. IPTG and induction temperature play an important role in determining the solubility of the recombinantly expressed protein which has an overall impact on the final product yield (Tolia and Joshua-Tor, 2006; Gutiérrez-González et al., 2019). To optimise these conditions, the IPTG and induction temperature parameters were investigated for clones 11B2 and 41B in both scFv and scAb formats. Cultures of each clone were induced with a range of IPTG concentrations and expressed at either 30°C or 25°C O/N. Lysates were then obtained for these cultures and tested in ELISA against the CP. For 41B, the scFv form was optimally expressed using 0.1mM IPTG and 25°C induction temperature (*Figure 4.10 (i)*), whereas the conditions of 1mM IPTG and 25°C were selected for the 41B scAb (*Figure 4.10 (ii)*). For 11B2, the optimal expression conditions were the same for both the scFv (*Figure 4.11 (i)*) and scAb (*Figure 4.11 (ii)*), and these were 0.1mM IPTG and 25°C. The identified conditions were used for subsequent expression of the recombinant antibodies.

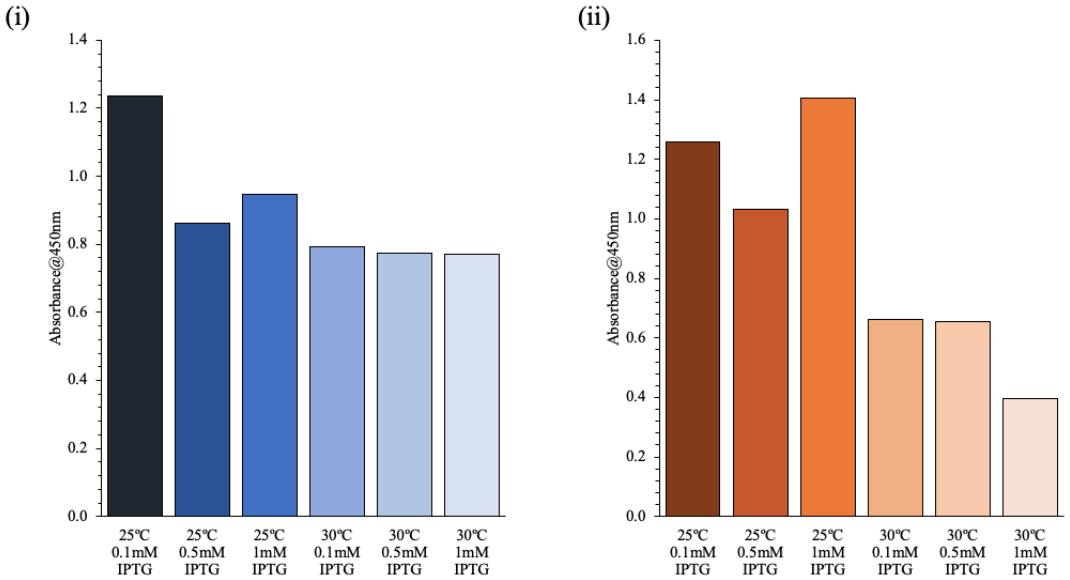

Figure 4.10 Optimisation of expression for the 41B scFv and scAb

Cultures of 41B scFv ***(i)*** *or scAb* ***(ii)*** *were induced with IPTG concentrations of 0.1mM, 0.5mM or 1mM, and left to express at either 30°C or 25°C O/N. Lysates from each condition were applied to wells coated with 1μg/mL CP. Bound antibody was detected using a HRP-labelled anti-HA antibody. The absorbance was then read at 450nm.*

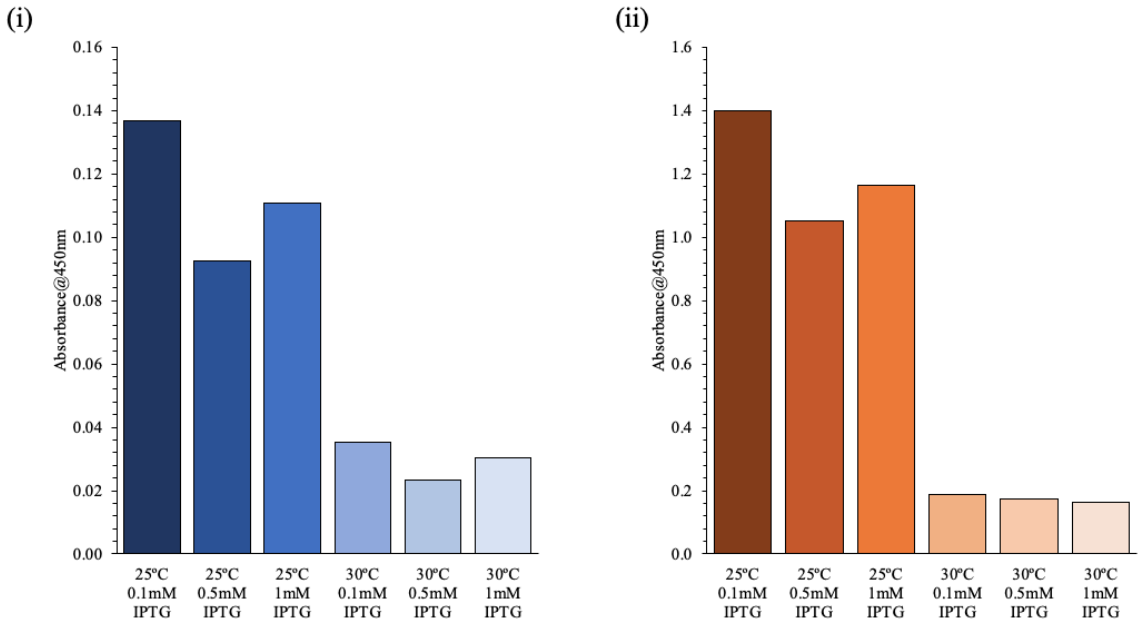

Figure 4.11 Optimisation of expression for the 11B2 scFv and scAb

Cultures of 11B2 scFv ***(i)*** *or scAb* ***(ii)*** *were induced with a range of IPTG concentrations (0.1mM ,0.5mM or 1mM) and left to express at either 30°C or 25°C O/N. Lysates from each condition were applied to wells coated with 1μg/mL CP. Bound antibody was detected using a HRP-labelled anti-HA antibody. The absorbance was then read at 450nm.*

4.2.4.2 Large-scale expression and purification of recombinant scFv and scAbs

Both the 41B and 11B2 scAbs and scFvs were grown in 2 x 300mL large-scale cultures each, with expression induced according to the previously determined optimal conditions (*Section 4.2.4.1)*. All recombinant proteins were purified separately via their 6X His tags on Ni-NTA resin, as per *Section 2.15.2*. The elution fractions for each were concentrated, and buffer exchanged into PBS. The purification fractions were run in SDS-PAGE and WB to assess the purification of 41B and 11B2 scAb and scFv formats. These are depicted in *Figure 4.12 (i)* and *(ii),* respectively. Purple-coloured bands at ~40kDa in the WBs for each scAb confirms the presence of scAb protein. The 11B2 scFv appeared at the expected size of ~27kDa, however, the major reactive band in the 41B scFv purified fraction ran lower, at ~20kDa, with only minimal band formation at the expected scFv size of ~27kDa. This suggests that the 41B scFv may be degrading. This can occur either during expression, purification or storage of the protein. It was noted after purification that the yield of 41B and 11B2 proteins in both scAb and scFv format was low, with only narrow bands present in the SDS-PAGE and WB analyses. Additionally, when used in a purified antibody titre, the resulting signal was restrictively low for both 11B2 recombinant antibodies (*Figure 14.12 (iv)*). While the 41B scFv elicited some signal when used in an antibody titre, shown in *Figure 4.12 (iii*), the scAb derivative of 41B presented a only a low signal, similar to that observed for the 11B2 scFv and scAbs.

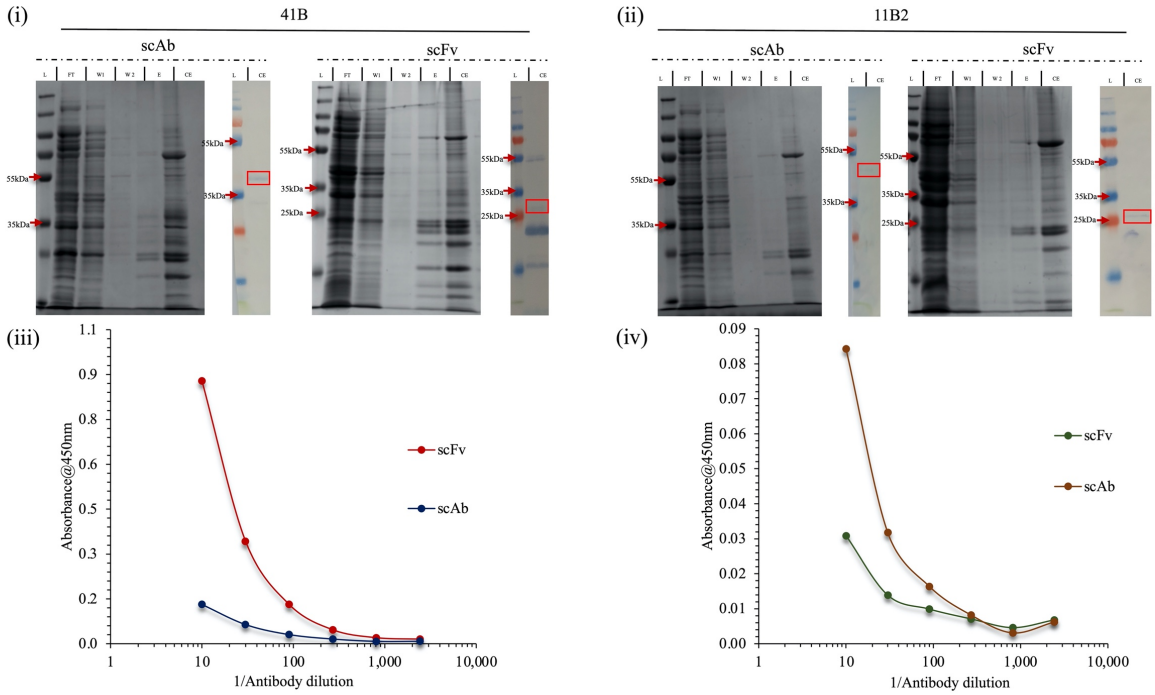

Figure 4.12 Purification and titration of the 11B2 and 41B scAb and scFv

(i) *Analysis of the 41B2 scAb and scFv purification in SDS-PAGE and WB.* ***(ii)*** *Analysis of the 11B2 scAb and scFv in SDS-PAGE and WB. Both the 11B2 and 41B scFv blots were probed with a HRP-labelled anti-HA antibody for WB analysis, while the scAb blots were probed with a HRP-labelled anti-chicken H+L. (Ladder = PageRuler Plus prestained, FT = flow through (1:2), W1 = 20mm imidazole buffer, W2 = 30mM imidazole buffer, E = 300mM imidazole buffer elution, CE = concentrated, buffer exchanged elution). The purified 41B scAb and scFv* ***(iii)*** *and purified 11B2 scAb and scFv* ***(iv)*** *were titred against 1µg/mL CP coated to the wells of an ELISA plate. Bound scFv was detected with a HRP-labelled anti-HA antibody while bound scAb detected with a HRP-labelled ant-chicken H+L antibody, respectively. Absorbance was read at 450nm.*

4.2.5 Soluble and insoluble fraction analysis

Based on the low titre obtained when using these purified antibodies in ELISA after large-scale expression and purification, it was decided to re-examine the protein expression characteristics, particularly with respect to analysing the solubility of each protein. This was achieved by testing both the soluble and insoluble fractions of a culture which had antibody expression induced overnight. Each of the 11B2 and 41B scAbs and scFvs were used is this analysis. From each culture, the bacteria were harvested, lysed by freeze thaw and the lysed cells pelleted by centrifugal action. The supernatant was retained as the soluble fraction,

while the lysed pellet resuspended in PBS represented the insoluble fraction. A sample of each of these fractions was run in SDS-PAGE in addition to analysis in WB (*Section 2.10.5* and *2.10.6*).

Based on the result, it appeared that the antibody protein for each clone was predominantly insoluble, demonstrated by thicker bands present in both SDS-PAGE (*Figure 4.13 (i)*) and WB (*Figure 4.13 (ii)*), around the expected sizes for the scAbs (~40kDa) and scFv (~25kDa) in the lanes where the insoluble fractions where analysed. Overexpression of recombinant proteins can result in rapid production of the protein of interest, which in turn can cause misfolding and aggregation of the protein, leading to subsequent insolubility and inclusion body formation (Rosano and Ceccarelli, 2014a). It was speculated that the observed insolubility of the recombinant antibodies potentially arose due to a combination of aggregation-prone residues and as a result of the codon optimisation performed on their respective DNA sequences. The optimisation of the codons for *E. coli* expression may have brought about rapid and high-level expression, which in turn, led to aggregation under the employed expression conditions. Furthermore, during this analysis it was noted that the recombinant forms of 41B appeared to have undergone degradation once more, demonstrated by the thicker reactive bands lower than the bands of expected scAb (~40kDa) and scFv (~27kDa) sizes. This was in agreement with previous observations during the purification of the 41B scFv (*Figure 4.12 (i)*). Due to the suggested degradation of 41B on multiple occasions, it was decided to focus solubilisation efforts on the 11B2 formats as these presented strong reactive bands at the expected size.

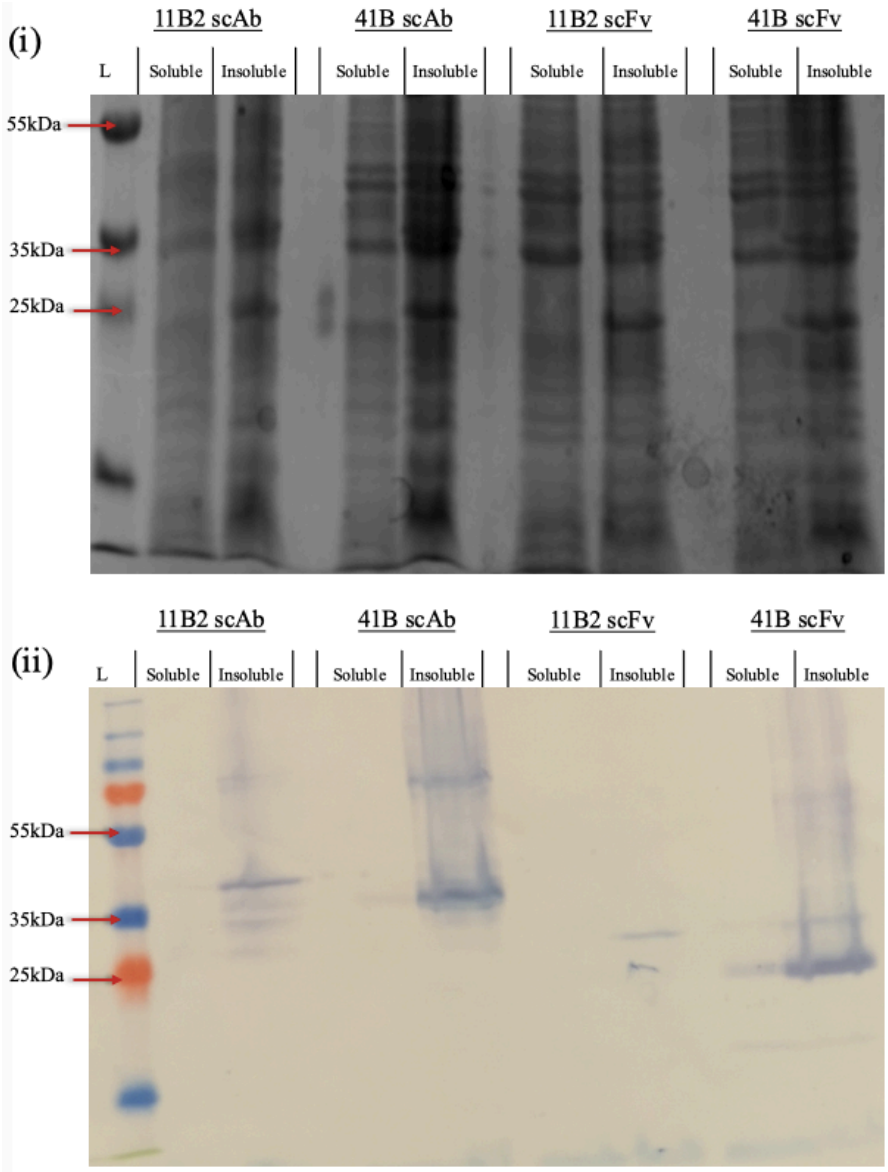

Figure 4.13 Solubility analysis of the 41B and 11B2 scAb and scFv antibodies

Both soluble and insoluble fractions were obtained for 41B and 11B2 scAb and scFv proteins and run in SDS-PAGE ***(i)*** *and WB* ***(ii)****. The WB was probed with a HRP-labelled anti-HA antibody. The WB analysis of these fractions revealed high levels of target protein present in the insoluble fractions, with limited soluble expression observed for all clones (Ladder = PageRuler Plus prestained).*

Based on the observed insolubility of the proteins, it was decided to re-evaluate the recombinant protein expression parameters in an attempt to bias expression toward the soluble fraction. This was achieved through the investigation of various parameters such as alternative incubation temperatures, media composition and the addition of glucose.

4.2.6 Modulation of soluble expression

4.2.6.1 Temperature optimisation

The expression of the 11B2 scAb and scFv at various temperatures was described previously under *Section 4.2.4.1*, in which the temperatures of 30°C and 25°C were investigated. From this analysis, it appeared that the expression greatly favoured lower temperatures. Based on this observation, a further reduction in overnight induction temperature was assessed by leaving scAb and scFv cultures to induce overnight at either room temperature (RT) or 25°C as per *Section 2.10.10*. Higher temperatures were not included due to the fact that they appeared to have a detrimental effect on expression (*Figure 4.11*). The results of the new temperature optimisations are shown in *Figure 4.14*. Again, it appeared that lower temperatures were favoured, with the cultures expressed at RT appearing to have a considerably higher signal that those expressed at 25°C. As previously discussed, expression at lower temperatures slows metabolism which, in turn, slows recombinant protein production, permitting time for correct folding and, therefore, enhanced solubility of the expressed protein. From this point, all further optimisations were performed using the pre-defined IPTG concentration of 0.1mM and overnight induction at RT.

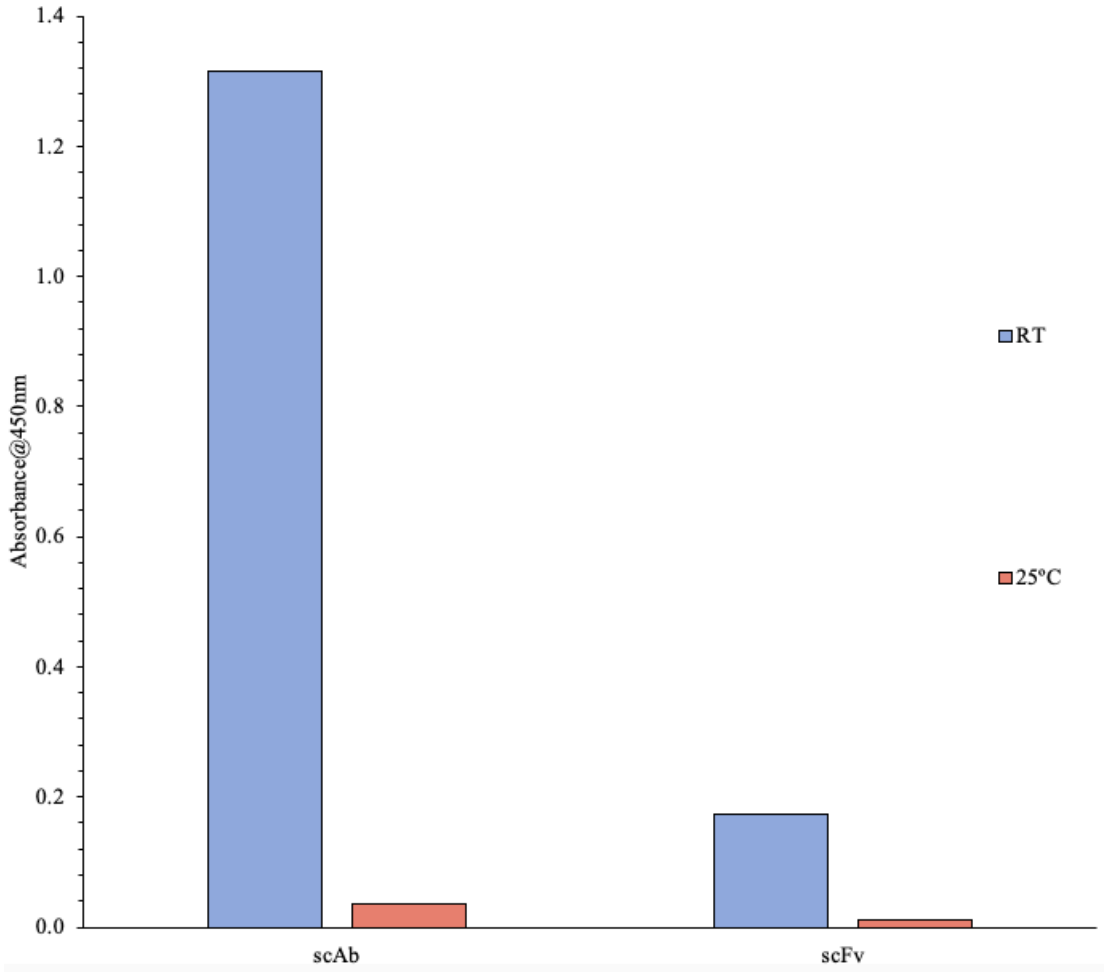

Figure 4.14 Induction temperature optimisation for the 11B2 scAb and scFv

The scAb and scFv clones were induced overnight at either RT or 25°C. The lysates from the cultures were applied to the wells of an ELISA plate coated with 1μg/mL CP. Bound scAb and scFv was detected via a HRP-labelled anti-HA antibody. Absorbance was read at 450nm.

4.2.6.2 Optimisation of media

For media optimisation, expression was performed in one of three media broths, either super broth (SB), Luria-Bertani broth (LB) or terrific broth (TB) (*Section 2.10.10)*. After expression, each sample was harvested, and the lysate examined by ELISA for scFv and scAb expression. Based on the result (*Figure 4.15*), SB was found to be the optimal broth as the highest signal was achieved in these wells. The clones expressed in LB presented a greatly diminished signal, while growth in TB only permitted scAb expression, with no signal generated in the wells containing scFv expressed in TB. The limited signal in the LB-expressed cultures could be attributed to the fact that LB has the lowest amount of yeast extract and tryptone out of the three medias tested, making it the least rich broth. It may be

that these cultures did not achieve the same cell density that is observed when growing bacteria in SB or TB. The apparent lack of expression in TB for the scFv and lower expression level for the scAb was somewhat unexpected as TB is also considered a rich media, however, it contains less tryptone than SB. Based on this it was postulated that tryptone was important for the scAb and scFv expression. From these findings, expression of both the scAb and scFv clones was performed in SB media.

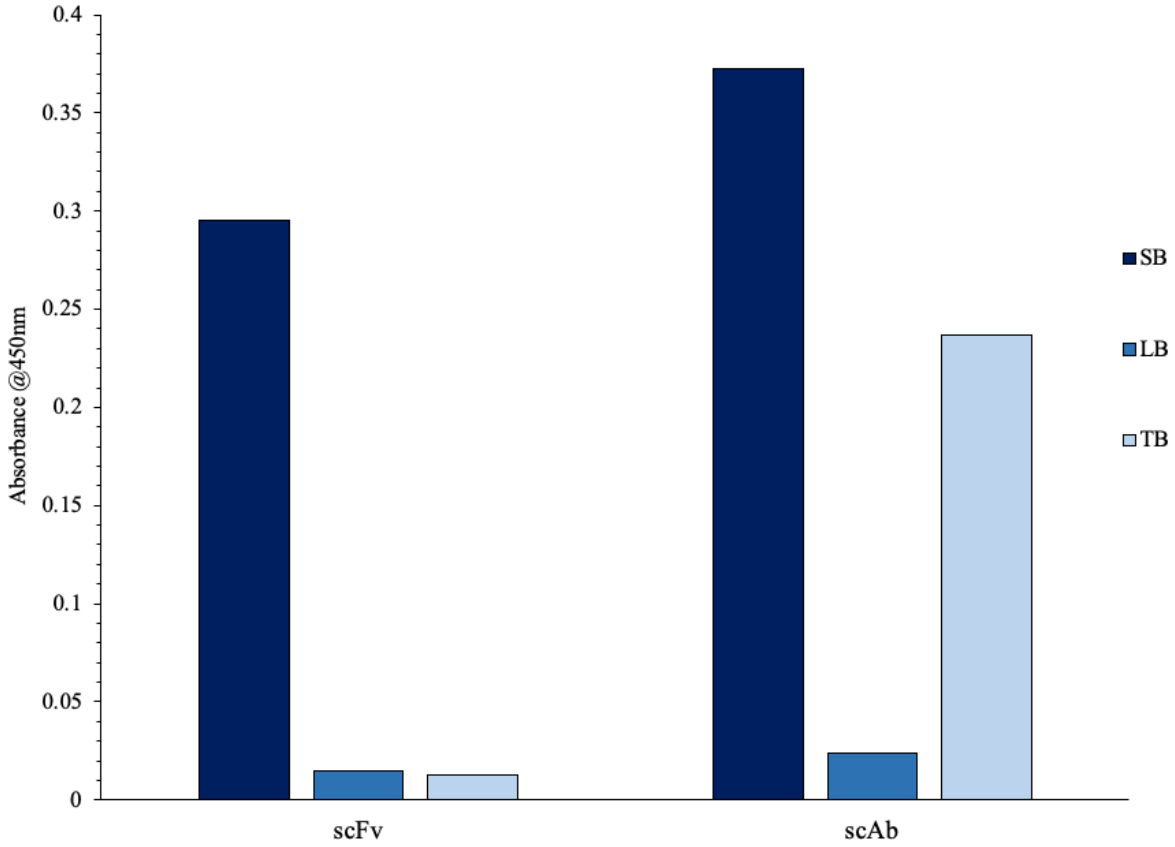

Figure 4.15 Broth optimisation for the 11B2 scAb and scFv

The scAb and scFv clones were grown in various media broths. The lysates from the cultures were applied to the wells of an ELISA plate coated with 1µg/mL CP. Bound scAb and scFv was detected via a HRP-labelled anti-HA antibody. Absorbance was read at 450nm.

4.2.6.3 Optimisation of glucose supplementation

The previously expressed cultures were supplemented with glucose and glycerol in the form of the 1X 505 (50% (v/v) glycerol and 5% (w/v) glucose). The addition of glucose is known to aid in the repression of leaky expression, reducing the level of unintended recombinant protein expression (Studier, 2005; Rosano and Ceccarelli, 2014a). In the scenario where the recombinant protein expressed is deleterious to the cells, repression of premature leaky

expression may increase recombinant protein yield by improving cell health up to the point at which protein expression is induced with IPTG. To investigate the effect of glucose supplementation, cultures were set up containing either 1% (v/v) glucose, 1X 505, or with no additional glucose (*Section 2.10.10)*. The results shown in *Figure 4.16* indicate that the scFv marginally favoured the addition of 505, however, practically no difference was observed when compared to scFv cultures which contained no glucose. The scAb protein expressed best in the absence of any glucose supplementation. It was also noted that the addition of 1% (v/v) glucose to both the scFv and scAb cultures effectively blocked recombinant protein expression. The addition of glucose is proposed to improve yield by suppressing leaky expression of the promoter, in this case the Lac promoter, as glucose will be selectively utilised over lactose, thereby preventing unwanted induction of protein expression. This may improve factors such as cell density and cell health by preventing premature expression of recombinant proteins, which can impart additional burden on the cells. However, in this scenario, the addition of 1% (v/v) glucose appeared to entirely block expression, even after overnight induction with IPTG. While this parameter could be optimised further, the protein appeared to be expressed well in the absence of a glucose source, therefore, it was decided to proceed without any further optimisation to glucose content in the media. Based on these findings, both the 11B2 scAb and scFv were expressed in SB media with the scAb containing no glucose supplementation and the scFv being supplemented with 1X 505. Induction of both clones was then performed at RT O/N.

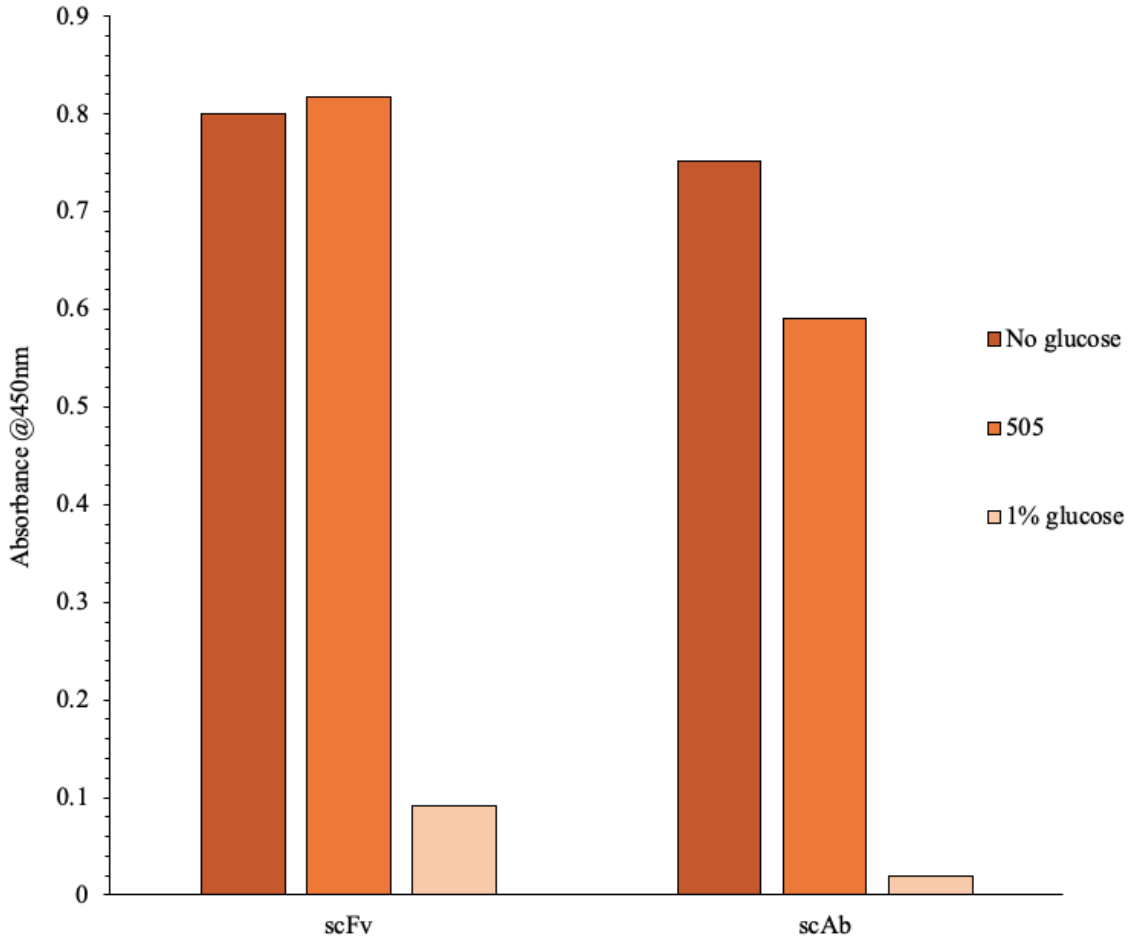

Figure 4.16 Optimisation of glucose supplementation

Cultures were grown in the presence of either no glucose, 1X 505 or 1% (v/v) glucose. The lysates from the expressed cultures were tested against 1µg/mL CP. Bound scFv and scAb was detected with an anti-HA HRP-labelled antibody. Absorbance was read at 450nm.

Having made further optimisation to incubation temperature, broth and media additives, the new expression conditions designated for the scAb and scFv were considered sufficient for commencement of large-scale expression of the recombinant clones.

4.2.7 Large-scale expression and purification of 11B2 scAb and scFv

4.2.7.1 Expression and purification of the 11B2 recombinants under optimised conditions

Both the scAb and scFv proteins were expressed under their defined optimal conditions in 400mL volumes each. From these cultures, the proteins were purified via their 6X His tags through IMAC on Ni-NTA resin (*Section 2.15*). The resulting elution fractions were concentrated, and buffer exchanged into PBS for use in subsequent characterisation assays. The purification fractions for the scAb and scFv were run in SDS-PAGE and WB. These are

depicted in *Figure 4.17 (i)* and *(ii)*, respectively. The success of the purification was confirmed by the presence of purified scAb and scFv proteins in the WB positioned at the expected sizes of roughly 40kDa and 27kDa, respectively.

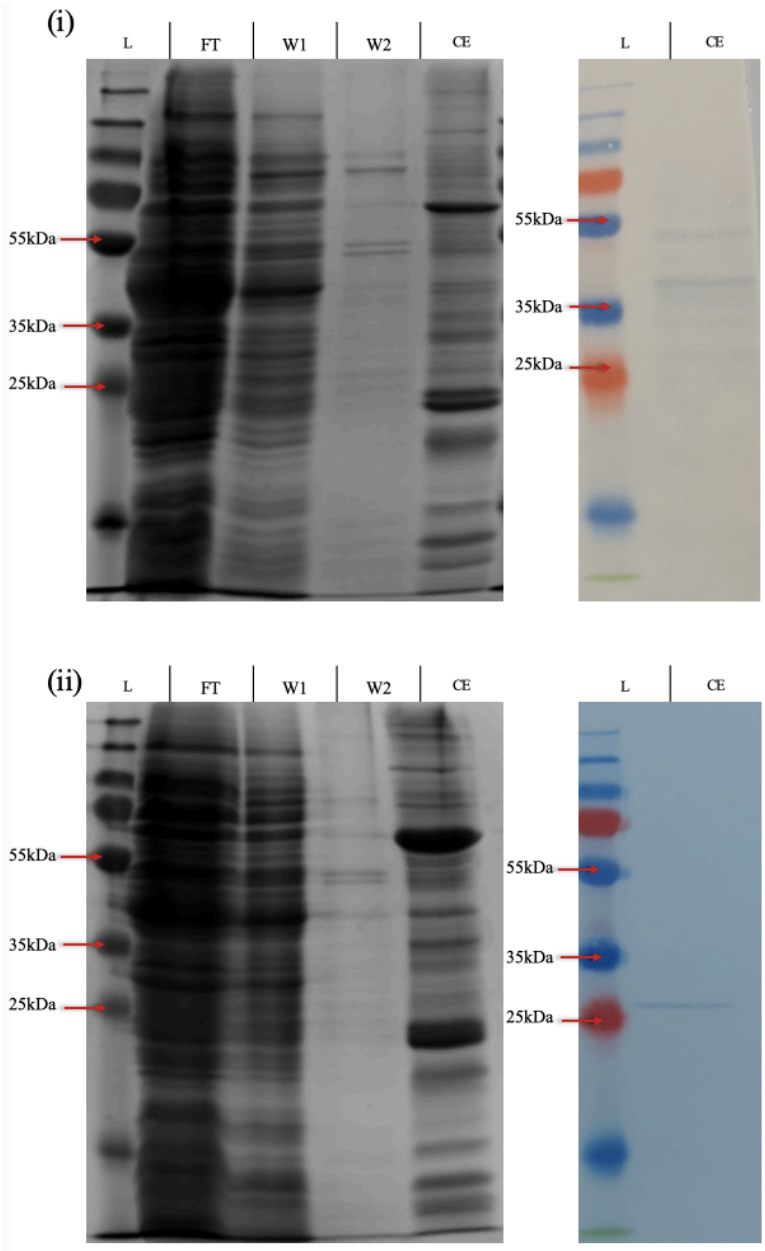

Figure 4.17 Ni-NTA chromatographic purification of the 11B2 scAb and scFv

(i) *SDS-PAGE (left) and WB (right) analysis of the purified of the 11B2 scAb. The WB was probed with a HRP-labelled anti-chicken H+L antibody.* ***(ii)*** *Analysis of the purification of the 11B2 scFv. The purified scFv fraction was probed with a HRP-labelled anti-HA antibody (Ladder = PageRuler Plus prestained, FT = flow through (1:2), W1 = 20mm imidazole buffer, W2 = 30mM imidazole buffer, CE = concentrated, buffer exchanged elution).*

4.2.7.2 Titration of purified 11B2 scAb and scFv

The scFv and scAb proteins which were isolated and purified after expression using the newly defined expression parameters were titred against the CP antigen, as per *Section 2.17.1*. The application of both the 11B2 scAb and scFv proteins to this analysis yielded good assay signal with a successful titre confirmed by an observed reduction in signal coinciding with an increase in dilution factor of the antibody (*Figure 4.18*). However, from this result, there was a notable difference in signal from the titrations, with the scAb protein presenting a higher signal and higher titre-point. This is in agreement with previous observations that the addition of the constant domain in scAb antibodies can aid in stability, solubility and expression, yielding higher quantities and more stable antibodies when compared to scFvs presenting the same variable heavy and variable light chain sequences (Maynard et al., 2002; Hayhurst et al., 2003; Hayes, Leonard, and O'Kennedy, 2012; Ayyar, Hearty, and O'Kennedy, 2015). The working dilution range was identified as 1 in 50 to 1 in 625 for the scAb due to the adequacy of the signal achieved in this dilution range. In contrast, the scFv working dilution was limited to a maximum of a 1 in 10 dilution.

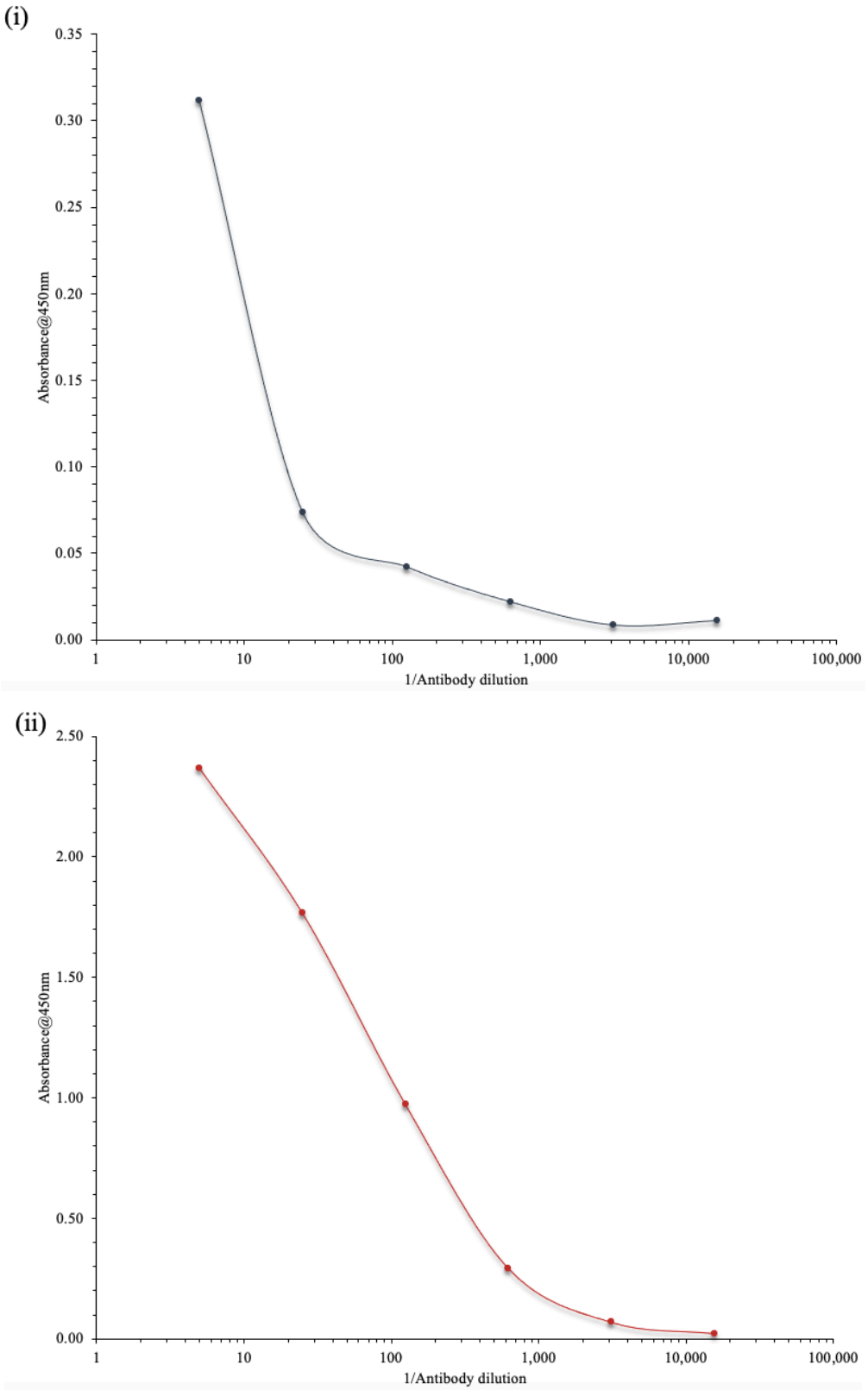

Figure 4.18 Titration of purified 11B2 scFv and scAb

Purified antibody was applied in a series of dilutions to the wells of an ELISA plate coated with 1μg/ml CP. Bound 11B2 scFv ***(i)*** *and scAb* ***(ii)*** *were detected using a HRP-labelled anti-HA antibody. The absorbance for both was read at 450nm.*

At this stage, each form of the 11B2 antibody, including the mAb, scAb and scFv, was purified and demonstrated to titre against the CP antigen. From here, in an effort to further characterise the isolated antibodies, investigations were performed with respect to immunoreactivity, antibody kinetics and the competitive detection capabilities of the selected antibodies. Initially, the 11B2 mAb and scAb were selected for immunoreactivity profiling in WB to confirm the specificity and selectivity of the antibodies for the CP antigen.

4.2.8 Immunoreactivity of 11B2 clones

4.2.8.1 Western blot analysis against recombinant CP

A WB was performed as per *Section 2.10.6* to ensure that the 11B2 mAb and its scAb derivate were specifically reactive with the 30kDa PVY CP. This analysis was performed with the mAb and scAb forms of the antibodies as these demonstrated the capacity to be used at relatively high working dilutions. Approximately 100ng of the recombinant CP was run in SDS-PAGE prior to transfer to a nitrocellulose membrane via WB. The blot was subsequently probed with either the 11B2 mAb or scAb. The results of the mAb and scAb analyses are shown in *Figure 4.19 (i)* and *(ii)*, respectively.

Both antibodies were found to be specifically reactive with a ~30kDa band, indicating binding to the recombinant CP. It was also noted that the 11B2 mAb bound to a protein at an apparently larger molecular weight of ~70kDa. As this is approximately double the size of the CP, it was postulated that this was a dimerised form of the CP, rather than a non-specific binding event between the mAb and an unrelated protein. While the scFv form of 11B2 was not used in this analysis, the scAb form of the antibody contains the same monovalent binding region as the scFv, therefore, it is likely that these would present a similar immunoreactivity profile.

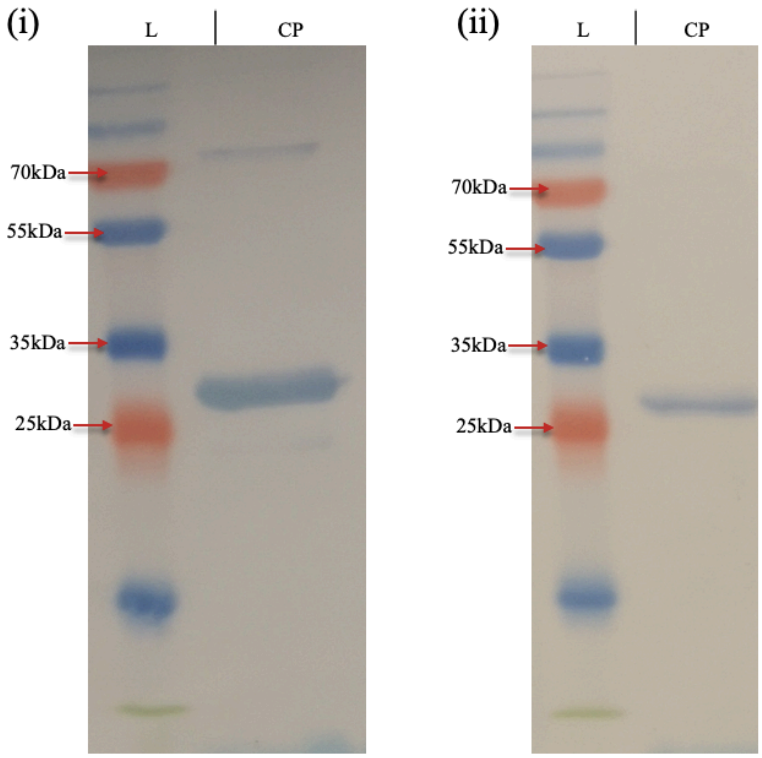

Figure 4.19 Detection of CP in WB by 11B2 mAb and scAb

A sample of the CP was run in SDS-PAGE at a final amount of 100ng. The resulting gel was transferred to a nitrocellulose membrane in WB. This blot was then probed with either the 11B2 mAb ***(i)*** *or scAb* ***(ii)****. Bound 11B2 mAb was detected with an anti-mouse H+L HRP-labelled secondary antibody while bound scAb was detected by a HRP-labelled anti-HA secondary antibody (Ladder = PageRuler Plus prestained, CP = recombinant CP).*

4.2.8.2 Western blot analysis of crude plant extracts

Further immunoblot analysis was performed with the 11B2 mAb and scAb to assess the their reactivity with plant samples known to be infected with PVY. This was achieved by running both the recombinant CP and samples of crude leaf extracts from PVY-infected plants in WB. The WB was subsequently probed with either the 11B2 mAb or scAb acting as the primary antibody. Detection of 11B2 mAb was facilitated by the action of a labelled anti-mouse antibody while the scAb was detected through probing for the HA tag. The result of the mAb and scAb blots are in *Figure 4.20 (i)* and *(ii)*, respectively.

In each lane for the mAb blot, colour formation can be seen at a molecular weight of ~30kDa, indicating successful detection of the CP by the mAb. It was noted that a slightly higher reactive band was observed in the recombinant CP lane of the mAb blot, with a faint band

of a similar molecular weight developing in the PVY^O lane also. These were of a similar molecular weight to those observed in previous analysis in *Figure 4.19*. The fact that the band appeared in both the recombinant CP samples and in a PVY-infected leaf extract sample strongly suggests this is actually a dimerised form of the CP which has the requisite epitope available for reactivity with 11B2 as these two samples would contain no crossover of extraneous proteins. The 11B2 scAb was also found to be capable of detecting CP from the crude leaf sample, however, the ~30kDa band was only observed in the PVY^O serotype and not PVY^N. As the signal was relatively low in the scAb blot for both the recombinant CP and PVY^O leaf sample, it is likely that the level of CP in the PVY^N sample was simply outside the detection limit of the scAb in this format, rather than a case where the scAb did not present binding to PVY^N. The comparatively reduced signal achieved for the PVY^N serotype in the mAb blot supports this proposal.

Additionally, it was noted that the 11B2 mAb reacted with both primary PVY serotypes, O and N, indicating successful broad-spectrum detection. As discussed, the lack of the N serotype detection by the scAb is likely due to the low concentration of CP in this sample, rather than a loss of reactivity with the N serotype as both the mAb and scAb contain the same variable binding regions. No comment could be made on whether 11B2 appeared more reactive with one serotype over the other as the level of PVY infection in the leaf samples was not ascertained and, therefore, could not be normalised for this WB.

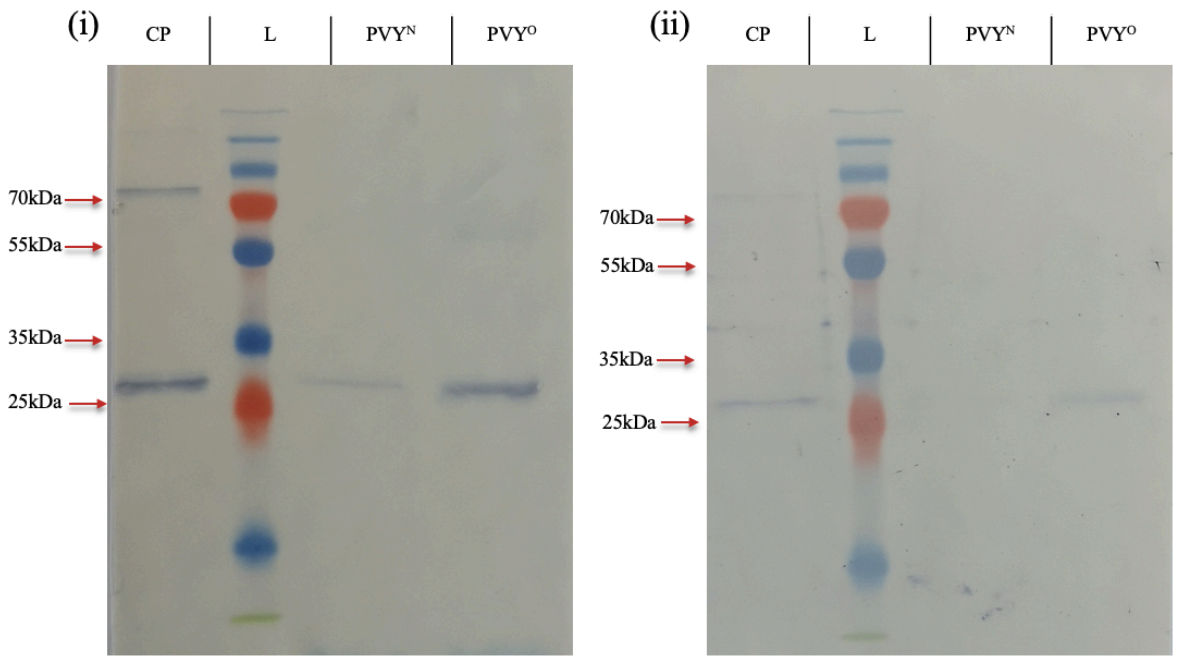

Figure 4.20 Detection of CP from plant extracts in WB by the 11B2 mAb and scAb

Samples of recombinant CP (100ng) or crude leaf samples infected with PVY were run in WB and probed with 11B2 mAb ***(i)*** *or scAb* ***(ii)****. Bound 11B2 mAb was subsequently detected with an anti-mouse H+L HRP-labelled secondary antibody, while bound scAb was detected with an anti-HA HRP-labelled antibody (Ladder = PageRuler Plus prestained, PVY^O/ PVY^N = Plant samples infected with the denoted PVY serotype, CP = recombinant CP).*

With specificity of the antibodies for the CP confirmed, work was progressed to attempt to characterise these antibodies further using surface plasmon resonance (SPR). This method allows the elucidation of kinetic constants. These constants provide valuable information about the binding characteristics of the antibody to its cognate antigen.

4.2.9 Kinetic analysis of antibodies by surface plasmon resonance

4.2.9.1 Kinetic evaluation of the 11B2 mAb

SPR technology permits the analysis of antibody-antigen interactions. It can be used to elucidate key binding characteristics such as association (k_a) and dissociation (k_d) constants, in addition to the equilibrium dissociation constant (K_D) value of the antibody, which reflects the overall affinity the antibody has for its cognate antigen. Kinetic evaluation was performed on a Biacore X100. The 11B2 mAb was captured by means of an anti-mouse Fc antibody coated onto the surface of a CM5 sensor chip via amine coupling, permitting re-use of the chip as 11B2 can be stripped away via a 20mM NaOH regeneration wash, while

the anti-mouse Fc remains coupled to the surface. Additionally, directed capture of the Fc region aids in signal generation as the binding regions of the mAb should face away from the sensor surface and be more available for antigen-capture. Details of the anti-mouse Fc immobilisation protocol are provided in *Section 2.18.1*. The X100 system provides two flow cells, one reference cell and one active cell where binding is monitored. Both flow cells were coated with anti-mouse Fc antibody to permit subtraction of non-specific signal arising from interactions between the CP antigen and the anti-mouse Fc antibody.

Kinetic interactions were monitored by capturing the 11B2 mAb on the chip surface and subsequently flowing over various concentrations of the CP antigen, as per *Section 2.18.2*. Antigen was allowed to associate with the antibody for 180s, and dissociation was monitored for 700s. Alongside subtraction of signal from the reference flow cell from the experimental dataset, signal arising from a 0μg/ml CP negative control was also subtracted from the data, leading to double-referencing of the 11B2 binding data. A duplicate concentration (1.66μg/mL) was included during the run to monitor systemic stability. The resulting kinetic data was fitted to a 1:1 Langmuir binding model (global fit). This fit is demonstrated by the black lines overlayed on each experimental concentration, which are colour-coded, in *Figure 4.21*. The predicted binding model was in good agreement with the experimental data, as demonstrated by the very close fit between the two. A good fit for the model increases experimental confidence that the elucidated kinetic constants are correct. From this fitting, the kinetic constants were determined. The k_a was found to be 2.12×10^4 while the k_d was 2.31×10^{-4}. Both the on and off rates are used in a ratio (k_a: k_d) to determine the overall K_D. This value indicates the affinity of the binding between antibody and antigen. Antibody K_D values can range depending on the strength of binding, ranging from those displaying micromolar concentrations (10^{-6}) to rare, extremely high affinity antibodies which achieve femtomolar values (10^{-12}) (Fujii, 2004; Wark and Hudson, 2006; Igawa et al., 2011). The K_D of the 11B2 mAb was determined as 1.09×10^{-8}, indicating binding in the nanomolar range.

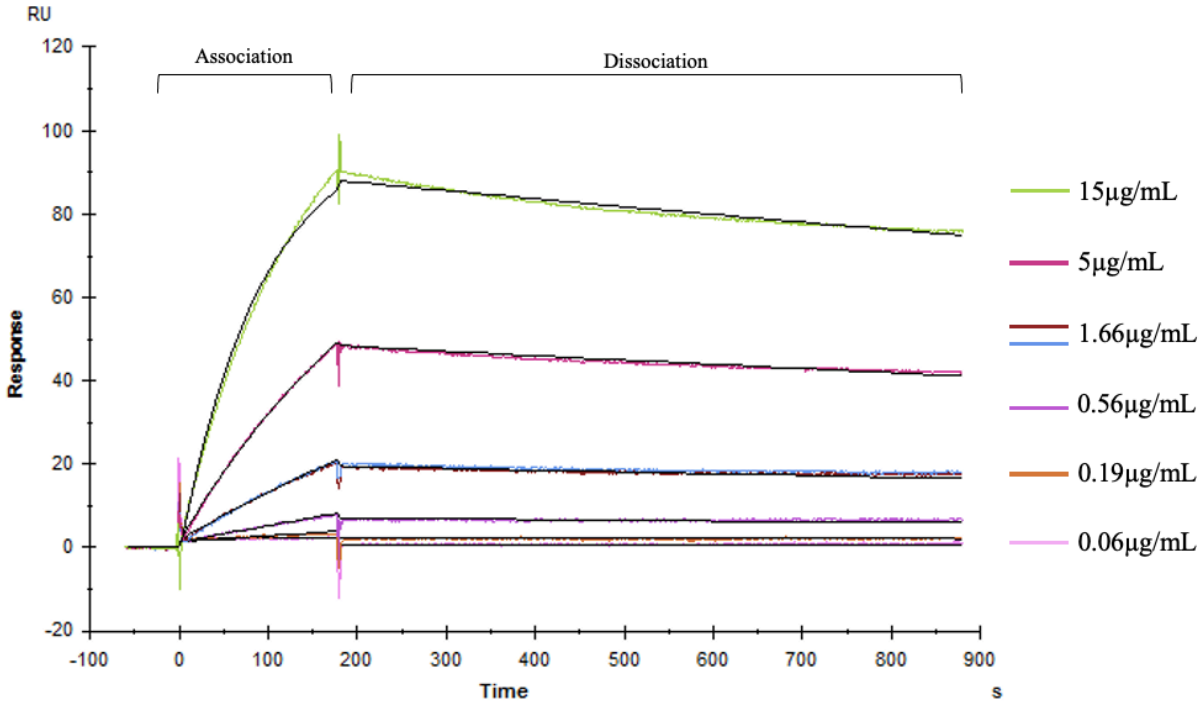

Figure 4.21 Kinetic interaction analysis of the 11B2 mAb

Various concentrations of CP (15µg/mL -0.06µg/mL) were passed over 11B2 mAb captured on the surface of a CM5 chip. Response is reported as arbitrary Response Units (RUs). Signal from both a 0µg/mL CP concentration, and from the reference cell were subtracted from the dataset. The equilibrium dissociation constant (K_D) was determined as 1.09 x 10^{-8}.

4.2.9.2 Kinetic evaluation of the 11B2 scAb

To achieve a level of comparison between the kinetics of the 11B2 mAb and a recombinant form of the antibody, kinetic evaluations were also performed using the 11B2 scAb. No kinetics analysis could be performed for the scFv due to the combination of low amounts of scFv protein after purification and relatively high reagent demand for kinetic analysis. A CM5 chip was functionalised with an anti-chicken Fab region antibody via amine coupling on both flow cells, as per *Section 2.18.1*. This facilitates the capture of the avian constant light region on the scAb, permitting functional orientation of the binding sites outward from the sensor surface which can allow for better antibody-antigen interaction, particularly for smaller recombinant antibody fragments.

Multicycle kinetics were performed on the 11B2 scAb, as described under *Section 2.18.3*, whereby a range of concentrations of CP were allowed to associate with the sensor surface for 180s prior to dissociation for 700s. One concentration, 17.5µg/mL, was run in duplicate

to monitor systemic stability. The results of the kinetics are shown in *Figure 4.22*. Subtracted from the dataset was a 0μg/mL CP concentration cycle, in addition to the subtraction of any signal arising from the reference flow cell, thus ensuring the experimental data was subjected to double-referencing. The resulting data was globally fit to a 1:1 Langmuir binding model. The predicted binding is demonstrated by black lines overlayed on the experimental data, shown in colour-coded lines. The predicted fit was relatively well aligned with the experimental data. The kinetic values k_a and k_d were determined as 9.23×10^{3} and 2.26×10^{-3}, respectively. Based on these values, an overall K_D of 2.44×10^{-7} was elucidated, indicating binding in the nanomolar range. It was noted that the mAb had a superior K_D value, indicating stronger binding between the antibody and antigen. Similar observations with respect to an alteration in K_D upon restructuring of a mAb into a recombinant form were made previously. In these studies, mAbs were reformatted into their scFv homologues and reductions in K_D values and dissociation values were observed (Patel and Andrien, 2010; Badescu et al., 2016). However, this is not always the case and the equilibrium constant between the parental and fragmented antibodies may also remain unchanged (Nuttall et al., 2011). This highlights the need for characterisation of the recombinant forms post-reformatting.

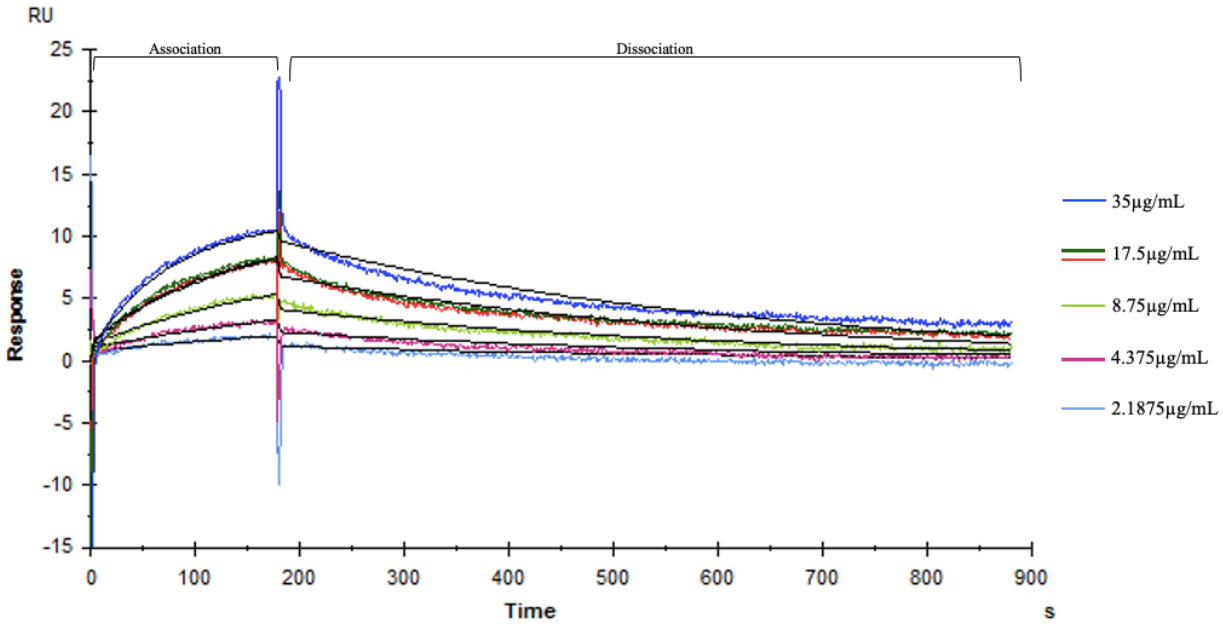

Figure 4.22 Kinetic interaction analysis of the 11B2 scAb

Various concentrations of CP (35µg/mL – 2.1875µg/mL) were passed over the 11B2 scAb captured on the surface of a CM5 chip. Response is reported as arbitrary RUs. Signal from both a 0µg/mL CP concentration and from the reference flow cell were subtracted from the dataset. The equilibrium dissociation constant was determined as 2.44 x 10^{-7}.

4.2.10 Development of competitive ELISAs for the detection of PVY

To investigate the applicability of the isolated 11B2 mAb, scAb and scFv antibodies in ELISA, the development of a competitive ELISA was undertaken employing each form of the 11B2 antibody (*Section 2.17.2*). The competitive ELISA method relies on the ability of the antibody to detect, and remain bound to, free antigen in solution. For competitive analysis, antibodies are applied at a fixed concentration alongside ranging concentrations of free CP antigen. If the antibodies are competitive for the CP, they will bind to the free antigen in solution and be washed away by subsequent wash steps. The higher the concentration of free antigen in the well, the less antibody is available to bind to the immobilised antigen, making the signal in competitive ELISA inversely proportional to the level of antigen in a given sample. The results of the competitive ELISA are typically expressed as A/A0, where wells containing free antigen (A) are expressed as a function of the absorbance of wells containing no free antigen (A0).

Competitive ELISA standard curves were developed for each of the 11B2 forms of antibody. From triplicate analyses of these standards, calibration curves were generated in

BiaEvaluation software according to a 4-parameter logistical equation fitted to the data. These curves follow the sigmoidal shape generally observed for immunoassays, which are linear over specific ranges while forming plateaus at upper and lower limits. The generated calibration curves for the mAb, scAb and scFv are shown in *Figure 4.23*, *Figure 4.24* and *Figure 4.25*, respectively. From these calibration curves, the LOD for each assay was calculated using a combination of mean absorbance signals and standard deviation (SD). This was achieved by first determining the limit of blank (LOB) through the equation "*LOB = mean of blank - 1.645(SD of blank)"*. The LOB value was then used to calculate the LOD in the equation "*LOD = LOB – 1.645 (SD of a low concentration sample)*". From this, the estimated LOD values of the designed ELISAs were determined as 651.7ng/mL, 303.6ng/mL and 162.7ng/mL for the mAb, scAb and scFv assays, respectively.

Additionally, a summary of the intra-day coefficients of variation (CV) for each triplicate standard within each curve, and the overall CV value for the developed assays, are provided in *Table 4.2*, *Table 4.3* and *Table 4.4* for the mAb, scAb and scFv, respectively. CV reflects the precision within an assay, with lower CV values indicative of greater reproducibility between samples. The CV values were calculated by the equation *"%CV = (SD/Mean of the standard) X 100*". The %CV values for the mAb fell in the range of 0.6% - 14.1%. The scAb %CVs ranged from 0.6% -8.5% and the scFv %CVs were found to be in the range of 3% - 13%. The average CV values were determined as 8.4% for the mAb, 4.9% for the scAb and 6.7% for the scFv. Each of these falls within the recommended %CV for immunoassay of 15-20% (Findlay et al., 2000; EMA, 2011).

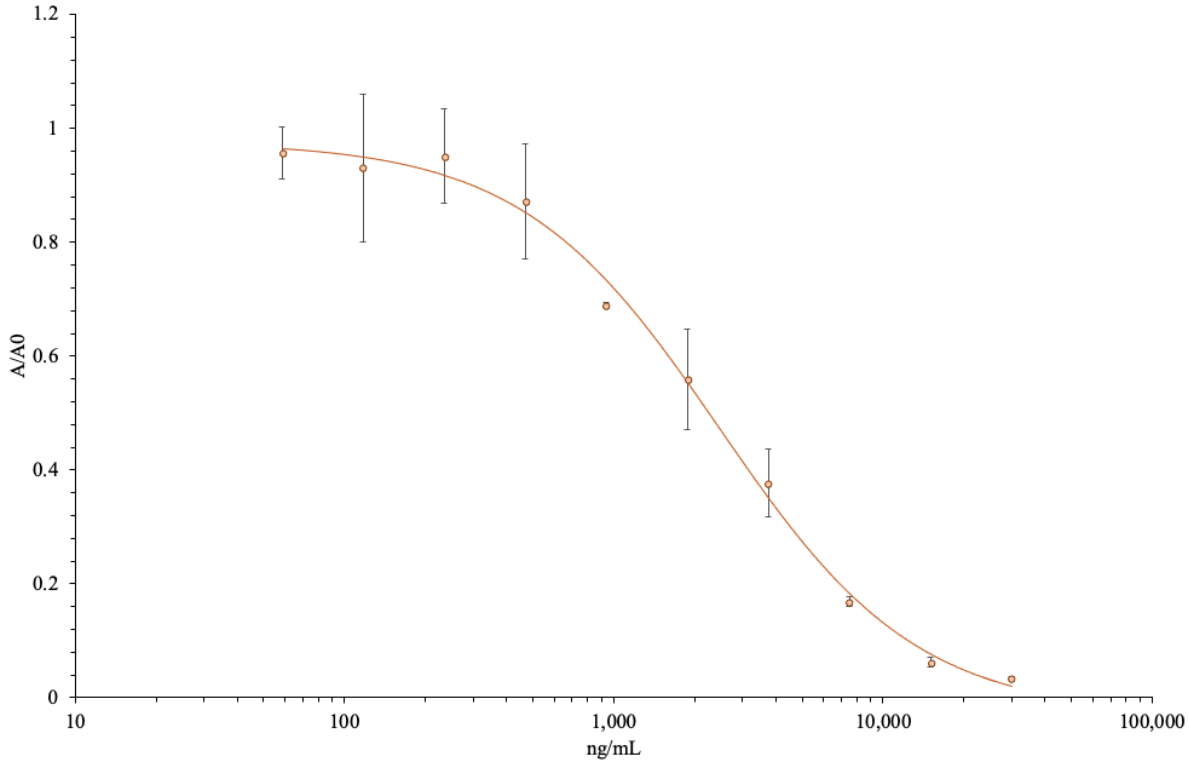

Figure 4.23 Calibration curve of the 11B2 mAb

The calibration curve was generated from ELISA data in BiaEvaluation according to a 4-parameter logistical fit. Free antigen concentrations ranged from 30,000ng/mL – 58.6ng/mL. Each data point represents a triplicate measurement of the standard concentration. Error bars represent SD between replicates.

Table 4.2 Intra-day CV (%) values for the anti-PVY 11B2 mAb

CV percentages were calculated by dividing the SD between triplicates of a given concentration by the mean absorbance of the same concentration and multiplying by 100. The average CV was found to be 8.4%.

Concentration (ng/mL)	CV (%)
30,000	4.3
15,000	12.1
7,500	4.7
3,750	14.1
1,875	13.9
937.5	0.6
468.8	10.3
234.4	7.7
117.2	12.3
58.6	4.2
Average	8.4

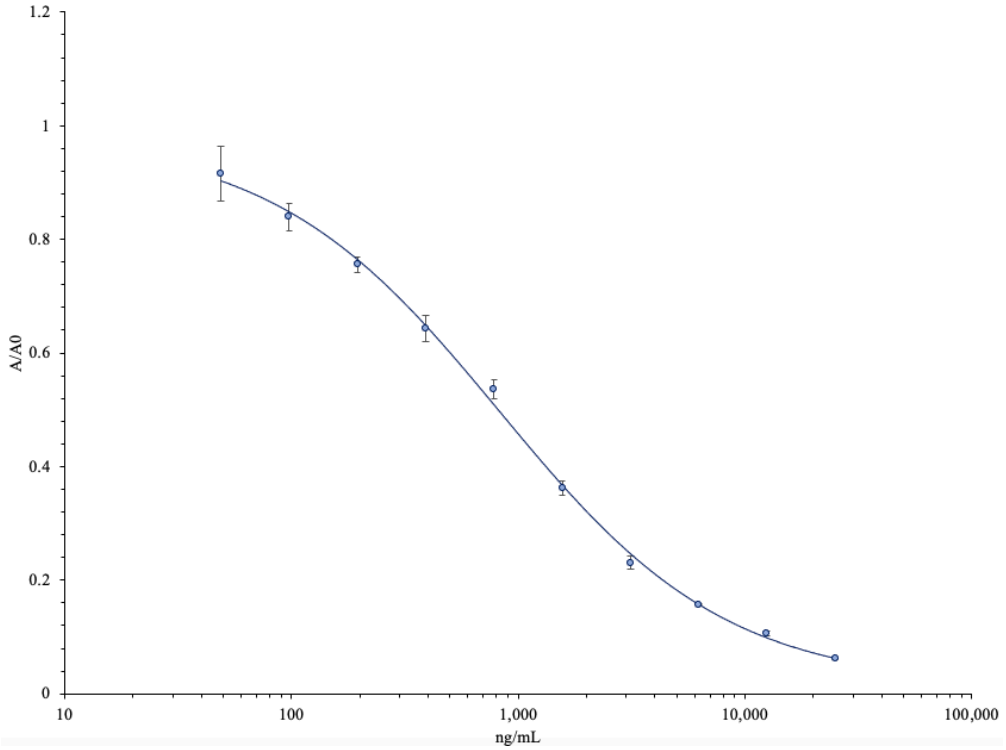

Figure 4.24 Calibration curve of the 11B2 scAb

The calibration curve was generated from ELISA data in BiaEvaluation according to a 4-parameter logistical equation. Free antigen concentrations ranged from 25,000ng/mL – 48.8ng/mL. Each data point represents a triplicate measurement of the standard concentration. Error bars represent SD.

Table 4.3 Intra-day CV (%) values for the anti-CP 11B2 scAb competitive curve

CV percentages were calculated by dividing the SD between replicates of a given concentration by the mean absorbance of the same concentration and multiplying by 100. The average CV was found to be 4.9%.

Concentration (ng/mL)	CV (%)
25,000	2.0
12,500	5.3
6,250	0.6
3,125	8.0
1,562.5	6.1
781.3	5.0
390.6	5.8
195.3	3.0
97.7	4.6
48.8	8.5
Average	4.9

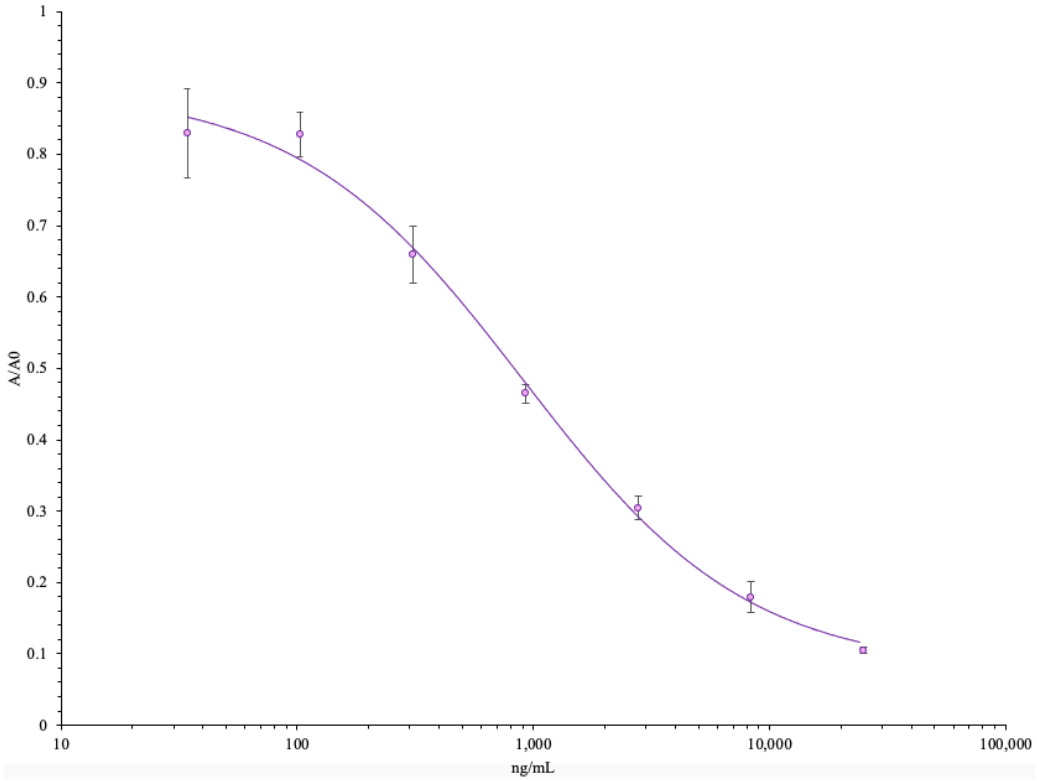

Figure 4.25 Calibration curve of the 11B2 scFv

The calibration curve was generated from ELISA data in BiaEvaluation according to a 4-parameter logistical equation. Free antigen concentrations range from 25,000ng/mL – 34.3ng/mL. Each data point represents a triplicate measurement of the standard concentration. Error bars represent SD.

Table 4.4 Intra-day CV (%) values for anti-CP 11B2 scFv competitive curve

CVs percentages were calculated by dividing the SD between replicates of a given concentration by the mean absorbance of the same concentration and multiplying by 100. The average CV was found to be 6.7%.

Concentration (ng/mL)	CV (%)
25,000	4.9
8,333.3	13.3
2,777.8	6.1
925.9	3.0
308.6	6.7
102.9	4.2
34.3	8.3
Average	6.7

4.2.11 Analysis of crude leaf samples in competitive ELISA

Having successfully designed competitive ELISA curves for each antibody, the assay development was progressed to testing crude leaf extracts previously confirmed to be infected with PVY. These were implemented in competitive ELISA format (*Section 2.17.2*) whereby the relevant antibody was applied alongside crude extracts containing PVY of serotypes O or N. Healthy leaf extracts were included as negative controls and acted as the "blank sample". A positive control sample was added whereby recombinant CP was spiked into healthy leaf at a final concentration of 15μg/mL. This analysis was performed with the 11B2 mAb, scAb and scFv. The data is expressed as A/A0 where the absorbances of the test wells (A) are a function of a blank control well (A0). In this analysis, the signal arising from wells containing healthy leaf extract acted as 'A0', while spiked and PVY-infected plants were 'A'. As this assay is competitive, a lower absorbance in the well is indicative of a positive result, as the detection antibody is bound by the PVY antigen in solution leaving less antibody to bind the immobilised antigen.

The results indicate that both the mAb (*Figure 4.26*), scAb (*Figure 4.27*) and scFv (*Figure 4.28*) can readily detect PVY from the PVY-infected leaf samples, with the signal derived from both PVY-positive samples falling outside the cut-off value of "*mean absorbance of the blank – (2 X SDs of the blank)*". No comment can be made on whether there is increased specificity of the 11B2 antibodies for either the PVY^{O} or PVY^{N} serotypes as the PVY concentration in the naturally infected samples was not normalised. However, it was confirmed by this assay that the 11B2 mAb, scAb and scFv are reactive with both primary serotypes (O and N) and therefore can act in a 'broad-spectrum' detection manner for future PVY-detection assays. Additionally, this assay demonstrated that all antibodies can function in a complex matrix such as a crude leaf extract, suggesting that limited sample preparation is required when incorporating these antibodies into future assays.

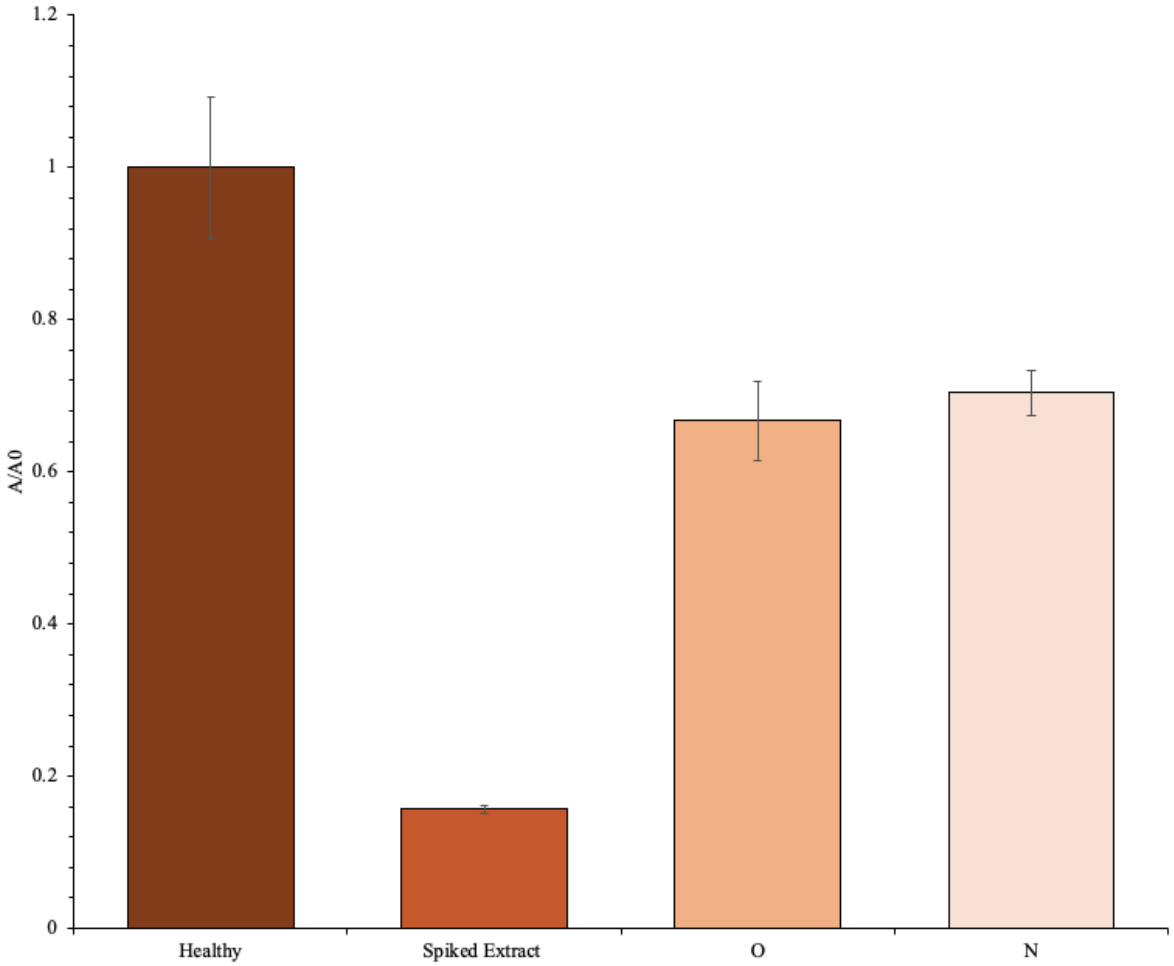

Figure 4.26 Detection of PVY from crude leaf extracts by 11B2 mAb

Crude leaf extracts and the 11B2 mAb were applied in triplicate to the wells of an ELISA plate coated with 1μg/mL CP. Alongside the mAb, samples of healthy, PVY-infected or PVY-spiked (15μg/mL CP) leaf extracts were applied. Bound 11B2 mAb was detected with a HRP-labelled anti-mouse H+L secondary antibody. Results were normalised by dividing the absorbance of the sample wells by the absorbance of the blank well (healthy leaf). Error bars represent SD.

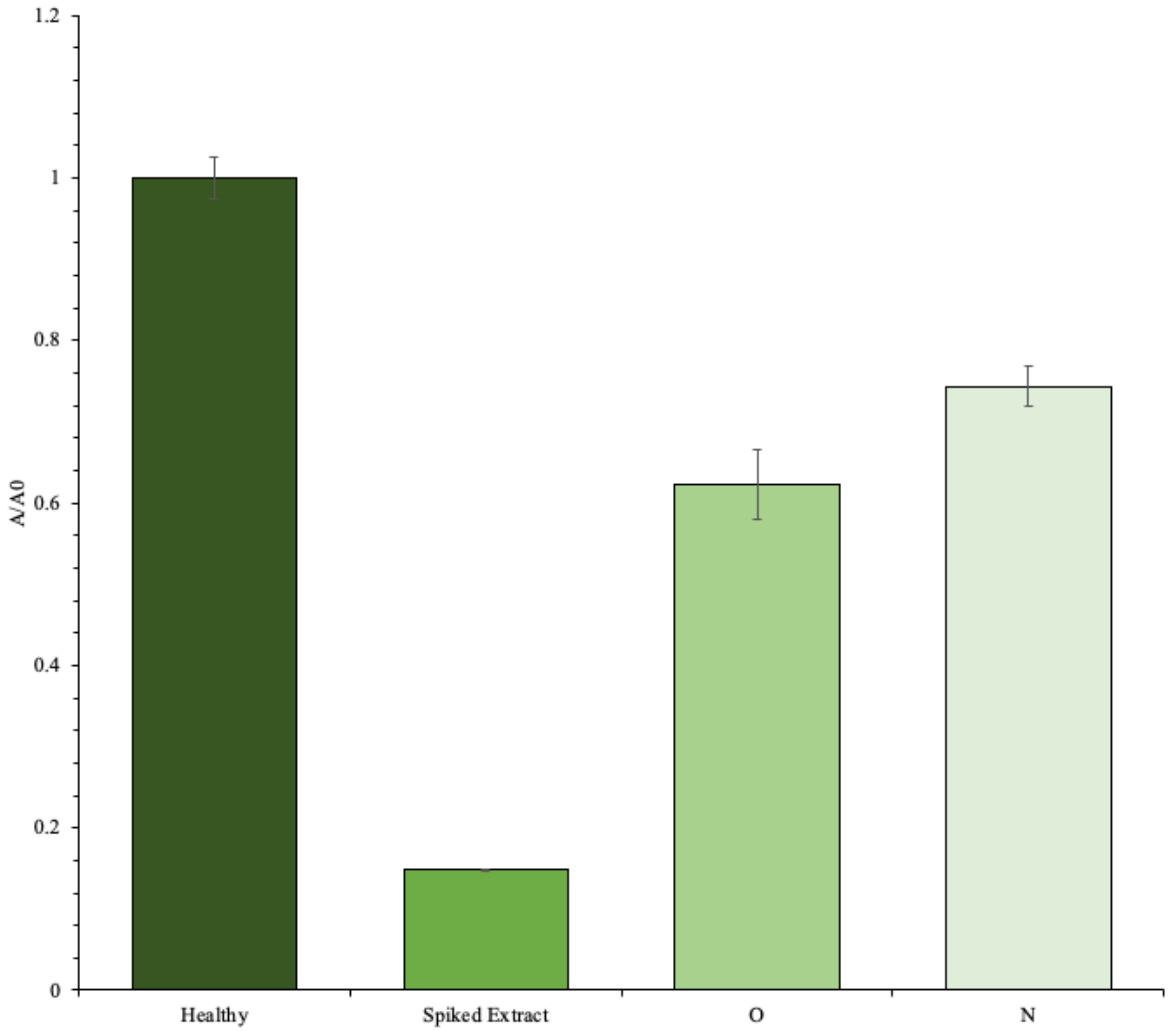

Figure 4.27 Detection of PVY from crude leaf extracts by 11B2 scAb

Crude leaf extracts were applied in triplicate alongside the 11B2 scAb to wells coated with 1μg/mL CP. Alongside the scAb, samples of healthy, PVY-infected or PVY-spiked (15μg/mL CP) leaf extracts were applied. Bound scAb was detected with a HRP-labelled anti-HA secondary antibody. Results were normalised by dividing the absorbance of the sample wells by the absorbance of the blank well (healthy leaf). Error bars represent SD.

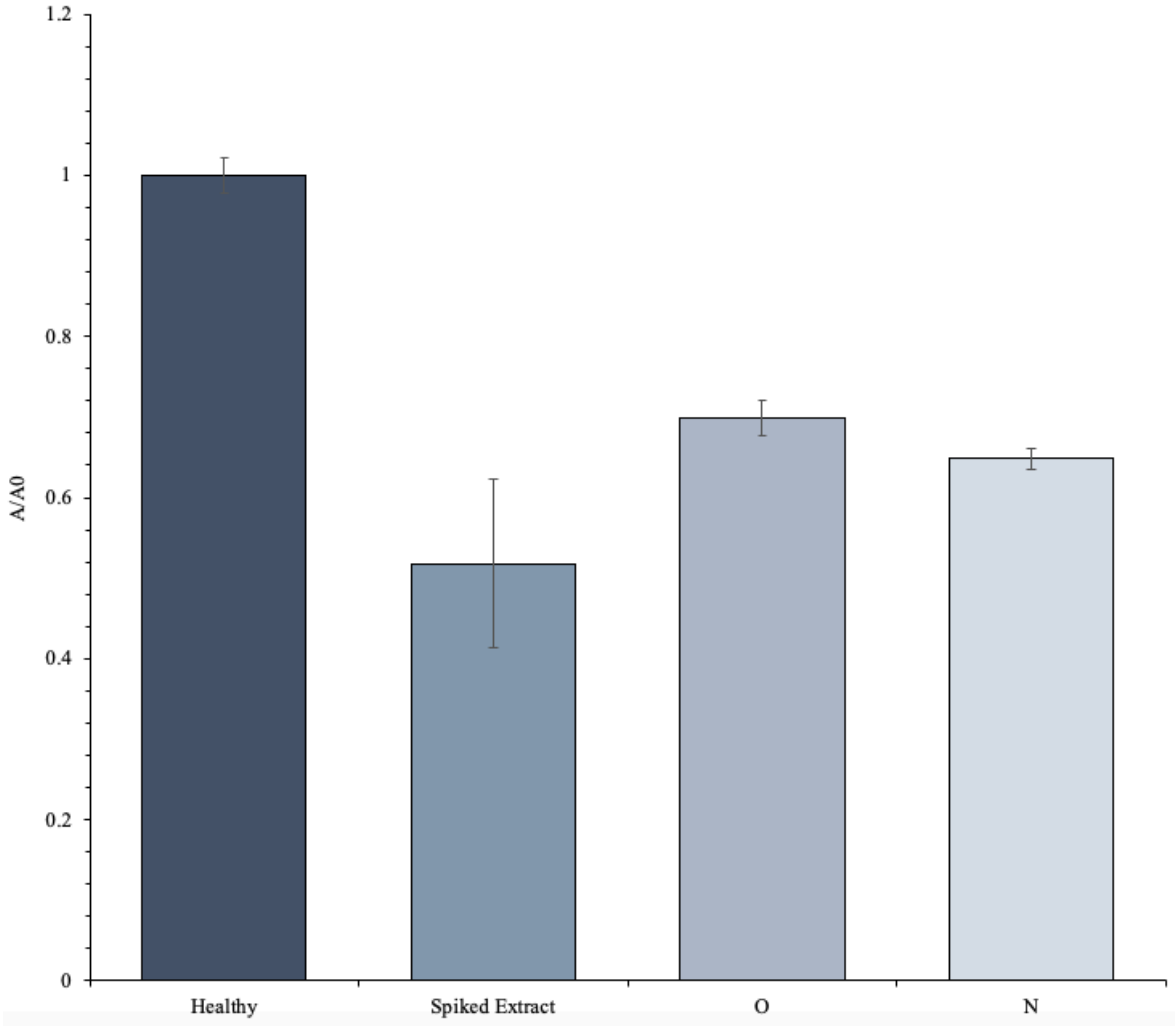

Figure 4.28 Detection of PVY from crude leaf extracts by 11B2 scFv

Crude leaf extracts were applied in triplicate alongside the 11B2 scFv to wells coated with 1μg/mL CP. Alongside the scFv, samples of healthy, PVY-infected or PVY-spiked (15μg/mL CP) leaf extracts were applied. Bound scFv was detected with a HRP-labelled anti-HA secondary antibody. Results were normalised by dividing the absorbance of the sample wells by the absorbance of the blank well (healthy leaf). Error bars represent SD.

Through these ELISAs, the applicability of the 11B2 mAb, scAb and scFv to the identification of infected PVY tissue directly from crude leaf samples was proven. As ELISA-based assays generally require additional equipment such as plate-readers it was decided to also develop paper-based alternatives to ELISA whereby PVY could be identified from similar crude extracts, without the need for such machinery.

4.2.12 Development of dot blot immunoassays for PVY detection

4.2.12.1 Detection of recombinant CP in dot blot

To provide a paper-based alternative to ELISA it was proposed to develop a dot blot. Dot blotting is a useful method by which plant pathogens can be detected from crude samples and, unlike WB, does not require any prior denaturation of the samples tested. This would provide a visual method through which PVY could be detected from infected leaf tissue without the need for sophisticated equipment. For these analyses, only the 11B2 mAb and scAb were implemented as these have relatively high working dilutions making them suitable for dot blot which typically requires a higher volume of diluted antibody for functionality than other immunoassays, for example, ELISA. Initial assessments were made with the recombinant form of the CP, as described in *Section 2.19*. A series of dilutions were performed on the CP and these were spotted onto a nitrocellulose membrane. This membrane was subsequently probed with the either the 11B2 mAb or scAb which, in turn, was detected with either an anti-mouse secondary antibody or an anti-HA antibody, respectively. A control blot was also included for each whereby a 1% (w/v) block solution was used in lieu of either the 11B2 mAb or scAb. From the results, it is clear that both forms of 11B2 readily react with the recombinant CP. With respect to the mAb, *Figure 4.29 (i)*, signal on the dot blot is clearly visible to 1.78ng CP for the mAb, with very faint signal observed at 0.44ng (440pg). For the scAb (*Figure 4.30 (i)*), a clear signal was observed to the point of 62.5ng, while a faint signal was observable at the 31.25ng amount. Additionally, no reactivity is observed on the control blot for either the mAb (*Figure 4.29 (ii)*) or scAb (*Figure 4.30 (ii)*). This confirms that the signal in the dot blot arose only from the 11B2 antibodies binding to the CP and not from non-specific interactions between the PVY sample and the labelled secondary antibodies.

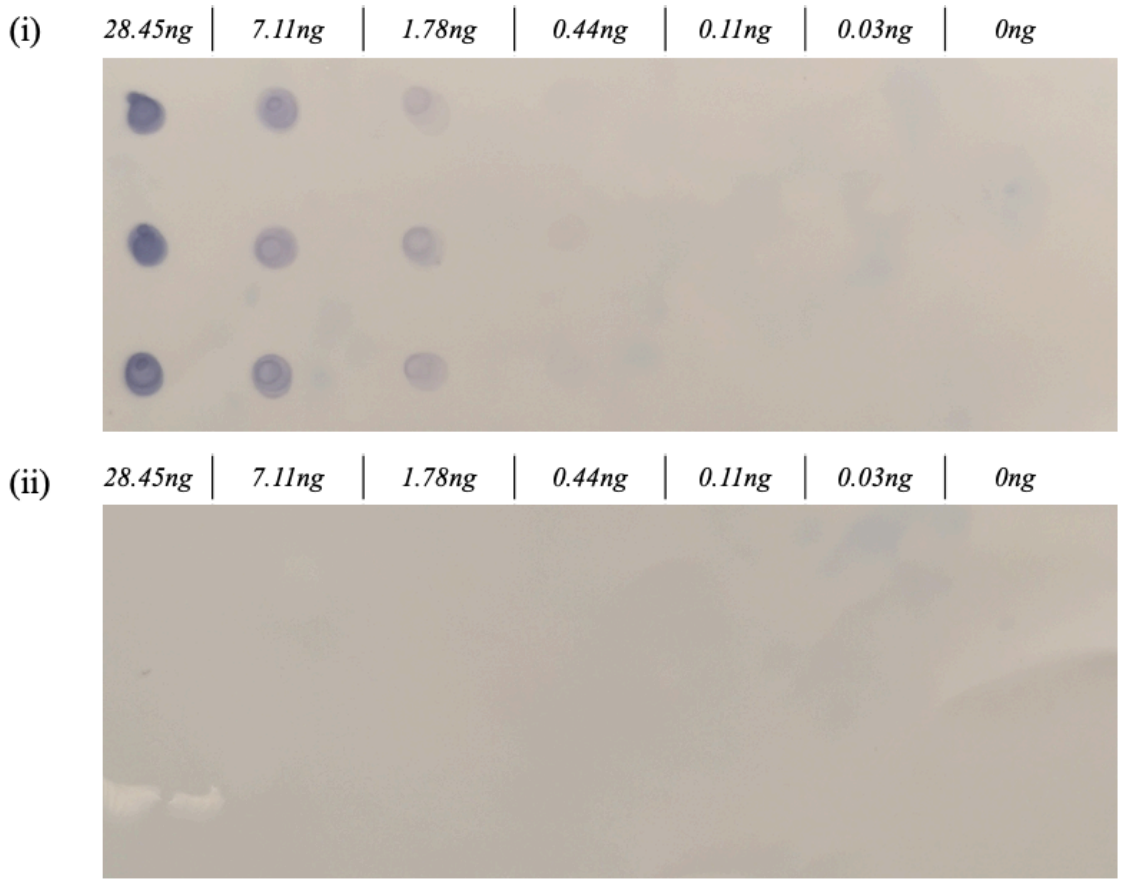

Figure 4.29 Detection of CP by the 11B2 mAb through dot blots

Samples of recombinant CP were dotted onto nitrocellulose membranes. ***(i)*** *One membrane was probed with the 11B2 mAb. Detection of the bound mAb was facilitated by the application of an anti-mouse H+L HRP-labelled secondary antibody.* ***(ii)*** *A control membrane was employed whereby 1%* (w/v) *block was used in lieu of 11B2. This membrane was then also probed with an anti-mouse H+L HRP-labelled secondary antibody.*

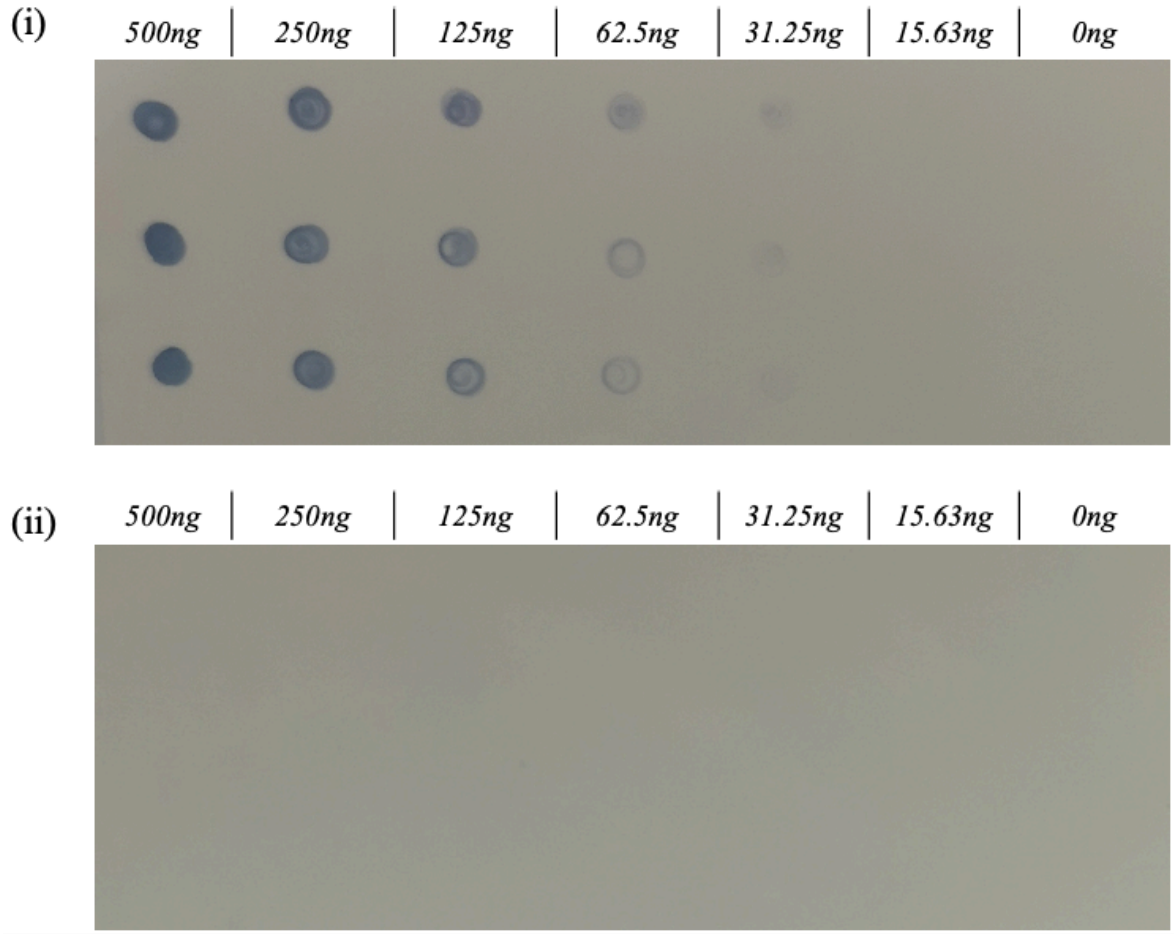

Figure 4.30 Detection of CP by the 11B2 scAb through dot blots

Samples of recombinant CP were dotted onto nitrocellulose membranes. ***(i)*** *One membrane was probed with the 11B2 scAb. Detection of the bound scAb was facilitated by the application of an anti-HA HRP-labelled secondary antibody.* ***(ii)*** *A control membrane was employed whereby 1% (w/v) block was used in lieu of the scAb. This membrane was then also probed with an anti-HA HRP-labelled secondary antibody.*

Based on the results of the dot blot analysis using the recombinant CP, it was determined that the mAb had greater sensitivity in dot blot when compared to the scAb, with a LOD around 440pg, as opposed to the scAb which appeared to have a lower limit near 31.25ng. As such, it was decided to carry the mAb forward for the examination of PVY-infected crude leaf extracts in dot blot.

4.2.12.2 Detection of PVY from crude leaf extracts in dot blot

The 11B2 mAb was incorporated in further dot blot analysis to determine its ability to detect CP from the samples of PVY-infected leaves. This was assessed as described in *Section 2.19*.

Dot blots were prepared by spotting samples of recombinant CP, PVY-infected plant extracts, or healthy plant extracts onto a membrane. Each of these samples was dotted onto a membrane which was then probed with the 11B2 mAb. Bound mAb was detected with a HRP-labelled anti-mouse antibody. As before, a control reaction was included whereby no 11B2 was applied for the primary antibody probing step, and instead only 1% (w/v) block was applied. From the result (*Figure 4.31*) it appeared that the 11B2 mAb was strongly reactive with both the recombinant CP and natural PVY-infected leaf extracts, while showing no reactivity with healthy leaf extracts or the control dot (PBS). The control blot also presented with no reactivity against any sample except for some weak reactivity of the anti-mouse H+L HRP-labelled antibody with the N-serotype sample. This non-specific binding of the secondary could be attributed to the complexity of the crude plant matrix and could be remedied by direct conjugation of the 11B2 mAb with a reporter molecule, e.g. HRP or biotin, as the 11B2 mAb itself appeared to have no reactivity with healthy leaf. Such dot blot assays are cheaper to perform than typical ELISAs and also allow for the possibility of large-scale sampling in-field through methods such as tissue blot whereby suspect plant components such as leaf or stems can be simply pressed into the membrane.

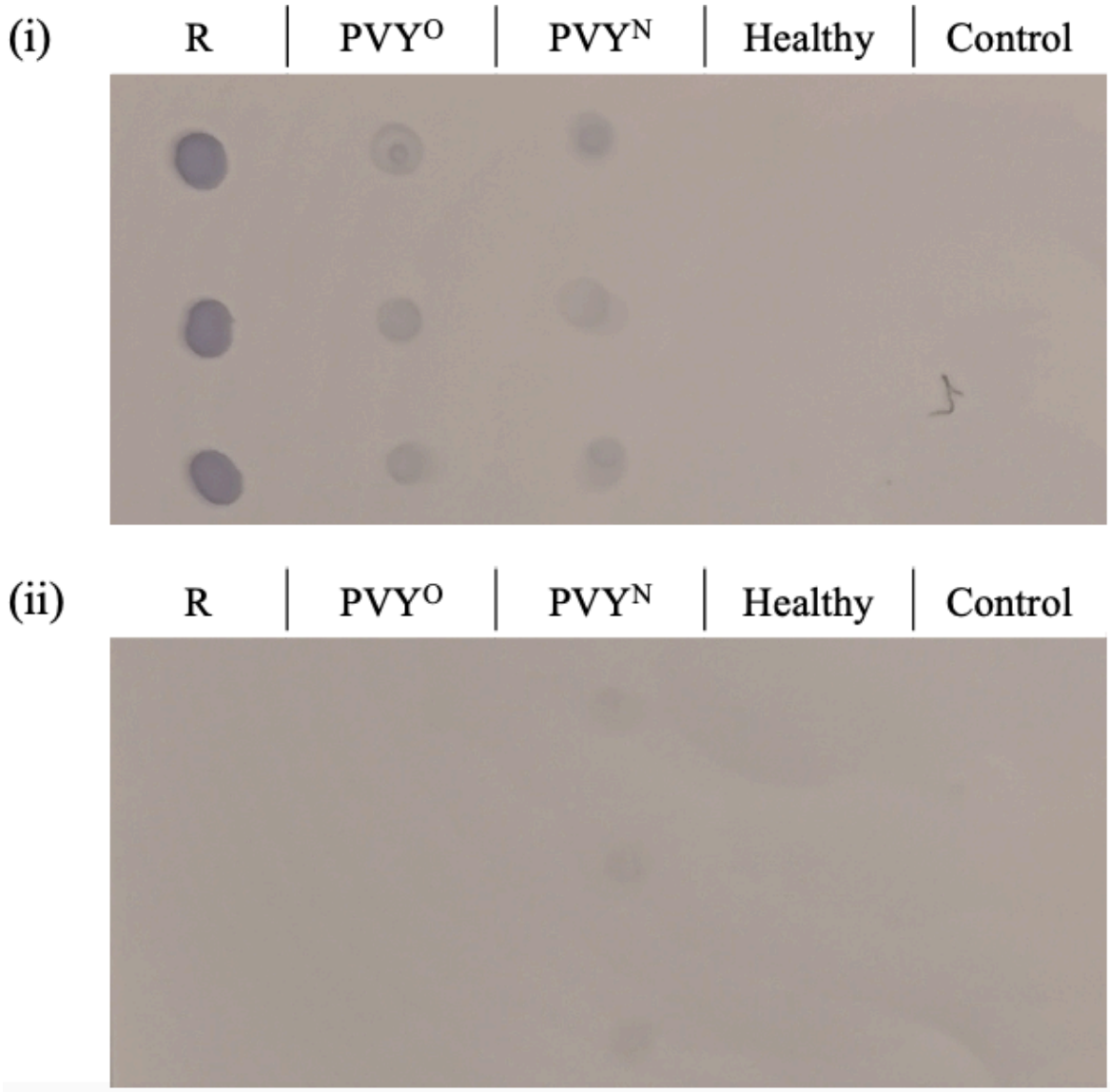

Figure 4.31 Detection of CP in crude leaf samples by the 11B2 mAb through dot blots
Samples of either recombinant CP, PVY-infected leaf samples from O and N serotypes, or healthy leaf were dotted onto nitrocellulose membranes. ***(i)*** *A test membrane was probed with the 11B2 mAb. Bound mAb was detected through the application of an anti-mouse H+L HRP-labelled secondary antibody.* ***(ii)*** *A control membrane was employed whereby instead of an application of 11B2, a 1% (w/v) block solution was used. This membrane was then similarly probed with an anti-mouse H+L HRP-labelled secondary antibody.*

In addition to the design and generation of competitive ELISAs and dot blot assays for PVY detection, it was considered important to develop a system by which PVY could be rapidly detected, as both of the aforementioned assays require several hours to complete. For this

purpose it was decided to develop a SPR-based assay which facilitates rapid, real-time and label free immunodetection of antigens.

4.2.13 Development of an SPR-based immunosensor assay for PVY detection

To further demonstrate the utility of 11B2 as a candidate for incorporation into a immunosensor detection platform, a biosensor assay was developed on a Biacore X100 as per *Section 2.20*. This was established in a capture assay format, whereby 11B2 was captured on the surface of the sensor chip via the action of an anti-mouse Fc antibody. Thereafter, antigen was flowed over, with a regeneration of the chips surface performed in between each antigen run. A sample sensorgram for a single cycle within the binding assay is depicted in *Figure 4.32.* In this diagram, markers are provided for each event in the cycle. Each cycle in the binding analysis follows a similar pattern to that shown in *Figure 4.32*.

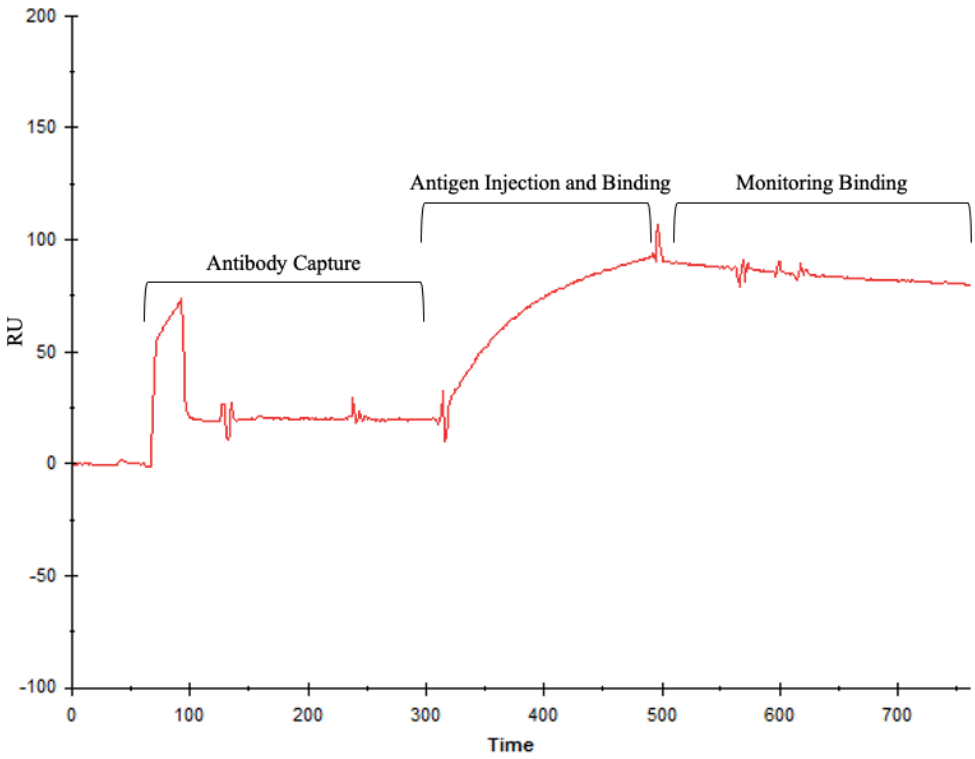

Figure 4.32 Single cycle sensorgram of CP detection in a SPR format

The 11B2 antibody is injected and captured to the sensor surface by an anti-mouse Fc antibody. The RUs increase due to the capture of 11B2 on the sensor surface. Thereafter, the CP antigen is injected where it is bound by 11B2. Binding of the antigen by the antibody elicits another increase in RU. An observed increase in RU is directly proportional to an increase in CP concentration across the linear range of the assay. The sensorgram baseline is adjusted to zero prior to antibody capture to demonstrate binding.

For this capture assay, a chip was functionalised on both flow cells with an anti-mouse Fc antibody, this was used to capture 11B2 (*Section 2.18.1*). A range of antigen concentrations, 70,000ng/mL – 4ng/mL, were passed over the 11B2-functionalised surface in triplicate and the response monitored. The RUs were recorded based on the stability measurement, which reflects the level of antigen remaining captured on the surface after sample injection. This accounts for any signal generated by effects the sample injection may have caused. The resulting data was fitted to a 4-parameter logistical curve in BiaEvaluation software (*Figure 4.33*). From this calibration curve, the LOD was calculated by first determining the LOB using the equation "*LOB = mean of blank + 1.645(SD of blank)"*. The LOB value was then used to calculate the LOD in the equation "*LOD = LOB + 1.645 (SD of low concentration sample)*". The LOD for the Biacore capture assay was found to be 148.7ng/mL. This is considerably lower than the LOD of 651.7ng/mL achieved in ELISA using the same mAb.

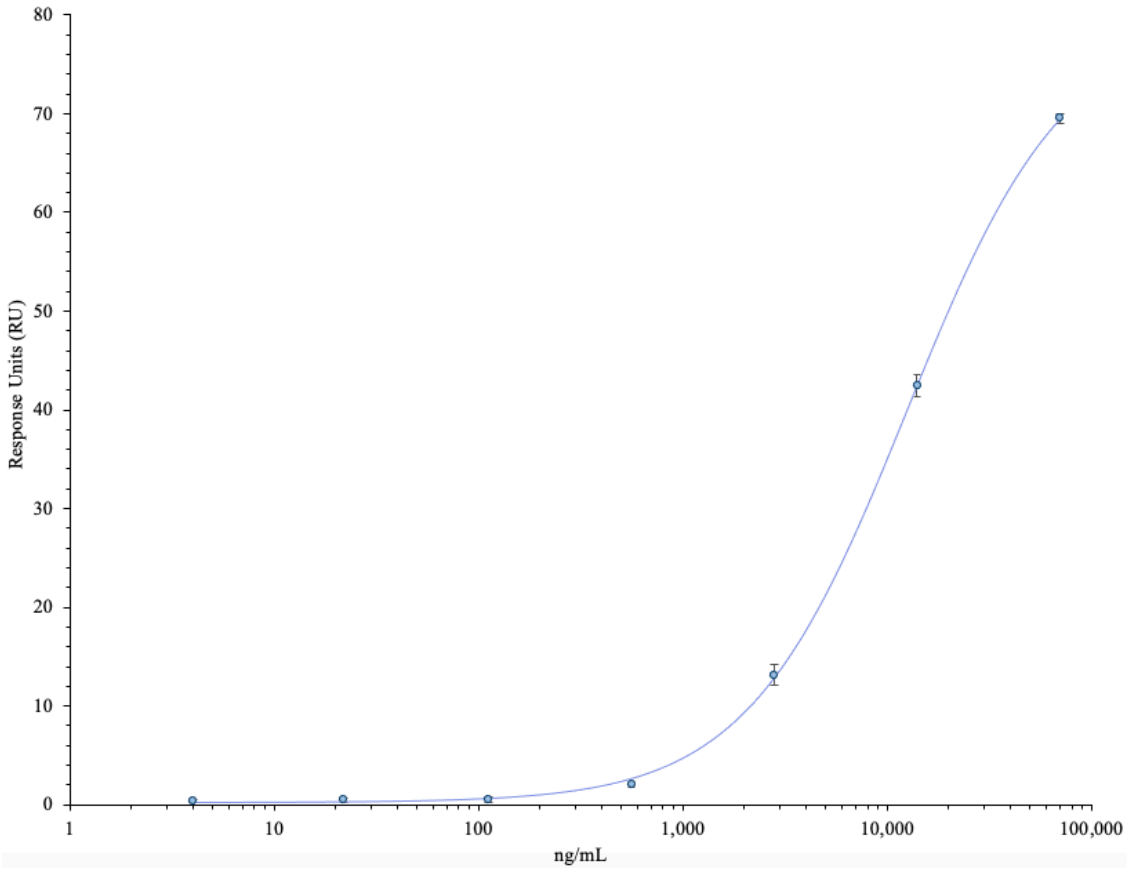

Figure 4.33 SPR-based sensing of CP by the 11B2 mAb

CP was passed over the surface of an 11B2-functionalised chip at a range of concentrations (70,000ng/mL - 4ng/mL). Signal was recorded in RUs, based on the stability reading of triplicate samples of each concentration. Calibration curves were generated in BiaEvaluation software using a 4-parameter logistical equation. Error bars represent SD.

This assay demonstrates the functionality of the 11B2 mAb in capture assay format, indicating that the antibody can readily capture free-flowing antigen from solution and trap it on the sensor surface, generating signal in a 'label-free' and 'real-time' system. This, therefore, acts as 'proof-of-concept' that the 11B2 mAb can be incorporated into future 'label-free' biosensor systems for PVY detection.

4.3 Discussion

The work in this chapter endeavoured to provide several antibody candidates to aid in the early detection of PVY. The aim was to restructure 'full-length' anti-CP mAbs into scAb and scFv derivatives and characterise the binding qualities of these fragmented forms, alongside characterisation of the 'full-length' parental antibodies. It was intended to use a combination of immunoblotting, SPR and ELISA analysis to elucidate the characteristics of each antibody. Additionally, it was aimed to devise a 'proof-of-concept' sensor through which PVY could be detected in real-time and with good sensitivity.

Four anti-PVY hybridoma lines were selected for reformatting. Initial characterisations of these lines were performed in scFv format. From this preliminary analysis, two clones, 41B and 11B2, presented themselves as suitable candidates due to a demonstrated detection of immobilised CP in addition to presenting competition for the CP antigen in solution. On this basis, these clones were selected for further analysis in mAb, scAb and scFv formats. The 41B parental mAb was successfully cultured and purified through affinity chromatography prior to analysis of both the 41B and 11B2 mAbs in WB. Thereafter, work was continued into the optimisation of the expression of the recombinant scAb and scFv forms of 41B and 11B2. Initial optimisations were performed with respect to IPTG concentration and induction temperature. Thereafter, the clones were expressed large-scale and purified. However, it was noted that after the purification, the expression levels of the clones were prohibitively low and the majority of the protein was present in the insoluble fraction, suggesting that the proteins had undergone aggregation and were unsuitable for use in assay development in their current state. In order to render the proteins applicable to immunoassay development, they were required in soluble form. Therefore, efforts to solubilise the scAb and scFv proteins were undertaken. These investigations were restricted to the 11B2 forms of recombinant antibody due to a noted propensity of the 41B scFv and scAb to possible degradation.

Based on the accumulation of scAb and scFv in the insoluble fraction, it was hypothesised that under the current expression conditions, these proteins were forming insoluble inclusion bodies. This may have arisen, in part, from rapid and high-level expression of the proteins brought about by the codon optimisation performed on the DNA sequence of the clones of interest. Codon optimisation methods replace codons rarely used in *E. coli* with synonymous, but more commonly used, codons. This, in turn, yields a sequence from which the *E. coli* host can more readily manufacture protein when compared to sequences which maintain the fidelity of the codons in the species from which they were derived (Francis and Page, 2010). Codon optimisation is highly useful as expression levels of optimised proteins can be significantly higher than those which remain un-optimised, however, rapid expression does not always yield protein of high solubility. If regions of hydrophobicity were present on the antibody proteins, for example strings of hydrophobic residues, this, in conjunction with misfolding of proteins due high protein expression levels, can lead to aggregation and protein insolubility as a result of hydrophobic interactions (Singh et al., 2015). The occurrence of higher levels of insolubility for some codon-optimised proteins was demonstrated previously whereby the re-introduction of non-optimised codons increased soluble protein yield by slowing protein production (Konczal, Bower, and Gray, 2019). It is also suggested that the presence of rare codons in naturally occurring protein-coding sequences in fact aids in correct folding by slowing protein synthesis at certain regions (Komar, 2009). To remedy the apparent insolubility of the 11B2 recombinants, it was decided to attempt to slow protein expression through the optimisation of the expression conditions, rather than retroactive 'de-optimisation' of certain codons, as often expression conditions can be tailored to decrease protein production rates. To achieve this, the 11B2 scAb and scFv were optimised under the parameters of induction temperature, media and glucose supplementation. Of these optimisations, the reduction of induction temperature to RT appeared to have the greatest impact, with considerably increased expression observed upon lowering the induction temperature from 25ºC to RT. This finding supports the idea that rapid expression was causing insolubility as temperature is linked to rate of metabolism in *E. coli*, with lower temperatures resulting in slower recombinant protein synthesis (Vera et al., 2007). Therefore, the reduced induction temperature may have provided sufficient time for the production and correct folding of the recombinant antibody proteins, preventing high levels of aggregation and increasing overall solubility. Upon optimising the 11B2 scAb and scFv to a suitable point and isolating purified forms of each protein through affinity chromatography, various characterisations were undertaken.

Initial assessment of the resulting antibodies was performed in immunoblotting whereby the 11B2 scAb and mAb were used in WB alongside the recombinant CP. Additionally, the mAb and scAb were also used in WB in conjunction with plant samples known to be infected with PVY. On each occasion, reactivity was only observed with the CP bands, demonstrating good specificity, even when challenging the antibodies against more complex matrices such as the crude leaf extract. Furthermore, the WB analysis implied the ability of the antibodies to be used in a 'broad-spectrum' detection manner, as they were found to be reactive with both serotypes associated with PVY, O and N. While the scFv was not assessed in this immunoblot analysis due to its comparatively low working dilution, it is expected that it should present the same binding pattern as the mAb and scAb, which contains homologous binding regions. Having confirmed the specificity of the antibodies for both the recombinant and natural forms of the CP, characterisations were progressed to investigate the impact of reformatting on the affinity of the parental mAb when compared to the recombinant forms. This was achieved through the employment of SPR.

SPR analysis facilitates the elucidation of factors known as kinetic constants. These constants provide information with respect to how fast an antibody will associate with its antigen (k_{on}/k_a) and for how long the antigen remains bound in the antibody-antigen complex (k_{off}/k_d). The ratio between the k_a and k_d is reported as the equilibrium dissociation constant, K_D, which can be used to ascertain the overall affinity an antibody has for its antigen. In this work, the kinetic analysis revealed that the 11B2 mAb and 11B2 scAb had K_D values of 1.09 x 10^{-8} and 2.44 x 10^{-7}, respectively, indicating both antibodies exhibited binding in the nanomolar range. The 11B2 mAb demonstrated a superior K_D value than that of the 11B2 scAb, an occurrence which has previously been recognised, as the defined affinity upon restructuring of a parental mAb is variable, with both gains and losses in affinity observed (Patel and Andrien, 2010; Nuttall et al., 2011; Badescu et al., 2016). This change in affinity, apparently brought about by the removal of constant regions from the parental IgG, not only demonstrates the importance of characterisation of restructured antibodies, but also highlights the role that regions other than the CDRs can play in antigen binding

In addition to kinetic analysis, the 11B2 mAb, scAb and scFv were characterised in a competitive ELISA format. All data points on developed competitive ELISAs were found to have intra-day CVs of <15%, indicating that each was within the recommended allowable variation in immunoassay and had acceptable levels of reproducibility (Findlay et al., 2000;

EMA, 2011). Additionally, the calibration curves generated for each of these proteins led to the estimation of LOD values of 651.7ng/mL, 303.6ng/mL and 162.7ng/mL for the mAb, scAb and scFv assays, respectively. While the LOD values for the scAb and scFv ELISAs appear lower than that of the mAb-based ELISA, this is not necessarily a definitive reflection of the antibody's detection limits as different secondary detection approaches were used for the recombinant antibody ELISAs and the mAb ELISA. Therefore, while overall it can be concluded that of the developed assays, the ELISAs using the recombinant antibody forms offer higher sensitivity, it should be noted that an absolute comparison of LOD in competitive ELISA could only be achieved through an alternative means such as direct labelling of the antibodies, or expressing each antibody with a uniform antigenic tag. The ELISAs implementing the scAb and scFv, however, did employ the same secondary antibody. Therefore, in this work, it appears that the scFv presented the lowest detection limit of the two recombinant formats, with an elucidated LOD of approximately half the concentration of the LOD of the scAb. This higher sensitivity may be attributed to the tendency that some scFv proteins have toward dimer formation. Dimerisation of scFv proteins can lead to an overall increase in avidity, the stability of the overall antibody-antigen complex (Lee et al., 2002). With respect to competitive immunoassay, the results suggest that the scFv could detect, and remain bound to, free antigen at lower concentrations than that of the scAb, allowing the detection of PVY with increased sensitivity. Of benefit to the developed competitive immunoassays would be assessment of the identified standards in a leaf-matrix and subsequent elucidation of LODs through the resulting curves. This would provide information on the impact of matrix effects on the developed assays. This was partially investigated through assessment of the antibodies in competitive ELISA alongside crude leaf samples, wherein the mAb, scAb and scFv could readily differentiate PVY-infected leaf samples from healthy crude leaf extracts. While no information with respect to the effect of the matrix on LOD could be ascertained from this analysis, it illustrated the ability of the antibodies to function even in crude matrices, therefore, generation of calibration curves in crude leaf matrices is not predicted to pose a challenge. Additionally, the expansion of the described crude-leaf competitive ELISA to field-trials would aid in the further validation the detection capacity of the 11B2 antibodies.

In an effort to develop a paper-based assay which could be employed at low cost with minimal equipment requirements, a dot blot assay was designed. Initial investigations were performed with the 11B2 mAb and scAb. In this analysis, it was found that the scAb

presented a LOD of ~31.25ng, while the detection limit of the mAb was closer to 440pg. Therefore, the latter, being more sensitive, was carried forward for investigation with crude plant samples. This further analysis demonstrated the applicability of 11B2 to the detection of PVY from crude extracts, with positive signal generated against PVY-infected plants, but none generated against healthy plants. This dot blot requires minimal hands-on operating time as crude samples can be used, meaning that very little preparation is required. The assay could feasibly be completed in one day, with the possibility of multiplexed testing of plant samples on the same blot. Additionally, the assay could be made more rapid via direct conjugation of the antibody, removing the need for any secondary antibody probing step.

While the dot blot is a useful and inexpensive assay, detection of PVY would benefit from additional methods which demonstrate higher sensitivity, as the level of virus in the plant can remain relatively low at the early window of infection. To offer a sensitive, real-time and label-free assay, it was proposed to develop a SPR-based immunosensor assay. This assay, developed using the 11B2 mAb, could detect PVY from solution at a LOD of 148.7ng/mL. This SPR-based assay offered the most sensitive PVY detection of the assays developed in this work. Additionally, the SPR-assay functions in 'real-time' without the need for labelling, facilitating rapid detection at low antigen concentrations. The developed assay acts as a 'proof-of-concept' for incorporating the 11B2 antibody into future biosensing assays for the real-time detection PVY with high sensitivity.

In conclusion, the work described in this chapter focused on the development and characterisation of antibodies against PVY in an effort to provide sensitive detection methods for the improved diagnosis of PVY. This was performed in conjunction with investigating the applicability of recombinant forms of restructured 'full-length' mAbs. From the research, recombinant versions of parental mAbs were generated and could be expressed rapidly and inexpensively in an *E. coli* host under optimised conditions. The isolated antibodies were proven to have specificity for the CP antigen through immunoblot analysis. Additionally, three competitive ELISAs were developed which demonstrated good sensitivity for the detection of PVY. These assays also illustrated retention of the antigen-binding properties of the recombinant forms of the parental mAb, with lower LODs achieved in the ELISAs implementing the recombinant fragments than the ELISA utilising the mAb. Assessment of PVY-infected leaf samples in further ELISA analysis confirmed the functionality of the developed assays. In addition to the generation of standard curves in

ELISA, the work in this chapter also offered a cheaper assay alternative in the form of a dot blot. This assay can be performed with minimal hands-on time and was shown to readily detect PVY from infected leaf samples with no cross-reactivity with healthy leaf material observed. Furthermore, in an effort to offer a detection method with increased sensitivity, an immunosensor assay was designed in an SPR-system. This sensing approach led to development of an assay with which the lowest demonstrated LOD was achieved. The developed assays provide evidence that the isolated and characterised antibodies are highly suited to the intended future application which is the development of biosensing systems for rapid, sensitive and early-stage PVY detection.

Chapter 5

Development of a Nucleic Acid Lateral Flow Immunoassay for the Rapid Detection of Potato Virus Y

5.1 Introduction

PVY is considered the most important pathogen of potatoes globally, causing yearly major losses and reduced food yields. As PVY can spread readily through crops as a result of infected seed potatoes, cross-contamination from machinery or through aphid vectors, it is important to develop rapid and sensitive methods by which users can detect this virus. Previously discussed in this thesis was the development of PVY-specific antibodies and the design of subsequent immunoassays employing these antibodies, however, the detection of virus-associated nucleic acids is another highly popular and valuable method of pathogen detection. Nucleic acid-based detection is typically more sensitive than standard immunoassay, for example ELISA. Incorporating nucleic acid detection methods could provide the potential for an earlier diagnostic window at very low virus levels. This, in turn, may permit early intervention in a crop which has tested positive for PVY, preventing widespread infection across the entire field. Furthermore, nucleic acid detection methods could be used in conjunction with the immunoassays developed in *Chapter 3* and *Chapter 4*, to increase diagnostic confidence by combining two confirmatory tests which implement different detection mechanisms.

One of the most widely used methods for the detection of nucleic acids is PCR, and its derivative qPCR, the latter of which facilitates accurate quantitation of the target pathogen through the use of oligonucleotide probes and dyes (Mullis et al., 1986; Heid et al., 1996). However, these traditional methods require sophisticated machinery, can be time consuming and generally require trained staff. This is not optimal for application to situations where on-site testing may be desired, for example, within a field of crops or at seed potato import/export sites. As an alternative to classic PCR, which requires controlled cyclical runs using stepwise temperatures, newer types of nucleic acid amplification methods which function at singular temperatures are proposed. These are termed isothermal amplification methods. A host of such isothermal amplification approaches are available such as nucleic acid sequence-based amplification (NASBA), strand-displacement amplification (SDA), rolling circle amplification (RCA), loop-mediated isothermal amplification (LAMP), exponential amplification reaction (EXPAR) and helicase-dependant amplification (HDA), (Compton, 1991; Walker et al., 1992; Lizardi et al., 1998; Notomi et al., 2000; Van Ness, Van Ness, and Galas, 2003; Vincent, Xu, and Kong, 2004). One of the more recently developed isothermal reactions, recombinase polymerase amplification (RPA), is particularly appealing due to the fact that it operates at relatively low temperatures, without

the need for DNA denaturation or preparation prior to the commencement of the reaction (Piepenburg et al., 2006).

While standard PCR amplification utilises cyclic temperatures, oligonucleotides and a polymerase to achieve strand denaturation and template amplification, RPA relies on the action of alternative proteins to achieve the same. These unique proteins consist of a recombinase, recombinase loading factor and single-stranded DNA binding protein (SSBP) which work together in tandem with other reaction components such as creatine kinase, phosphocreatine and polyethylene glycol (PEG). Creatine kinase contributes energy in the form of ATP by acting on phosphocreatine, while PEG acts as a crowding agent, enhancing amplification (Daher et al., 2016). The recombinase forms a nucleoprotein complex with target-specific oligonucleotides (primers). This complex scans the DNA template for the primer cognate binding sites. Once identified, strand exchange occurs at the primer-binding regions on the template, forming a D-loop structure, making this region of the DNA template available for amplification. In the reaction, ATP is hydrolysed to ADP, which induces spontaneous dissociation of the recombinase. SSBPs are recruited to replace the recombinase and these act to support the unwound, single-stranded DNA and permit stable binding of the primers. A strand displacing polymerase then extends from the 3' end of the primers, permitting template amplification. This balance between nucleoprotein formation and recombinase dissociation gives rise to the exponential nature of RPA (Piepenburg et al., 2006; Daher et al., 2016; Li, Macdonald, and Von Stetten, 2019).

The reaction is performed at temperatures between 22ºC - 45ºC, with the optimal range lying between 37ºC and 42ºC. This means little to no heating equipment is required to perform to the reaction. The high flexibility associated with this reaction temperature is helpful for on-site amplification where slight variations could occur based on environmental changes. While amplification at ambient temperature is limited to warmer climates, successful RPA can be performed in colder ambient temperatures through the employment of exothermal chemical heaters, for example sodium acetate trihydrate (SAT), commonly used in hand-warmers, or by using body heat incubations alone (Crannell, Rohrman, and Richards-Kortum, 2014; Lillis et al., 2014; Wang et al., 2017). The reaction can be completed in as little as 20 min, facilitating rapid point-of-use testing and diagnosis. In addition to the advantages of flexible operating temperatures and rapid assay performance, a further advantage of RPA is its apparent tolerance to base mismatches between primers and the

target region (Abd El Wahed et al., 2013; Daher et al., 2015; TwistDx, 2021). PVY is a diverse virus with new recombinant forms likely to increase in abundance in the future based on current trends and the ongoing globalisation of the food and agriculture industry. Each recombinant form has unique characteristics and variations can occur across many regions of the genome, as such, there is potential for some heterogeneity across the targeted regions. The ability of RPA to function even in the presence of several base mismatches between primer, probes and the target DNA is advantageous in this scenario as it suggests that even in the case where some mismatches occur, the reaction could still commence. This, in turn, lowers the likelihood of false negative reporting arising from a diversity-driven inability to amplify the PVY target. However, this tolerance to mismatches also emphasises the need for vigilance in primer and probe design to ensure a limited level of sequence similarity occurs between the chosen oligonucleotides and non-target pathogen DNA. Additionally, in some scenarios, mismatches were observed to decrease amplification efficiency, therefore, it is preferable to maintain as low a number of mismatches between the template and designed oligos as feasible (Liu et al., 2019).

The amplicons resulting from RPA can be detected in a number of ways (*Figure 5.1*). At the most basic, DNA agarose gel electrophoresis can be used, however, this requires additional equipment, reagents and is relatively slow, making it unsuited to on-site testing. DNA intercalating dyes such as SYBR Green or Eva Green can also be used (Singpanomchai et al., 2019; Zhang et al., 2020a). Fluorescence from the binding of these dyes to double stranded DNA is observable with the naked eye, making it suited to on-site detection, however, such dyes will bind indiscriminately to any double-stranded DNA in the reaction. Given that RPA proceeds at lower temperatures, the likelihood of some non-specific amplification occurring is increased when compared to other applications where intercalating dyes are used, such as PCR, where higher operating temperatures enhance specificity. For this reason, unless there is certainty that no double-stranded non-target DNA is formed in the reaction, DNA dyes should be avoided. The employment of probes overcomes the specificity issues associated with the use of DNA dyes. Such probes are incorporated into RPA for quantitative and real-time analysis, these are termed exo and fpg. These probes feature quencher and fluorophore labels which, when bound to specific target regions on the amplicon, undergo cleavage resulting in the permittance of fluorescence as the quencher is removed from the fluorophore (Daher et al., 2016). As cleavage, and resulting fluorescence, only occurs in the presence of the correct internal sequence on the

amplicon, probes are expected to be more specific than DNA dyes. The exo probe is cleaved by exonuclease III and can act as a new primer upon cleavage, while the fpg probe is cleaved by the action of a DNA glycosylase and cannot act as a new primer (Li, Macdonald, and Von Stetten, 2019). Incorporation of these probes into the RPA assay provides measurable fluorescent signal, allowing quantification of unknowns through comparison of sample signal against known standards (Euler et al., 2013; Yang et al., 2015). While such probes are useful for quantitatively reflecting the burden of pathogen in the sample, these methods also require extra equipment to monitor the result, e.g. fluorimeters, making transition to point-of-use challenging. The ideal point-of-use system would require minimal equipment and hands-on time, while still permitting pathogen detection in a rapid manner. These point-of-use qualities can be achieved through the employment of an alternative RPA probe, termed nfo. The incorporation of this probe permits amplicon analysis on lateral flow immunoassay strips. Through this analysis method, the amplicon is dual-labelled with antigenic tags. Detection of the labelled amplicon is usually by sandwich immunoassay, meaning that the amplicon is bound at either end by molecules specific for the antigen tags. This method is termed nucleic acid lateral flow immunoassay (NAFLIA) (Powell et al., 2018).

The combination of NALFIA and RPA could provide a rapid, on-site and sensitive means for the detection of PVY, requiring minimal equipment and hands-on time. Due to this potential, it was decided to develop such an assay in an attempt to offer an effective means of virus detection. However, in order to develop a PVY-specific approach, a suitable target region was required. It is imperative that this target region is unique to PVY, with minimal similarity to other pathogens which may be present in the sample. Another desirable factor of this target is a relatively high level of sequence conservation observed across PVY strains, as this would facilitate broad-spectrum detection. For this purpose, the PVY CP was employed as this contains regions of high homology across viral strains, permitting the opportunity for broad-spectrum strain detection in molecular-based assays (Kogovšek et al., 2008).

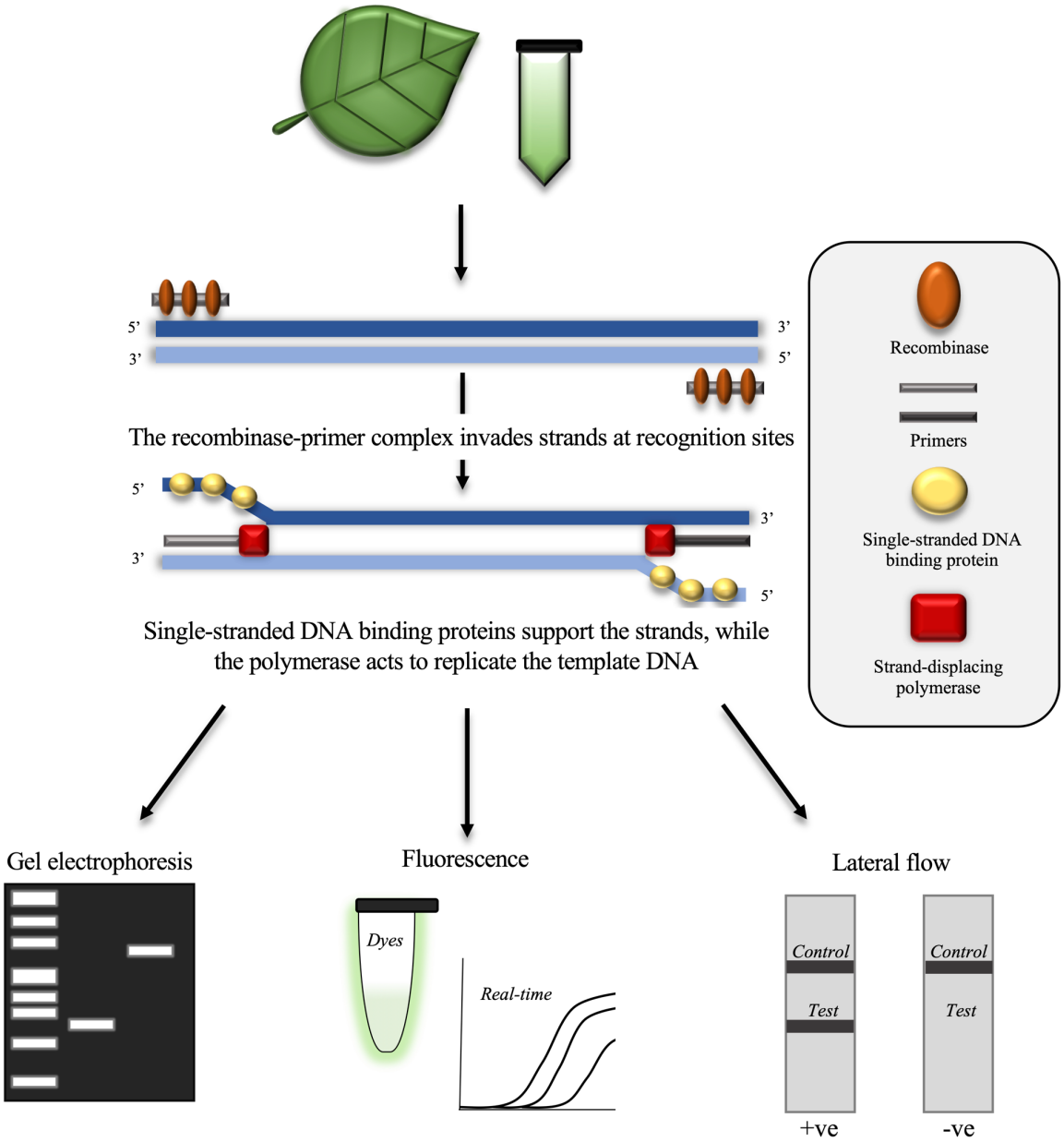

Figure 5.1 Schematic for the amplification and detection of nucleic acids in RPA

Nucleic acids are sourced from plant tissue, for example, suspect leaf tissue. RPA is performed to enrich for the target sequence. Primer pairs are bound by the recombinase. This primer-recombinase complex scans the DNA template for regions of primer-recognition. Upon identification of sequences complementary to the primers, strand invasion occurs and DNA replication proceeds through the action of a strand-displacing polymerase. This process is repeated in an exponential fashion, yielding large quantities of target amplicon. The amplified product can be detected in a number of ways. Some common methods are gel electrophoresis, fluorescent detection through the use of intercalating dyes or probes (real-time detection), or detection on lateral flow strips.

5.2 Results

5.2.1 Primer design

5.2.1.1 Identification of RPA primer pairs

The recommended length for RPA primers is roughly 30-35 nucleotides (TwistDx), moderately longer than standard PCR primers which are usually 18-22 nucleotides long (van Pelt-Verkuil, van Belkum, and Hays, 2008). Additionally, the suggested size for RPA amplicons ranges from 80bp to 500bp as longer amplicons can slow the rate of amplification. With respect to amplicon length, previous studies have indicated that smaller amplicons of ~150bp may be more suited for subsequent lateral flow analysis and could aid in achieving higher sensitivity (Safenkova et al., 2020). Considering each of these factors, it was decided to design primer sets, each primer being at least 30 bases long, which would facilitate the amplification of ~150bp regions on the PVY CP gene. Identification of suitable regions of the target template was achieved by aligning multiple CP sequences in Clustal. These sequences were elucidated by Della Bartola, Byrne and Mullins (2020) from various strains of PVY-infected Irish crops. Some preliminary sequences were provided by collaborators in Teagasc prior to formalisation and publication on Genbank (Della Bartola, Byrne, and Mullins, 2020). The associated Genbank sequences are filed under accession numbers MT264731, MT264732, MT264733, MT264734, MT264735, MT264736, MT264737 and MT264738. The sequence alignment was manually scanned for paired regions of high similarity across PVY strains which were roughly 30 bases long and which facilitated the amplification of a 150bp product. As discussed, RPA primers are reported to be tolerant of mismatches between the template and the designed oligonucleotides, with studies demonstrating successful amplification in the presence of up to nine base mismatches (Boyle et al., 2013; TwistDx, 2021). However, during assay design, the aim was to limit the number of mismatches to maintain efficient amplification and specificity for PVY, while still achieving suitable primer pair design and amplicon size. The highest number of mismatches between the chosen templates and individual primers and probes in this study were three. In cases where mismatches were present between sequences, the sequence from strain PVY^{NTN} was chosen as this strain was found to be most abundant in Ireland at the time of testing (Della Bartola, Byrne, and Mullins, 2020). Three primer pairs were identified under these parameters, the sequences of which are listed in *Table 2.14*.

5.2.2 Primer screening in PCR

5.2.2.1 PCR amplification of target regions

Upon identification of suitable primers sets, a dsDNA template corresponding to the CP of PVY was sourced commercially. Two other templates were acquired to reflect CP sequences of potato virus X (PVX) and potato virus A (PVA). Alongside PVY, PVX and PVA are among some of the most common potato viruses affecting Irish crops. In a 2015 survey of Irish crops, of the viruses tested, PVX and PVA were found to be the second and third most prevalent viruses in Irish seed potato, respectively, with PVY being the most prevalent potato crop pathogen (Hutton et al., 2015). While later in 2020, PVA was found to be third and PVX the fourth most common of the viruses tested, again with PVY being the most abundant (Della Bartola, Byrne, and Mullins, 2020). The details of the various DNA template sequences and corresponding template-specific primers for PVA and PVX are detailed in *Table 2.15* and *Table 2.16*, respectively.

Initially, a standard PCR assay was performed to ensure that the PVA and PVX DNA templates could be used successfully alongside their requisite primers to amplify the target regions. The templates were assessed as per *Section 2.21.2*. Both PVA and PVX amplified successfully, with distinct DNA bands at the expected size visible for each (*Figure 5.2*).

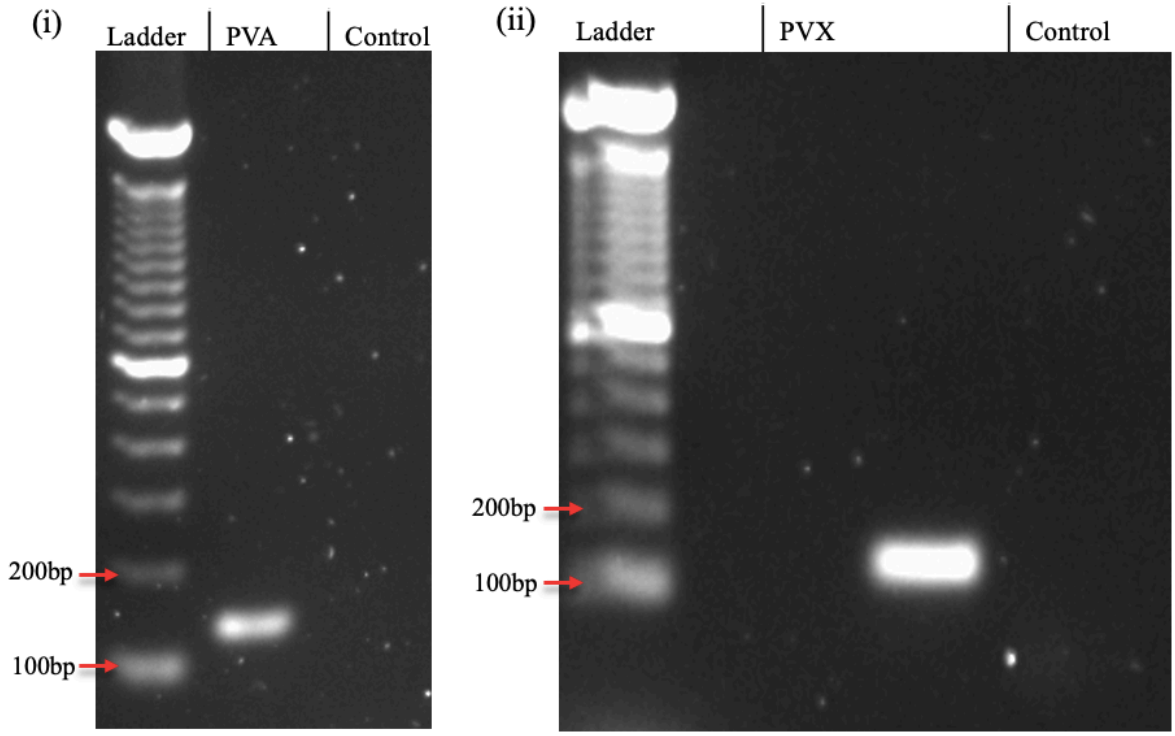

Figure 5.2 Amplification of PVA and PVX templates

*The **(i)** PVA and **(ii)** PVX templates were used alongside their respective primers to ensure functionality. Successful amplification was demonstrated by DNA bands at ~132bp and ~101bp for PVA and PVX, respectively (Ladder = Invitrogen 100bp ladder, control = no template control (NTC)).*

This confirmed, further PCRs were performed to assess the efficacy and specificity of the designed PVY RPA primers. It was important to ensure that no cross-reactivity was present between the PVY-specific RPA primers and the PVX or PVA templates. Given that these viruses may occur simultaneously within a single potato crop, any cross-reactivity between the PVY primers and other co-infecting viruses would pose a problem with respect to false positive results, and subsequent misdiagnosis.

As such, to investigate primer specificity, the PCR reaction also included reactions consisting of the three PVY primer pairs (RPA1, RPA2 and RPA3) in conjunction with either PVY, PVX or PVA templates (*Section 2.21.3*). While RPA primers are longer than typical primers, it was predicted that they should still function in PCR, albeit with potentially slightly lower efficiency as the longer primers may take more time to anneal to the template. The results of this PCR analysis are shown in *Figure 5.3*. All three primer pairs successfully amplified the 150bp insert from the PVY template. Additionally, it was observed that there

was no cross-reactivity between the any of the PVY primer pairs and PVX or PVA in PCR format, as evidenced by the absence of any DNA product in any lanes where PVA or PVX were used as template in lieu of PVY. This confirmed that the three selected primer sets were suitable for subsequent analysis in RPA.

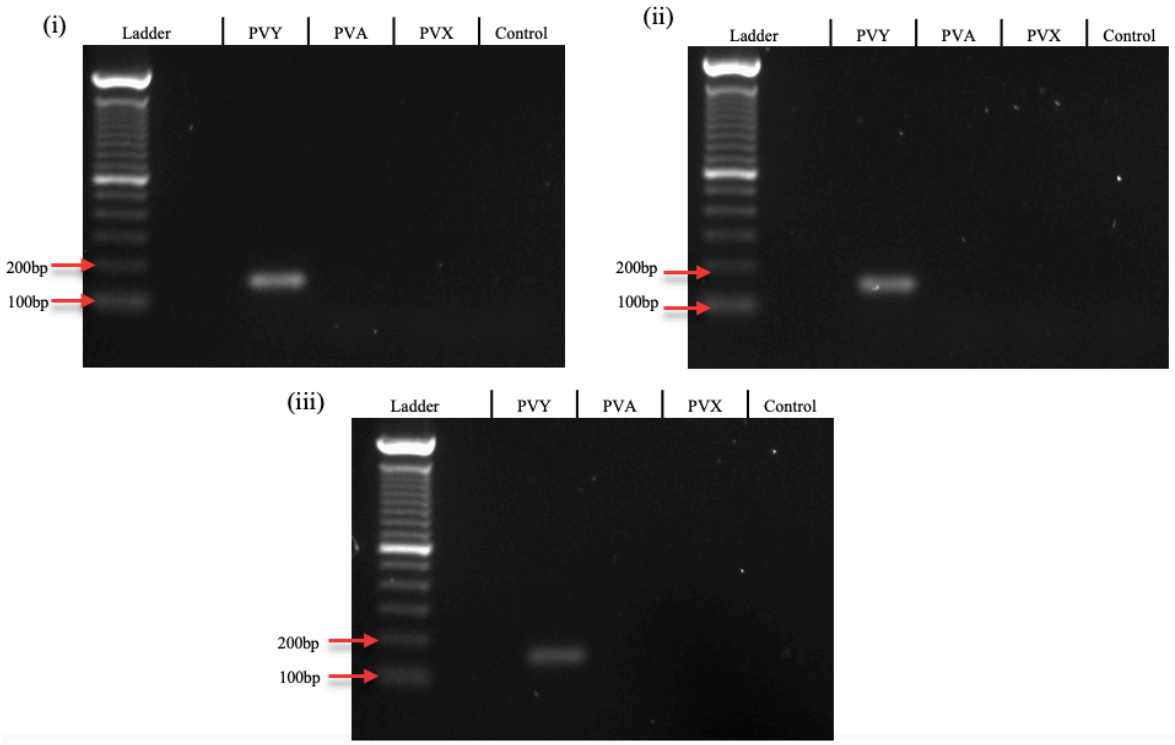

Figure 5.3 Specificity of PVY RPA primers

*Amplification was successful when PVY primers (**(i)** = RPA1, **(ii)** = RPA2, **(iii)** = RPA3) were used in conjunction with the PVY template, however, no such amplification was observed when substituting PVA or PVX as templates into the reaction. This indicates that the designed primers are PVY-specific in PCR (Ladder = Invitrogen 100bp ladder, control = NTC).*

5.2.3 Primer screening in RPA

5.2.3.1 RPA of PVY

RPA is an isothermal amplification method, whereby the reaction is performed at a single temperature, as opposed to PCR, which consists of multiple temperature cycles. Once the specificity and functionality of the PVY primers and templates were confirmed in classic PCR, the assay was progressed to the RPA format. Initially, tests were carried out, as per *Section 2.21.4*, to ensure that the target region on the PVY template could be successfully

amplified using the designed primers in RPA. Additionally, the suitability of the three primer pairs could be compared based on specificity and efficiency of amplification.

It is recommended that the RPA products be "cleaned-up", typically using a PCR clean up kit, post-reaction as some of the components in the RPA reaction can interfere with gel electrophoresis if not removed (TwistDx). However, an alternative option to using a clean-up kit is to apply heat to the RPA sample post amplification. This is suggested to be an adequate and rapid alternative for the purpose of preparing RPA samples for gel electrophoresis (Londoño, Harmon, and Polston, 2016). To assess this, RPA was performed using the three primer pairs alongside the PVY template. After amplification, the samples were divided and treated either using a PCR clean-up kit, or by incubating the samples at 65°C for 10 min prior to electrophoresis. Untreated RPA reactions were also run alongside clean-up kit and heat-treated samples for the purposes of comparison. Controls from each reaction were prepared in the same manner.

From the results (*Figure 5.4*), it is clear that treatment of the samples is necessary after RPA, with double, smeared bands observed in the untreated RPA products for all primer pairs. Contrastingly, usage of the either the PCR clean up kit or heating to 65°C for 10 min resulted in a single distinct band at the expected size of 150bp, with no other bands observed in the lanes, for each primer set. As such, either method was considered suitable for post-RPA sample preparation. It was noted that faint, low weight bands were present in the NTC reactions, regardless of the post-RPA treatment method used. This was postulated to be a result of primer-dimer formation, as the combination of long primers and a low operating temperature means RPA is more prone to dimer product formation. Overall, the results showed positive amplification of the PVY template with the expected size amplicon, 150bp, observed for all primer pairs. Since the primer pairs RPA2 (*Figure 5.4 (ii)*) and RPA3 (*Figure 5.4 (iii)*) presented brighter DNA bands, indicating more efficient amplification, these were chosen for further analysis.

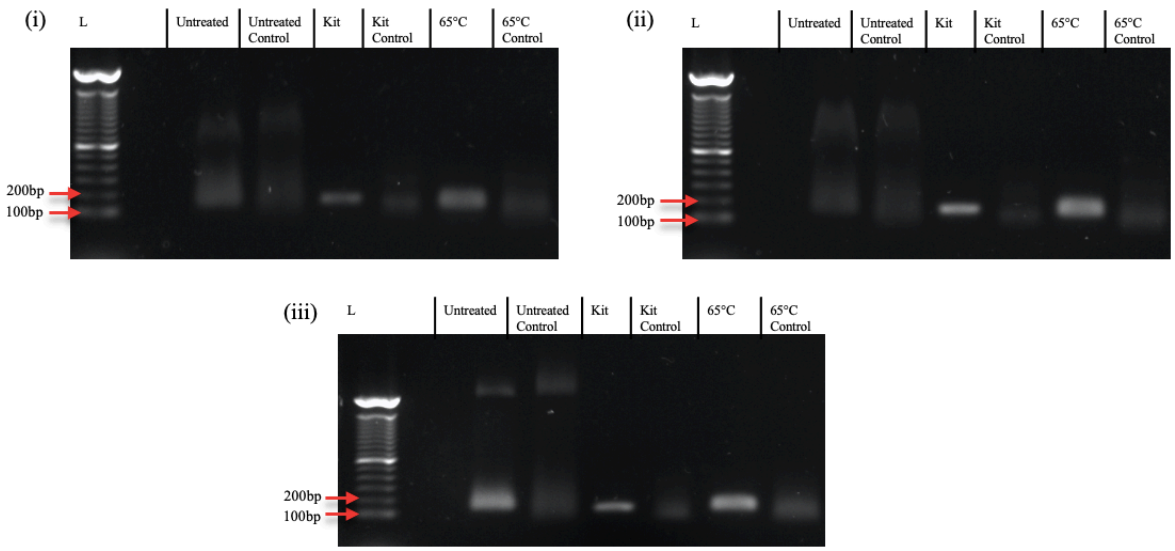

Figure 5.4 Primer screening and comparison of post-RPA treatments

*Amplification was present using all PVY primer pairs (**(i)** = RPA1, **(ii)** = RPA2, **(iii)** = RPA3). In the untreated sample lanes, two smeared bands were observed in both the positive and control reactions for all pairs. When performing clean-up on the products, either through use of a kit or through heating, the only band observed in the positive reactions was the expected size of 150bp (L = Invitrogen 100bp ladder, Untreated = RPA product without post-amplification clean up, Kit = RPA products cleaned up with PCR clean up kit, 65°C = RPA products heated to 65°C for 10 min, controls = NTC).*

5.2.3.2 Specificity of PVY primers in RPA

The specificity of the PVY primers in RPA was assessed as per *Section 2.21.4*. This was performed in a similar fashion to the previously described specificity assessment in standard PCR. RPA was performed using the PVY-specific primers, with either a PVY, PVA or PVX template. The products were cleaned-up and analysed on an agarose gel. The results of the amplification show strong, clear bands at the expected size of 150bp for both RPA2 (*Figure 5.5 (i)*) and RPA3 (*Figure 5.5 (ii)*) when using PVY as the template. Contrastingly, when the PVX or PVA templates are used in lieu of the PVY template, no specific amplification occurred, and only smeared bands were present. Similarly sized bands of comparable intensity also appeared in the NTC lanes, again suggesting that these arose from primer dimer formation, rather than from amplification of the templates. Based on this analysis, both primer sets were considered specific to the PVY template in the RPA format and were taken forward for development into a lateral flow immunoassay-based detection system.

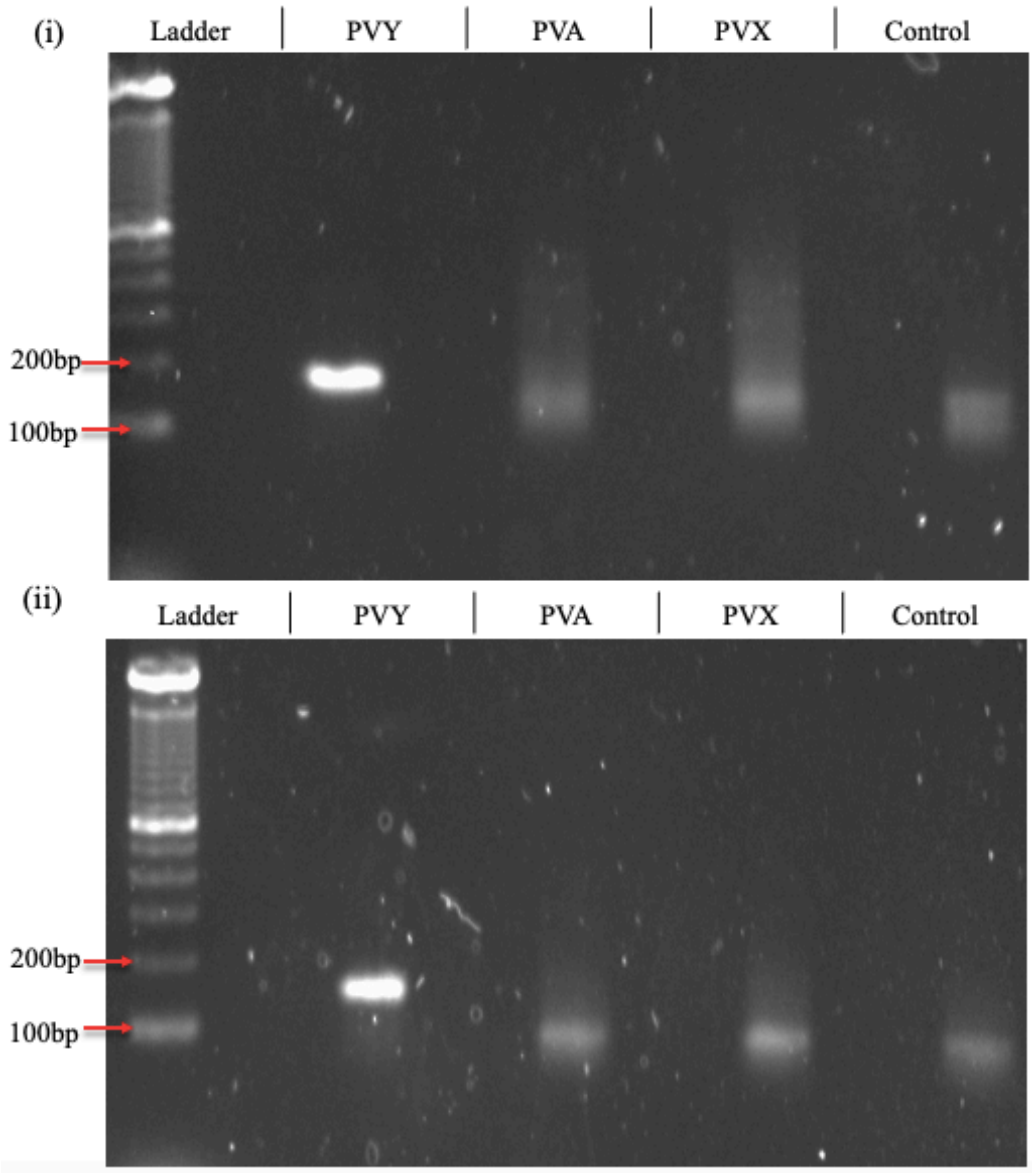

Figure 5.5 Specificity of the PVY primer pairs in RPA format

*Both selected primer pairs (**(i)** = RPA2 and **(ii)** = RPA3)) were found to be specific for the PVY template with strong amplification only occurring in reactions containing the PVY template (Ladder = Invitrogen 100bp ladder, control = NTC).*

5.2.4 Development of nucleic acid lateral flow immunoassay with dual-labelled primers

5.2.4.1 Assessment of dual-labelled primer pairs

RPA is an efficient and rapid method of amplifying nucleic acids, however, without the introduction of probes, or the modification of primers, analysis of products is limited to methods such as gel electrophoresis. This method of results visualisation can be time-consuming, of low sensitivity and requires additional equipment and reagents, detracting from the appeal of RPA. Considering that ideally the developed assay would be applicable

to in-field use for PVY detection, the application of NALFIA was investigated to permit visual detection of the RPA products, without the requirement for additional equipment.

This was initially attempted through incorporation of two unique antigenically-labelled primers into the RPA reaction. These primers, in turn, dual label any resulting amplicons. The labelled amplicons are then mixed with an appropriate buffer prior to their introduction to the lateral flow strip, on which immunodetection of the labels is achieved. This facilitates rapid detection of the amplified product, in an easy-to-use format, making this detection system appealing for on-site diagnostics. The lateral flow-based detection process is presented in *Figure 5.6***.**

In this work, commercial lateral flow strips (PCRD) were employed for the NAFLIA analysis. These PCRD cassettes feature a control line, and two test lines. Test line 1 contains immobilised anti-digoxigenin (DIG) antibodies, while test line 2 features anti-FAM/FITC (fluorescein derivatives) antibodies immobilised at this line, permitting multiplexed detection, if desired. For the purposes of this thesis, only the anti-FAM line (line 2) was utilised. RPA primer pairs RPA2 and RPA3 were dual labelled with a 5' 6-FAM label on the forward primer and a 5' biotin on the reverse primer, and further details are outlined in *Table 2.22*. RPA and subsequent NALFIA detection were performed as per *Section 2.22.1*. Bands on the lateral flow strip were generally visible within the first few minutes of sample application, however, the results were recorded after roughly 10 min. Any results after 10 min were disregarded. Images of lateral flow assays are reported in grayscale.

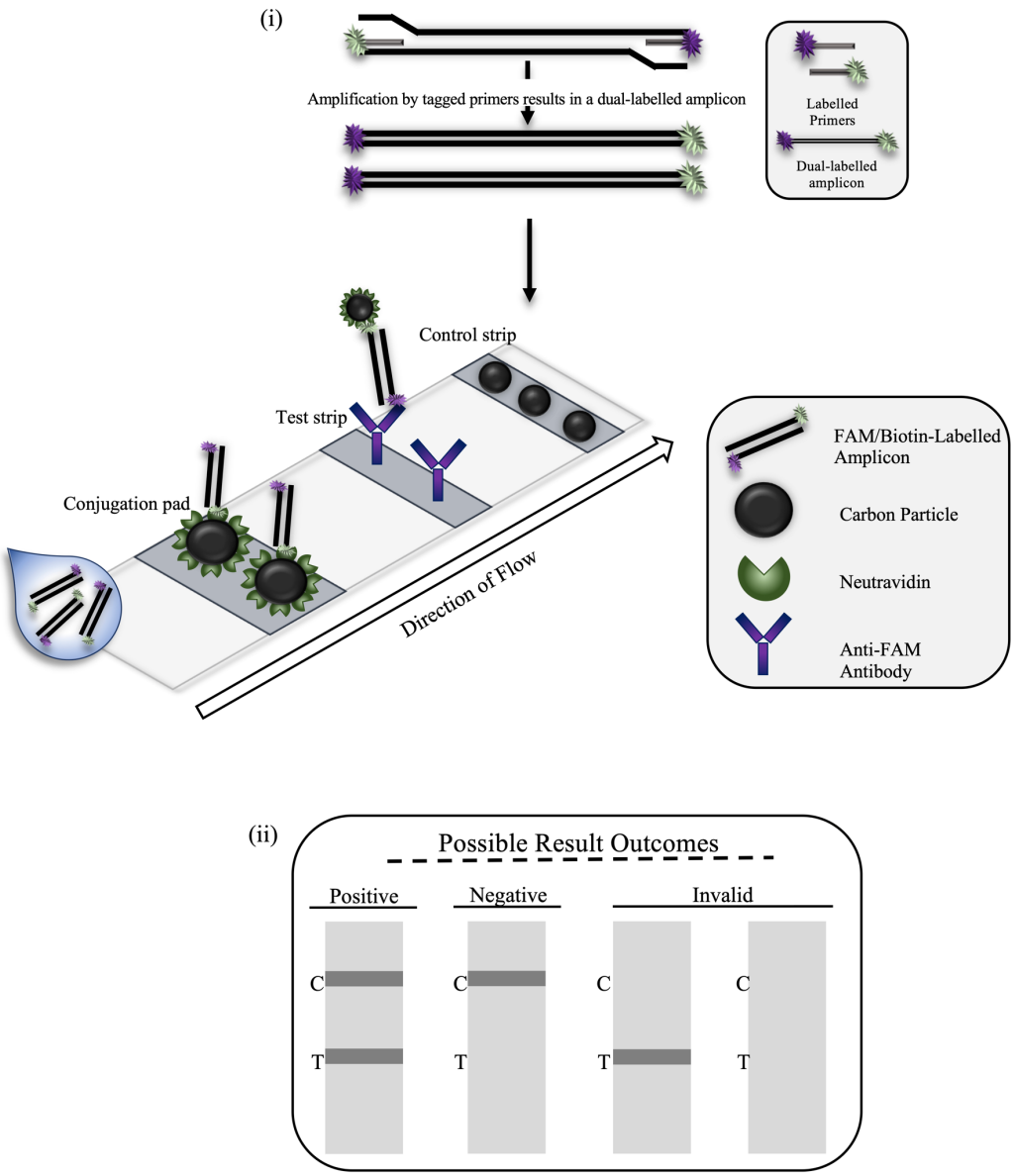

Figure 5.6 Nucleic acid lateral flow immunoassay using dual-labelled primers

(i) *Amplification using dual-labelled primers results in an amplicon presenting with the same labels as the primers, e.g. biotin and FAM. The reaction is applied to the sample pad and traverses the lateral flow strip until it encounters the conjugation pad. Here, it is bound by neutravidin-coated carbon particles which bind the biotin label. The particle-amplicon complex continues along the strip to the test line where it encounters anti-FAM antibodies. These react with the FAM tag, capturing the amplicon, and hence carbon particles, eliciting colour formation at this line. Other carbon particles proceed to the control line where they are captured, validating the assay.* ***(ii)*** *A visible band at the control line is essential for ensuring the assay was functional. No band at the control is considered an invalid assay. A positive test result requires a band at the test line and control line, while a negative result will only present a band at the control line.*

The results of the initial NALFIA analysis of both primer pairs are depicted in *Figure 5.7*. When using RPA2 (*Figure 5.7 (i)*), the positive reaction presents two strong bands at the test and control lines, as expected for a successful amplification of the target region. However, bands are also present at the both the test and control lines in the negative control cassette. For the RPA3 primers (*Figure 5.7 (ii)*) strong bands are present at the test and control lines of the positive reaction, while the control reaction features a strong band at the control line, and a very faint band at the test line. Both control reactions contained no template DNA, therefore, the false positive band presenting at the test line was attributed to the presence of primer dimers within the reaction. This is in agreement with the previously observed faint low weight bands on the agarose gel analysis of RPA products, for examples see *Figures 5.4* and *Figure 5.5*. When using dual-labelled primers, dimerisation of the pair can cause the formation of similarly dual-labelled DNA products, which present as false positives in the NALFIA system. The false positive band observed on the RPA3 primer pair cassette appeared very faint, therefore, attempts to optimise the reaction such that primer dimers were no longer observable were performed.

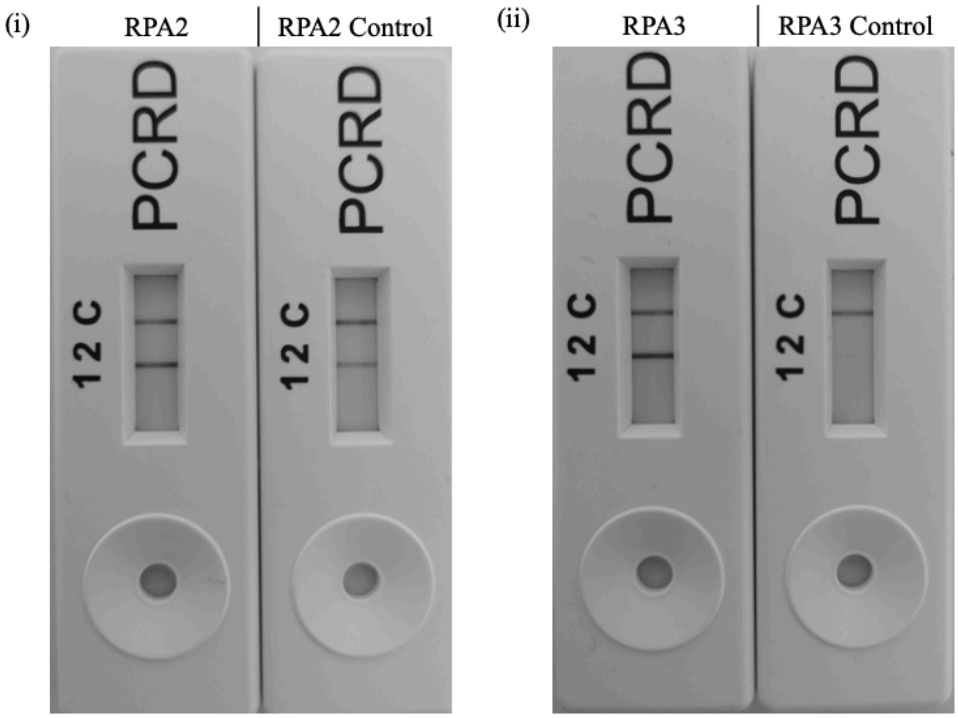

Figure 5.7 NALFIA analysis of dual-labelled PVY amplicons

(i) *NALFIA analysis products formed when using the RPA2 primer pair.* ***(ii)*** *RPA3 primer-mediated amplification of the target region (Template = 10^6 gene copies, control = NTC).*

5.2.4.2 Optimisation of dual-labelled RPA3 primer pair

The first effort to reduce the presence of the false positive band was to apply heat to the resulting RPA product in an attempt to denature the dual-labelled primer dimer product, thus preventing its detection in the NALFIA. A sample of RPA product was heated to 70°C for 10 min. Heating the amplification products was previously shown to sometimes ameliorate difficulties with primer dimer formation through melting of the dimer, but not the specifically amplified template (Liu et al., 2017). After the incubation, the RPA3 amplification samples were re-run on lateral flow strips. The results (*Figure 5.8*) indicate that the heating of the sample was not successful in denaturing the primer dimer, as a band persisted at the test line of the strip on the negative control assay.

Figure 5.8 Heating of RPA3-amplified products to reduce primer dimer formation

The RPA products were heated to 70°C for 10 min in an attempt to remove the false positive band on the control strip (Template = 10^6 gene copies, control = NTC).

Since this method did not improve the result, another optimisation was investigated. This was to reduce the level of primer used in the reaction. TwistAmp™ recommend starting with

an initial primer concentration for each primer of 480nM but suggest that this can be optimised between 100nM and 600nM per reaction. Therefore, several further RPA reactions were performed as previously described, however, with the change that a range of alternative primer concentrations were employed (*Section 2.22.2*) Results are depicted in *Figure 5.9*. Initially, 360nM and 240nM primer concentrations were assessed. Concentrations of 240nM showed only a very faint dimer band. Thereafter, 180nM and 120nM concentrations were analysed, followed by a final assessment of a 100nM concentration. Upon reduction of the primers to concentrations of 180nM, 120nM or 100nM, the false positive band at the test line disappeared. Positive controls included in the 100nM primer reactions confirmed that successful amplification could still be achieved even when using the lower limit of the recommended primer concentration.

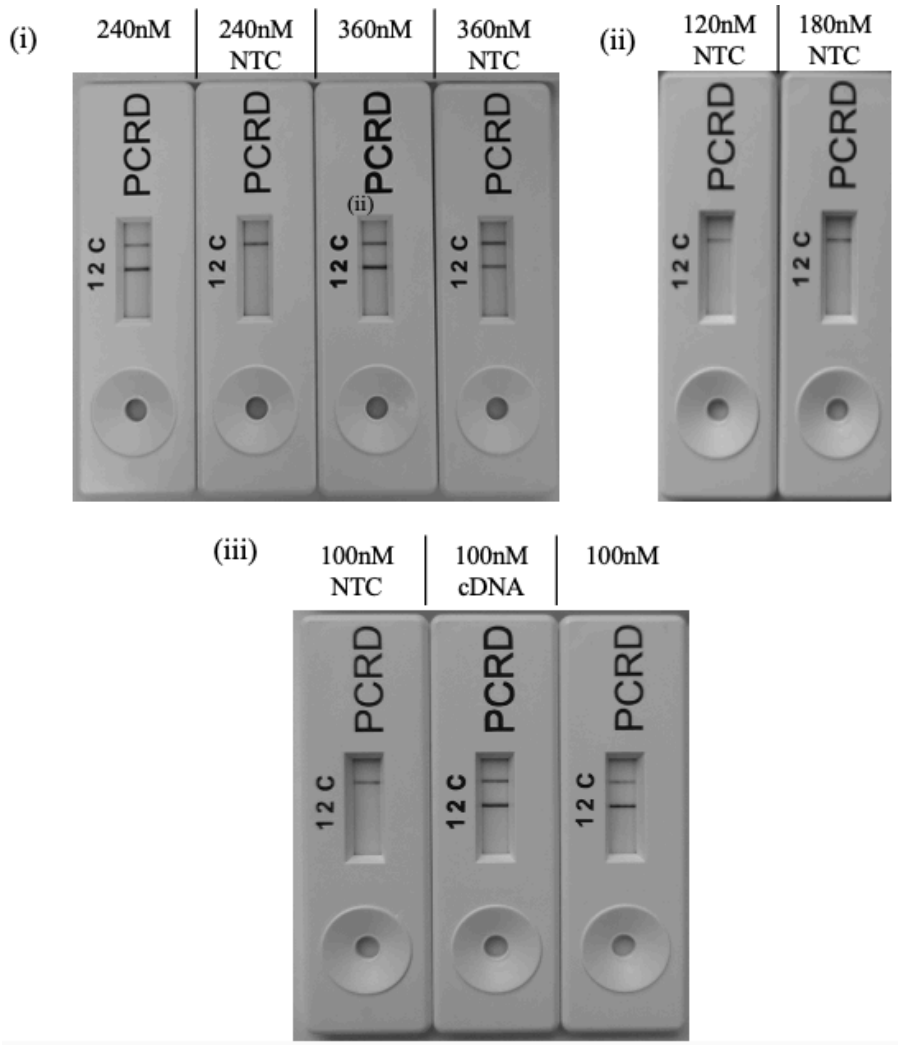

Figure 5.9 Optimisation of primer concentration for RPA and NALFIA

A range of primer concentrations were utilised in an attempt to reduce the false positive band. ***(i)*** *Analysis of 360nM and 240nM primer concentrations. Positive reactions contained 10^6 copies of template while negative reactions were NTCs.* ***(ii)*** *NTC reactions using primers at 180nM and 120nM concentrations.* ***(iii)*** *RPA performed with 100nM primer concentrations. Reactions contained either 10^6 gene copies (100nM) or 20ng of cDNA from a PVY positive plant (100nM cDNA). Negative reactions in the form of NTCs were included.*

While optimisation of the primer concentration successfully removed the false positive band on the lateral flow strip when using primer concentrations below 180mM each, it was not found to be a suitable solution for the assay upon progression to specificity analysis. When performing this specificity analysis, RPA was performed on cDNA samples extracted from plants which tested positive for the potato viruses PVA and potato leafroll virus (PLRV) alongside cDNA from a healthy plant. Initial investigations were performed using 180nM

primers as this was identified as the highest employable primer concentration with which false positives arising from primer dimers were not observed. However, it was found the assay did not offer reliability based on the fact that false positive outcomes/non-specific amplifications were observed throughout the specificity analysis. Attempts were made to investigate other parameters such as altering primer concentrations to 120nM and 100nM concentrations. Additionally, supplementation of betaine, which is proposed to increase specificity, was investigated (Luo et al., 2019). However, none of these optimisations yielded a sustainable or reliable solution, with false positives persisting. Select examples of the type of results obtained under these investigations are presented in *Appendix A*. As the aim was to generate a rapid, reliable assay with good diagnostic confidence for PVY, it was decided to amend the RPA-NALFIA experiment to incorporate a probe. Probes typically confer additional specificity as they require template-specific internal sequences for functionality. Furthermore, the addition of probe oligos in RPA greatly reduces the likelihood of false positives arising from oligo dimerisation.

5.2.5 Development of a primer-probe-based NALFIA

5.2.5.1 Design and application of a RPA probe

The RPA probe is advised to be 46-52 nucleotides long, part of which can overlap the primer of the same directionality as the probe, but none should overlap with the primer of opposing direction to the probe in order to avoid unwanted dimerisation between the probe and opposing primer (TwistDx, 2021). In this work, the oligos were designed such that no overlap occurred between either the sense or antisense primer and the probe. Other features of the RPA probe are an internal abasic site (THF residue), a 5' antigen label and a 3' blocking group. Alongside the addition of the probe oligo, this RPA format also requires the incorporation of an endonuclease, endonuclease IV (Nfo). This endonuclease cleaves THF sites on oligonucleotides only under the circumstance where the THF site is flanked by complementary DNA sequences, for example, when binding their cognate DNA template (Piepenburg et al., 2006).

The function of the probe is to recognise and anneal to an internal sequence on the DNA product amplified by the forward and reverse primers. Upon binding to its complementary DNA region, the probe is cleaved at its abasic residue by Nfo. This, in turn, removes the 3' blocking group, effectively permitting the probe to act as a new primer. This permits the production of a DNA product that is dual-labelled with the probe label and the label of the

opposing primer. Importantly, only when the probe is cleaved and acts as a primer is the amplicon dual-labelled. This, therefore, offers reassurance that positive signal in the assay arises from specific amplification of the target as not only must the target sequence first be amplified by the forward and reverse primer set, but the amplicon then requires the correct internal sequence to permit probe-binding and subsequent cleavage and labelling. In addition to added target specificity, the likelihood of false positives occurring due to non-specific amplification interactions between the labelled probe and opposing primer is largely reduced. Only in the scenario where the probe contains nucleotide sequences either side of its THF residue which were complementary to the opposing primer would this occur. This can largely be avoided by rigorous probe design. The dual-labelled amplicon can then be detected in lateral flow in the same manner as described previously. The concept of the RPA probe-based NALFIA is depicted in *Figure 5.10*.

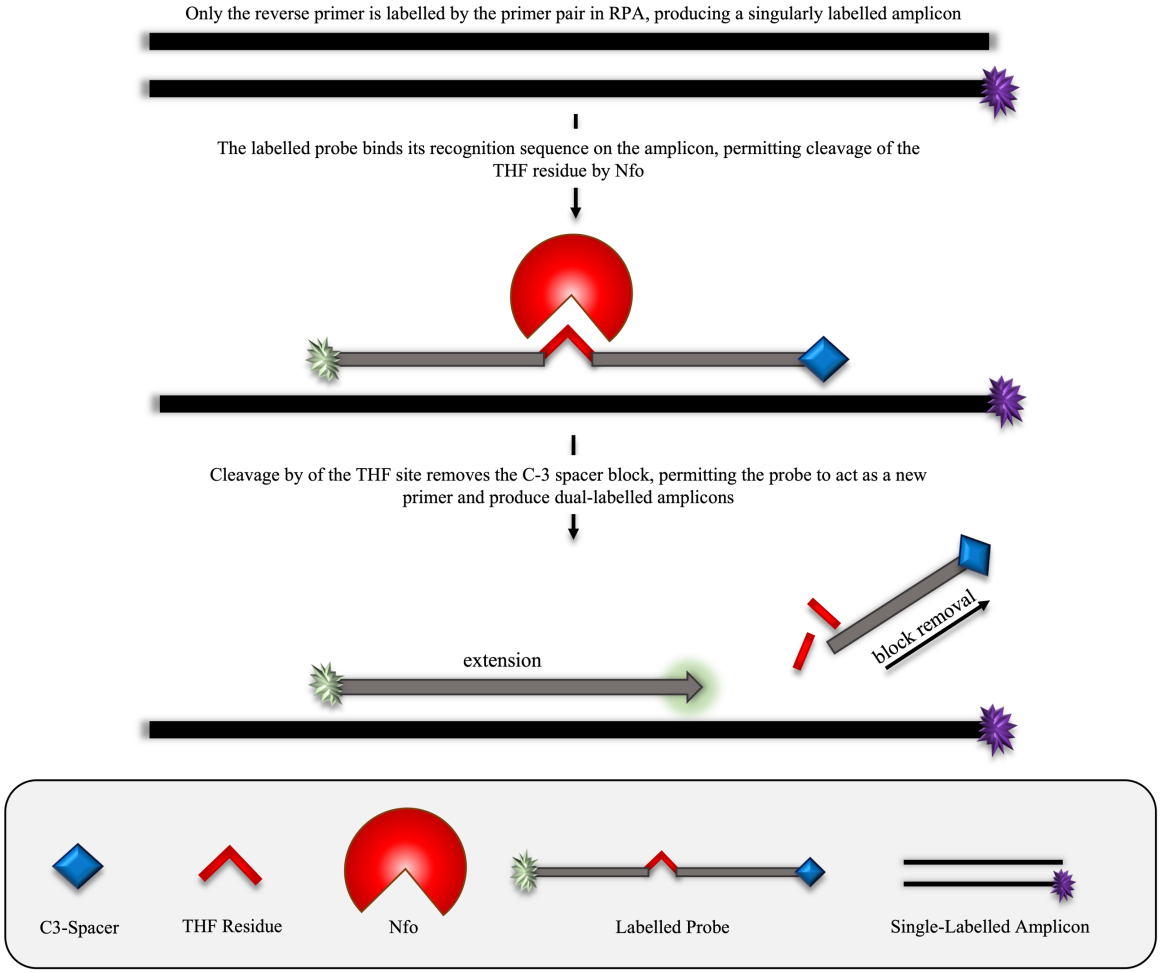

Figure 5.10 NALFIA detection of PVY through incorporation of a probe to RPA

The target DNA is first amplified by the forward and reverse RPA primer pair; at this stage it features only one antigenic label, derived from a labelled reverse primer. Upon generation of the target amplicon, the probe binds to its cognate sequence. Only when hybridisation of complementary nucleotides either side of the THF site is achieved can this abasic residue be cut by the endonuclease Nfo, resulting in cleavage away of the 3' C3-spacer. The probe is now permitted to act as a new primer, producing a dual-labelled amplicon which can be detected in lateral flow.

As the RPA3 primer pair had shown good ability to amplify the target sequence, and appeared to have minimal dimerisation interactions with each other, it was decided to design a probe to target the amplicon of this primer pair (details of primers and probe listed in *Table 2.23*). In this work, the probe was labelled with a 5' FAM antigenic label and a 3' C3-Spacer was used as the block. The reverse primer remained labelled with 5' biotin while the forward

primer was unlabelled. Initial trials of the probe were performed as per *Section 2.22.4*. The results of the probe incorporation are depicted in *Figure 5.11*. The presence of two bands on the test cassette, and only one band on the control cassette indicated that the probe is binding to a PVY-related amplicon and being cleaved. No false positives were observed on the control cassette test line.

Figure 5.11 Amplification of PVY sequences with primer-probe combination
(i) *Amplification of PVY from 10^6 gene copies. Strong bands are observable at both the control and test lines.* ***(ii)*** *In the NTC reaction, a single band is present at the control line, with no signal observed at the test line.*

5.2.5.2 Detection of various strains of PVY

PVY is a highly diverse virus, with many recombinant versions reported, mainly derived from the parental PVY^N and PVY^O strains (Green et al., 2017) Given the multitude of different non-recombinant and recombinant PVY genotypes, it was deemed important to ensure that the RPA assay was inclusive and could effectively identify PVY from the nucleic acids of multiple strains, acting in a "broad-spectrum" manner. This ensures that false-negative results are avoided. This was theoretically achieved by considering the primer- and probe-binding regions and ensuring that these regions were relatively conserved across all

strains. However, in addition to this, the effectiveness of the primer and probe design was investigated *in-vitro* through performing RPA analysis on cDNA using cDNA sourced from several PVY strains (*Figure 5.12*). As evidenced by the strong bands at the test lines, all strains of PVY tested could be effectively detected from cDNA, demonstrating the suitability of this assay for generalised PVY-detection.

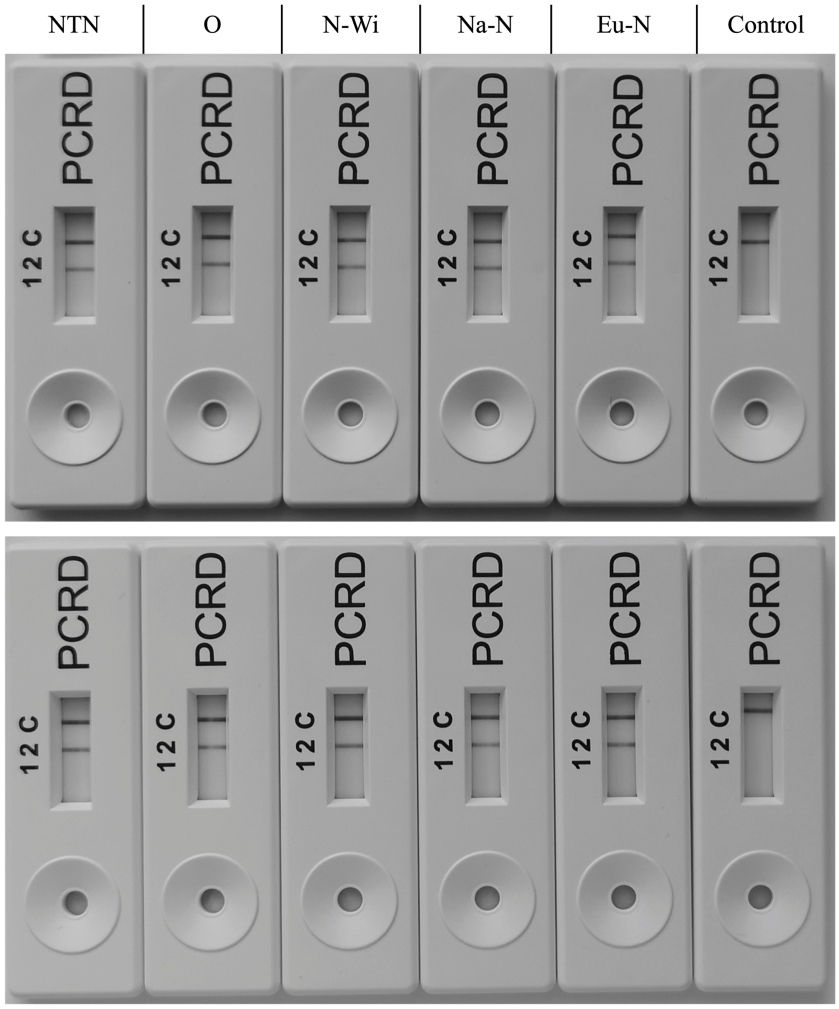

Figure 5.12 Detection of various PVY strains

RPA reactions were set up containing 10ng of either PVY^{NTN}, PVY^{O}, $PVY^{N\text{-}Wi}$, $PVY^{Na\text{-}N}$ or $PVY^{Eu\text{-}N}$ cDNA. Analysis was performed in duplicate RPA reactions and each reaction run on a separate cassette. Colour formation is observed at the test band of all assays performed with PVY cDNA, regardless of the strain from which the cDNA was derived (Control = NTC).

The inclusivity of the primers and probe for PVY was further assessed *in-silico* by aligning the sequences of the designed primers and probe with the genomes of 401 PVY genotypes

in Blastn. The accession numbers were sourced from, and are listed in, Green *et al*., (2018). The analysis of the alignments of the forward primer (*Appendix B*), reverse primer (*Appendix C*) and probe (*Appendix D*) revealed good inclusivity for PVY. The forward primer contained two common mismatches between primer and target at bases 6 and 7 of the primer. These mismatches were experimentally shown to not prevent amplification as the strains PVY^{O} and $PVY^{N\text{-}Wi}$, which contain the same mismatches, were successfully amplified by RPA in this work (*Figure 5.12*). The reverse primer binding region appeared highly conserved, with only rare mismatches observed between reverse primer and target templates. The probe, which acts as a new primer upon cleavage by nfo, also appeared to target a relatively well conserved region. A common mismatch at base 32 of the probe was replaced by the THF site as one base of the probe is required to be replaced by this abasic residue, therefore, this was not considered a true mismatch. Other common mismatches occurred at bases 5, 8, 11 and 17 between the probe and PVY, the majority of which were associated with the $PVY^{NE\text{-}11}$ genotype. This genotype was not detected in Irish PVY populations and, therefore, was not tested experimentally in this work (Della Bartola, Byrne, and Mullins, 2020). However, RPA is shown to tolerate as many as nine mismatches across oligonucleotides and templates, therefore it is possible that amplification would be still proceed (Boyle et al., 2013; Daher et al., 2015). Additionally, the mismatches occur toward the 5' end of the probe, further suggesting the possibility of successful amplification, however, this would need to be experimentally verified. The alignments between all amplification oligonucleotides and the PVY genotypes suggest that the designed primers and probe could be suitable for application to broad-spectrum PVY detection.

5.2.6 Specificity and sensitivity analysis of the developed NALFIA

5.2.6.1 Specificity of primer-probe-based RPA and NALFIA

It was also considered essential to ensure that the RPA assay would not amplify DNA sequences from non-target nucleic acids which may also be present in the potato crop. Analysis of the assays exclusivity for PVY was achieved by assembling reaction mixtures using various template DNAs. For these investigations, cDNA extracted from healthy and virus-infected plants was utilised as this would reflect the true specificity of the assay when using a complex DNA sample containing potentially cross-reactive templates. For non-targets, cDNA sourced from healthy plants, or cDNA from plants infected with PLRV and PVA were used. PVY-associated cDNA was incorporated as a positive control. This was performed, as per *Section 2.22.5*, using 10ng of each cDNA sample. The outcome of the

analysis (*Figure 5.13*) demonstrated that the probe endows the requisite specificity to the assay, with no signal observed on any test line except the reaction in which PVY-associated cDNA was added.

Figure 5.13 Specificity of the primer-probe-based NALFIA

Reactions were set up containing 10ng of either healthy plant, PVA, PLRV or PVY cDNA. Analysis was performed in duplicate RPA reactions and each reaction run on a separate cassette. Colour formation can only be seen on the test line of the cassette in which PVY cDNA was used as the template (Control = NTC).

5.2.6.2 Sensitivity of primer-probe-based RPA and NALFIA

To assess the sensitivity of the RPA-NALFIA, a series of dilutions was performed on the PVY template DNA and RPA performed as per *Section 2.22.6*. Each dilution corresponded to a gene copy number of the PVY standard DNA, ranging from 10^4 copies to 1 copy. The results of the analysis (*Figure 5.14*) revealed that the assay could detect as low as 100 copies per reaction of the target template.

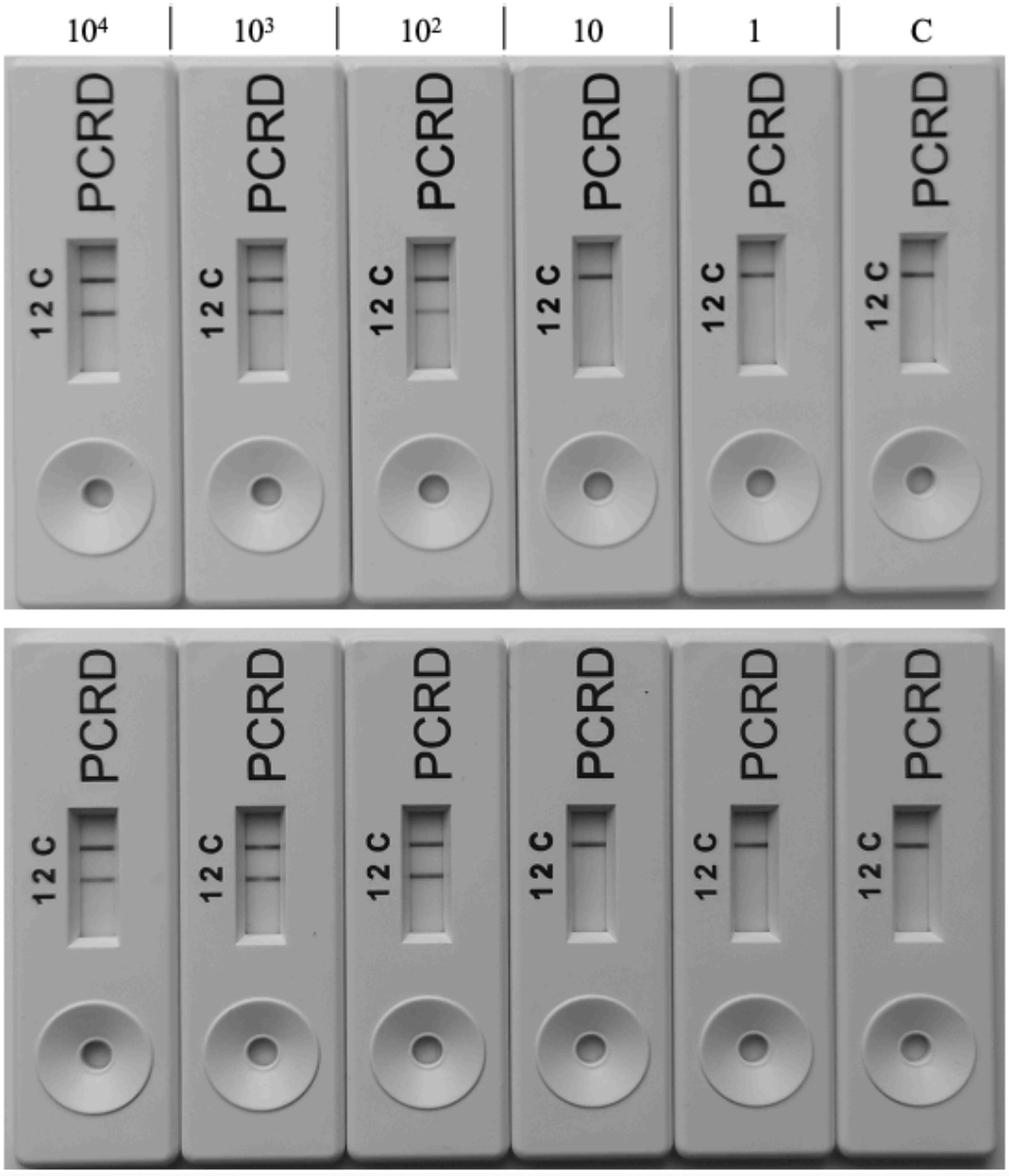

Figure 5.14 Sensitivity of the NALFIA for the detection of PVY

Template was added to the reaction at concentrations of 10^4, 10^3, 10^2, 10 and 1 copies. Analysis was performed in duplicate RPA reactions and each reaction run on a separate cassette. The assay was capable of detecting 100 copies per reaction, confirmed by colour formation on the test line up until this copy number (Control = NTC).

5.2.7 Development of a one-step reverse-transcription RPA for PVY

5.2.7.1 Reverse transcription-RPA of PVY

As PVY is a single-stranded RNA virus, the further development of the described RPA assay into a one-step reverse-transcription-RPA (RT-RPA) was considered highly important and beneficial as it would mean the assay could be readily deployed in-field, without the requirement for prior reverse-transcription of isolated RNA. In RPA, amplification of RNA targets can be achieved via the addition of a reverse transcriptase (RT) enzyme directly into the RPA mixture in a 'one-step' approach, making the reaction time-friendly for RNA-detection (Euler et al., 2012; Daher et al., 2016).

To investigate this, the Maxima H Minus RT enzyme was incorporated into the RPA assay and the assay performed as per *Section 2.23.1*. This assessment utilised 10ng of total RNA from a PVY-infected plant in lieu of the previously employed cDNA or PVY template. In addition, a negative control comprising of 10ng of healthy plant total RNA was also assessed, alongside a NTC. The results of the RT-RPA are presented in *Figure 5.15*. Bands observable at the test and control lines in the reaction performed with PVY-RNA confirm successful single-step reverse transcription, amplification and labelling of the amplicon. No bands observed at the test lines of either the healthy plant control or the NTC confirm that the RT-RPA is both specific for PVY and that no false positives are generated in this assay.

Figure 5.15 Direct amplification of PVY from RNA in RT-RPA

Amplification of PVY from 10ng PVY-positive total RNA. Bands are observable at both the test line and the control line, suggesting effective amplification of the target sequence. Negative control amplifications consisted of reactions containing 10ng of total RNA from a healthy plant and a NTC. Neither control reaction produce signal at the test line, only forming colour at the control line (Control = NTC).

5.2.8 Sensitivity of the one-step RT-RPA NALFIA

5.2.8.1 Sensitivity of one-step RT-RPA

To determine the sensitivity of the one-step RT-RPA, a series of dilutions was performed on the total plant PVY RNA. Each of these RNA concentrations were added to individual reactions, with final RNA concentrations ranging from 1000pg-1pg/reaction. RPA was performed, as described in *Section 2.23.2,* using each of these dilutions as a template. Results (*Figure 5.16*) show that the LOD for the RT-RPA was 100pg/reaction when using a one-step approach where no prior reverse transcription of RNA was performed.

Figure 5.16 Sensitivity of the one-step RT-RPA NALFIA

Template was added to the reaction at concentrations of 1000pg, 100pg, 10pg or 1pg. Analysis was performed in duplicate RPA reactions and each reaction run on a separate cassette. The assay was capable of detecting 100pg of RNA per reaction, confirmed by colour formation on the test line up until this concentration (Control = NTC).

5.3 Discussion

PVY is a damaging virus which can spread rapidly amongst a crop population causing a loss in yield and crop quality. Control of PVY is aided in part by diagnostic detection methods such as PCR and ELISA, however, these methods cannot be readily transferred to on-site testing and generally require removal of the suspect plant material from the field prior to analysis. The inability to test on-site using these methods delays the time to detection of

PVY and could result in further proliferation of the virus in the population before interventions can be taken.

Isothermal techniques are a rapidly growing sector of diagnostics largely due to their amenability to on-site functionality and minimal equipment requirement, while still offering good sensitivity and specificity. Of these methods, RPA offers a rapid and convenient alternative to typical nucleic acid detection via standard PCR or qPCR. The single temperature of isothermal amplification means that only basic heating equipment is required, making it easily applicable to on-site testing such as import/export site or directly in fields of crops. Furthermore, since RPA is performed at lower operating temperatures, incubation at ambient temperatures in warmer climates, or through use of body heat can be sufficient for amplification (Crannell, Rohrman, and Richards-Kortum, 2014; Lillis et al., 2014; Abd El Wahed et al., 2015; Wang et al., 2017). Other rapid isothermal methods are proposed for PVY detection, predominantly LAMP assays. LAMP-based assays are generally more sensitive than those relying on RPA, with femtogram levels detection of PVY-associated nucleic acids achieved for some LAMP systems (Nie, 2005; Hasiów-Jaroszewska et al., 2015; Przewodowska et al., 2015; Treder et al., 2018). This high sensitivity could be attributed to the use of multiple primers, generally four - six, and the consequently large amount of target DNA which is generated over a relatively short space of time. However, while typically more sensitive than other isothermal amplification methods, LAMP assays require higher operating temperatures, around 60ºC, which increases the burden of equipment requirement and prevents the use of body temperature-mediated incubation for basic LAMP assays, placing it at a disadvantage for in-field testing. This is in contrast to RPA where body temperature incubations are shown to be sufficient to permit RPA, meaning there is no prerequisite for use of a heating apparatus (Wang et al., 2017). Furthermore, the suggested operating time for LAMP is slightly longer, with reported assays performed for 30-60 min, as opposed to the 20 min used for RPA within this research. Overall, these differences between LAMP and RPA suggest that while LAMP is highly useful in well-equipped settings, RPA is likely the more favourable isothermal method when the aim is to perform point-of-use testing in-field due to its low equipment demands and rapidity of amplification. Due to this suitability of RPA to in-field testing, previous investigation into RPA-based isothermal amplification of PVY is also published (Glais and Jacquot, 2015; Babujee et al., 2019; Wang et al., 2020b). However, each of these have requirements such as pre-amplification reverse transcription, post-amplification sample clean-up, or

prerequisites for additional monitoring equipment such as fluorimeters, limiting their point-of-use application. The work described herein extends upon these by providing a method through which amplification and detection of PVY could be performed directly from RNA with results obtained in less than 10 min on a user-friendly lateral flow strip. This method, therefore, provides a rapid, sensitive and accessible means to monitor PVY infection at whichever location there was a requirement for testing.

The diagnostic strength of lateral flow technology coupled with RPA was demonstrated through the detection of PVY from both DNA and RNA templates. This pairing provides an easy-to-interpret result output whereby nucleic acids can be detected. Initially, dual labelled primers were investigated. While initial optimisation of primer concentration suggested that this may be an efficient method to control the formation of primer dimers, progression to specificity analysis using cDNA templates with increased complexity revealed that dimerisation and/or non-specific amplification persisted, which could lead to the reporting of false-positives if left unaddressed. This highlights the need for rigorous primer design and thorough analysis of primer pairs in order to avoid dimerisation. To overcome these false positives, a probe was introduced to the system which alleviated the previously observed issues with dimers. The RPA probe can only be cleaved when the featured THF site is flanked on either side by highly complementary nucleic acids. Hence, the likelihood of false positives caused by dimerisation is greatly decreased. Additionally, the probe binds a region on the amplicon and therefore offers enhanced assay specificity. This primer and probe RPA system proved successful for the detection of PVY with a LOD of 100 copies/reaction achieved. Furthermore, the assay showed excellent specificity and exclusivity, as demonstrated by the absence of amplification in healthy plants or when other plant virus nucleic acids are substituted in lieu of PVY. Alongside good specificity for PVY, the NALFIA was also proved to have reactivity with all tested strains of PVY, indicating the ability of the assay to detect PVY in a broad-spectrum manner. This was further confirmed by extensive *in-silico* analysis comparing the designed oligonucleotides against hundreds of known PVY genotypes. This investigation revealed that overall the designed amplification set was inclusive and should readily amplify the vast majority PVY genotypes. Therefore, the ability for broad-spectrum detection is promising.

The RPA assay was further developed into a one-step RT-RPA NALFIA. PVY is a single-stranded RNA virus, therefore, reverse transcription of the RNA is required prior to any

further amplification. Reverse transcription was achieved via the addition of the Maxima H Minus RT enzyme directly to the RPA mixture alongside PVY-associated RNA. This led to the successful detection of PVY directly from RNA on lateral flow strips with a LOD of 100pg/reaction, or 2pg/μL, achieved within a 20 min reaction time. In addition to the rapid assay turnaround time, RPA is ideal for application to on-site RNA detection as it is shown to be robust when used alongside crude and complex matrices. The generation of crude leaf extracts can be achieved without the need for complicated or costly preparatory steps. Grinding or maceration of leaf or fruit tissue in buffers via mechanical action, for example using a pestle, or through incubation of leaf tissue with extraction buffers alone is shown to be sufficient template preparation for RPA (Mekuria, Zhang, and Eastwell, 2014; Zhang et al., 2014; Londoño, Harmon, and Polston, 2016; Kapoor et al., 2017; Silva et al., 2018; Babujee et al., 2019; Munawar et al., 2020). Therefore, although not investigated in this work, the detection of PVY RNA directly from leaf tissue is not predicted to pose a challenge for this system, further highlighting its applicability to on-site use.

With respect to further development of this diagnostic method, application to field-trials would be of great benefit. While this assay has been shown to be functional and permit the sensitive detection of PVY from RNA samples acquired from PVY-infected plants, application to a genuine in-field setting would demonstrate the assays robustness to external and uncontrollable factors such as ambient temperature, exposure and weather. In addition, it would provide the opportunity to assess the assays efficacy when implementing a crude sample preparation strategy. Shown in *Figure 5.17* is the proposed future workflow and theoretical timeline of PVY detection using the designed RT-RPA assay upon optimisation of crude nucleic acid extraction methods. The entire protocol could be performed within an hour.

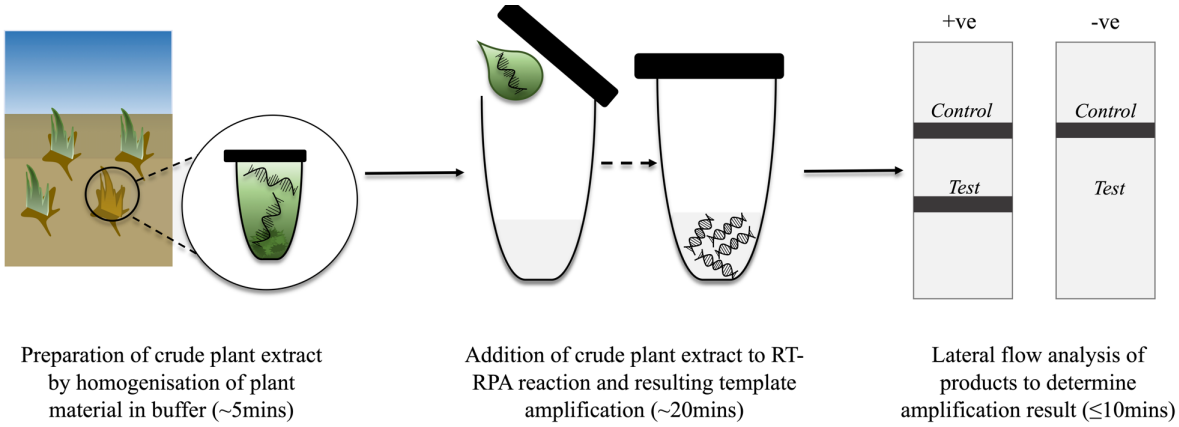

Figure 5.17 Overview of the potential workflow for NAFLIA detection

Suspect plant samples can be selected, or crops chosen at random. Plant tissue such as leaf material is prepared in an appropriate buffer prior to addition to the RT-RPA reaction mixture. Amplification commences and after roughly 20 min products can be analysed in lateral flow for a rapid and visual confirmatory test.

Ideally, the developed NALFIA assay could be deployed on-site in a field which may contain PVY-infected crops. Diagnosis of the crop could be performed *in situ* by RT-RPA-mediated lateral flow analysis, while samples of the same plants are retained for later testing by ELISA and qPCR. The previously described antibodies and immunoassays generated in *Chapter 3* and *Chapter 4* could also be incorporated into this analysis to provide a broad-scale assessment of the developed detection methods. Through this type of investigation, a comparison could be obtained between the developed RT-RPA assay and the currently used methods. Additionally, given that the PCRD strip used in this work features two test lines, a second RPA assay could be developed using new primer sets to allow either strain-specific detection and differentiation of PVY, or to permit multiplexed testing for other plant viruses such as PVX, PVA, PVS or PLRV, alongside PVY, if desired.

Chapter 6

The Generation of Antibodies for the Detection of Rhynchosporium commune

6.1 Introduction

Rhynchosporium commune (*R. commune*) is a fungal pathogen which affects *Hordeum vulgare* (barley) crops globally. Infection with *R. commune* results in damage to the barley foliage and grain, reducing yield and marketability. As barley is the fourth most widely produced cereal worldwide and is used commonplace in animal feed and within the food production sector, it is important to monitor this pathogen from both food security and economic outlooks (Looseley et al., 2018). Currently, *R. commune* infection is largely managed through the use of disease-resistant crops, crop rotation and fungicide spraying. However, the development of fungicide-resistant *R. commune* strains, and strains capable of avoiding the plant host-resistance genes means that the current methods of management do not always lead to the eradication of the pathogen (Zhan et al., 2008). Therefore, a method by which the level of *R. commune* in the field can be determined is necessary.

Although *R. commune* is an important pathogen, methods through which it can be detected are lacking. Current methods of *R. commune* diagnosis are heavily reliant on visual inspection of the crop. Nucleic acid-based diagnostic assays are available, but their uptake does not appear widespread as evidenced by the limited number of recent publications, with some publications more focused on monitoring of mutations within the fungal genome (Lee *et al.*, 2001; 2002; Fountaine *et al.*, 2007; Phelan *et al.*, 2017). There is also a paucity of reporting on immunoassay-based detection of *R. commune* (Foroughi-Wehr, Zuchner, and Rabenstein, 1996). The development of specific immunoassays and other diagnostic assays is not largely investigated. Perhaps the present focus on breeding *R. commune*-resistant crops has meant that interest is more greatly concentrated on the field of understanding *R. commune* pathogenicity or effector proteins, rather than on identifying diagnostic markers. While this approach is beneficial, it is evidently not sufficient in negating the losses suffered yearly in the barley crop, a large portion of which can be attributed to primary and secondary pathogenic activity by fungi, while the barley is growing, or under storage.

R. commune infection can occur through a number of avenues, including sowing infected seed, splash dispersal by nearby colonised crops, or by fungal spread to new crops sown in fields containing debris from past infected crops. Upon harvesting of infected crops, the pathogen can continue to proliferate, particularly if storage conditions are not adequate. This can cause major spoilage, rendering grain unmarketable. Incorporating diagnostic assays to monitor fungal pathogen burden at the various life stages of the crop, from sowing to storage,

would provide another avenue of control by permitting earlier detection of crop pathogens. For example, *Figure 6.1* demonstrates the various checkpoint testing sites which could be incorporated into *R. commune* control.

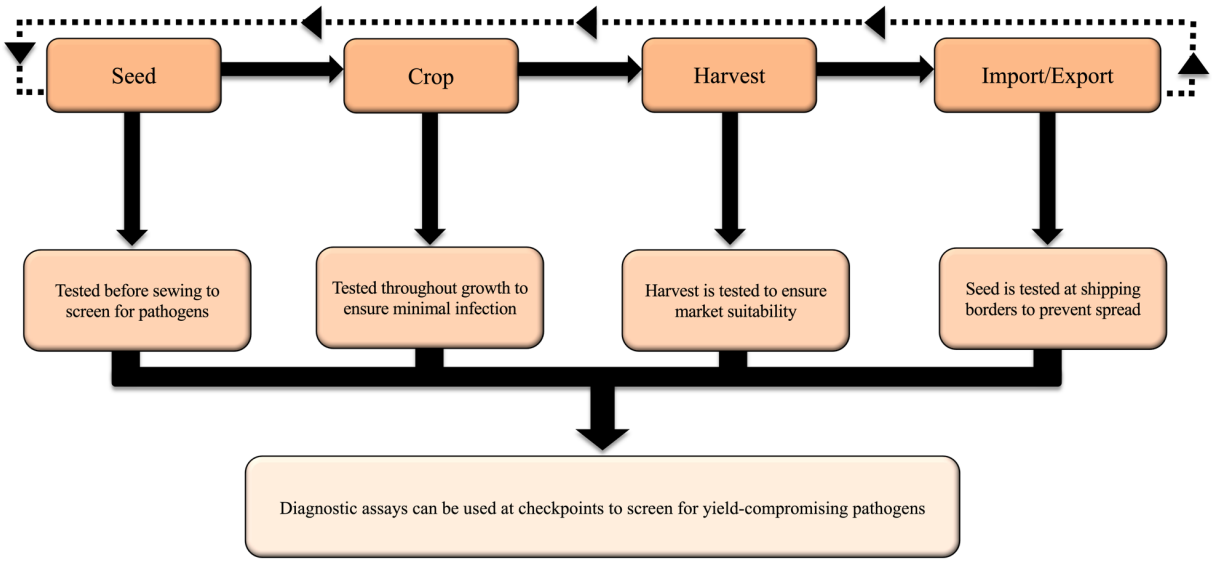

Figure 6.1 Flowchart of the multiple ways in which on-site crop testing can be used
Portable detection platforms would be useful at numerous locations along the crop production and import/export chain. The routine testing of crops at these stages helps to decrease the levels of infected crop which become available to the market. Accessible, rapid and facile assays would be extremely useful at these stages as it would permit testing and disease monitoring, without the requirement for training of staff or expensive equipment.

Part of the difficultly in controlling *R. commune* proliferation can be attributed to the fact that the fungus possesses a haploid genome, meaning that only one genetic alteration is required for progenies to present with different genotypes. This is advantageous for the fungus from two perspectives. Firstly, the development of resistance to fungicides is made more facile by the requirement for only a single change, therefore, chemical resistance in such fungi is prevalent. For example, there is a history of *R. commune* developing resistance to fungicides such as methyl benzimidazole carbamates (MBCs), quinone outside inhibitors (QoIs) and demethylation inhibitors (DMIs), the former two of which required only a single mutation to confer resistance. The development of fungal resistance to DMIs is more challenging as these chemicals act on multiple genes, however, there are cases of resistance and current recommendations include the application of additional alternative acting chemicals alongside DMIs to ensure control (Avrova and Knogge, 2012; Phelan et al., 2017).

With the current emphasis on reduction of chemical usage in crop production, it is uncertain as to which control measures will be permitted moving into the future. This is exacerbated by the fact that *R. commune* may develop resistance to certain fungicides at any given time, sometimes with as little as a single point mutation required to permit this. In a similar manner, mutations, or loss of genes, in *R. commune* also hinders the breeding of resistant crops. An example of this includes the complete loss of the *R. commune* effector protein NIP1 to evade the resistance system of certain barley cultivars (Schürch et al., 2004; Zhang, Ovenden, and Milgate, 2020). Therefore, breeding of resistance crops must focus on the selective targeting of essential *R. commune* genes. While measures such as understanding *R. commune*-host interactions, growing disease-resistant crops and applying various fungicides aid in reducing *R. commune*-associated losses, the disease still persists. Therefore, the field could stand to benefit from additional control measures such as the further development and application of diagnostic assays. This would allow the detection of low-level infection in growing crops, on seed, and on debris in the field. Such assays would work in tandem with current approaches to provide an enhanced *R. commune* management system. Hence, this work proposes the development of a diagnostic assay for the specific detection of *R. commune*.

With respect to diagnostic assays, immunoassays are relatively cheap to produce and can be translated into user-friendly technologies such as lateral flow, making them an appealing diagnostic tool. Therefore, it was decided to take an immunoassay focused approach when developing an *R. commune* detection method. Due to the fact that recombinant antibodies possess desirable attributes such as the ability to be genetically engineered and the capability of expression in *E. coli*, it was decided to produce a recombinant library with the capacity of generating/expressing scFv to *R. commune* (Basu et al., 2019). Typically, to isolate anti-pathogen antibodies, a target-specific antigen is required, however, presently, no unique antigens are proposed for *R. commune* detection and there is limited investigation into the identification of associated novel antigenic proteins. Previously, immunoassay-based detection of *R. commune* was reported, whereby researchers successfully utilised polyclonal anti-sera, raised against total protein, rather than antibodies with single antigen-specificity (Foroughi-Wehr *et al*., 1996). In light of this, the proposed method for antibody generation was to employ a total protein extract from the *R. commune* mycelium as an antigen. However, while this approach is demonstrated as functional for the detection of *R. commune* in-field, it runs the risk of producing false-positives in immunoassay as a result of cross-

reactivity with other fungal pathogens. This is exacerbated by the fact that barley is susceptible to multiple concurrent fungal infections, potentially increasing the likelihood of false positives when testing is performed in the presence of fungi with shared homology to *R. commune*. Therefore, in addition to the development of polyclonal antibodies, it was proposed to attempt to isolate scFv antibodies of single epitope binding in the hope that their single-antigen binding properties would enhance specificity.

Screening recombinant antibody libraries is ideally performed using a known, pathogen-specific antigen, however, given that such an antigen was not available for *R. commune*, it was important to employ a screening method by which the chance of cross-reactivity with other fungal pathogens would be reduced. Accounting for this, it was proposed to perform a 'depletion panning' strategy, also termed invert or subtractive biopanning (Bakhshinejad et al., 2016; Rahbarnia et al., 2016; Lebani et al., 2017). By this method, the scFv-displaying phage pools are exposed to antigens of other co-infecting fungi of barley, with the aim to deplete the library of cross-reacting scFv clones prior to subsequent enrichment against the *R. commune* proteins. This concept is depicted in *Figure 6.2*. In this way, the resulting final phage pool after biopanning should only harbour scFv which bind to antigens of *R. commune*, rather than other fungal pathogens.

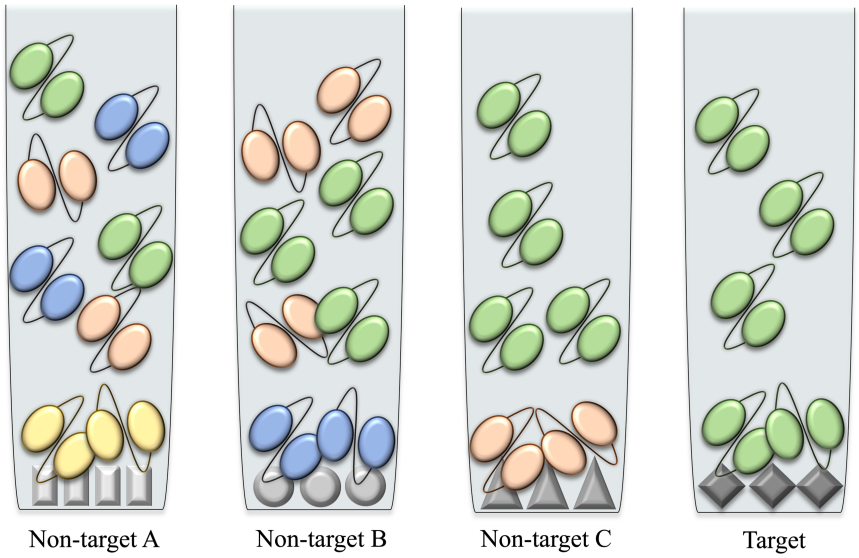

Figure 6.2 Depletion panning strategy for identifying R. commune-specific scFv

By exposing the scFv pool to proteins from other co-infecting fungi, i.e. "non-targets" (yellow, blue and orange), cross reactive clones are depleted. This increases the likelihood of isolating anti-R. commune, "target" scFv (green) which do not bind to common co-infecting pathogens of barley.

6.2 Results

6.2.1 Generation of an anti- R. commune scFv library

6.2.1.1 Determination of serum response to antigens

Total protein extracts were acquired from two separate *R. commune* isolates, denoted 20.16 and 44.07. These two isolates were expected to have similar compositions. They were administered as immunogens to a hen (*Section 2.11.1)*. A serum titre was used to determine the generated immune response against the target antigens. The *R. commune* antigens were coated to the wells of an ELISA plate at a concentration of 2µg/mL. Sera were applied to these wells in a series of dilutions (*Section 2.11.2*). "Pre-bleed" samples were used in the assay as a comparison to the post-immunisation response. An initial response at lower dilutions is observed in the pre-bleed serum titres for both *R. commune* isolates (*Figure 6.3*). This response is likely due to background interference caused by the complexity of the serum matrix and quantity of different proteins in the *R. commune* protein extract. The pre-bleed signal diminishes at a serum dilution of roughly 1:1,000, further indicating that the observed signal is cross-reactivity as opposed to a specific interaction with the antigens. The signal observed against the antigens, *R. commune* 44.07 and 20.16, was adequate. A similar response was observed against both isolates, with a final titre in the range of 1:1,000,000 - 1:10,000,000 achieved for both (*Figure 6.3*). Having confirmed a satisfactory immune response to the antigens, the work proceeded into the recombinant library generation stage, with the intention of isolating *R. commune*-specific scFv.

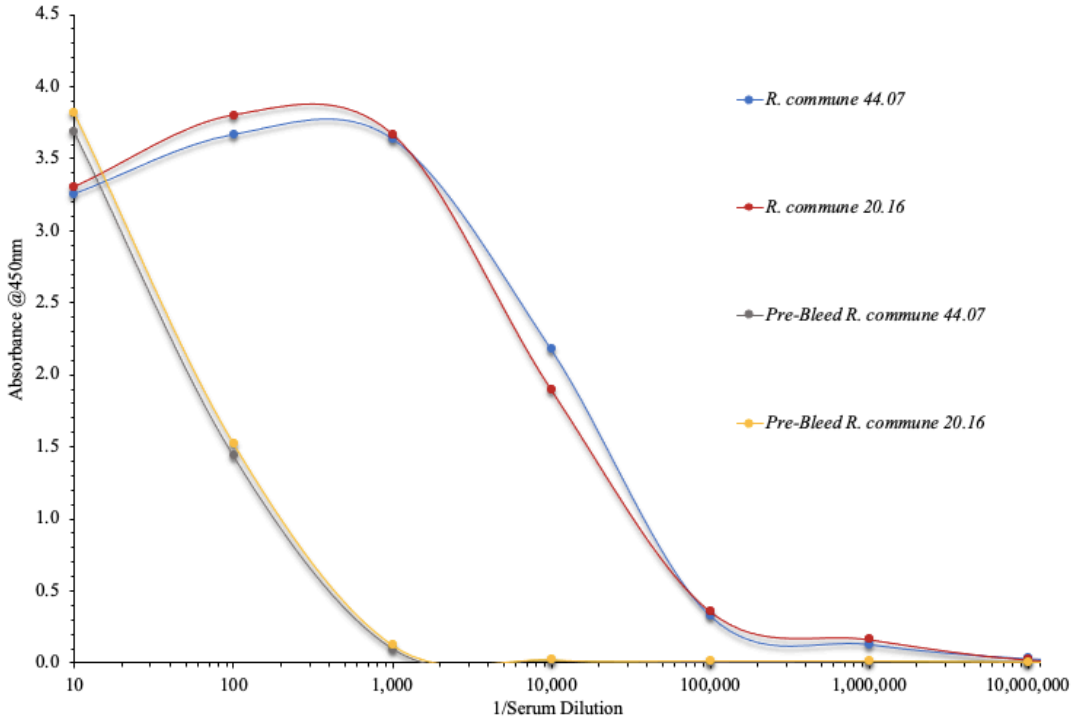

Figure 6.3 Serum antibodies were titred against the R. commune antigens

The sera was applied in serial dilutions to the wells of an ELISA plate coated with 2µg/mL R. commune antigen. Bound serum antibodies were detected using a HRP-labelled anti-chicken VHH antibody. The absorbance was then determined at 450nm.

6.2.1.2 Isolation and reverse transcription of RNA to cDNA

Spleen tissue was homogenised in TriZol® reagent as per *Section 2.11.3*. The total RNA phase was carefully removed from the sample and quantified on a Nanodrop™ 1000. Subsequently, the RNA was utilised in a first-strand synthesis reaction, by which a cDNA template is generated from RNA (*Section 2.11.4*). This cDNA pool was employed as a template in subsequent PCR reactions to facilitate the construction of the scFv immune library.

6.2.1.3 Amplification of V_H and V_L chains from cDNA

The first step in library building was the amplification of the antibody heavy (V_H) and light (V_L) chains using avian variable region-specific primer sets and PCR. This was performed as per *Section 2.11.5*, with the addition of 1.5mM $MgCl_2$. Both the V_H and V_L chains amplified successfully, as demonstrated by the bands around 400bp for V_H and around 350bp for V_L. The V_H and V_L products are depicted in in *Figure 6.4 (i) and Figure 6.4 (ii),* respectively.

Having achieved successful amplification, each chain was run separately on agarose gels, from which they were excised and purified. The purified chains were then quantified on a Nanodrop™ 1000. The following step in the library building process included the use of both chains in a splice by overlap extension (SOE)-PCR.

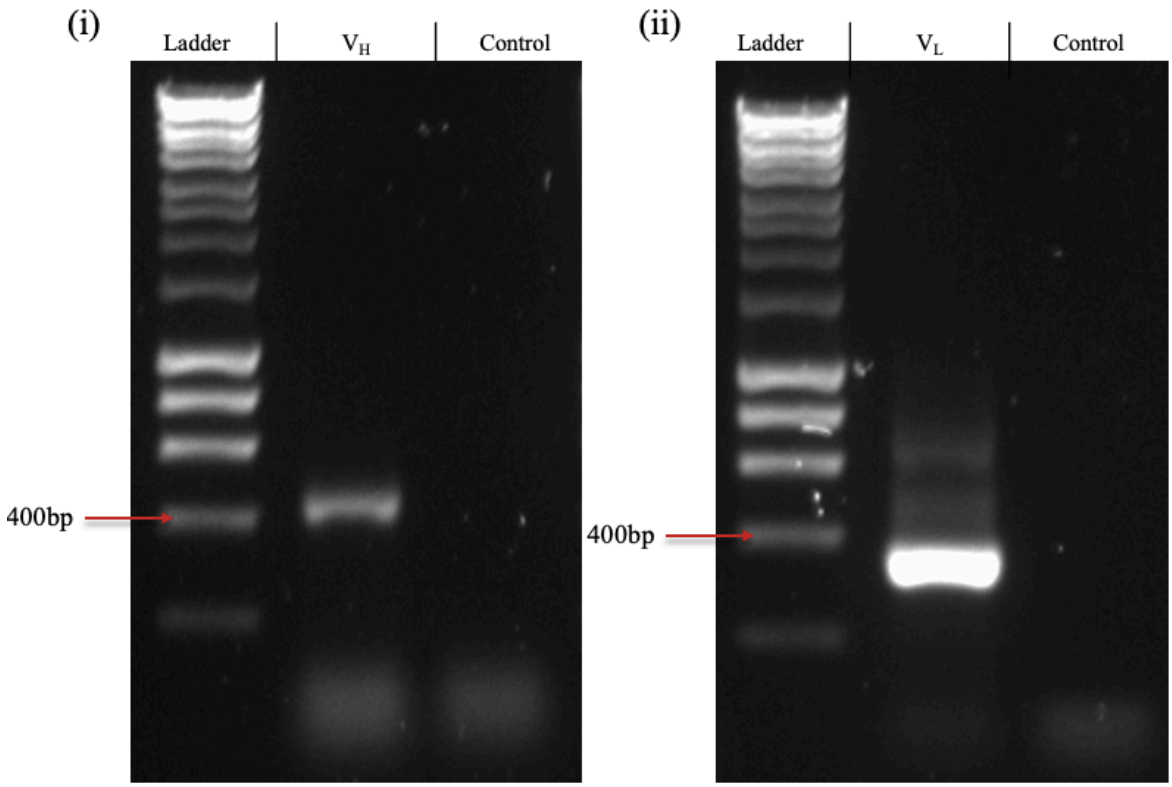

Figure 6.4 Amplification of V_H and V_L from cDNA

(i) *Successful amplification of the V_H is evidenced by the band present at ~400bp.* ***(ii)*** *Amplification of the V_L was also successful, as demonstrated by the ~350bp DNA band (Ladder = Hyperladder™ 1 kb, V_L = variable light chain, V_H = variable heavy chain, control = PCR without cDNA template).*

6.2.1.4 Generation of splice by overlap extension product

SOE-PCR is performed to facilitate the joining of the VL and VH antibody chains via a glycine-serine $(G_4S)_4$ linker. By this method, random combinations of each chain are joined, creating a highly diverse pool of VH and VL chain pairs. To permit this, the purified VL and VH chains were used at equal concentrations and act as the template DNA in the SOE-PCR, as per *Section 2.11.6*. The resulting SOE product is roughly 750-800bp, comprising of the 400bp VH, 350bp VL and the linker. The SOE amplification was considered successful as a

strong band was observed on the agarose gel at a position around 800bp (*Figure 6.5)*. Further SOE PCRs were performed under these conditions.

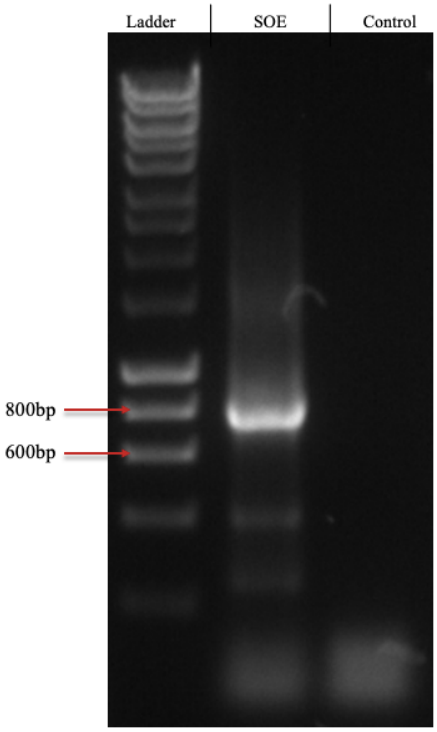

Figure 6.5 Splice by overlap extension-PCR to join V_L and V_H

A DNA band present at roughly 750-800bp indicated successful joining of the V_L and V_H. This amplification incorporates a glycine serine linker to endow flexibility to the resultant scFv proteins (Ladder = Hyperladder™ 1 kb, Control = PCR without cDNA template).

6.2.1.5 Library construction

The SOE-PCR products were run on an agarose gel and purified. The products were quantified on a Nanodrop™ 1000. Concurrently, a single colony, picked from an agar plate, containing the pComb3XSS vector was grown overnight. The plasmid was purified using a plasmid mini-prep kit and quantified on the Nanodrop™ 1000. In separate reactions, the pComb3XSS vector and the SOE products were subjected to *Sfi*I digestion as per *Section 2.11.7*. The digested SOE and vector were run on separate agarose gels, shown in *Figure 6.6 (i)* and *Figure 6.6 (ii)*, respectively. Digestion of the pComb3XSS vector generally yields three products, undigested vector (~4900bp), digested stuffer fragment (~1600bp) and the digested vector segment of interest (~3300bp). Caution is exercised to ensure that the resolution of the digested vector is sufficient to isolate only the digested vector of interest, as carry-over of stuffer fragment or undigested vector can result in inefficient assembly of

the final scFv library. Digestion of the SOE fragment is performed in order to introduce complementary sticky ends for subsequent ligation to the vector; as such, no major size difference can be observed between undigested and digested SOE. Both the digested SOE and pComb3XSS bands were excised from their respective gels and purified prior to quantification on a Nanodrop™ 1000. Following this, a ligation reaction was performed to permit incorporation of the SOE products into the pComb3XSS vector, yielding an assembled scFv library (*Section 2.11.8*).

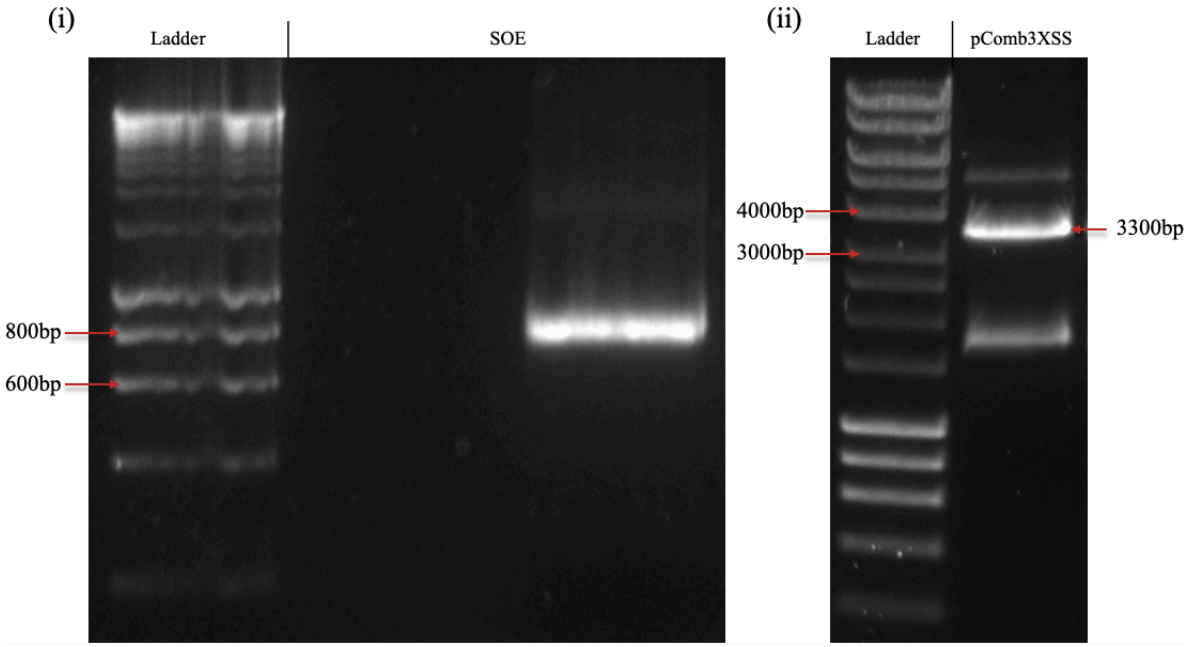

Figure 6.6 SfiI digestion of the SOE and pComb3XSS vector

(i) *Analysis of the digested SOE product (~750-800bp) on a 2% agarose gel.* ***(ii)*** *Digested pComb3XSS vector, run on a 0.7% agarose gel. With respect to the digested vector, the product of interest is present at ~3300bp (Ladder = Hyperladder™ 1 kb).*

6.2.1.6 Transformation into electrocompetent E. coli

The assembled anti-*R. commune* scFv library was subsequently transformed into electrocompetent XL1-Blue *E. coli* cells (*Section 2.11.9*). Post transformation, a colony-pick PCR was performed to assess the transformation efficiency of the insert-harbouring vector (*Section 2.11.10*). This reflects the quality of the library construction and indicates whether or not the SOE insert was effectively ligated into the pComb3XSS vector. Ten colonies were selected at random from the transformation plates, and from these, the SOE insert was selectively amplified. The resulting products were assessed on an agarose gel. In *Figure 6.7*, ~750-800bp inserts can be observed in all ten of the selected colonies, indicating a

transformation efficiency of 100%. At this stage, the library was considered ready to screen for anti- *R. commune* scFv.

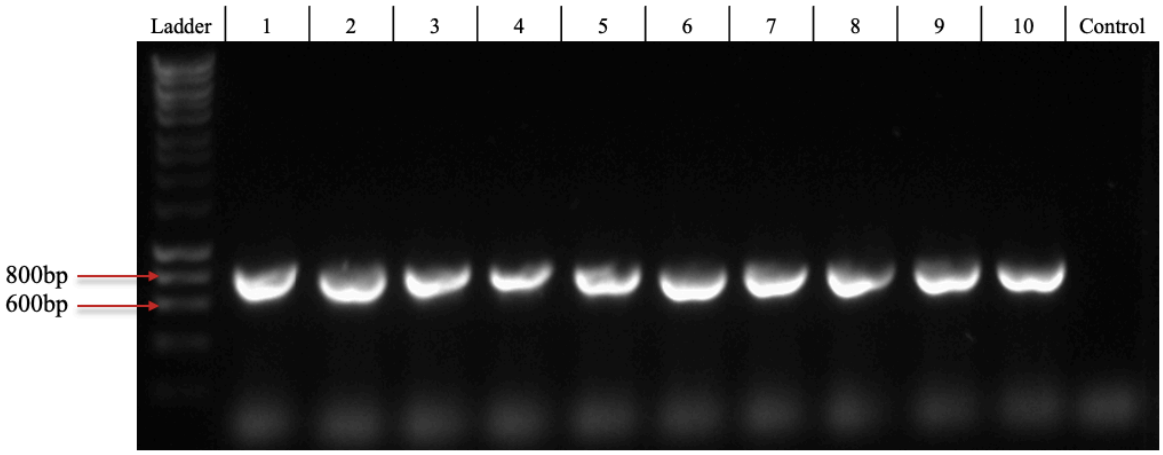

Figure 6.7 Analysis of colony-pick PCR on transformed scFv library

Ten randomly selected colonies were picked, and a colony-pick PCR performed to determine the transformation efficiency of the library into XL1-Blue E. coli cells (Ladder = Hyperladder™ 1 kb, 1 - 10 = random colonies, control = PCR with no colony).

6.2.2 Screening of an anti-R. commune scFv library for antigen-specific antibodies

6.2.2.1 Pre-panning library screening

Pre-panning analysis was performed to assess the response of random colonies prior to the enrichment process. From the transformation plates of the *R. commune* library, 192 clones were selected, grown and soluble scFv expression induced. The lysates from each clone were obtained via freeze-thaw lysis and then used in monoclonal ELISA analysis against the *R. commune* antigen (*Section 2.13.1*). The results of this analysis are depicted in *Figures 6.8* and *Figure 6.9*. Based on the monoclonal ELISA, it appeared that a number of scFv clones showed a positive signal against *R. commune*, as suggested by an elevation in absorbance when compared to that of other tested clones.

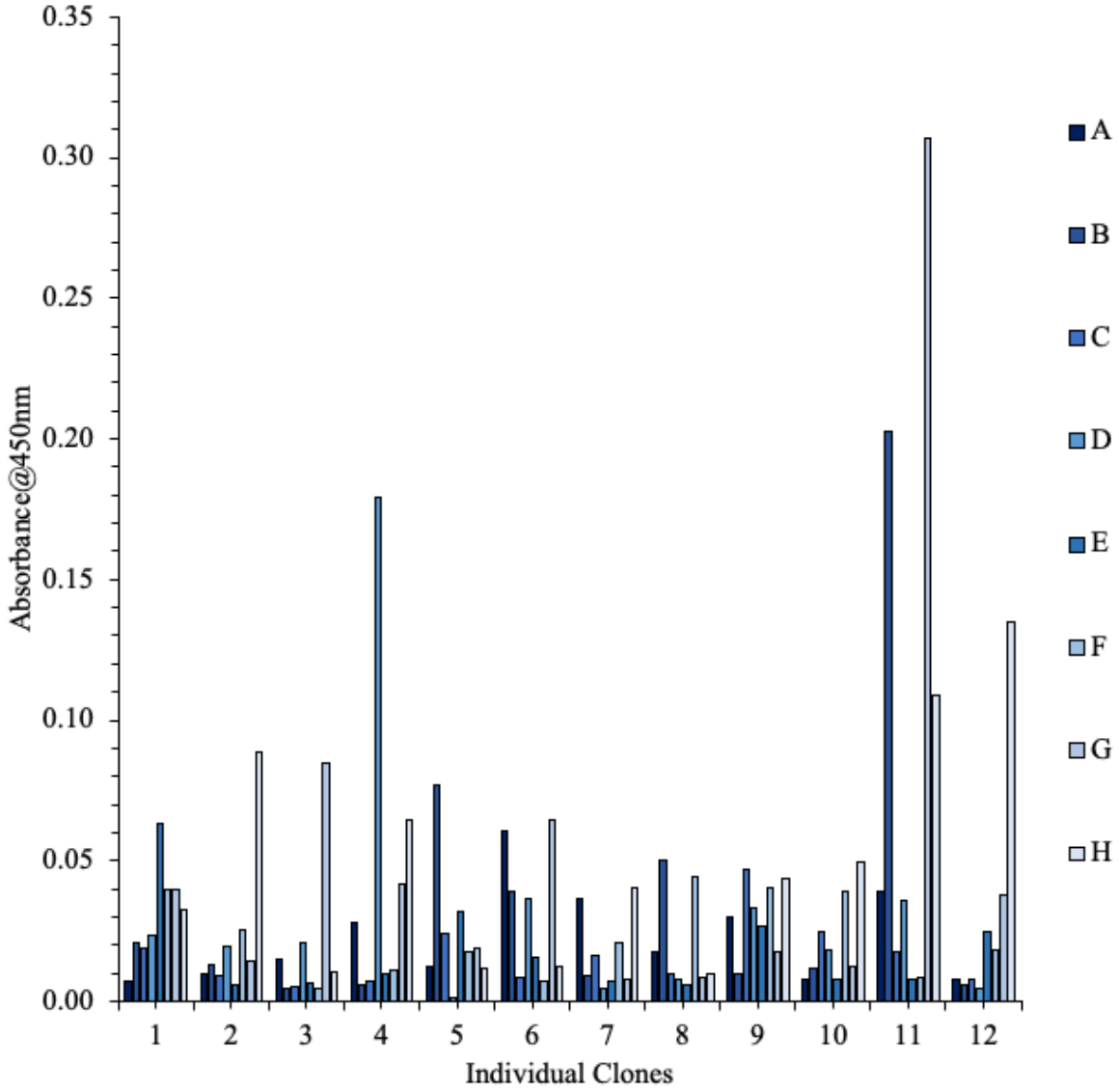

Figure 6.8 Pre-panning monoclonal ELISA against R. commune

ScFv-enriched lysates from single clones (1-12; A-H) were applied to ELISA wells coated with 4μg/mL R. commune. Bound scFv were detected using a HRP-labelled anti-HA antibody. The absorbance was then read at 450nm.

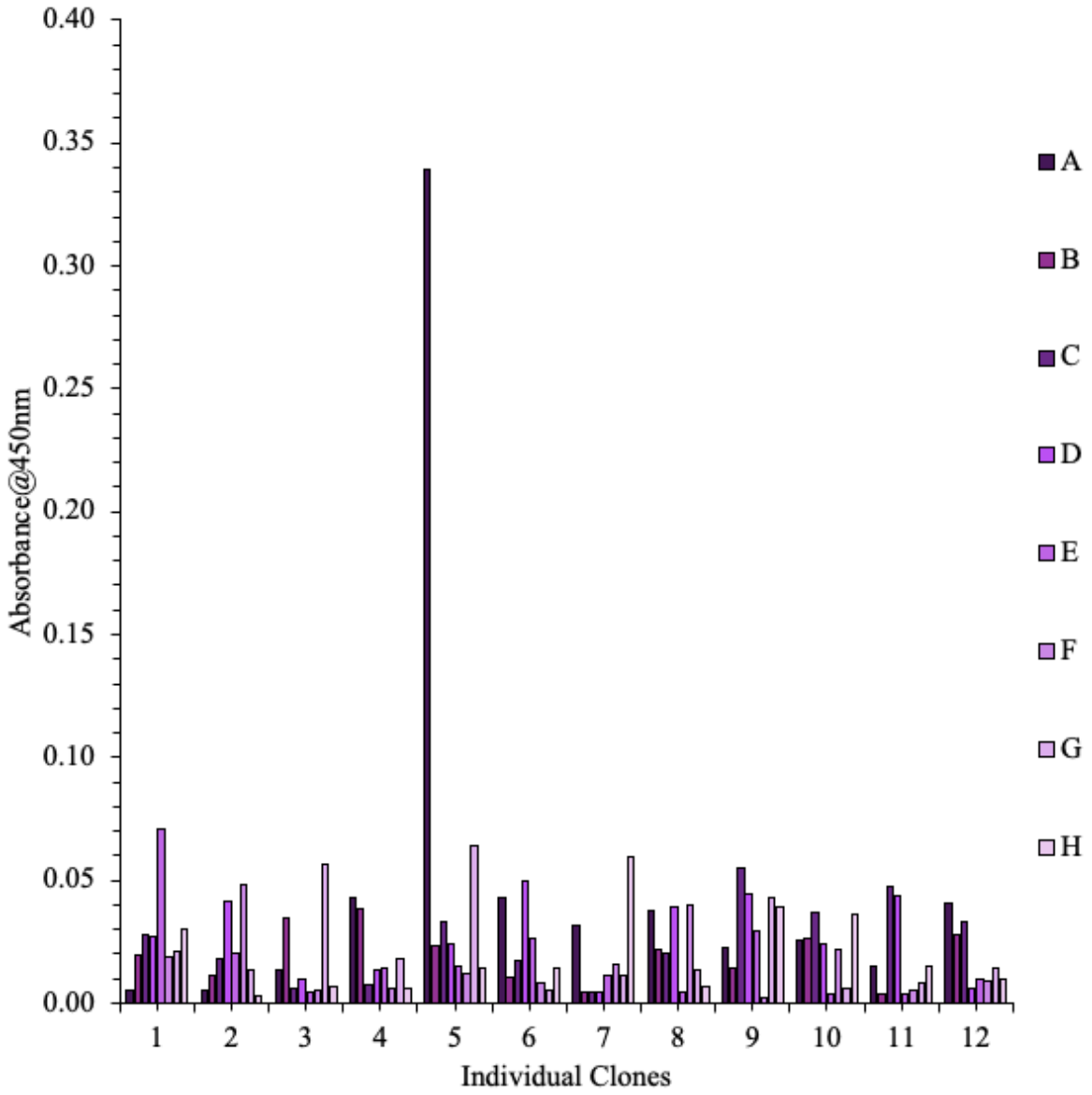

Figure 6.9 Pre-panning monoclonal ELISA against R. commune

ScFv-enriched lysates of single clones (1-12; A-H) were applied to ELISA wells coated with 4μg/mL R. commune. Bound scFv were detected using a HRP-labelled anti-HA antibody. The absorbance was then read at 450nm.

6.2.2.2 Indirect ELISA analysis of binding clones

Five clones of interest presenting an elevated signal (absorbance <0.1) in the monoclonal ELISA analysis were selected for further investigation. To permit this, the clones were re-grown, and expression induced. Lysate for each clone was obtained as per *Section 2.13.2* and applied in doubling dilutions to an ELISA plate coated with *R. commune* proteins. The titre, shown in *Figure 6.10*, indicated that of the selected clones, two titred successfully

against the *R. commune* proteins, 11G and 5A, as demonstrated by a reduction in the observed signal corresponding with an increasing dilution of the lysate.

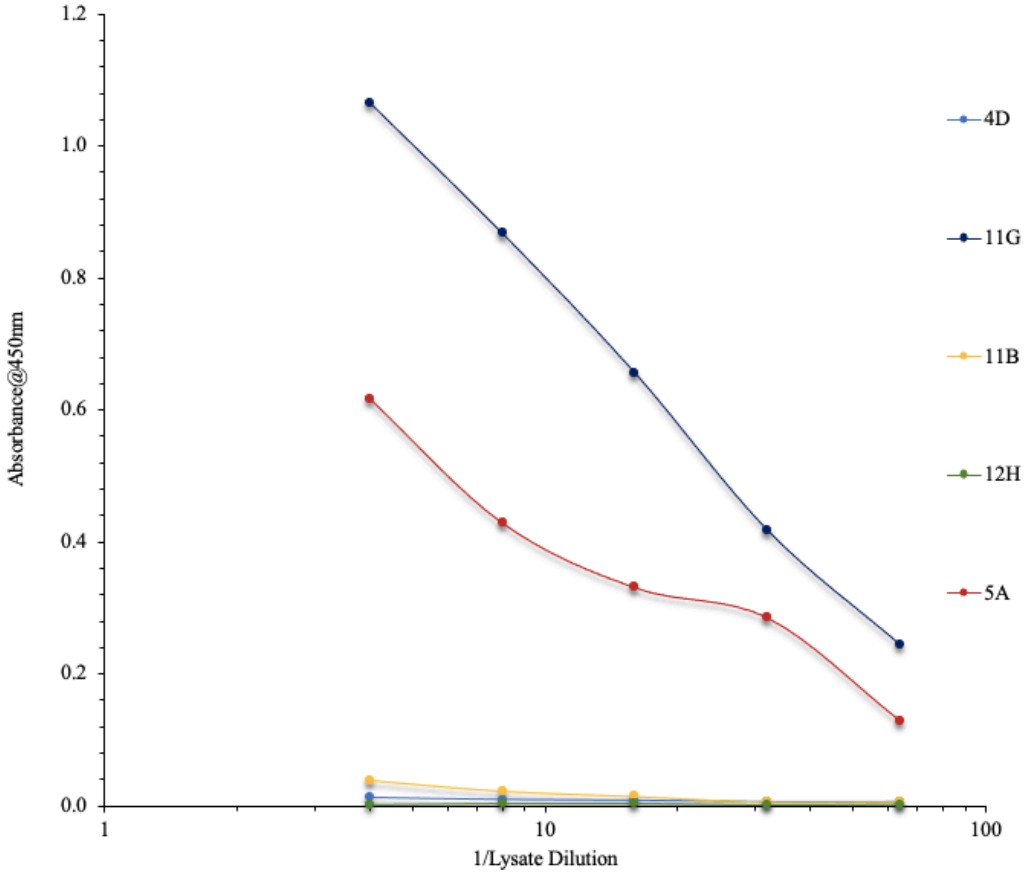

Figure 6.10 Titration of scFv-enriched lysates against R. commune

ScFv-containing lysate sourced from five clones was applied in a series of dilutions to the wells of an ELISA plate coated with 4µg/ml R. commune. Any bound scFv protein was detected using a HRP-labelled anti-HA antibody. The absorbance was then read at 450nm.

All five clones of interest were also tested in competitive ELISA format using *R. commune* total protein as a free antigen to compete with immobilised *R. commune* protein for scFv binding. The results are reported as A/A0 where A is a function of A0. This value reflects the reduction in absorbance value in wells containing free antigen (A) when compared to wells containing no free antigen (A0). However, the results indicated that no clones showed the capacity for competitive detection, as demonstrated by no change in A/A0 regardless of the concentration of free antigen present. *Figure 6.11* depicts a sample result of the competitive analysis when using the two clones which presented with a positive titre in indirect analysis, 5A and 11G. Results for the other clones are not shown.

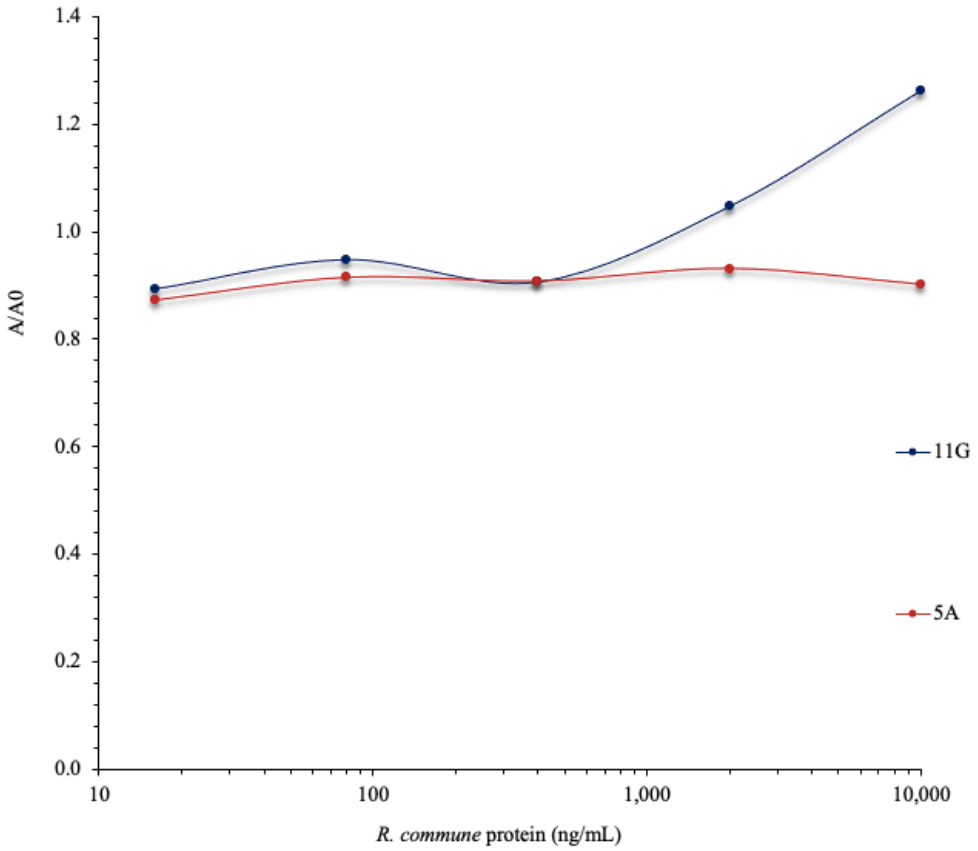

Figure 6.11 Competitive ELISA analysis of clones of interest

ScFv-containing lysates, at a final dilution of 1 in 4, from the clones of interest were applied to the wells of an ELISA plate coated with 4µg/ml R. commune alongside free R. commune protein at range of concentrations. Any bound scFv protein was detected using a HRP-labelled anti-HA antibody. The absorbance was then read at 450nm.

The library was also screened through phage display and biopanning in an attempt to enrich for, and isolate, further positively-binding clones. However, as aforementioned, due to the risk of enriching for cross-reactive scFv, in addition to employing standard biopanning, an alternative procedure termed subtractive biopanning was proposed.

6.2.2.3 Enrichment of the phage library via subtractive biopanning

Subtractive biopanning, also termed depletion biopanning, was suggested as a method by which to ensure that any scFv isolated from the biopanning process were not cross-reactive with proteins associated with other common co-infecting fungi of barley. This method involves the exposure of the antibody library to the proteins of the cross-reactants prior to enrichment against the antigen of interest. There are several fungal pathogens which infect barley crops, however, in Ireland, *Ramularia collo cygni* (*R. collo cygni*), *Fusarium*

culmorum (*F. culmorum*) and *Fusarium graminearum* (*F. graminearum*) are among the more common pathogens, in addition to *R. commune*. This considered, the depletion steps were performed using proteins from these fungal pathogens as there was a greater likelihood of these being found growing on the same crops which *R. commune* infects.

Exposure to potentially cross-reacting antigens should deplete any undesired clones, leaving pools of target-specific scFv remaining. With respect to this work, the depletion step was not performed during the first round of biopanning as at this point the 'unpanned' library still contains a plethora of clones with no *R. commune* specificity. Performing the depletion step at this stage in the process poses a risk of losing rare anti-*R. commune* clones. This considered, the first round of biopanning was performed as standard, by exposing the scFv pool to the *R. commune* antigen and recovering the enriched pool of clones. Depletion was then performed during the second round of biopanning, as at this stage the scFv pool should contain multiple iterations of *R. commune*-binding scFv, and the risk of losing clones of interest is reduced. When employing subtractive biopanning, the phage pools in round two were incubated sequentially, first in an immunotube coated with protein extracts associated with *F. graminearum*, *F. culmorum* or *R. collo cygni* (depletion tube). After exposure to the cross reactants, the phage remaining in solution were retrieved and applied to a second, *R. commune* coated immunotube (enrichment tube). After incubation in this tube, unbound phage and loosely bound phage were washed away, and any remaining *R. commune*-binding phage were eluted. The third round was then performed as standard, with no further depletion step incorporated. Protocols were as per *Section 2.12*, with the deviation that 300µL input phage was added to the immunotube for round 2. Alongside this depletion strategy, a "typical" panning was also performed whereby no depletion step was included. The details of the parameters employed in each of the biopanning rounds are provided in *Table 6.1*.

Table 6.1 Parameters for biopanning of an scFv library for anti- R. commune scFv

Both standard and subtractive biopanning approaches were implemented. The antigen coating concentration and washing stringency is altered in each subsequent round to apply selective pressure for the isolation of high sensitivity and specificity clones. Depletion of cross-reactive scFv was performed in round 2 when using the depletion panning strategy.

Round	**Antigen Coating Concentration**		**Wash Steps**
1	30µg/mL *R. commune*		3X PBS-T (0.05%, v/v), 3X PBS
2 (Depletion)	Depletion tube: 3µg/mL each of *F. culmorum, F. graminearum* and *R. collo cygni*	Enrichment tube: 3µg/mL *R. commune*	3X PBS-T (0.05%, v/v), 3X PBS
2 (No Depletion)	3µg/mL *R. commune*		
3	1 µg/mL *R. commune*		5X PBS-T (0.05%, v/v), 5X PBS

6.2.2.4 Polyclonal phage ELISA

Upon completion of the three biopanning rounds, a polyclonal phage ELISA was performed using input phage pools sourced from each round of panning, as per *Section 2.12.4*, with the deviation that half volumes of reagents were used due to limited sample size for phage pools. It should be noted that due to a low output in round three of panning, no input phage pool could be obtained for this round. The phage ELISA was performed using input phage from the unpanned library, alongside phage pools from rounds one and two. This analysis should reflect whether *R. commune*-specific enrichment was occurring, as even after one round panning, the library should indicate bias toward the target antigen. The phage pools were tested against the antigen of interest, *R. commune*, and the other potentially cross-reactive proteins. The analysis is shown in *Figure 6.12*. The results indicate that the depletion step in the biopanning process appeared to remove some cross-reactive scFv, as demonstrated by the reduction in signal against *R. collo cygni* and *F. graminearum* when comparing the signal against these pathogens in the continuous panning strategy to the depletion strategy.

However, no such reduction was observed against *F. culmorum*. This may be a result of a shared, or very similar, protein composition between *R. commune* and *F. culmorum*, resulting in an inability to remove all cross-reactive scFv. However, it should be noted that overall there did not appear to be strong selective enrichment for *R. commune*-specific scFv, as indicated by the low absorbance values achieved in the assay.

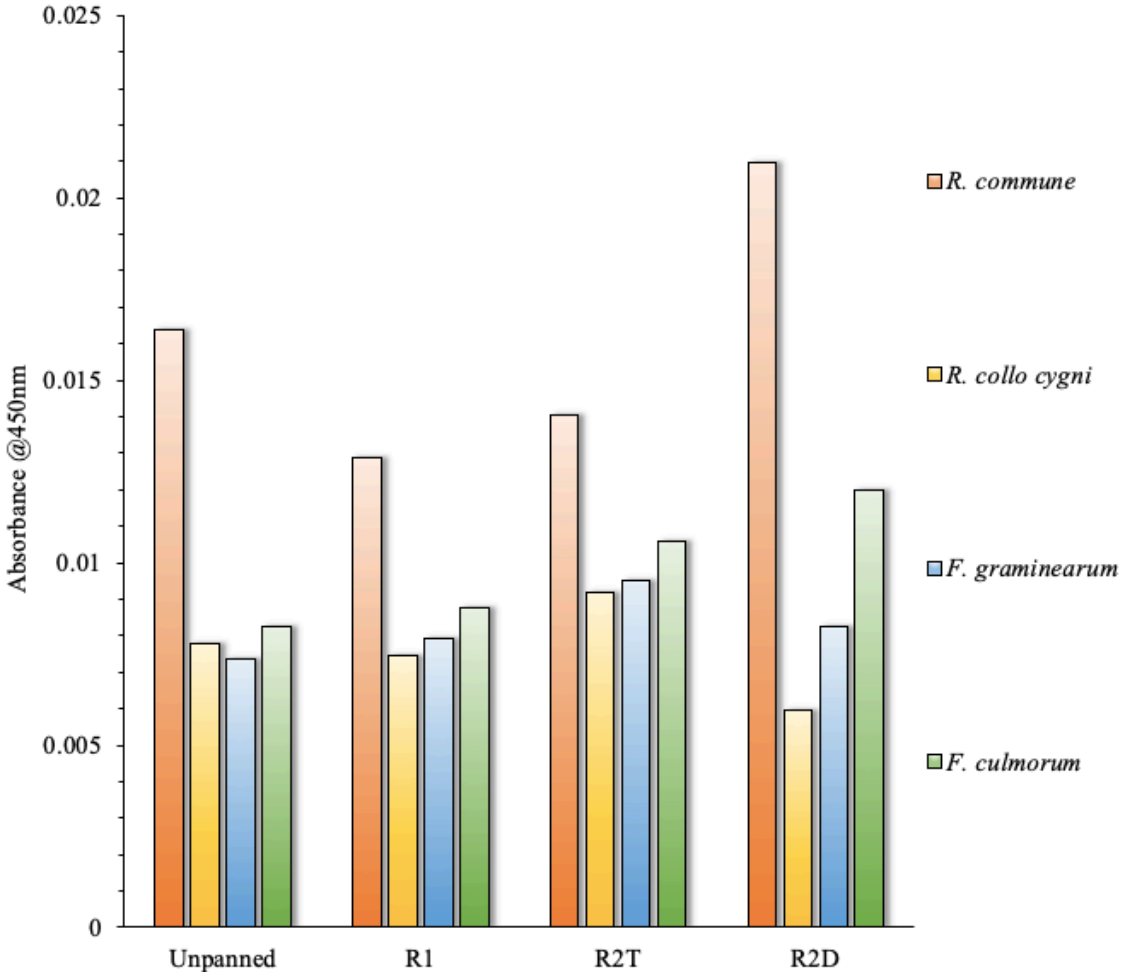

Figure 6.12 Analysis of phage pool-binding from biopanning rounds

Input phage pools from each round of panning were diluted 1:3 and applied in triplicate to wells coated with 4μg/mL of each antigen. Bound phage were detected using a HRP-labelled anti-HA antibody. The absorbance was read at 450nm (R2T = "typical" panning round 2, R2D = depletion panning round 2).

6.2.2.5 Monoclonal ELISA analysis

To evaluate the scFv clones carried forward through panning, monoclonal ELISA analysis was performed by picking single colonies across biopanning rounds two and three from both the continuous and depletive strategies. The clones were grown and expression of scFv

induced. Lysates were obtained from each of these expressed clones and used in ELISA to determine if there was a response against the *R. commune* antigen. The results of the screening are shown in *Figure 6.13* and *Figure 6.14*.

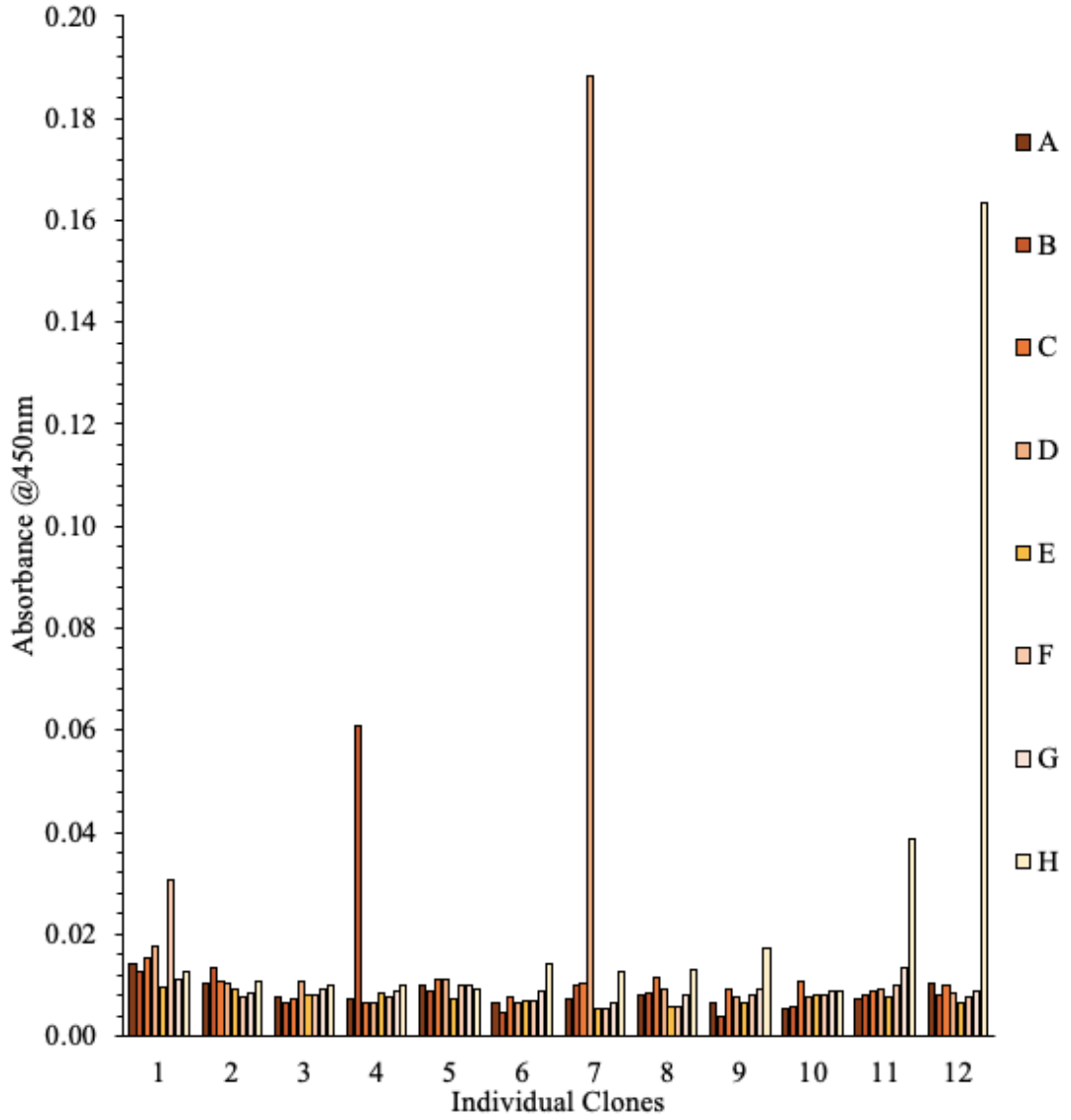

Figure 6.13 Monoclonal ELISA analysis of clones from biopanning rounds

Lysates from single clones (1-12; A-H) sourced from continuous panning rounds were applied to the wells of an ELISA plate coated with 4µg/mL R. commune protein extract. The bound clones were detected with a HRP-labelled anti-HA secondary antibody. The absorbance was then read at 450nm.

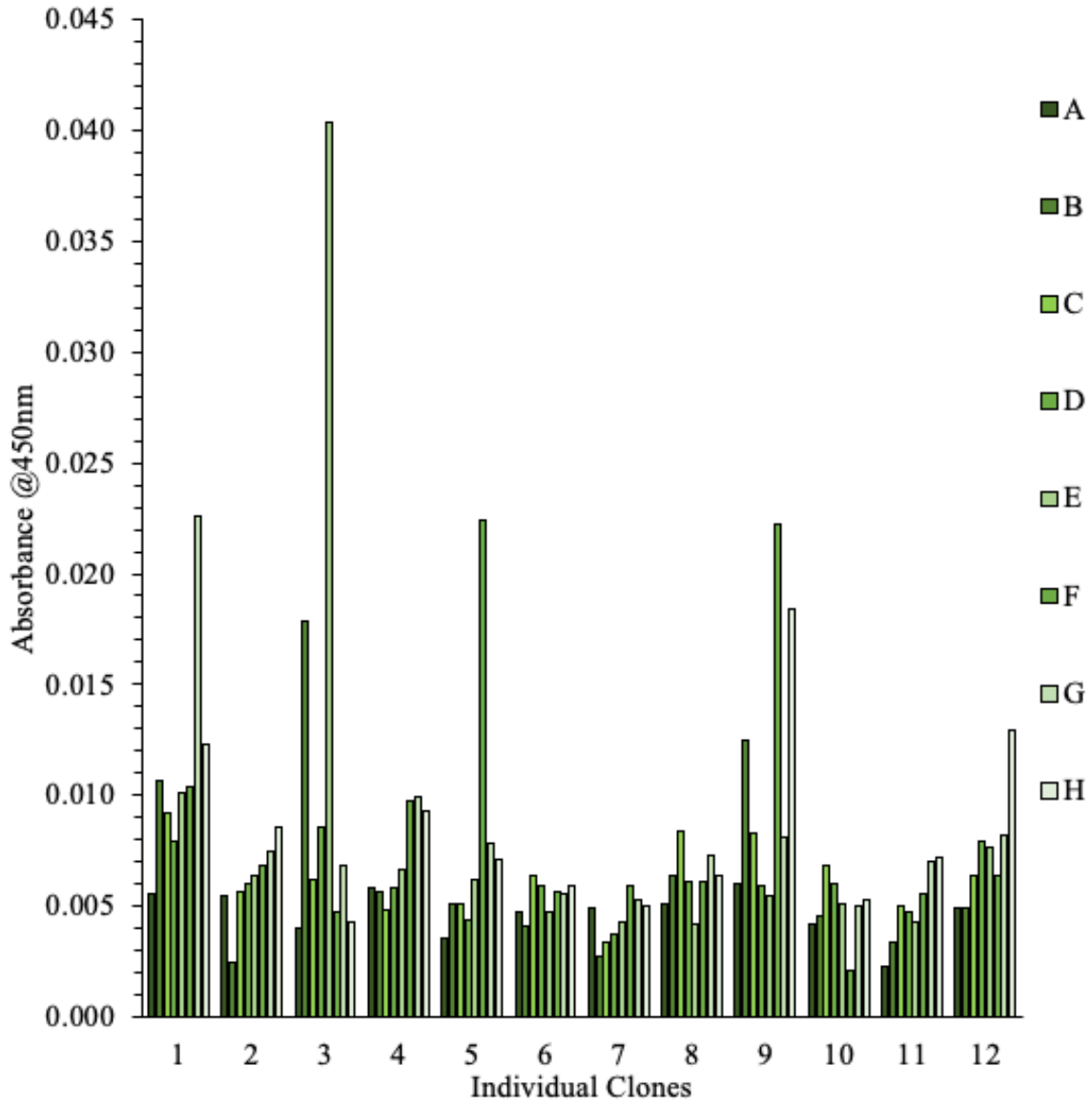

Figure 6.14 Monoclonal ELISA analysis of clones from depletion biopanning rounds

Lysates from single clones (1-12; A-H) from depletion panning rounds were applied to the wells of an ELISA plate coated with 4μg/mL R. commune protein extract. The bound clones were detected with a HRP-labelled anti-HA secondary antibody. The absorbance was then read at 450nm.

6.2.2.6 Lysate titre analysis

From the monoclonal ELISA, nine clones were selected for further analysis across both plates of monoclones. Each clone of interest was re-grown and soluble expression of scFv induced overnight. Lysates were obtained and used in a lysate titre against the *R. commune* antigen (*Section 2.13.2*). Results of this analysis are depicted in *Figure 6.15*. Of the clones tested, two had apparent signal when titred against the *R. commune* antigen, 7D and 4B.

Clone 4B was not considered further for analysis as the low in-assay signal and low titre meant it would not be suitable for application to further immunoassay development in its current state. Clone 7D provided a slightly improved signal at low dilutions, however, when the plasmid was isolated and sent for sequencing with Source Bioscience Ltd., it was revealed that no scFv insert was present in the plasmid. In addition, when attempting to identify an scFv protein in WB, no 27kDa band was observed, further confirming the absence of scFv expression. Hence, it was deduced that the signal observed upon titration of this clone was a result of non-specific binding, therefore, no further characterisation of this clone was performed.

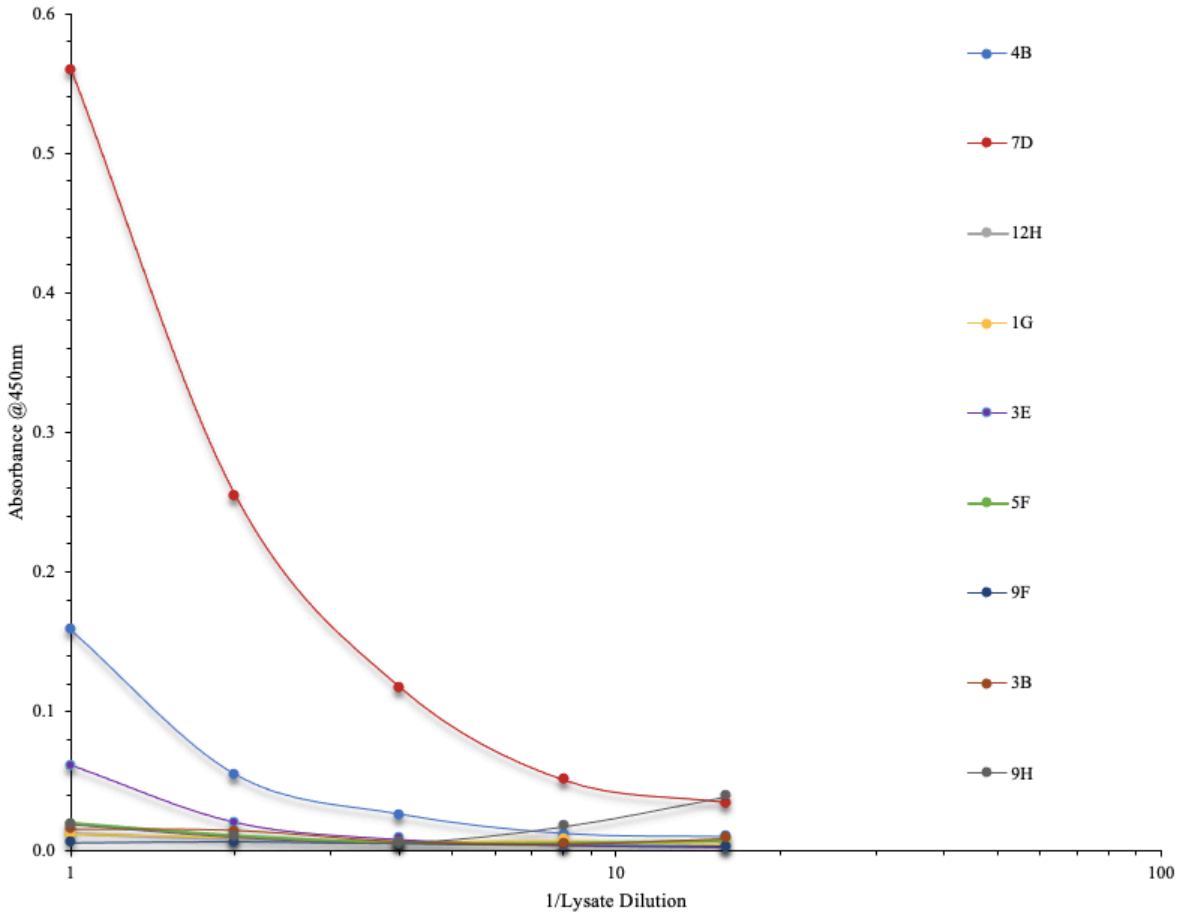

Figure 6.15 Lysate titre of clones of interest

ScFv-enriched lysates were obtained from clones which displayed a positive response in monoclonal ELISA. The lysates were diluted and applied to wells coated with 4µg/mL R. commune antigen. Bound scFv were detected with a HRP-labelled anti-HA secondary antibody. The absorbance was then read at 450nm.

6.2.3 Characterisation of anti-R. commune scFv

6.2.3.1 Optimisation of expression of 5A and 11G

The two positive clones identified from screening of the anti-*R. commune* library, 5A and 11G, were transformed via heat shock (*Section 2.10.11*) into Top10F' cells to permit soluble expression of the scFv without the PIII protein. Top10F' cells are a non-suppressor strain. In this context, that means that the amber stop codon located between the scFv gene insert and the phage PIII protein is read, permitting expression of the scFv as a stand-alone protein. Contrastingly, in suppressor strains, such as XL1-Blue, the stop codon is read-through and the scFv is expressed as an scFv-PIII fusion. While the fusion to PIII does not impact binding, it is preferable to express and characterise the scFv without it. The expression of 5A and 11G was optimised under the parameters of IPTG concentration and induction temperature as described in *Section 2.10.10*. IPTG concentration plays a role in how strongly the promoter is activated and the level of IPTG used to induce expression is linked to protein solubility. Similarly, protein solubility and production rates are also affected by temperature (Tolia and Joshua-Tor, 2006; Gutiérrez-González et al., 2019). Results of the optimisations are depicted in *Figure 6.16*. Based on these, the apparent optimal conditions were 0.1mM IPTG and a temperature of 25°C for both 5A and 11G, as demonstrated by the highest absorbance observed in the wells containing lysates from cultures expressed under these conditions. Induction temperature appeared to have a greater effect on 5A than 11G, with a reduced signal observed in all cultures expressed O/N at 30°C for this clone. In comparison, each 11G culture presented similar signals, aside from 0.1mM IPTG and 25°C, indicating that this clone is not as greatly affected by these parameters.

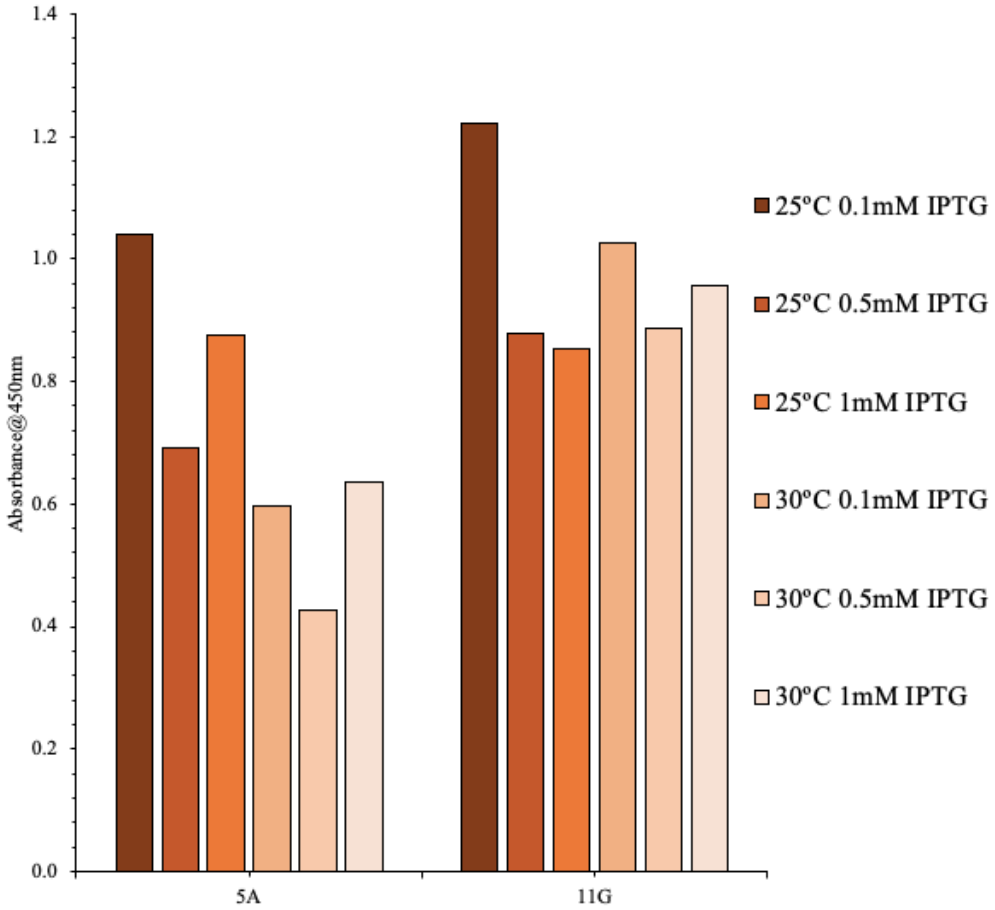

Figure 6.16 Optimisation of expression for 5A and 11G scFv

Cultures of 5A or 11G were induced with a range of IPTG, 0.1mM ,0.5mM and 1mM and expressed overnight at either 30°C or 25°C. Lysates from each condition were applied to wells coated with 4μg/mL R. commune. Bound scFv were detected using a HRP-labelled anti-HA antibody. The absorbance was then read at 450nm.

6.2.3.2 Sequence analysis of 11G and 5A scFv

Plasmids were isolated from 5A and 11G clones and sent for sequencing by Source Bioscience Ltd. The returned sequences were translated in Expasy Translate and the CDRs identified via manual identification, in line with the Kabat antibody numbering scheme. The sequences were subsequently aligned in Multalin. The alignment of the CDR regions between the two clones is shown in *Table 6.2*. Diversity amongst the CDRs is demonstrated by the dissimilarity between these regions when comparing the 5A and 11G sequences. The CDR-H3 of clone 11G favoured small residues such as glycine (G), serine (S), threonine (T) and alanine (A). This is in agreement with previous observations that avian repertoires are more biased toward small residues in CDR-H3, appearing at a frequency of 54%, as opposed to murine or human counterparts which employ such residues at 35% and 36%, respectively.

The 5A CDR-H3 contains larger AAs such as two large, aromatic tryptophans (W). This 5A CDR-H3 also features a cysteine (C) residue. Cysteines are known to appear more frequently in avian repertoires and previously it was suggested that avian antibodies could be subtyped based on the presence of C in the heavy chain binding regions. The presence of one C in the CDR-H3 and a further single C in the CDR-H1 suggests that scFv 5A aligns with the suggested structural avian subtype, "type 3", which features residues at these locations. This type is suggested to comprise of <5% of the overall repertoire. Contrastingly, scFv 11G appears to contain no non-canonical C residues, suggesting is falls under the "type 2" subtype, which makes up 33% of the avian pool (Wu et al., 2012).

Table 6.2 CDR sequence alignment of 5A and 11G scFv

The sequences were translated in Expasy and aligned in Multalin to highlight variation between the two clones.

	CDR-L1	***CDR-L2***	***CDR-L3***
11G	SGSSGS-YG	KNTKRPS	GTWESSAAA--
5A	SGSTGNAYG	GNNQRPS	GSGDSNTGAGI

	CDR-H1	***CDR-H2***	***CDR-H3***
11G	FTFSSFYMF	QISGSGRYTYYAPAVKG	SA----GTAADTDA
5A	FTFNTYCMQ	LIYNDGG-TDYGAAVKG	GGVWCWDAAGNIDA

6.2.3.3 Large-scale expression and purification of 5A and 11G

The two clones were grown large-scale under their previously defined optimal conditions and purified in IMAC as per *Sections 2.15.2*. The results of the purification process are presented in *Figure 6.17 (i)* and *(ii)*. It was confirmed that both clones were successfully purified based on the presence of bands around the 27kDa MW in the elution fractions, the typical size for scFv migration. In conjunction with this, probing of the elution fractions in WB with an anti-HA antibody revealed a concurrently sized band, confirming isolation of the scFv protein. A faint band, reactive with the anti-HA antibody in WB, can be seen around the 55kDa size in the 11G WB analysis. The size is roughly double that of an scFv,

suggesting that this could be a dimerised form of 11G. It was noted that in the concentrated elution fractions for 5A, a high amount of scFv was not observed, based on visualisation of protein bands in the SDS-PAGE gel. In contrast, thick protein bands were observed for the purified 11G samples in both SDS-PAGE and WB.

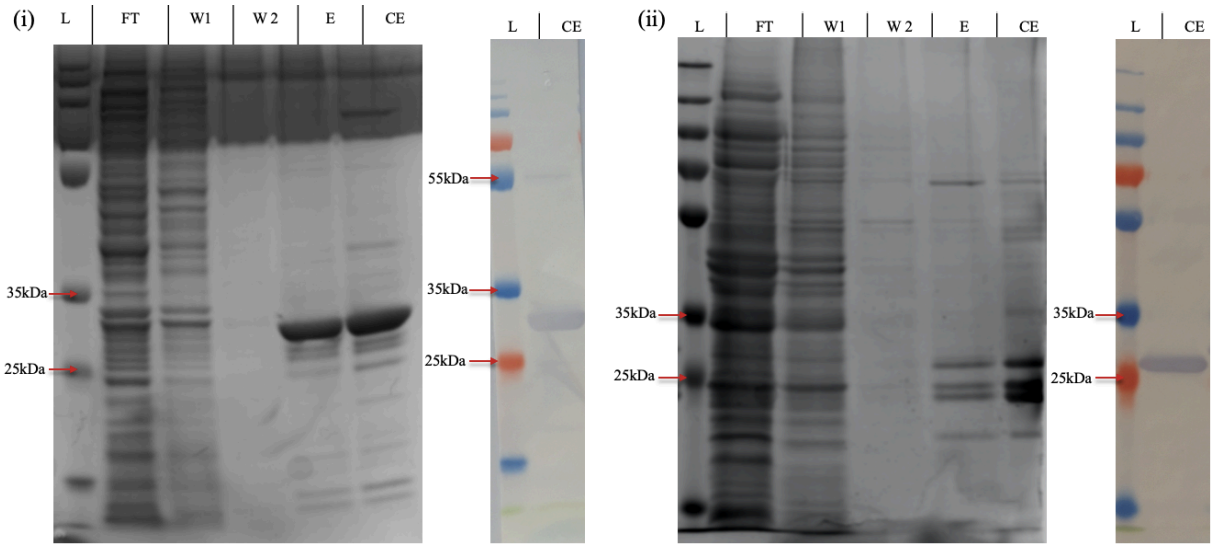

Figure 6.17 Ni-NTA purification of 5A and 11G scFv

(i) *SDS-PAGE (left) and WB (right) analysis of the Ni-NTA purification of scFv 11G.* ***(ii)*** *Analysis of 5A purification fractions in SDS-PAGE (left) and WB (right). The antibodies were purified on Ni-NTA resin and unbound protein was removed through a series of wash steps, prior to elution with a high imidazole concentration elution buffer (Ladder = PageRuler plus prestained, FT = flow through (1:2), W1 = 20mm imidazole buffer, W2 = 30mM imidazole buffer, E = 300mM imidazole buffer elution, CE = concentrated and buffer exchanged elution).*

6.2.3.4 Titration of purified 5A and 11G

The purified sample of each clone was used in an antibody titre against the *R. commune* antigen as per *Section 2.17.1* From the results in *Figure 6.18*, the 5A clone did not appear to achieve a good titre, indicating that post-purification this clone did not retain good binding to *R. commune*, or that the expression level of this clone may be too low to elicit high signal. This is somewhat confirmed by the analysis, where apparently low amounts of purified 5A were observed based on the visual analysis of the protein bands in the SDS-PAGE gel. However, the 11G scFv titred well against *R. commune*, producing good in-assay signal, suggesting that this antibody may be suitable for the detection of *R. commune*.

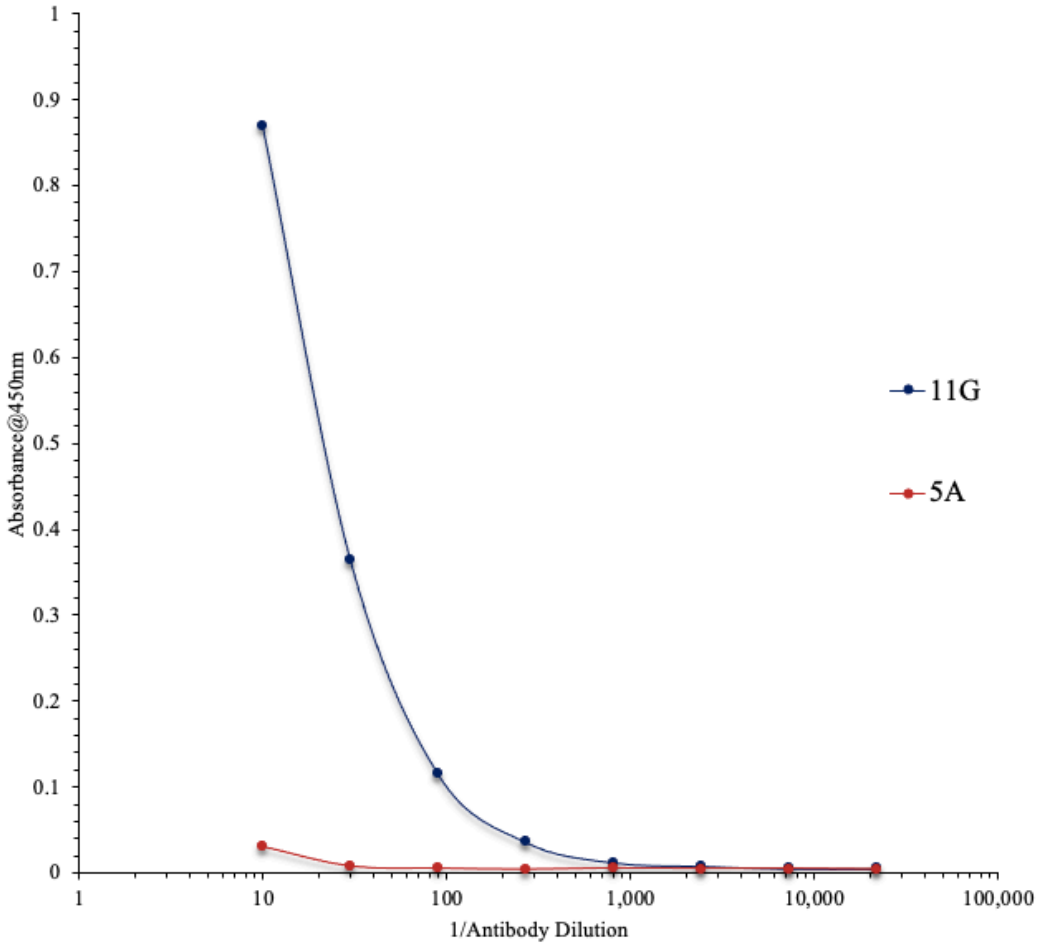

Figure 6.18 Titration of anti-R. commune scFv 11G and 5A against R. commune

The purified scFv were applied in duplicate in a series of dilutions to ELISA wells coated with 4µg/mL R. commune. Bound scFv was detected via the application of an anti-HA HRP-labelled antibody. Absorbance was read at 450nm.

6.2.3.5 Cross-reactivity analysis of 11G

To investigate the reactivity of 11G with other non-target pathogens of barley, the scFv was titred against equally coated concentrations of *R. commune*, *F. graminearum*, *F. culmorum* and *R. collo cyngi*. The results (*Figure 6.19*) indicate that the scFv does cross-react with the other pathogens. Similar absorbance readings were obtained against all pathogens, with the signal against *F. graminearum* presenting as the lowest. Overall, this suggests that 11G may bind a shared, or highly similar, antigen amongst these fungal pathogens. This means that while it may prove a useful capture antibody in the scenario where screening indiscriminately for various fungal pathogens is the intended goal, it will not suffice for the specific detection of *R. commune*. Based on this result, it was decided to pursue the application of polyclonal antibodies (pAbs) for the detection of *R. commune*.

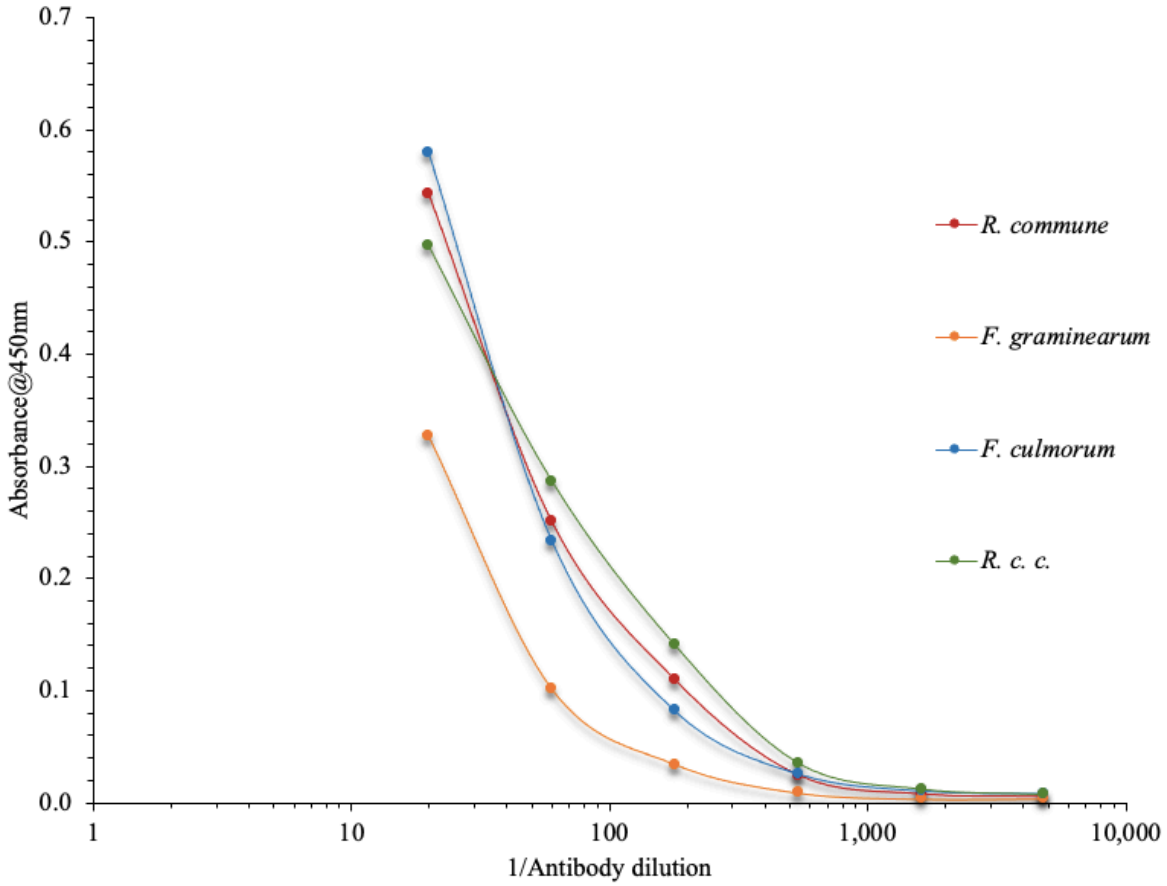

Figure 6.19 Assessment of 11G reactivity with non-target proteins

Purified 11G was applied in a series of dilutions to wells coated with 4µg/mL of either R. commune, F, graminearum, F. culmorum or R. collo cygni. Bound scFv was detected with an anti-HA HRP labelled antibody and the absorbance was read at 450nm.

6.2.4 Isolation and characterisation of anti-R. commune polyclonal antibodies

6.2.4.1 Isolation of IgY

Typically, purification of IgG from murine or leporine derived sources can be achieved through the use of Protein A/G/L resins, however, this option is not available for the purification of the avian homologue, IgY, due to the absence of binding between the IgY Fc and Proteins A/G/L. Therefore, isolation of IgY pAbs requires alternative approaches such as ammonium sulphate precipitation. This was performed on anti-*R. commune* antibody enriched serum as per *Section 2.24*. Three successive rounds of precipitation were performed to increase the purity of the isolated pAb. To confirm the successful precipitation of the pAb from serum, the samples were run in SDS-PAGE and WB. The heavy and light chains are clearly visible in the SDS-PAGE gel at ~70kDa and 25-30kDa, respectively (*Figure 6.20 (i)*). The presence of the avian heavy chain is further confirmed by the WB analyses in *Figure*

6.20 (ii) which depicts a clear purple band at ~70kDa. This is around the expected size of the IgY heavy chain, which appears larger than the mammalian IgG heavy chain (~50kDa) due to the presence of an additional constant region. The resulting isolated pAb was quantified by BCA assay.

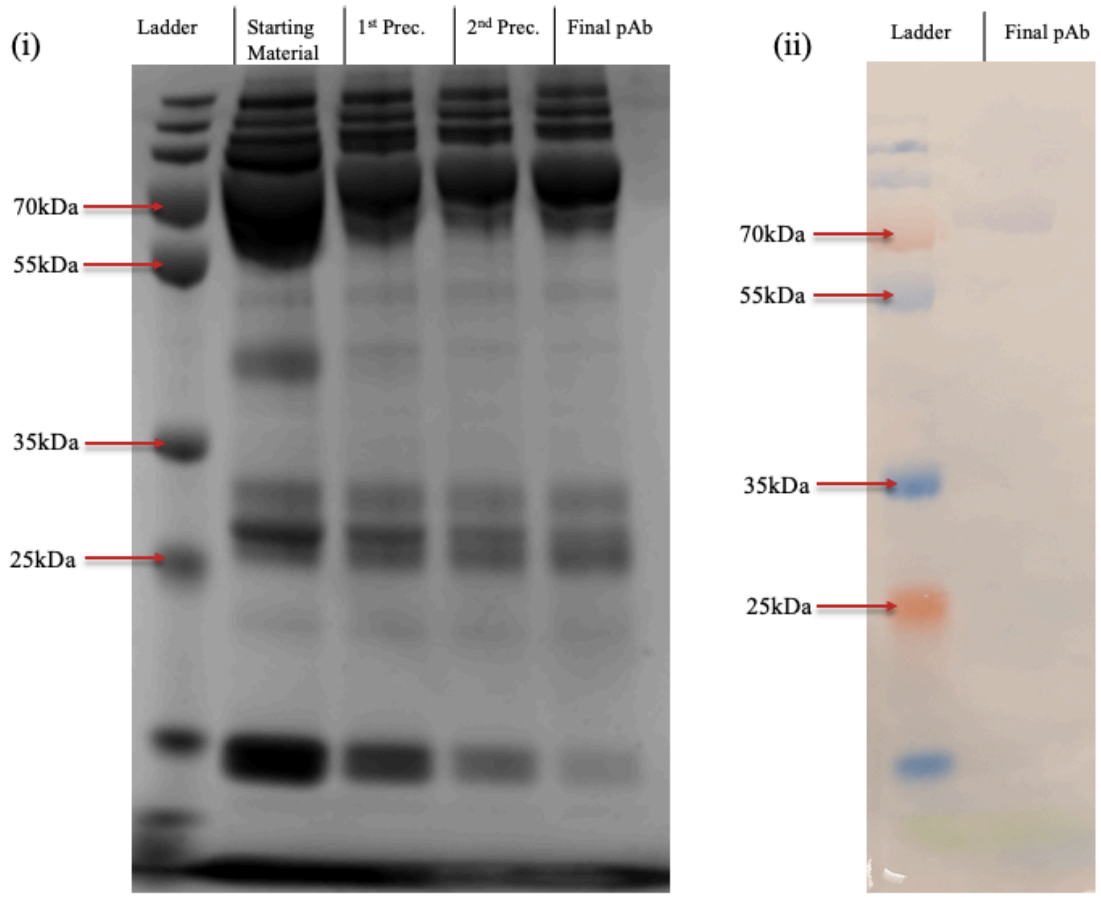

Figure 6.20 Ammonium sulphate precipitation of pAb

(i) *SDS-PAGE gel depicting three successive ammonium sulphate precipitations.* ***(ii)*** *The final sample of pAb was analysed in WB and probed with a HRP-labelled anti-chicken VHH antibody (Ladder = PageRuler plus prestained, Starting material = serum prior to any precipitations, 1st/2nd prec. = the first and second iterations of the precipitation, Final pAb = the 3rd precipitation buffer-exchanged into PBS; all samples were diluted 1:20).*

6.2.4.2 Checkerboard ELISA analysis

Upon the successful isolation of the pAb, a checkerboard ELISA was performed to determine the reactivity of the pAb with the *R. commune* antigen (*Section 2.25.1*). This is a useful assay to determine both a range for the working concentration of the antibody, and a suitable coating concentration for the antigen. It can be used to ensure that the most

economical quantity of each resource is used in subsequent assays. The results of the checkboard ELISA are shown in *Figure 6.21*. Based on this analysis, a coating concentration of 4µg/mL *R. commune* protein and a working dilution of pAb in the range of 1 in 4,000 and 1 in 10,000 was chosen for future assay development.

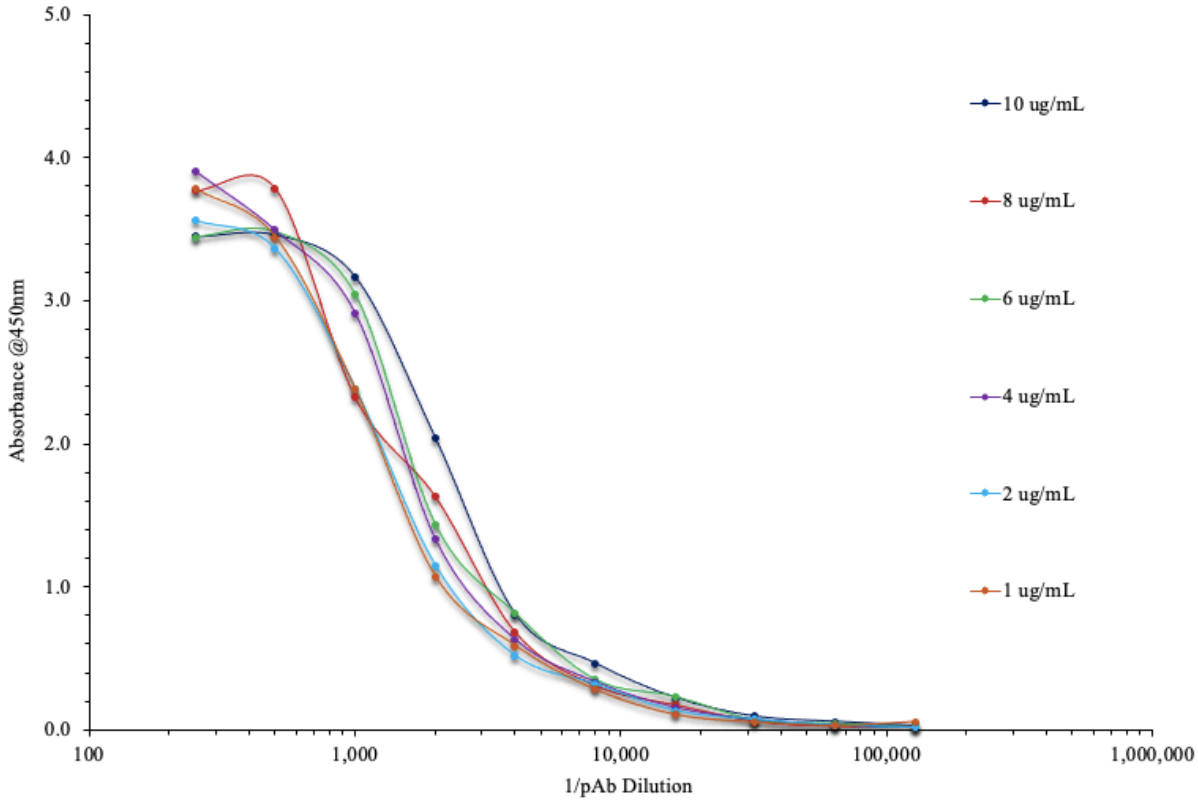

Figure 6.21 Checkboard ELISA of pAb against the R. commune antigen

Varying concentrations of R. commune were coated to the wells of an ELISA plate and each probed with a range of concentrations of pAb. Bound pAb was detected with a HRP-labelled anti-IgY H+L antibody. The absorbance was read at 450nm.

6.2.4.3 Cross-reactivity analysis

An assessment was performed to determine if cross-reactivity between the pAb and other common fungal pathogens was present (*Section 2.25.2*). This was performed by means of an antibody titre whereby the anti-*R. commune* pAb was titred against protein extracts from *R. commune*, *R.collo cygni*, *F. graminearum* and *F. culmorum* (*Figure 6.22*). Based on the results of the titre, the cross-reactivity appeared low, with the absorbance signal achieved in wells coated with *R. commune* antigens considerably higher than those coated with non-target protein extracts. While there appears to be some cross-reactivity, it is important to note that some pathogens such as *F. culmorum* and *F. graminearum,* which produced the

first and second highest signals of the cross-reactants respectively, are found predominantly in the head of the barley crops (McMullen et al., 2012). While others, such as *R. collo cygni* occupy the barley foliage (Havis et al., 2015). Similarly, *R. commune* is primarily a foliar disease meaning that it is largely found on the leaves of the plant, although the fungal growth will proceed into the head of the barley as the disease develops. Therefore, a correct sampling strategy targeting only leaf tissue, used in conjunction with visual inspection, could reduce the likelihood of high quantities of cross-reactive pathogens being present in the sample to be tested.

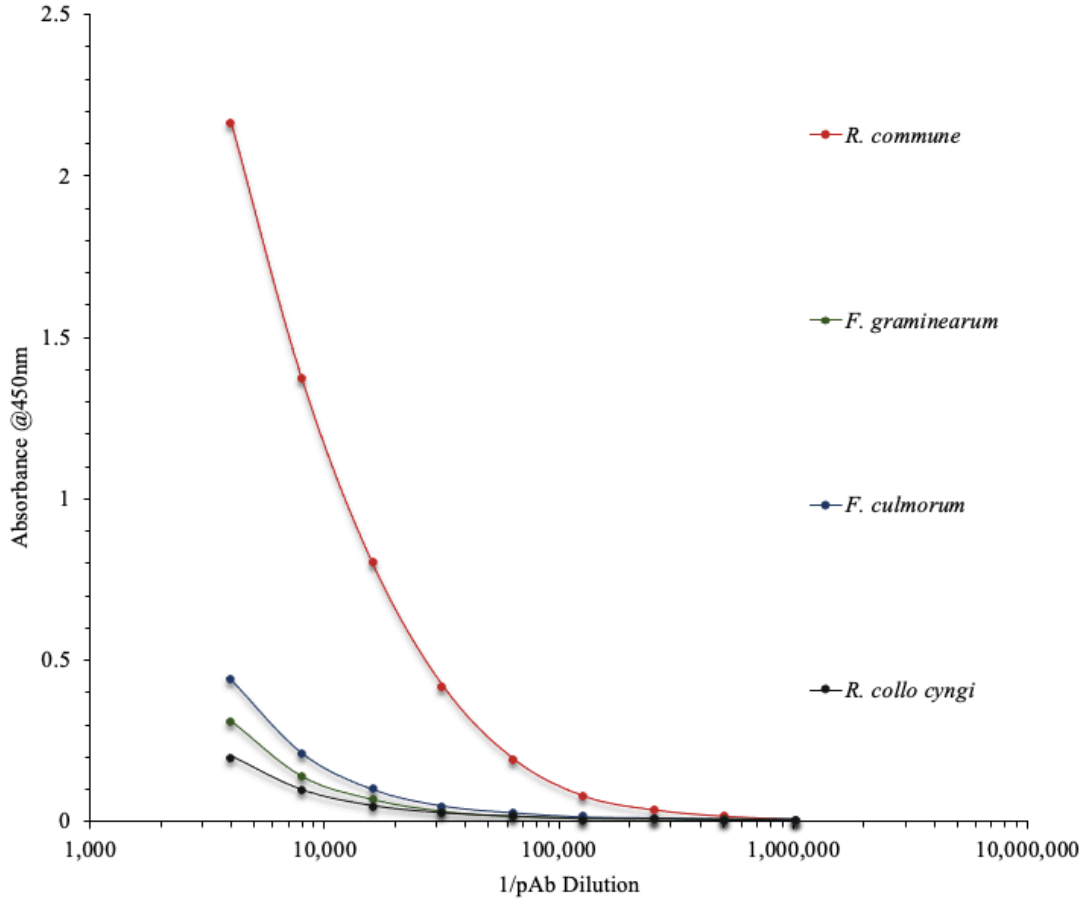

Figure 6.22 Cross-reactivity analysis of the pAb

Doubling dilutions of pAb, starting from 1 in 4,000, were applied in triplicate to wells coated with 4µg/mL of either R. commune, R. collo cygni, F. graminearum or F. culmorum total proteins. Bound IgY was detected with a HRP-labelled anti- IgY H+L chain antibody. The absorbance was then read at 450nm.

6.2.5 Dot blot analysis

The dot blot is a paper-based immunoassay whereby proteins are blotted onto a membrane, and these blotted proteins can be subsequently detected through protein-specific antibodies. Dot blots make a good alternative to other immunoassays such as WB as they do not require denaturation or separation of the proteins, rather, the total protein content is immobilised at one site. In addition, dot blots retain proteins in the natural 3D structure, as opposed to western blot were proteins are typically denatured, meaning that dot blots reflect the detection of naturally folded proteins. To permit dot blot analysis, *R. commune* protein was spotted onto a nitrocellulose membrane at various concentrations, the membrane blocked and the proteins subsequently detected through an anti-*R. commune* pAb (*Section 2.26*). Results of initial analysis are shown in *Figure 6.23*. The pAb shows clear detection of the *R. commune* proteins, with a reduced dot intensity observable as the quantity of *R. commune* protein decreases (*Figure 6.23 (i)*). No cross-reactivity between the secondary antibody was observed with *R. commune* at any concentration in the control blot (*Figure 6.23 (ii)*), confirming that the generated signal was attributed to the pAb binding only.

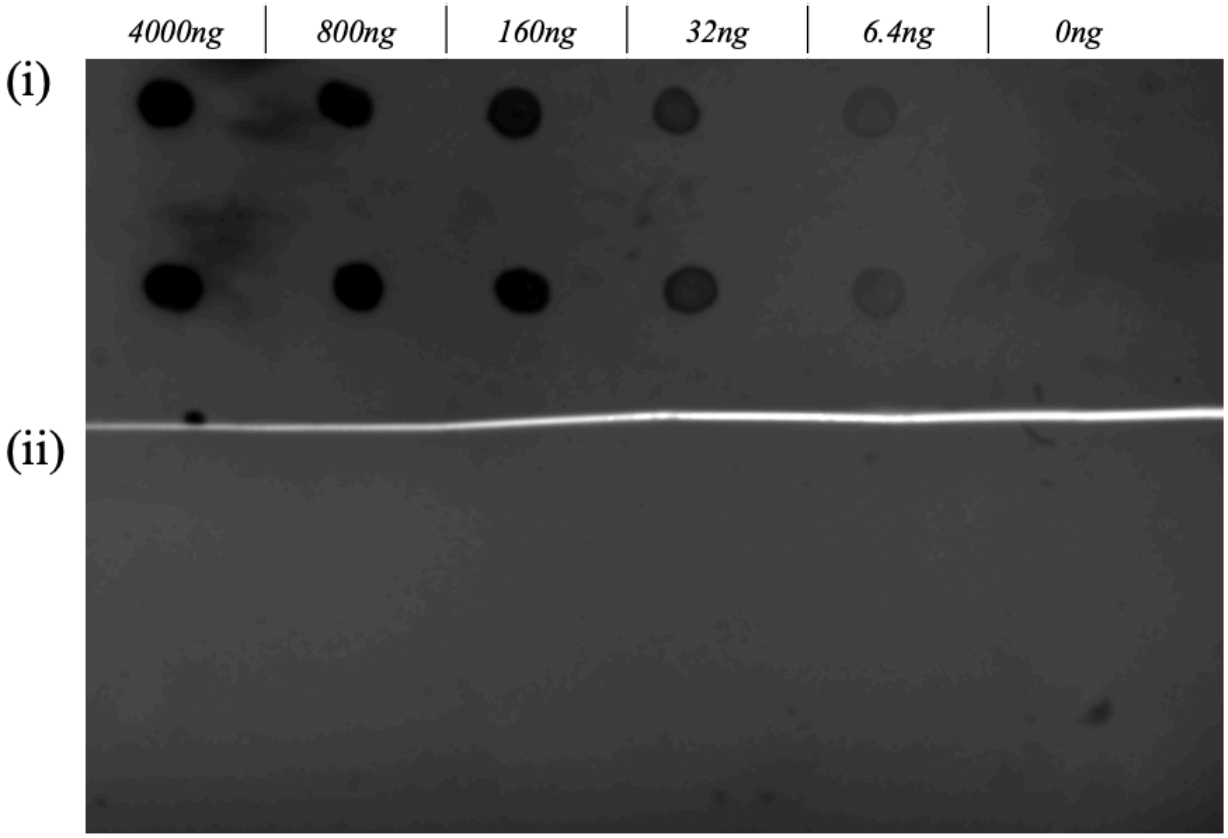

Figure 6.23 Dot blot analysis of pAb binding to R. commune proteins

R. commune proteins were dotted onto a membrane at a range of protein amounts in duplicate (4000ng-6.4ng, including a 0ng control). ***(i)*** *The pAb (1 in 4,000 dilution) was washed over the membrane and detected with an anti-chicken H+L HRP antibody.* ***(ii)*** *Control experiments were run concurrently, whereby the same concentrations of R. commune proteins were dotted to the membrane, however, no pAb was added. Anti-chicken H+L HRP was washed over the membrane thereafter.*

From the dot blot in *Figure 6.23*, it is apparent that the pAb could readily detect down to 6.4ng of protein, as evidenced by a clear colour change at this concentration spot. To elucidate an estimated LOD for this method, the concentration range was expanded to $4x10^6$pg – 25pg of *R. commune* protein. This is shown in *Figure 6.24*. On this occasion, the pAb failed to detect the lowest amount of 25pg *R. commune*, however detected all other amounts, with only a weak signal observed at 500pg (*Figure 6.24 (i)*). Again, no signal was observed in the control reactions (*Figure 6.24 (ii)*). This analysis revealed that the pAb could detect 500pg of *R. commune* protein blotted onto a membrane.

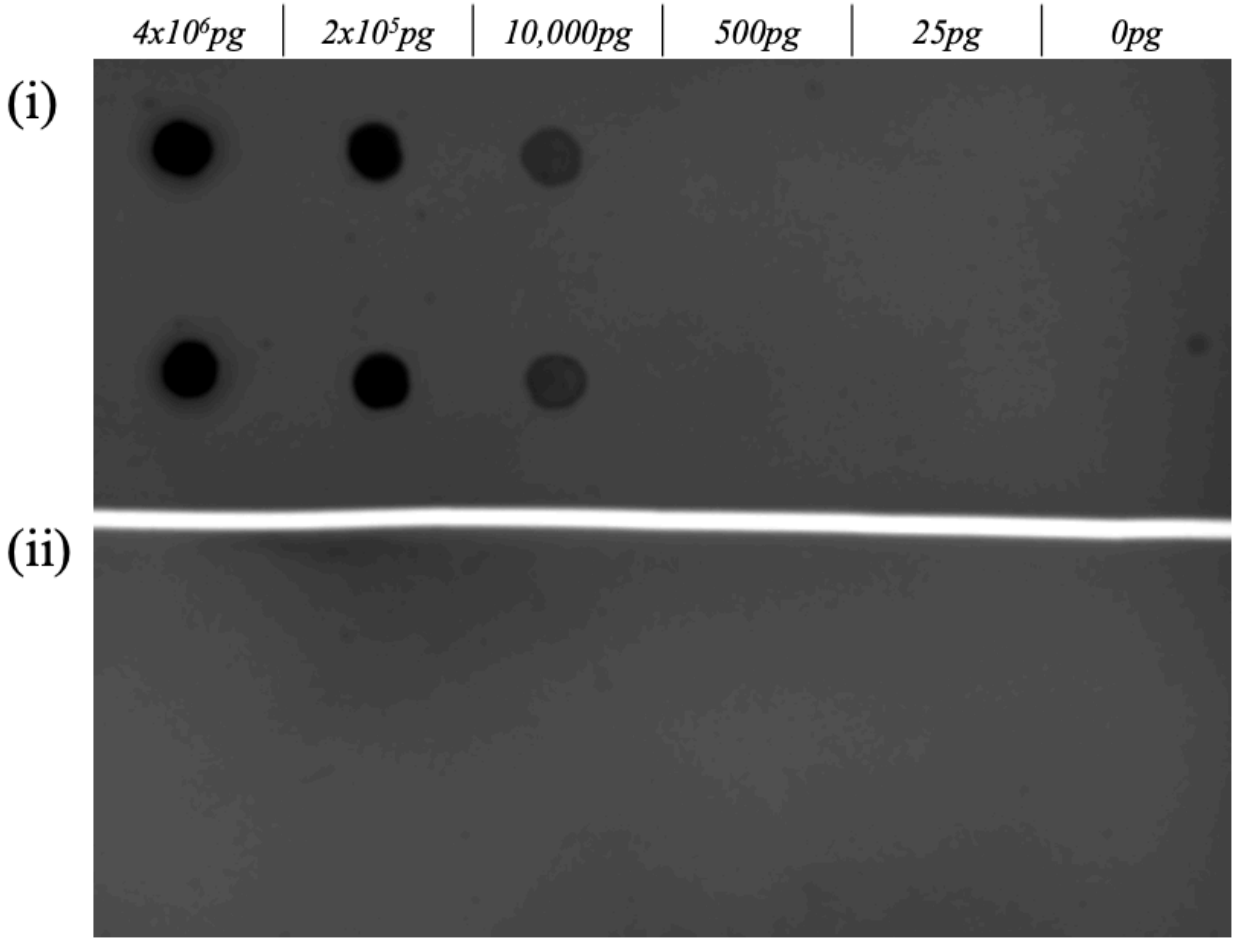

Figure 6.24 Dot blot analysis of pAb binding to R. commune at low concentrations

R. commune proteins at a range of 4x10⁶pg – 25pg were spotted onto a membrane in duplicate. ***(i)*** *The pAb was washed over the membrane at a 1 in 4,000 dilution and detected with an anti-chicken H+L HRP antibody.* ***(ii)*** *Control experiments were performed whereby the same concentrations of R. commune proteins were dotted to the membrane, however, no pAb was added. Anti-chicken H+L HRP was washed over the membrane thereafter.*

6.3 Discussion

This aim of this chapter was to contribute to the development of control methods for *R. commune* infection via the design of immunoassays against *R. commune* proteins. It was proposed to take an immunoassay-based approach as these methods are generally robust and can be incorporated into user-friendly endpoint assays, simplifying deployment into the various sectors in which testing may be required.

To facilitate this, an anti- *R. commune* scFv recombinant antibody library was constructed. As aforementioned, currently, no single protein is proposed as a suitable biomarker for *R.*

commune detection, therefore, the library was screened using a total protein extract. However, given that enrichment of the library against this antigen could have led to enrichment against only proteins that would be cross-reactive with broad-range fungal proteins, it was decided to incorporate a depletion step into the panning procedures, alongside the typically employed panning strategy. This depletion method was previously demonstrated to be effective at depleting cross-reactive antibodies from phage pools, leaving only a target-specific pool remaining (Bakhshinejad et al., 2016; Rahbarnia et al., 2016; Lebani et al., 2017). However, for the work herein, the depletion step failed to efficiently and simultaneously remove the response against the other fungal pathogens while enriching for *R. commune*-binding scFv. While the response of the polyclonal phage pools against *R. commune* was observed to increase, the signal generated in these wells was relatively low. In addition to this, the signal observed against the cross-reactive proteins in the phage pools which had been subjected to depletion were not observed to be much lower than that of the phage pools sourced from the non-depletive panning strategy, further suggesting that the depletion method was inefficient.

This may be partly attributed to the employed antigen preparation. The fungal pathogens *R. commune, F, graminearum, F. culmorum and R. collo cyngi* likely share homology across several proteins, rendering it challenging to deplete away cross-reactive scFv while still maintaining a good response against *R. commune*. However, it was also noted that the signal generated in the traditional panning approach did not encourage high levels of enrichment of phage against *R. commune* either. Therefore, the difficulties in isolating scFv through panning may be linked to issues regarding the complexity of the total protein extract being used. Such an extract has the possibility to encourage non-specific binding of the phage pools to the immunotube surface, resulting in the carry-through of scFv clones with no true binding to *R. commune*, or when performing depletion, could have resulted in the loss of *R. commune*-specific scFv clones which were weakly bound to the depletion tube. Elevated non-specific binding may additionally have prevented true binding as high levels of interaction at the coated antigen interface may occlude antigenic epitopes. This would be particularly detrimental at earlier panning rounds whereby only a limited number of target-specific scFv are present. Furthermore, when using a heterogenous mixture, the coating of the proteins to immunotubes or ELISA wells would be affected by factors such as the abundance of the protein and size of the protein, as such, some proteins may not be

accurately represented in the coating on the plate. ScFv with binding to these proteins could have been lost or overlooked as no, or a low signal would be generated.

Nonetheless, pre-panning analysis of the library revealed two scFv which demonstrated binding to *R. commune* in indirect ELISA, indicating that the library did contain scFv with *R. commune*-binding capabilities. However, no binding was observed in a competitive ELISA format. ScFv antibodies are monospecific, binding only a singular epitope, however, given that they were identified by screening against a total protein extract, it is unknown what protein or epitope they are reactive with in the extract. After confirmation of binding, both scFv were optimised with respect to expression level and subsequently purified. Upon analysis of the purification, it was revealed that the expression level and purification efficiency of one of the scFv, 5A, was low, as evidenced by minimal scFv protein and a failure to titre in ELISA. Given that the other clone, 11G, presented high signal and good expression, further analysis was performed with this scFv. The first point of the characterisation analysis was to examine the reactivity of 11G with other non-target fungal proteins as minimal cross-reactivity was required. However, upon titration of 11G against proteins associated with *R. commune, F, graminearum, F. culmorum and R. collo cyngi*, it appeared that the scFv bound to all protein extracts tested, which suggests binding of 11G to a shared antigen. Overall, this cross-reactivity limits the use of 11G with respect to the specific detection of *R. commune*. For future applications, this scFv would have to undergo considerable investigation into binding analysis, cross-reactivity, and characterisation, therefore, the pursuit of suitable and characterised *R. commune* biomarker candidates is suggested.

With respect to the future work required for the isolation of *R. commune*-specific recombinant antibodies, it is recommended that single, pure antigens (or a panel of pure antigens) should be identified and used for the intended screening. The complexity of the total protein extract did not provide adequate opportunity for enrichment against the *R. commune* proteins, even though a strong polyclonal response was observed, suggesting the presence of *R. commune*-specific antibodies in the repertoire. To confer added specificity to the assay, ideally several antigens would be identified which would provide enhanced certainty that the detection of *R. commune* was accurate and specific. Caution should be exerted with respect to the identification of *R. commune* biomarker, or biomarkers, as it is observed that some fungal infection-related proteins can be expressed at alternate life stages

of the fungus, while remain unexpressed, or only present at low levels, at late-stage growth (Zhang, Ovenden, and Milgate, 2020). As such, care must be taken to ensure that the chosen antigen is expressed at a relatively high level throughout the life cycle of the pathogen. In addition to confirming consistent antigen expression, it is also important that the selected antigen could provide good specificity for *R. commune*. Identification of such an antigen would entail proteomic analysis of *R. commune* at all life stages and comparative analysis of the selected proteins to ensure minimal cross-reactivity between *R. commune* and other fungal pathogens. In addition, genomic examination would likely be required to ensure that gene deletions are not commonplace for the chosen target, for example the gene deletion observed for the *NIP1* protein in certain *R. commune* isolates (Schürch et al., 2004). Furthermore, investigation into secreted molecules, the secretome, of *R. commune* would also be of benefit in the effort to elucidate suitable biomarkers as it is demonstrated that pathogenic fungi often secrete a suite of molecules (Girard et al., 2013; McCotter, Horianopoulos, and Kronstad, 2016). Such secreted molecules could prove suitable antigens for *R. commune* pathogen detection, therefore, comprehensive analysis of these targets could also be performed in the endeavour for *R. commune* antigen identification. Upon identification of a suitable candidate biomarker, the scFv library constructed in this work could be re-screened for antigen-binding clones which should permit detection of *R. commune* with enhanced specificity.

To further investigate the application of antibodies for the detection of *R. commune*, a pAb was isolated. This pAb showed strong reactivity with *R. commune* proteins in indirect ELISA while presenting much lower reactivity with other common fungal pathogens of barley. PAbs are naturally polyspecific, meaning that the antibodies bind to multiple epitopes on the antigen. In this scenario, the antigen is multiple proteins, therefore, the pAb is likely binding to a range of epitopes over many *R. commune*-associated proteins. The strong reactivity of the pAb with *R. commune* indicates that the immunogenic proteins of *R. commune* were distinct enough from other fungal pathogens to elicit a response biased toward *R. commune*. This was demonstrated by the comparatively elevated signal observed against *R. commune* upon titration of the pAb against similar protein extracts from non-target fungal species. The specificity of this pAb could be enhanced by methods such immunoaffinity chromatography, whereby the pAb would be purified against an *R. commune*-specific protein, or proteins, however, as discussed, this would require further analysis into the *R. commune* proteome and in-depth comparison against other fungal pathogens which infect barley.

In addition to analysis in ELISA, dot blot analysis was employed for the characterisation of the pAb, whereby *R. commune* antigens were immobilised on the surface of a membrane and detected by the pAb. Dot blots are cost effective and offer advantages such as the requirement for a small sample volume, the ability to detect antigens directly from the sample and the fact that blotted membranes can be stored for a number of days before testing, facilitating the testing of numerous membranes simultaneously. In some circumstances, sample preparation may be unnecessary as simple pressing of the suspect tissue onto the membrane can be sufficient to facilitate antigen immobilisation (Garzo et al., 2011; Komor, 2011; Boukari et al., 2020). A sample dot blot workflow for the detection of *R. commune* antigens from infected foliage is shown in *Figure 6.25*. While dot blots generally have a longer run-time than some other paper-based immunoassays such as lateral flow, they can be made more rapid by use of strategies such as direct labelling of the detection antibody, or by optimisation of steps such as incubation times. Optimisation of these parameters has the potential to reduce the assay time to result to as little as two-three hours. This, in conjunction with the fact that multiple samples can be assessed on the same blot, makes the assay a convenient, cost-effective and relatively quick method. Additionally, dot blots can be made semi-quantitative by employing software which can determine each dot intensity, thereby allowing comparison of an unknown sample to a sample standard and permitting quantitation.

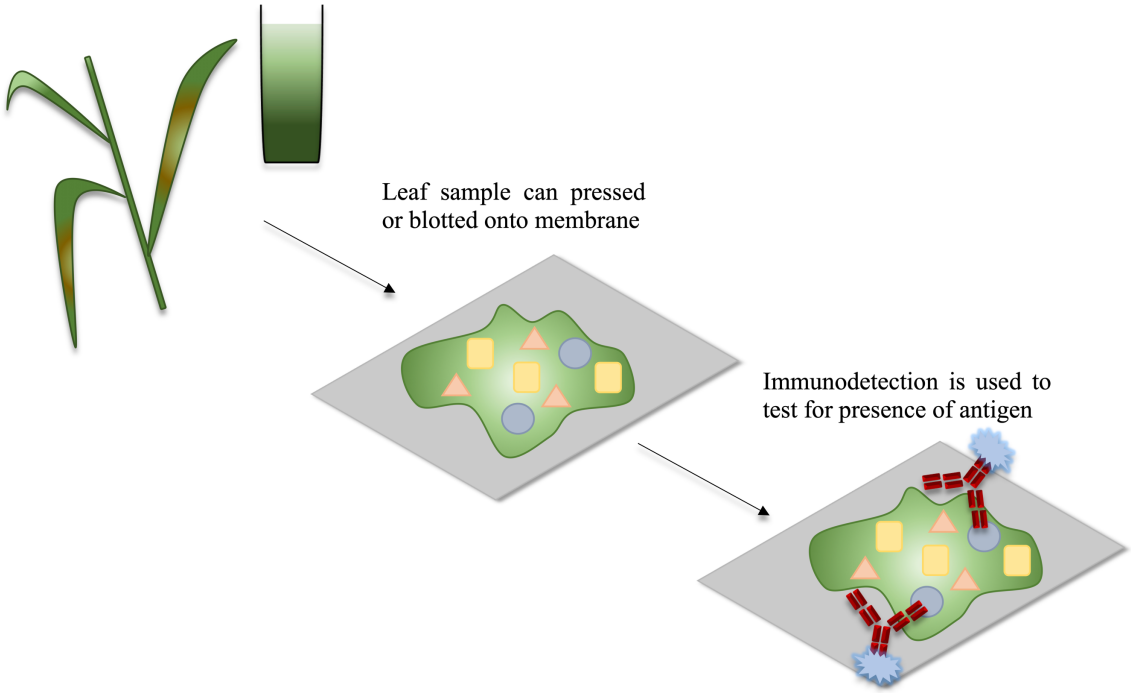

Figure 6.25 Schematic of dot blot-based detection of R. commune proteins

Foliar samples can be harvested and ground in a suitable buffer, or pressed directly onto the support membrane, facilitating antigen immobilisation. Thereafter, the blotted sample can be probed with target-specific antibodies which produce signal, the intensity of which is related to the amount of antigen of interest present on the blot.

In conclusion, this chapter describes the isolation of scFvs and pAbs with reactivity to *R. commune* proteins. In this work, two scFv were identified, however, the 5A scFv was found to have poor expression making it unsuitable for future assay development without further investigation into its expression characteristics. The 11G scFv was found to express well and was confirmed to titre against *R. commune*. However, this scFv was also found to have reactivity with protein extracts from non-target fungi. For any future work with this scFv, rigorous analysis into its antigen-binding properties would be required. With respect to future approaches for the development of recombinant anti- *R. commune* antibodies, identification of suitable antigens and screening using these targets is recommended. In addition to recombinant antibodies, a pAb was also isolated. The pAb demonstrated a good reactivity with *R. commune*-proteins and showed a higher response against *R. commune* when compared to signal generated in indirect ELISA against proteins from other fungal co-infectors of barley, demonstrating favourable capacity for *R. commune* detection. The pAb was also applied successfully in dot blot, presenting a convenient assay by which *R. commune* proteins could be identified.

Chapter 7

Overall Conclusions

7.1 Overall Conclusions and Outcomes

The aim of this work was to develop diagnostic methods by which the important crop pathogens PVY and *R. commune* could be detected in a sensitive and timely manner. Infection of potatoes or barley with PVY or *R. commune*, respectively, yields poor crop quality, reduced marketability and can result in major harvest losses. As these pathogens can proliferate in-field while undetected, particularly at early stages of infection, the development of sensitive methods to permit routine testing for these diseases would greatly benefit crop-growers. Additionally, the introduction of environmentally-friendly control measures, in lieu of chemical control, is encouraged and will continue to be of great value for the future as the employment of chemical control means becomes increasingly restricted. To allow sensitive and early detection, it was proposed within this work to develop immunoassays and hybrid molecular-immunoassay methods for the specific detection of PVY and *R. commune*.

Chapter 3 described the generation and screening of a recombinant scFv library for PVY-binding antibodies. To generate a suitable antigen with which to screen the library, a recombinant form of the PVY CP was constructed. The expression of this construct was optimised prior to subsequent purification and incorporation into a screening campaign using a combination of monoclonal ELISA, phage-display and biopanning techniques. This screening yielded one primary scFv of interest, 12D. The clone initially demonstrated a high titre point and good competition for the CP, however, throughout the characterisation process it became apparent that further optimisations of the immunoassay conditions were required due to the occurrence of potential non-specific binding events. To address this non-specific binding, it is proposed to perform future assay optimisation and to subject the 12D clone to site-directed mutagenesis methods. Of great interest would be the directed mutagenesis of the CDR-H3 as this region is strongly implicated in antigen-specificity determination. Furthermore, clone 12D was found to have charged residues in this region, which are suggested to play a role in non-specific assay signal. Therefore, engineering of this clone, and subsequent characterisation of the resulting 12D mutant derivatives, may yield scFv candidates with improved sensitivity and specificity over the wild-type.

In a continued effort to provide panels of recombinant anti-PVY antibodies, *chapter 4* describes the engineering of ‘full-length’ anti-CP IgG antibodies into recombinant forms, namely scFv and scAb derivates. Analysis of these restructured clones through a series of

indirect and competitive ELISAs, in conjunction with SDS-PAGE and WB, revealed that recombinant antibodies derived from the parental 11B2 mAb proved the most favourable for future assay development. It was noted that the expression level of the 11B2 recombinant antibodies was poor, with the majority of the antibody protein located in the insoluble fraction. Optimisation of these expression conditions led to a shift toward the soluble fraction, highlighting the need to investigate these parameters when developing recombinant antibodies. Characterisation of the 11B2 mAb, scAb and scFv was performed in immunoblot, ELISA and SPR formats. Immunoblot analysis against the CP revealed that the clones demonstrated good specificity for the PVY antigen and could detect CP in both recombinant and natural forms. Additionally, successful detection of CP from crude plant extracts was performed in WB, highlighting the specificity of the antibodies, even when challenged with a crude matrix. Subsequent analysis involved the elucidation of kinetic constants for the 11B2 mAb and scAb forms. From this, equilibrium dissociation constants of 1.09×10^{-8} and 2.44×10^{-7} were found for the mAb and scAb, respectively. This result suggested that while both antibodies presented binding in the nanomolar range, with the mAb displaying a higher affinity for the CP than its engineered scAb form. Continued characterisation of these antibodies led to the development of competitive calibration curves in ELISA for each form. This work yielded three competitive ELISAs with estimated LODs of 651.7ng/mL, 303.6ng/mL and 162.7ng/mL for the mAb, scAb and scFv assays, respectively. Furthermore, it was shown in additional competitive ELISA analyses that the clones could distinguish between healthy and infected leaf material when using natural crude leaf extracts, demonstrating their applicability to future field-testing. In addition to providing ELISA-based detection assays, the work in this chapter endeavoured to offer simpler detection methods in the form of dot blots. In these assays, both the mAb and scAb could detect CP spotted onto a membrane support at LODs of ~440pg and ~31.25ng, respectively. Furthermore, it was shown that the mAb could also detect CP from crude plant extracts used in dot blots, providing a means through which PVY antigens may be readily detected in a paper-based assay. Finally, as the ultimate fate of these developed antibodies is intended to be incorporation into an on-site sensing system, which would permit point-of-use PVY detection, a ‘proof-of-concept’ biosensor assay was developed using the 11B2 mAb in conjunction with SPR sensing technology. This assay provided good confidence that the antibody could work efficiently in a ‘label-free’ and ‘real-time’ biosensor system, with the final LOD of the assay calculated as 148.7ng/mL. The antibodies developed and characterised provide promising candidates for incorporation into future PVY-sensing

assays, alongside furnishing suitable options for immediate incorporation into ELISA, immunoblot and SPR diagnostic techniques.

While *chapter 3* and *chapter 4* focused on the development of novel anti-PVY antibodies, primarily in recombinant forms, *chapter 5* described the application of molecular methods in conjunction with lateral flow immunoassay in an effort to facilitate early-stage PVY detection. The described assay relied on the use of an isothermal amplification technique, RPA, which permits amplification at a low singular temperature. Primers and probes specific for the PVY CP were designed in such a way that successful amplification of their target region would produce amplicons with dual antigenic labels. These labelled amplicons could then be detected in lateral flow which facilitates rapid, visual and easy-to-interpret results analysis from the amplification. The application of NALFIA to the identification of PVY dsDNA permitted detection at a LOD of 100 copies per reaction. The designed RPA was also shown to have wide-reaching detection capabilities and good inclusivity for the various PVY strains, both experimentally and computationally. *In-vitro* analysis revealed that the developed assay could successfully detect PVY nucleic acids from the strains PVY^{NTN}, PVY^{O}, $PVY^{N\text{-}Wi}$, $PVY^{Na\text{-}N}$ and $PVY^{Eu\text{-}N}$, while further *in-silico* analysis of the primers and probes against hundreds of PVY genotypes demonstrated that the oligos maintained good homology to the sequences of the vast majority. Overall, this suggests that broad-spectrum detection is feasible and that the designed assay could be used universally. In addition to maintaining good inclusivity for PVY, it was also found that the assay had exclusivity for PVY, with no amplification of non-target templates from other plant viruses, or from healthy plants, observed. In an enhancement to applicability of the assay for point-of-use testing, the RPA assay was further developed into a one-step RT-RPA assay. This permitted the amplification of PVY ssRNA directly, with no need for prior reverse transcription. The LOD of the RT-RPA method was determined as 100pg RNA per reaction. Based on these findings, the generated one-step RT-RPA, in conjunction with NALFIA, has the potential to be applied directly in-field to allow early-stage and rapid detection of PVY, with the ability to analyse results in an easy-to-use lateral flow format.

In addition to developing methods for the identification of PVY, this work also endeavoured to provide early detection methods for *R. commune* in the form of antibody-based diagnostics. This was achieved through the construction of an scFv recombinant antibody library and subsequent screening of this library using a total protein extract derived from the

R. commune pathogen. Screening of this library led to the isolation of two candidate scFv, 5A and 11G. Of the two, 11G demonstrated good expression and a high titre against *R. commune* antigens. Upon purification and further characterisation of the scFv, cross-reactivity analysis of 11G with total protein extracts sourced from other common fungal pathogens of barley was performed. It was found that the scFv was reactive with all pathogens tested, suggesting that 11G bound a relatively conserved antigen across the fungal species, rendering it non-specific for *R. commune* alone. In addition to the recombinant antibodies, an anti-*R. commune* pAb was also isolated. This pAb showed improved specificity for the *R. commune* antigen and apparently limited cross-reactivity with the non-target pathogens tested. This pAb was subsequently incorporated in ELISA and dot blot-based characterisation formats where it showed good sensitivity for *R. commune* antigens. The dot blot provided a paper-based method through which *R. commune* proteins could be identified through immunoassay.

In conclusion, this work led to the production and characterisation of multiple anti-PVY antibodies, and the subsequent incorporation of these antibodies into immunoassays for sensitive PVY antigen detection. This body of research also provided a further diagnostic method in the form of a rapid one-step RT-RPA which could detect PVY nucleic acids in a lateral flow immunoassay system. Additionally, anti-*R. commune* pAbs and immunoblot assays were designed for the detection of *R. commune*-associated antigens. The work in this thesis contributed to a multi-institutional project involving collaboration with Teagasc (Oak Park) and the Tyndall National Institute (UCC). It is hoped that the techniques and reagents generated in this work may be further exploited in future molecular and sensor-based approaches designed by these collaborators. It is envisaged that the described antibodies would be incorporated into a portable biosensing platform destined for use on-site to aid in pathogen detection, while the RT-RPA assay could be deployed simultaneously for increased diagnostic confidence. Overall, these methods could be employed in tandem with the currently implemented control measures for PVY and *R. commune* to offer enhanced diagnostic and control capabilities.

Chapter 8

Bibliography

Abd El Wahed, A., El-Deeb, A., El-Tholoth, M., Abd El Kader, H., Ahmed, A., Hassan, S., Hoffmann, B., Haas, B., Shalaby, M. A., Hufert, F. T. and Weidmann, M. (2013). A portable reverse transcription recombinase polymerase amplification assay for rapid detection of foot-and-mouth disease virus. *PLoS One*, 8 (8), e71642.

Abd El Wahed, A., Patel, P., Faye, O., Thaloengsok, S., Heidenreich, D., Matangkasombut, P., Manopwisedjaroen, K., Sakuntabhai, A., Sall, A. A., Hufert, F. T. and Weidmann, M. (2015). Recombinase polymerase amplification assay for rapid diagnostics of Dengue infection. *PLoS One*, 10 (6), e0129682.

Agindotan, B. O., Shiel, P. J. and Berger, P. H. (2007). Simultaneous detection of potato viruses, PLRV, PVA, PVX and PVY from dormant potato tubers by TaqMan® real-time RT-PCR. *J. Virol. Methods*, 142 (1–2), 1–9.

Al-Shehadah, E., Al-Daoude, A. and Jawhar, M. (2018). Survival and germinability of *Rhynchosporium secalis* conidia exposed to solar radiation. *Hell. Plant Prot. J*., 11 (2), 47–53.

An, L., Tang, W., Ranalli, T. A., Kim, H. J., Wytiaz, J. and Kong, H. (2005). Characterization of a thermostable UvrD helicase and its participation in helicase-dependent amplification. *J. Biol. Chem*., 280 (32), 28952–28958.

Andris-Widhopf, J., Rader, C., Steinberger, P., Fuller, R. and Barbas 3rd, C. F. (2000). Methods for the generation of chicken monoclonal antibody fragments by phage display. *J. Immunol. Methods*, 242 (1–2), 159–181.

Anjum, R., Khan, M. A., Olawale, K. O. and Baber, R. (2017). Field evaluation and enzyme-linked immunosorbent assay detection of potato leaf roll virus, potato virus X and potato virus Y in potato germplasm. *J. Agric. Sci.*, 9 (7), 229-235.

Arbatova, J., Lehto, K., Pehu, E. and Pehu, T. (1998). Localization of the P1 protein of potato Y potyvirus in association with cytoplasmic inclusion bodies and in the cytoplasm of infected cells. *J. Gen. Virol*., 79 (10), 2319–2323.

Arora, S., Saxena, V. and Ayyar, B. V. (2017). Affinity chromatography: A versatile technique for antibody purification. *Methods*, 116, 84–94.

Arzanlou, M., Karimi, K. and Mirabi, F. (2016). Some evidence for skewed mating type distribution in Iranian populations of *Rhynchosporium commune*, the cause of barley scald disease. *J. Plant Prot. Res*., 56 (3), 237–243.

Avrova, A. and Knogge, W. (2012). *Rhynchosporium commune*: A persistent threat to barley cultivation. *Mol. Plant Pathol*., 13 (9), 986–997.

Ayyar, B. V., Hearty, S. and O'Kennedy, R. (2015). Facile domain rearrangement abrogates expression recalcitrance in a rabbit scFv. *Appl. Microbiol. Biotechnol*., 99 (6), 2693–2703.

Babujee, L., Witherell, R. A., Mikami, K., Aiuchi, D., Charkowski, A. O. and Rakotondrafara, A. M. (2019). Optimization of an isothermal recombinase polymerase amplification method for real-time detection of potato virus Y O and N types in potato. *J. Virol. Methods*., 267, 16–21.

Badescu, G. O., Marsh, A., Smith, T. R., Thompson, A. J. and Napier, R. M. (2016). Kinetic characterisation of a single chain antibody against the hormone abscisic acid: Comparison with its parental monoclonal. *PLoS One*, 11 (3), e0152148.

Bak, A., Cheung, A. L., Yang, C., Whitham, S. A. and Casteel, C. L. (2017). A viral protease relocalizes in the presence of the vector to promote vector performance. *Nat. Commun*., 8, 14493.

Bakhshinejad, B., Zade, H. M., Shekarabi, H. S. Z. and Neman, S. (2016). Phage display biopanning and isolation of target-unrelated peptides: In search of nonspecific binders hidden in a combinatorial library. *Amino Acids*, 48, 2699–2716.

Balodi, R., Bisht, S., Ghatak, A. and Rao, K. H. (2017). Plant disease diagnosis: Technological advancements and challenges. *Indian Phytopathol*., 70 (3), 275–281.

Banér, J., Nilsson, M., Isaksson, A., Mendel-Hartvig, M., Antson, D. O. and Landegren, U. (2001). More keys to padlock probes: Mechanisms for high-throughput nucleic acid analysis. *Curr. Opin. Biotechnol*., 12 (1), 11–15.

Baran, D., Pszolla, M. G., Lapidoth, G. D., Norn, C., Dym, O., Unger, T., Albeck, S., Tyka, M. D. and Fleishman, S. J. (2017). Principles for computational design of binding antibodies. *Proc. Natl. Acad. Sci. U. S. A*., 114 (41), 10900–10905.

Barbas, C., Burton, D., Scott, J. and Silverman, G. (2001). Phage display: A laboratory manual. New York: Cold Spring Laboratory Press.

Barderas, R., Shochat, S., Martínez-Torrecuadrada, J., Altschuh, D., Meloen, R. and Ignacio Casal, J. (2006). A fast mutagenesis procedure to recover soluble and functional scFvs containing amber stop codons from synthetic and semisynthetic antibody libraries. *J. Immunol. Methods*, 312 (1–2), 182–189.

Basu, K., Green, E. M., Cheng, Y. and Craik, C. S. (2019). Why recombinant antibodies — benefits and applications. *Curr. Opin. Biotechnol*., 60, 153–158.

Batista, F. D. and Harwood, N. E. (2009). The who, how and where of antigen presentation to B-cells. *Nat. Rev. Immunol*., 9, 15–27.

Batra, V., Beard, W., Shock, D., Krahn, J., Pederson, L. and Wilson, S. (2006). Magnesium-induced assembly of a complete DNA polymerase catalytic complex. *Structure*, 14 (4), 757–766.

Bebber, D. P. and Gurr, S. J. (2015). Crop-destroying fungal and oomycete pathogens challenge food security. *Fungal Genet. Biol*., 74, 62–64.

Benedict, C. A., McMoran, D. W., Inglis, D. A. and Karasev, A. V. (2015). Tuber symptoms associated with recombinant strains of potato virus Y in specialty potatoes under Western Washington growing conditions. *Am. J. Potato Res*., 92, 593–602.

Birtalan, S., Zhang, Y., Fellouse, F. A., Shao, L., Schaefer, G. and Sidhu, S. S. (2008). The intrinsic contributions of tyrosine, serine, glycine and arginine to the affinity and specificity of antibodies. *J. Mol. Biol*., 377 (5), 1518–1528.

Borrebaeck, C. A. K. (2000). Antibodies in diagnostics - From immunoassays to protein chips. *Immunol. Today*, 21 (8), 379–382.

Boukari, W., Wei, C., Tang, L., Hincapie, M., Naranjo, M., Nuessly, G., Beuzelin, J., Sood, S. and Rott, P. (2020). Lack of transmission of sugarcane yellow leaf virus in Florida from Columbus grass and sugarcane to sugarcane with aphids or mites. *PLoS One*, 15 (3), e0230066.

Boyd, L. A., Ridout, C., O'Sullivan, D. M., Leach, J. E. and Leung, H. (2013). Plant-pathogen interactions: Disease resistance in modern agriculture. *Trends Genet*., 29 (4), 233–240.

Boyle, D. S., Lehman, D. A., Lillis, L., Peters, D., Singhal, M., Armes, N., Park, M., Piepenburg, O. and Overbaugh, J. (2013). Rapid detection of HIV-1 proviral DNA for early infant diagnosis using recombinase polymerase amplification. *mBio*, 4 (2), e00135-13.

Bratsch, S. A., Olszewski, N. and Lockhart, B. (2021). Incidence of *cymbidium* mosaic, *odontoglossum* ringspot, and orchid fleck virus in orchids in Minnesota and production of antibodies for use in ELISA to detect orchid fleck virus. *Eur. J. Plant Pathol*., 159, 543–554.

Brault, V., Uzest, M., Monsion, B., Jacquot, E. and Blanc, S. (2010). Aphids as transport devices for plant viruses. *Comptes Rendus Biol*., 333 (6–7), 524–538.

Bustin, S. A. (2000). Absolute quantification of mRNA using real-time reverse transcription polymerase chain reaction assays. *J. Mol. Endocrinol*., 25 (2), 169–193.

Cerda, R., Avelino, J., Gary, C., Tixier, P., Lechevallier, E. and Allinne, C. (2017). Primary and secondary yield losses caused by pests and diseases: Assessment and modelling in coffee. *PLoS One*, 12 (1), e0169133.

Chikh-Ali, M., Vander Pol, D., Nikolaeva, O. V., Melzer, M. J. and Karasev, A. V. (2016). Biological and molecular characterization of a tomato isolate of potato virus Y (PVY) of the PVY-C lineage. *Arch. Virol*., 161 (12), 3561–3566.

Chung, B. Y. W., Miller, W. A., Atkins, J. F. and Firth, A. E. (2008). An overlapping essential gene in the *Potyviridae*. *Proc. Natl. Acad. Sci. U. S. A*., 105 (15), 5897–5902.

Clasen, B. M., Stoddard, T. J., Luo, S., Demorest, Z. L., Li, J., Cedrone, F., Tibebu, R., Davison, S., Ray, E. E., Daulhac, A., Coffman, A., Yabandith, A., Retterath, A., Haun, W., Baltes, N. J., Mathis, L., Voytas, D. F. and Zhang, F. (2016). Improving cold storage and processing traits in potato through targeted gene knockout. *Plant Biotechnol. J*., 14 (1), 169–176.

Compton, J. (1991). Nucleic acid sequence-based amplification. *Nature (Lond.)*, 350 (6313), 91–92.

Crannell, Z. A., Rohrman, B. and Richards-Kortum, R. (2014). Equipment-free incubation of recombinase polymerase amplification reactions using body heat. *PLoS One*, 9 (11), 1–7.

Crosslin, J. M. (2013). PVY: An old enemy and a continuing challenge. *Am. J. Potato Res*., 90, 2–6.

Crowther, J. R. (1995). "ELISA: Theory and practice." in Methods in Molecular Biology., ed. J. R. Crowther (Totowa, NJ: Humana Press).

Cui, H. and Wang, A. (2016). Plum pox virus 6K1 protein is required for viral replication and targets the viral replication complex at the early stage of infection. *J. Virol*., 90 (10), 5119–5131.

Daher, R. K., Stewart, G., Boissinot, M. and Bergeron, M. G. (2016). Recombinase polymerase amplification for diagnostic applications. *Clin. Chem*., 62 (7), 947–958.

Daher, R. K., Stewart, G., Boissinot, M., Boudreau, D. K. and Bergeron, M. G. (2015). Influence of sequence mismatches on the specificity of recombinase polymerase amplification technology. *Mol. Cell. Probes*, 29 (2), 116–121.

Davie, K., Holmes, R., Pickup, J. and Lacomme, C. (2017). Dynamics of PVY strains in field grown potato: Impact of strain competition and ability to overcome host resistance mechanisms. *Virus Res*., 241, 95–104.

Dean, F. B., Nelson, J. R., Giesler, T. L. and Lasken, R. S. (2001). Rapid amplification of plasmid and phage DNA using Phi29 DNA polymerase and multiply-primed rolling circle amplification. *Genome Res*., 11 (6), 1095–1099.

Della Bartola, M., Byrne, S. and Mullins, E. (2020). Characterization of potato virus Y isolates and assessment of nanopore sequencing to detect and genotype potato viruses. *Viruses*, 12 (4), 478.

Demain, A. L. and Vaishnav, P. (2009). Production of recombinant proteins by microbes and higher organisms. *Biotechnol. Adv.*, 27 (3) 297-306.

Dias da Silva, W. and Tambourgi, D. V. (2010). IgY: A promising antibody for use in immunodiagnostic and in immunotherapy. *Vet. Immunol. Immunopathol*., 135 (3), 173–180.

Ecker, C., Ertl, A., Pulverer, W., Nemes, A., Szekely, P., Petrasch, A., Linsberger-Martin, G. and Cichna-Markl, M. (2013). Validation and comparison of a sandwich ELISA, two competitive ELISAs and a real-time PCR method for the detection of lupine in food. *Food Chem*., 141 (1), 407–418.

Elmore, J. and Coaker, G. (2011). The role of the plasma membrane H+-ATPase in plant–microbe interactions. *Mol. Plant*, 4 (3), 416–427.

EMA (2011). Guideline on bioanalytical method validation. (https://www.ema.europa.eu/en/documents/scientific-guideline/guideline-bioanalytical-method-validation_en.pdf).

Estrela, P. F. N., Mendes, G. de M., de Oliveira, K. G., Bailão, A. M., Soares, C. M. de A., Assunção, N. A. and Duarte, G. R. M. (2019). Ten-minute direct detection of Zika virus in serum samples by RT-LAMP. *J. Virol. Methods*, 271, 113675.

Euler, M., Wang, Y., Heidenreich, D., Patel, P., Strohmeier, O., Hakenberg, S., Niedrig, M., Hufert, F. T. and Weidmann, M. (2013). Development of a panel of recombinase polymerase amplification assays for detection of biothreat agents. *J. Clin. Microbiol*., 51 (4), 1110–1117.

Euler, M., Wang, Y., Nentwich, O., Piepenburg, O., Hufert, F. T. and Weidmann, M. (2012). Recombinase polymerase amplification assay for rapid detection of Rift Valley fever virus. *J. Clin. Virol*., 54 (4), 308–312.

European Commission Statistical Office-Eurostat (2021). Agricultural production - crops. Eurostat. (https://ec.europa.eu/eurostat/web/main/home)

Findlay, J. W. A., Smith, W. C., Lee, J. W., Nordblom, G. D., Das, I., Desilva, B. S., Khan, M. N. and Bowsher, R. R. (2000). Validation of immunoassays for bioanalysis: A pharmaceutical industry perspective. *J. Pharm. Biomed. Anal*., 21 (6), 1249–1273.

Fitzgerald, J., Leonard, P., Darcy, E., Danaher, M. and O'Kennedy, R. (2011). Light-chain shuffling from an antigen-biased phage pool allows 185-fold improvement of an anti-halofuginone single-chain variable fragment. *Anal. Biochem*., 410 (1), 27–33.

Folwarczna, J., Plchova, H., Moravec, T., Hoffmeisterova, H., Dedic, P. and Cerovska, N. (2008). Production of polyclonal antibodies to a recombinant coat protein of potato virus Y. *Folia Microbiol*., 53 (5), 438–442.

Foroughi-Wehr, B., Zuchner, S. and Rabenstein, F. (1996). Enzyme-linked immunosorbent assay for detection *Rhynchosporium secalis* (Oud) J J. Davis in winter barley. *J. Plant Dis. Prot*., 103 (3), 267–271.

Fountaine, J. M., Shaw, M. W., Napier, B., Ward, E. and Fraaije, B. A. (2007). Application of real-time and multiplex polymerase chain reaction assays to study leaf blotch epidemics in barley. *Phytopathology*, 97 (3), 297–303.

Fox, A., Collins, L. E., Macarthur, R., Blackburn, L. F. and Northing, P. (2017). New aphid vectors and efficiency of transmission of potato virus A and strains of potato virus Y in the UK. *Plant Pathol*., 66 (2), 325–335.

Francis, D. M. and Page, R. (2010). Strategies to optimize protein expression in *E. coli*. *Curr. Protoc. Protein Sci*., 5 (1), 21–29.

Francois, P., Tangomo, M., Hibbs, J., Bonetti, E. J., Boehme, C. C., Notomi, T., Perkins, M. D. and Schrenzel, J. (2011). Robustness of a loop-mediated isothermal amplification reaction for diagnostic applications. *FEMS Immunol. Med. Microbiol*., 62 (1), 41–48.

Frenzel, A., Hust, M. and Schirrmann, T. (2013). Expression of recombinant antibodies. *Front. Immunol*., 4, 217.

Fuentes, S., Jones, R. A. C., Matsuoka, H., Ohshima, K., Kreuze, J. and Gibbs, A. J. (2019). Potato virus Y; the Andean connection. *Virus Evol*., 5 (2), vez037.

Fujii, I. (2004). "Antibody affinity maturation by random mutagenesis," in Antibody Engineering. Methods in Molecular Biology, ed. B. K. C. Lo (Totowa: Human Press), 345–359.

Fux, R., Söckler, C., Link, E. K., Renken, C., Krejci, R., Sutter, G., Ritzmann, M. and Eddicks, M. (2018). Full genome characterization of porcine circovirus type 3 isolates reveals the existence of two distinct groups of virus strains. *Virol. J*., 15, 25.

Galimberti, A., Alyokhin, A., Qu, H. and Rose, J. (2020). Simulation modelling of potato virus Y spread in relation to initial inoculum and vector activity. *J. Integr. Agric*., 19 (2), 376–388.

Garzo, E., Bonani, J. P., Fereres, A. and Moriones, E. (2011). Whitefly resistance traits derived from the wild tomato. *Virology*, 101 (10), 1191–1201.

Geißinger, C., Hofer, K., Habler, K., Heß, M., Huckelhoven, R., Rychlik, M., Becker, T. and Gastl, M. (2017). Fusarium species on barley malt: Is visual assessment an appropriate tool for detection? *Cereal Chem*., 94 (4), 659–669.

Gibbs, A. J., Ohshima, K., Yasaka, R., Mohammadi, M., Gibbs, M. J. and Jones, R. A. C. (2017). The phylogenetics of the global population of potato virus Y and its necrogenic recombinants. *Virus Evol*., 3 (1), vex002.

Gilgunn, S., Martín, S. M., Wormald, M. R., Zapatero-Rodríguez, J., Conroy, P. J., O'Kennedy, R. J., Rudd, P. M. and Saldova, R. (2016). Comprehensive N-glycan profiling of avian immunoglobulin Y. *PLoS One*, 11 (7), e0159859.

Girard, V., Dieryckx, C., Job, C. and Job, D. (2013). Secretomes: The fungal strike force. *Proteomics, 13* (3–4), 597–608.

Glais, L., Bellstedt, D. U. and Lacomme, C. (2017). "Diversity, characterisation and classification of PVY," in Potato Virus Y: Biodiversity, Pathogenicity, Epidemiology and Management eds. C. Lacomme, L. Glais, D. Bellstedt, B. Dupuis, A. Karasev, E. Jacquot, (Cham: Springer International Publishing), 43–76.

Glais, L. and Jacquot, E. (2015). "Detection and Characterization of Viral Species/Subspecies Using Isothermal Recombinase Polymerase Amplification (RPA) Assays," in Plant Pathology. Methods in Molecular Biology, vol. 1302, ed. C. Lacomme, (New York, Humana Press), 207–225.

Green, K. J., Brown, C. J., Gray, S. M. and Karasev, A. V. (2017). Phylogenetic study of recombinant strains of potato virus Y. *Virology*, 507, 40–52.

Green, K. J., Brown, C. J. and Karasev, A. V. (2018). Genetic diversity of potato virus Y (PVY): Sequence analyses reveal ten novel PVY recombinant structures. *Arch. Virol*., 163, 23–32.

Gururani, M. A., Venkatesh, J., Upadhyaya, C. P., Nookaraju, A., Pandey, S. K. and Park, S. W. (2012). Plant disease resistance genes: Current status and future directions. *Physiol. Mol. Plant Pathol*., 78, 51–65.

Gutiérrez-González, M., Farías, C., Tello, S., Pérez-Etcheverry, D., Romero, A., Zúñiga, R., Ribeiro, C. H., Lorenzo-Ferreiro, C. and Molina, M. C. (2019). Optimization of culture conditions for the expression of three different insoluble proteins in *Escherichia coli*. *Sci. Rep*., 9, 1–11.

Hamidi, S. V., Ghourchian, H. and Tavoosidana, G. (2015). Real-time detection of H5N1 influenza virus through hyperbranched rolling circle amplification. *Analyst*, 140 (5), 1502–1509.

Hammers, C. M. and Stanley, J. R. (2014). Antibody phage display: Technique and applications. *J. Invest. Dermatol*., 134 (2), e17.

Handford, C. E., Elliott, C. T. and Campbell, K. (2015). A review of the global pesticide legislation and the scale of challenge in reaching the global harmonization of food safety standards. *Integr. Environ. Assess. Manag*., 11 (4), 525–536.

Hasiów-Jaroszewska, B., Stachecka, J., Minicka, J., Sowiński, M. and Borodynko, N. (2015). Variability of potato virus Y in tomato crops in Poland and development of a reverse-transcription loop-mediated isothermal amplification method for virus detection. *Phytopathology*, 105 (9), 1270–1276.

Havis, N. D., Brown, J. K. M., Clemente, G., Frei, P., Jedryczka, M., Kaczmarek, J., Kaczmarek, M., Matusinsky, P., McGrann, G. R. D., Pereyra, S., Piotrowska, M., Sghyer, H., Tellier, A. and Hess, M. (2015). *Ramularia collo-cygni* - An emerging pathogen of barley crops. *Phytopathology*, 105 (7), 895–904.

Hayes, C. J., Leonard, P. and O'Kennedy, R. (2012). Overcoming antibody expression and screening limitations by smart design: Applications to PSA immunoassay development. *Protein Expr. Purif*., 83 (1), 84–91.

Hayhurst, A., Happe, S., Mabry, R., Koch, Z., Iverson, B. L. and Georgiou, G. (2003). Isolation and expression of recombinant antibody fragments to the biological warfare pathogen *Brucella melitensis*. *J. Immunol. Methods*, 276 (1–2), 185–196.

He, J. (2013). "Practical Guide to ELISA Development," in The immunoassay handbook: theory and applications of ligand binding, ELISA and related techniques., ed. D. Wild (Oxford: Elsevier), 381–394.

Heid, C. A., Stevens, J., Livak, K. J. and Williams, P. M. (1996). Real time quantitative PCR. *Genome Res*., 6 (10), 986–994.

Himananto, O., Yoohat, K., Danwisetkanjana, K., Kumpoosiri, M., Rukpratanporn, S., Theppawong, Y., Phuengwas, S., Makornwattana, M., Charlermroj, R., Karoonuthaisiri, N., Thummabenjapone, P., Kositcharoenkul, N. and Gajanandana, O. (2020). Double antibody pairs sandwich-ELISA (DAPS-ELISA) detects *Acidovorax citrulli* serotypes with broad coverage. *PLoS One*, 15 (8), e0237940.

Holliger, P. and Hudson, P. J. (2005). Engineered antibody fragments and the rise of single domains. *Nat. Biotechnol*., 23 (9), 1126–1136.

Hoogenboom, H. R. (2005). Selecting and screening recombinant antibody libraries. *Nat. Biotechnol*., 23 (9), 1105–1116.

Hutton, F., Spink, J. H., Griffin, D., Kildea, S., Bonner, D., Doherty, G. and Hunter, A. (2015). Distribution and incidence of viruses in Irish seed potato crops. *Irish J. Agric. Food Res*., 54 (2), 98–106.

Igawa, T., Tsunoda, H., Kuramochi, T., Sampei, Z., Ishii, S. and Hattori, K. (2011). Engineering the variable region of therapeutic IgG antibodies. *MAbs*, 3 (3), 243–252.

International Barley Sequencing Consortium (2012). A physical, genetic and functional sequence assembly of the barley genome. *Nature (Lond.)*, 491 (7426), 711–716.

Ivanov, K. I., Eskelin, K., Bašic, M., De, S., Lõhmus, A., Varjosalo, M. and Mäkinen, K. (2016). Molecular insights into the function of the viral RNA silencing suppressor HCPro. *Plant J*., 85 (1), 30–45.

Ivanov, K. I., Eskelin, K., Lõhmus, A. and Mäkinen, K. (2014). Molecular and cellular mechanisms underlying *Potyvirus* infection. *J. Gen. Virol*., 95 (7), 1415–1429.

Jeevalatha, A., Kaundal, P., Sharma, N. N., Thakur, P., Chakrabarti, S. K. and Singh, B. P. (2013). Expression of coat protein of an ordinary strain of potato virus Y in *Escherichia coli* and production of polyclonal antibodies for diagnosis. *J. Phytopathol*., 161 (9), 671–674.

Jones, H., Civá, P., Cockram, J., Leigh, F. J., Smith, L. M. J., Jones, M. K., Charles, M. P., Molina-Cano, J. L., Powell, W., Jones, G. and Brown, T. A. (2011). Evolutionary history of barley cultivation in Europe revealed by genetic analysis of extant landraces. *BMC Evol. Biol*., 11, 320.

Jung, D., Giallourakis, C., Mostoslavsky, R. and Alt, F. W. (2006). Mechanism and control of V(D)J recombination at the immunoglobulin heavy chain locus. *Annu. Rev. Immunol*., 24, 541–570.

Kanyavuz, A., Marey-Jarossay, A., Lacroix-Desmazes, S. and Dimitrov, J. D. (2019). Breaking the law: Unconventional strategies for antibody diversification. *Nat. Rev. Immunol*., 19, 355–368.

Kapoor, R., Srivastava, N., Kumar, S., Saritha, R. K., Sharma, S. K., Jain, R. K. and Baranwal, V. K. (2017). Development of a recombinase polymerase amplification assay for the diagnosis of banana bunchy top virus in different banana cultivars. *Arch. Virol*., 162 (9), 2791–2796.

Kasamatsu, H. and Vinograd, J. (1974). Replication of circular DNA in eukaryotic cells. *Annu. Rev. Biochem*., 43 (1), 695–719.

Kennedy, P. J., Oliveira, C., Granja, P. L. and Sarmento, B. (2017). Monoclonal antibodies: technologies for early discovery and engineering. *Crit. Rev. Biotechnol*. 38 (3), 394–408.

Kenneth, M., Paul, T., Mark, W. and Charles, J. (2016). Janeway's Immunobiology. 9th ed. New York: Garland Science.

Kežar, A., Kavčič, L., Polák, M., Nováček, J., Gutiérrez-Aguirre, I., Žnidarič, M. T., Coll, A., Stare, K., Gruden, K., Ravnikar, M., Pahovnik, D., Žagar, E., Merzel, F., Anderluh, G.

and Podobnik, M. (2019). Structural basis for the multitasking nature of the potato virus Y coat protein. *Sci. Adv*., 5 (7), eaaw3808.

Kim, H. J., Lee, H. R., Jo, K. R., Mortazavian, S. M. M., Huigen, D. J., Evenhuis, B., Kessel, G., Visser, R. G. F., Jacobsen, E. and Vossen, J. H. (2012). Broad spectrum late blight resistance in potato differential set plants MaR8 and MaR9 is conferred by multiple stacked R genes. *Theor. Appl. Genet*., 124 (5), 923–935.

King, K. M., West, J. S., Fitt, B. D. L. and Dyer, P. S. (2015). Differences in MAT gene distribution and expression between *Rhynchosporium* species on grasses. *Plant Pathol*., 64 (2), 344–354.

Klein, F., Diskin, R., Scheid, J. F., Gaebler, C., Mouquet, H., Georgiev, I. S., Pancera, M., Zhou, T., Incesu, R. B., Fu, B. Z., Gnanapragasam, P. N. P., Oliveira, T. Y., Seaman, M. S., Kwong, P. D., Bjorkman, P. J. and Nussenzweig, M. C. (2013). Somatic mutations of the immunoglobulin framework are generally required for broad and potent HIV-1 neutralization. *Cell*, 153 (1), 126–138.

Kogovšek, P., Gow, L., Pompe-Novak, M., Gruden, K., Foster, G. D., Boonham, N. and Ravnikar, M. (2008). Single-step RT real-time PCR for sensitive detection and discrimination of potato virus Y isolates. *J. Virol. Methods*, 149 (1), 1–11.

Köhler, G. and Milstein, C. (1975). Continuous cultures of fused cells secreting antibody of predefined specificity. *Nature (Lond.)*, 256, 495–497.

Komar, A. A. (2009). A pause for thought along the co-translational folding pathway. *Trends Biochem. Sci*., 34 (1), 16–24.

Komor, E. (2011). Susceptibility of sugarcane, plantation weeds and grain cereals to infection by Sugarcane yellow leaf virus and selection by sugarcane breeding in Hawaii. *Eur. J. Plant Pathol*., 129, 379–388.

Konczal, J., Bower, J. and Gray, C. H. (2019). Re-introducing non-optimal synonymous codons into codon-optimized constructs enhances soluble recovery of recombinant proteins from *Escherichia coli*. *PLoS One*, 14 (4), e0215892.

Lacomme, C. and Jacquot, E. (2017). “General characteristics of potato virus Y (PVY) and its impact on potato production: an overview,” in Potato Virus Y: Biodiversity, Pathogenicity, Epidemiology and Management, eds. C. Lacomme, L. Glais, D. Bellstedt, B. Dupuis, A. Karasev, E. Jacquot, (Cham: Springer International Publishing), 1–19.

Langridge, P. (2018). “Economic and Academic Importance of Barley,” in The Barley Genome. Compendium of Plant Genomes., eds. N. Stein and G. Muehlbauer (Cham: Springer), 1–10.

Larkin, R. P., Griffin, T. S. and Honeycutt, C. W. (2010). Rotation and cover crop effects on soilborne potato diseases, tuber yield, and soil microbial communities. *Plant Dis*., 94 (12), 1491–1502.

Lebani, K., Jones, M. L., Watterson, D., Ranzoni, A., Traves, R. J., Young, P. R. and Mahler, S. M. (2017). Isolation of serotype-specific antibodies against dengue virus non-structural protein 1 using phage display and application in a multiplexed serotyping assay. *PLoS One*, 12 (7), e0180669.

Ledsgaard, L., Kilstrup, M., Karatt-Vellatt, A., McCafferty, J. and Laustsen, A. (2018). Basics of antibody phage display technology. *Toxins,* 10 (6), 236.

Lee, H. K., Tewari, J. P. and Turkington, T. K. (2001). A PCR-based assay to detect *Rhynchosporium secalis* in barley seed. *Plant Dis*., 85 (2), 220–225.

Lee, H. K., Tewari, J. P. and Turkington, T. K. (2002). Quantification of seedborne infection by *Rhynchosporium secalis* in barley using competitive PCR. *Plant Pathol*., 51 (2), 217–224.

Lee, H., Tewari, J. and Turkington, T. (2001b). Symptomless infection of barley seed by *Rhynchosporium secalis*. *Can. J. Plant Pathol*., 23 (3), 315–317.

Lee, W., Syed Atif, A., Tan, S. C. and Leow, C. H. (2017). Insights into the chicken IgY with emphasis on the generation and applications of chicken recombinant monoclonal antibodies. *J. Immunol. Methods*, 447, 71–85.

Lee, Y. C., Boehm, M. K., Chester, K. A., Begent, R. H. J. and Perkins, S. J. (2002). Reversible dimer formation and stability of the anti-tumour single-chain Fv antibody MFE-

23 by neutron scattering, analytical ultracentrifugation, and NMR and FT-IR spectroscopy. *J. Mol. Biol*., 320 (1), 107–127.

Leighton, P. A., Morales, J., Harriman, W. D. and Ching, K. H. (2018). V(D)J rearrangement is dispensable for producing CDR-H3 sequence diversity in a gene converting species. *Front. Immunol*., 9, 1317.

Li, J., Macdonald, J. and Von Stetten, F. (2019). Review: a comprehensive summary of a decade development of the recombinase polymerase amplification. *Analyst*, 144 (1), 31–67.

Li, X. H., Zhang, X. L., Wu, J., Lin, N., Sun, W. M., Chen, M., Ou, Q. S. and Lin, Z. Y. (2019). Hyperbranched rolling circle amplification (HRCA)-based fluorescence biosensor for ultrasensitive and specific detection of single-nucleotide polymorphism genotyping associated with the therapy of chronic hepatitis B virus infection. *Talanta*, 191, 277–282.

Lillis, L., Lehman, D., Singhal, M. C., Cantera, J., Singleton, J., Labarre, P., Toyama, A., Piepenburg, O., Parker, M., Wood, R., Overbaugh, J. and Boyle, D. S. (2014). Non-instrumented incubation of a recombinase polymerase amplification assay for the rapid and sensitive detection of proviral HIV-1 DNA. *PLoS One*, 9 (9), e108189.

Linsell, K. J., Keiper, F. J., Forgan, A. and Oldach, K. H. (2011). New insights into the infection process of *Rhynchosporium secalis* in barley using GFP. *Fungal Genet. Biol*., 48 (2), 124–131.

Lipman, N. S., Jackson, L. R., Trudel, L. J. and Weis-Garcia, F. (2005). Monoclonal versus polyclonal antibodies: Distinguishing characteristics, applications, and information resources. *ILAR J*., 46 (3), 258–268.

Liu, H. B., Zang, Y. X., Du, X. J., Li, P. and Wang, S. (2017). Development of an isothermal amplification-based assay for the rapid visual detection of *Salmonella* bacteria. *J. Dairy Sci*., 100 (9), 7016–7025.

Liu, J. (2014). The history of monoclonal antibody development – Progress, remaining challenges and future innovations. *Ann. Med. Surg*., 3 (4), 113–116.

Liu, X., Yan, Q., Huang, J., Chen, J., Guo, Z., Liu, Z., Cai, L., Li, R., Wang, Y., Yang, G. and Lan, Q. (2019). Influence of design probe and sequence mismatches on the efficiency of fluorescent RPA. World *J. Microbiol. Biotechnol*., 35, 95.

Lizardi, P. M., Huang, X., Zhu, Z., Bray-Ward, P., Thomas, D. C. and Ward, D. C. (1998). Mutation detection and single-molecule counting using isothermal rolling-circle amplification. *Nat. Genet*., 19 (3), 225–232.

Lobato, I. M. and O'Sullivan, C. K. (2018). Recombinase polymerase amplification: Basics, applications and recent advances. *TrAC - Trends Anal. Chem*., 98, 19–35.

Londoño, M. A., Harmon, C. L. and Polston, J. E. (2016). Evaluation of recombinase polymerase amplification for detection of begomoviruses by plant diagnostic clinics. *Virol. J*., 13, 48.

Looseley, M. E., Griffe, L. L., Büttner, B., Wright, K. M., Middlefell-Williams, J., Bull, H., Shaw, P. D., Macaulay, M., Booth, A., Schweizer, G., Russell, J. R., Waugh, R., Thomas, W. T. B. and Avrova, A. (2018). Resistance to *Rhynchosporium commune* in a collection of European spring barley germplasm. *Theor. Appl. Genet*., 131, 2513–2528.

Looseley, M. E., Newton, A. C., Atkins, S. D., Fitt, B. D. L., Fraaije, B. A., Thomas, W. T. B., Keith, R., Macaulay, M., Lynott, J. and Harrap, D. (2012). Genetic basis of control of *Rhynchosporium secalis* infection and symptom expression in barley. *Euphytica*, 184, 47–56.

López-Soriano, P., Noguera, P., Gorris, M. T., Puchades, R., Maquieira, Á., Marco-Noales, E. and López, M. M. (2017). Lateral flow immunoassay for on-site detection of *Xanthomonas arboricola pv. Pruni* in symptomatic field samples. *PLoS One*, 12 (4), e0176201.

Lorenz, T. C. (2012). Polymerase chain reaction: Basic protocol plus troubleshooting and optimization strategies. *J. Vis. Exp*., 63, e3998.

Luan, H., Shine, M., Cui, X., Chen, X., Ma, N., Kachroo, P., Zhi, H. and Kachroo, A. (2016). The potyviral P3 protein targets eukaryotic elongation factor 1A to promote the unfolded protein response and viral pathogenesis. *Plant Physiol*., 172 (1), 221–234.

Luo, G. C., Yi, T. T., Jiang, B., Guo, X. L. and Zhang, G. Y. (2019). Betaine-assisted recombinase polymerase assay with enhanced specificity. *Anal. Biochem*., 575, 36–39.

Ma, H. and O'Kennedy, R. (2015). "The structure of natural and recombinant antibodies," in Peptide Antibodies. Methods in Molecular Biology, vol 1348, ed. G. Houen, (New York: Humana Press), 7–11.

Ma, H. and O'Kennedy, R. (2017). Recombinant antibody fragment production. *Methods*, 116, 23–33.

Magan, N. and Aldred, D. (2007). Post-harvest control strategies: Minimizing mycotoxins in the food chain. *Int. J. Food Microbiol*., 119 (1–2), 131–139.

Mai-Prochnow, A., Hui, J., Kjelleberg, S., Rakonjac, S., McDougald, D. and Rice, S. (2015). Big things in small packages: The genetics of filamentous phage and effects on fitness of their host. *FEMS Microbiol. Rev*., 39 (4), 465–487.

Mariani, S. and Minunni, M. (2014). Surface plasmon resonance applications in clinical analysis. *Anal. Bioanal. Chem*., 406 (9-10), 2303–2323.

Marincevic-Zuniga, Y., Gustavsson, I. and Gyllensten, U. (2012). Multiply-primed rolling circle amplification of human papillomavirus using sequence-specific primers. *Virology*, 432 (1), 57–62.

Maul, R. W. and Gearhart, P. J. (2010). Controlling somatic hypermutation in immunoglobulin variable and switch regions. *Immunol. Res*., 47 (1–3), 113–122.

Maynard, J. A., Maassen, C. B. M., Leppla, S. H., Brasky, K., Iverson, B. L. and Georgiou, G. (2002). Protection against anthrax toxin by recombinant antibody fragments correlates with antigen affinity. *Nat. Biotechnol*., 20 (6), 597–601.

McCafferty, J., Griffiths, A., Winter, G. and Chiswell, D. J. (1990). Phage antibodies: Filamentous phage displaying antibody variable domains. *Nature (Lond)*, 348 (6301), 552-554.

McCotter, S. W., Horianopoulos, L. C. and Kronstad, J. W. (2016). Regulation of the fungal secretome. *Curr. Genet*., 62, 533–545.

McDonald, B. A. (2015). How can research on pathogen population biology suggest disease management strategies? The example of barley scald (*Rhynchosporium commune*). *Plant Pathol*., 64 (5), 1005–1013.

McMullen, M., Bergstrom, G., De Wolf, E., Dill-Macky, R., Hershman, D., Shaner, G. and Van Sanford, D. (2012). A unified effort to fight an enemy of wheat and barley: Fusarium head blight. *Plant Dis*., 96 (12), 1712–1728.

Mekuria, T. A., Zhang, S. and Eastwell, K. C. (2014). Rapid and sensitive detection of little cherry virus 2 using isothermal reverse transcription-recombinase polymerase amplification. *J. Virol. Methods*, 205, 24–30.

Mello, A. F. S., Olarte, R. A., Gray, S. M. and Perry, K. L. (2011). Transmission efficiency of potato virus Y strains PVY O and PVY N-Wi by five aphid species. *Plant Dis*., 95 (10), 1279–1283.

Mezger, A., Öhrmalm, C., Herthnek, D., Blomberg, J. and Nilsson, M. (2014). Detection of rotavirus using padlock probes and rolling circle amplification. *PLoS One*, 9 (11), e111874.

Mohd-Assaad, N., McDonald, B. A. and Croll, D. (2019). The emergence of the multi-species NIP1 effector in *Rhynchosporium* was accompanied by high rates of gene duplications and losses. *Environ. Microbiol*., 21 (8), 2677–2695.

Mohsen, M. G. and Kool, E. T. (2016). The discovery of rolling circle amplification and rolling circle transcription. *Acc. Chem. Res*., 49 (11), 2540–2550.

Mondal, S. and Gray, S. M. (2017). Sequential acquisition of potato virus Y strains by *Myzus persicae* favors the transmission of the emerging recombinant strains. *Virus Res*., 241, 116–124.

Moreno, A., Tjallingii, W. F., Fernandez-Mata, G. and Fereres, A. (2012). Differences in the mechanism of inoculation between a semi-persistent and a non-persistent aphid-transmitted plant virus. *J. Gen. Virol*., 93 (3), 662–667.

Motohashi, K. (2019). Development of highly sensitive and low-cost DNA agarose gel electrophoresis detection systems, and evaluation of non-mutagenic and loading dye-type DNA-staining reagents. *PLoS One*, 14 (9), e0222209.

Mullis, K., Faloona, F., Scharf, S., Saiki, R., Horn, G. and Erlich, H. (1986). Specific enzymatic amplification of DNA in vitro: The polymerase chain reaction. *Cold Spring Harb. Symp. Quant. Biol*., 51, 263–273.

Munawar, M. A., Martin, F., Toljamo, A., Kokko, H. and Oksanen, E. (2020). RPA-PCR couple: An approach to expedite plant diagnostics and overcome PCR inhibitors. *Biotechniques*, 69 (4), 271–280.

Murphy, C., Stack, E., Krivelo, S., Breheny, M., Ma, H. and O'Kennedy, R. (2018). Enhancing recombinant antibody performance by optimally engineering its format. *J. Immunol. Methods*, 463, 127–133.

Navarro, E., Serrano-Heras, G., Castaño, M. J. and Solera, J. (2015). Real-time PCR detection chemistry. *Clin. Chim. Acta*, 439, 231–250.

Nguyen, H. H., Park, J., Kang, S. and Kim, M. (2015). Surface plasmon resonance: A versatile technique for biosensor applications. *Sensors*, 15 (5), 10481–10510.

Nie, B., Singh, M., Sullivan, A., Singh, R., Xie, C. and Nie, X. (2010). Recognition and molecular discrimination of severe and mild PVY O variants of potato virus Y in potato in New Brunswick, Canada. *Plant Dis*., 95 (2), 113–119.

Nie, X. (2005). Reverse transcription loop-mediated isothermal amplification of DNA for detection of potato virus Y. *Plant Dis*., 89 (6), 605–610.

Notomi, T., Mori, Y., Tomita, N. and Kanda, H. (2015). Loop-mediated isothermal amplification (LAMP): Principle, features, and future prospects. *J. Microbiol*., 53 (1), 1–5.

Notomi, T., Okayama, H., Masubuchi, H., Yonekawa, T., Watanabe, K., Amino, N. and Hase, T. (2000). Loop-mediated isothermal amplification of DNA. *Nucleic Acids Res*., 28 (12), e63.

Nunes, C. (2012). Biological control of postharvest diseases of fruit. *Eur. J. Plant Pathol*., 133, 181–196.

Nuttall, S. D., Wilkins, M. L., Streltsov, V. A., Pontes-Braz, L., Dolezal, O., Tran, H. and Liu, C. Q. (2011). Isolation, kinetic analysis, and structural characterization of an antibody

targeting the *Bacillus anthracis* major spore surface protein BclA. *Proteins Struct. Funct. Bioinforma*., 79 (4), 1306–1317.

Olspert, A., Carr, J. P. and Firth, A. E. (2016). Mutational analysis of the *Potyviridae* transcriptional slippage site utilized for expression of the P3N-PIPO and P1N-PISPO proteins. *Nucleic Acids Res*., 44 (16), 7618–7629.

Pagliaccia, D., Shi, J., Pang, Z., Hawara, E., Clark, K., Thapa, S. P., De Francesco, A., Liu, J., Tran, T. T., Bodaghi, S., Folimonova, S. Y., Ancona, V., Mulchandani, A., Coaker, G., Wang, N., Vidalakis, G. and Ma, W. (2017). A pathogen secreted protein as a detection marker for citrus huanglongbing. *Front. Microbiol*., 8, 2041.

Pande, J., Szewczyk, M. M. and Grover, A. K. (2010). Phage display: Concept, innovations, applications and future. *Biotechnol. Adv*., 28 (6), 849–858.

Panferov, V. G., Safenkova, I. V., Byzova, N. A., Varitsev, Y. A., Zherdev, A. V. and Dzantiev, B. B. (2017). Silver-enhanced lateral flow immunoassay for highly-sensitive detection of potato leafroll virus. *Food Agric. Immunol*., 29 (1), 445–457.

Parida, M., Sannarangaiah, S., Dash, P. K., Rao, P. V. L. and Morita, K. (2008). Loop mediated isothermal amplification (LAMP): A new generation of innovative gene amplification technique; perspectives in clinical diagnosis of infectious diseases. *Rev. Med. Virol*., 18 (6), 407–421.

Parray, H. A., Shukla, S., Samal, S., Shrivastava, T., Ahmed, S., Sharma, C. and Kumar, R. (2020). Hybridoma technology a versatile method for isolation of monoclonal antibodies, its applicability across species, limitations, advancement and future perspectives. *Int. Immunopharmacol*., 85, 106639.

Patel, R. and Andrien, B. A. (2010). Kinetic analysis of a monoclonal therapeutic antibody and its single-chain homolog by surface plasmon resonance. *Anal. Biochem*., 396 (1), 59–68.

Phelan, S., Barthe, M. S., Tobie, C. and Kildea, S. (2017). Detection of the cytochrome b mutation G143A in Irish *Rhynchosporium commune* populations using targeted 454 sequencing. *Pest Manag. Sci*., 73 (6), 1154–1160.

Piepenburg, O., Williams, C. H., Stemple, D. L. and Armes, N. A. (2006). DNA detection using recombination proteins. *PLoS Biol*., 4 (7), e204.

Powell, M. L., Bowler, F. R., Martinez, A. J., Greenwood, C. J., Armes, N. and Piepenburg, O. (2018). New Fpg probe chemistry for direct detection of recombinase polymerase amplification on lateral flow strips. *Anal. Biochem*., 543, 108–115.

Przewodowska, A., Zacharzewska, B., Chołuj, J. and Treder, K. (2015). A one-step, real-time reverse transcription loop mediated isothermal amplification assay to detect potato virus Y. *Am. J. Potato Res*., 92, 303–311.

Quenouille, J., Vassilakos, N. and Moury, B. (2013). Potato virus Y: A major crop pathogen that has provided major insights into the evolution of viral pathogenicity. *Mol. Plant Pathol*., 14 (5), 439–452.

Rabia, L. A., Zhang, Y., Ludwig, S. D., Julian, M. C. and Tessier, P. M. (2018). Net charge of antibody complementarity-determining regions is a key predictor of specificity. *Protein Eng. Des. Sel*., 31 (11), 409–418.

Rahbarnia, L., Farajnia, S., Babaei, H., Majidi, J., Veisi, K., Tanomand, A. and Akbari, B. (2016). Invert biopanning: A novel method for efficient and rapid isolation of scFvs by phage display technology. *Biologicals*, 44 (6), 567–573.

Rakonjac, J., Russel, M., Khanum, S., Brooke, S. J. and Rajič, M. (2017). "Filamentous phage: Structure and biology," in Advances in Experimental Medicine and Biology, vol 1053, ed. T. Lim, (Cham: Springer), 1–20.

Rangnoi, K., Choowongkomon, K., O'Kennedy, R., Rüker, F. and Yamabhai, M. (2018). Enhancement and analysis of human anti-aflatoxin B1 (AFB1) scFv antibody-ligand interaction using chain shuffling. *J. Agric. Food Chem*., 66 (22), 5713–5722.

Reader, R. H., Workman, R. G., Maddison, B. C. and Gough, K. C. (2019). Advances in the production and batch reformatting of phage antibody libraries. *Mol. Biotechnol*., 61, 801–815.

Rosano, G. L. and Ceccarelli, E. A. (2014a). Recombinant protein expression in *Escherichia coli*: Advances and challenges. *Front. Microbiol*., 5, 172.

Rosano, G. L. and Ceccarelli, E. A. (2014b). Recombinant protein expression in microbial systems. *Front. Microbiol*., 5, 341.

Ryder, L. S. and Talbot, N. J. (2015). Regulation of appressorium development in pathogenic fungi. *Curr. Opin. Plant Biol*., 26, 8–13.

Sadofsky, M. J. (2001). The RAG proteins in V(D)J recombination: More than just a nuclease. *Nucleic Acids Res*., 29 (7), 1399–1409.

Safenkova, I. V., Ivanov, A. V., Slutskaya, E. S., Samokhvalov, A. V., Zherdev, A. V. and Dzantiev, B. B. (2020). Key significance of DNA-target size in lateral flow assay coupled with recombinase polymerase amplification. *Anal. Chim. Acta*, 1102, 109–118.

Safenkova, I. V, Zaitsev, I. A., Varitsev, Y. A., Byzova, N. A., Drenova, N. V., Zherdev, A. V. and Dzantiev, B. B. (2017). Development of a lateral flow immunoassay for rapid diagnosis of potato blackleg caused by *Dickeya* species. *Anal. Bioanal. Chem*., 409 (7), 1915–1927.

Sanderkar, M. and Nielsen, K. L. (2011). Genome sequence and analysis of the tuber crop potato : The Potato Genome Sequencing Consortium. *Nature (Lond.)*, 475 (7355), 189–195.

Savary, S., Ficke, A., Aubertot, J. N. and Hollier, C. (2012). Crop losses due to diseases and their implications for global food production losses and food security. *Food Security*, 4, 519–537.

Savary, S., Willocquet, L., Pethybridge, S. J., Esker, P., McRoberts, N. and Nelson, A. (2019). The global burden of pathogens and pests on major food crops. *Nat. Ecol. Evol*., 3, 430–439.

Schatz, D. G. (2004). V(D)J recombination. *Immunol. Rev*., 200, 5–11.

Schürch, S., Linde, C. C., Knogge, W., Jackson, L. F. and McDonald, B. A. (2004). Molecular population genetic analysis differentiates two virulence mechanisms of the fungal avirulence gene NIP1. *Mol. Plant-Microbe Interact*., 17 (10), 1114–1125.

Schweitzer, B. and Kingsmore, S. (2001). Combining nucleic acid amplification and detection. *Curr. Opin. Biotechnol*., 12 (1), 21–27.

Scott, P., Bader, M. K. F., Burgess, T., Hardy, G. and Williams, N. (2019). Global biogeography and invasion risk of the plant pathogen genus *Phytophthora*. *Environ. Sci. Policy*, 101, 175–182.

Seepiban, C., Charoenvilaisiri, S., Warin, N., Bhunchoth, A., Phironrit, N., Phuangrat, B., Chatchawankanphanich, O., Attathom, S. and Gajanandana, O. (2017). Development and application of triple antibody sandwich enzyme-linked immunosorbent assays for begomovirus detection using monoclonal antibodies against tomato yellow leaf curl Thailand virus. *Virol. J.*, 14 (1), 99.

Silva, G., Oyekanmi, J., Nkere, C. K., Bömer, M., Kumar, P. L. and Seal, S. E. (2018). Rapid detection of potyviruses from crude plant extracts. *Anal. Biochem*., 546, 17–22.

Singh, A., Upadhyay, V., Upadhyay, A. K., Singh, S. M. and Panda, A. K. (2015). Protein recovery from inclusion bodies of *Escherichia coli* using mild solubilization process. *Microb. Cell Fact*., 14, 41.

Singh, J., and Kaur, L. (2016). Advances in Potato Chemistry and Technology: Second Edition. (Oxford, Elsevier).

Singpanomchai, N., Akeda, Y., Tomono, K., Tamaru, A., Santanirand, P. and Ratthawongjirakul, P. (2019). Naked eye detection of the *Mycobacterium tuberculo*sis complex by recombinase polymerase amplification—SYBR green I assay. *J. Clin. Lab. Anal*., 33 (2), e22655.

Smith, G. (1985). Filamentous fusion phage: novel expression vectors that display cloned antigens on the virion surface. *Science*, 228 (4705), 1315–1317.

Sorel, M., Garcia, J. A. and German-Retana, S. (2014). The *Potyviridae* cylindrical inclusion helicase: A key multipartner and multifunctional protein. *Mol. Plant-Microbe Interact*., 27 (3), 215–226.

Spillner, E., Braren, I., Greunke, K., Seismann, H., Blank, S. and du Plessis, D. (2012). Avian IgY antibodies and their recombinant equivalents in research, diagnostics and therapy. *Biologicals*, 40 (5), 313–322.

Stergiopoulos, I. and de Wit, P. J. G. M. (2009). Fungal effector proteins. *Annu. Rev. Phytopathol*., 47, 233–263.

Straus, S. K. and Bo, H. E. (2018). "Filamentous Bacteriophage Proteins and Assembly," in Virus Protein and Nucleoprotein Complexes, eds. J. Harris and D. Bhella, (Singapore: Springer), 261–279.

Studier, F. W. (2005). Protein production by auto-induction in high density shaking cultures. *Protein Expr. Purif*., 41 (1), 207–234.

Tavert-Roudet, G., Anne, A., Barra, A., Chovin, A., Demaille, C. and Michon, T. (2017). The potyvirus particle recruits the plant translation initiation factor eIF4E by means of the VPg covalently linked to the viral RNA. *Mol. Plant-Microbe Interact*., 30 (9), 754–762.

Teng, G. and Papavasiliou, F. N. (2007). Immunoglobulin somatic hypermutation. *Annu. Rev. Genet*., 41, 107–120.

Teo, J. W. P., Chiang, D., Jureen, R. and Lin, R. T. P. (2015). Clinical evaluation of a helicase-dependant amplification (HDA)-based commercial assay for the simultaneous detection of HSV-1 and HSV-2. *Diagn. Microbiol. Infect*., Dis. 83 (3), 261–262.

Tian, Y.-P., Hepojoki, J., Ranki, H., Lankinen, H. and Valkonen, J. P. T. (2014). Analysis of potato virus Y coat protein epitopes recognized by three commercial monoclonal antibodies. *PLoS One*, 9 (12), e115766.

Tiller, K. E., Li, L., Kumar, S., Julian, M. C., Garde, S. and Tessier, P. M. (2017). Arginine mutations in antibody complementarity-determining regions display context-dependent affinity/specificity trade-offs. *J. Biol. Chem*., 292 (40), 16638–16652.

Tolia, N. H. and Joshua-Tor, L. (2006). Strategies for protein co-expression in *Escherichia coli*. *Nat. Methods*, 3, 55–64.

Tomita, N., Mori, Y., Kanda, H. and Notomi, T. (2008). Loop-mediated isothermal amplification (LAMP) of gene sequences and simple visual detection of products. *Nat. Protoc*. 3 (5), 877–882.

Topp, C. F. E., Hughes, G., Nevison, I. M., Butler, A., Oxley, S. J. P. and Havis, N. D. (2019). *Rhynchosporium* leaf scald disease incidence: Seed source and spatial pattern. *Plant Pathol*., 68 (6), 1179–1187.

Treder, K., Chołuj, J., Zacharzewska, B., Babujee, L., Mielczarek, M., Burzyński, A. and Rakotondrafara, A. M. (2018). Optimization of a magnetic capture RT-LAMP assay for fast and real-time detection of potato virus Y and differentiation of N and O serotypes. *Arch. Virol*., 163 (2), 447–458.

TwistDx (2021). TwistAmp® DNA Amplification Kits Assay Design Manual. (https://www.twistdx.co.uk/docs/default-source/RPA-assay-design/twistamp-assay-design-manual-v2-5.pdf?sfvrsn=b3be0efc_29).

Ullrich, S. (2010). Barley: Production, Improvement, and Uses. (Chichester, Wiley-Blackwell).

Unverdorben, F., Richter, F., Hutt, M., Seifert, O., Malinge, P., Fischer, N. and Kontermann, R. E. (2016). Pharmacokinetic properties of IgG and various Fc fusion proteins in mice. *MAbs*, 8 (1), 120–128.

Van der Vlugt, R. A. A., Leunissen, J. and Goldbach, R. (1993). Taxonomic relationships between distinct potato virus Y isolates based on detailed comparisons of the viral coat proteins and 3′-nontranslated regions. *Arch. Virol*., 131 (3–4), 361–375.

Van Ness, J., Van Ness, L. K. and Galas, D. J. (2003). Isothermal reactions for the amplification of oligonucleotides. *Proc. Natl. Acad. Sci. U. S. A*., 100 (8), 4504–4509.

van Pelt-Verkuil, E., van Belkum, A. and Hays, J. P. (2008). “PCR Primers,” in Principles and Technical Aspects of PCR Amplification, eds. E. van Pelt-Verkuil, A. van Belkum, and J. P. Hays (Dordrecht: Springer, Dordrecht), 63-90.

Vera, A., González-Montalbán, N., Arís, A. and Villaverde, A. (2007). The conformational quality of insoluble recombinant proteins is enhanced at low growth temperatures. *Biotechnol. Bioeng*., 96 (6), 1101–1106.

Verbeek, M., Piron, P. G. M., Dullemans, A. M., Cuperus, C. and Van Der Vlugt, R. A. A. (2010). Determination of aphid transmission efficiencies for N, NTN and Wilga strains of potato virus Y. *Ann. Appl. Biol*., 156 (1), 39–49.

Vijayapalani, P., Maeshima, M., Nagasaki-Takekuchi, N. and Miller, W. A. (2012). Interaction of the trans-frame potyvirus protein P3N-PIPO with host protein PCaP1 facilitates potyvirus movement. *PLoS Pathog*., 8 (4), e1002639.

Vincent, M., Xu, Y. and Kong, H. (2004). Helicase-dependent isothermal DNA amplification. *EMBO Rep*., 5 (8), 795–800.

Vincke, C., Loris, R., Saerens, D., Martinez-Rodriguez, S., Muyldermans, S. and Conrath, K. (2009). General strategy to humanize a camelid single-domain antibody and identification of a universal humanized nanobody scaffold. *J. Biol. Chem*., 284 (5), 3273–3284.

Vuento, M., Paananen, K., Vihinen-Ranta, M. and Kurppa, A. (1993). Characterization of antigenic epitopes of potato virus Y. *Biochim. et Biophysica Acta* 1162 (1–2), 155–160.

Walker, G. T., Fraiser, M. S., Schram, J. L., Little, M. C., Nadeau, J. G. and Malinowski, D. P. (1992). Strand displacement amplification - an isothermal, *in vitro* DNA amplification technique. *Nucleic Acids Res*., 20 (7), 1691–1696.

Wang, R., Zhang, F., Wang, L., Qian, W., Qian, C., Wu, J. and Ying, Y. (2017). Instant, visual, and instrument-free method for on-site screening of GTS 40-3-2 soybean based on body-heat triggered recombinase polymerase amplification. *Anal. Chem*., 89 (8), 4413–4418.

Wang, S., Liu, N., Zheng, L., Cai, G. and Lin, J. (2020a). A lab-on-chip device for the sample-in-result-out detection of viable *Salmonella* using loop-mediated isothermal amplification and real-time turbidity monitoring. *Lab Chip*, 20 (13), 2296–2305.

Wang, Y., Chen, R., Nie, X., Zhong, Z., Li, C., Li, K., Huang, W., Fu, X., Liu, J. and Nie, B. (2020b). Rapid and sensitive detection of potato virus Y by isothermal reverse transcription-recombinase polymerase amplification assay in potato. *Mol. Cell. Probes*, 50, 101505.

Wark, K. L., and Hudson, P. J. (2006). Latest technologies for the enhancement of antibody affinity. *Adv. Drug Deliv. Rev*., 58 (5–6), 657–670.

Wei, T., Huang, T., McNeil, J., Laliberte, J.-F., Hong, J., Nelson, R. S. and Wang, A. (2010). Sequential recruitment of the endoplasmic reticulum and chloroplasts for plant potyvirus replication. *J. Virol*., 84 (2), 799–809.

Wen, R. H. and Hajimorad, M. R. (2010). Mutational analysis of the putative PIPO of soybean mosaic virus suggests disruption of PIPO protein impedes movement. *Virology*, 400 (1), 1–7.

Whitfield, A., Falk, B. and Rotenberg, D. (2015). Insect vector-mediated transmission of plant viruses. *Virology*, 479–480, 278–289.

Wijesinha-Bettoni, R. and Mouillé, B. (2019). The contribution of potatoes to global food security, nutrition and healthy diets. *Am. J. Potato Res*., 96, 139–149.

Winter, G., Griffiths, A. D., Hawkins, R. E. and Hoogenboom, H. R. (1994). Making antibodies by phage display technology. *Annu. Rev. Immunol*., 12, 433–455.

Woonton, B. W., Jacobsen, J. V., Sherkat, F. and Stuart, I. M. (2005). Changes in germination and malting quality during storage of barley. *J. Inst. Brew*., 111 (1), 33–41.

Wu, L., Oficjalska, K., Lambert, M., Fennell, B. J., Darmanin-Sheehan, A., Ní Shúilleabháin, D., Autin, B., Cummins, E., Tchistiakova, L., Bloom, L., Paulsen, J., Gill, D., Cunningham, O. and Finlay, W. J. J. (2012). Fundamental characteristics of the immunoglobulin V_H repertoire of chickens in comparison with those of humans, mice, and camelids. *J. Immunol*., 188 (1), 322–333.

Wu, X., Kong, D., Song, S., Liu, L., Kuang, H. and Xu, C. (2015). Development of sandwich ELISA and immunochromatographic strip methods for the detection of *Xanthomonas oryzae pv. oryzae*. *Anal. Methods*, 7 (15), 6190–6197.

Xu, J. L. and Davis, M. M. (2000). Diversity in the CDR3 region of V(H) is sufficient for most antibody specificities. *Immunity*, 13 (1), 37–45.

Yang, L., Arora, K., Beard, W. A., Wilson, S. H. and Schlick, T. (2004). Critical role of magnesium ions in DNA polymerase β's closing and active site assembly. *J. Am. Chem. Soc*., 126 (27), 8441–8453.

Yang, Y., Qin, X., Wang, G., Zhang, Y., Shang, Y. and Zhang, Z. (2015). Development of a fluorescent probe-based recombinase polymerase amplification assay for rapid detection of Orf virus. *Virol. J*., 12, 206.

Zeng, H., Guo, W., Liang, B., Li, J., Zhai, X., Song, C., Zhao, W., Fan, E. and Liu, Q. (2016). Self-paired monoclonal antibody lateral flow immunoassay strip for rapid detection of *Acidovorax avenae* subsp. *citrulli*. *Anal. Bioanal. Chem*., 408 (22), 6071–6078.

Zhan, J., Fitt, B. D. L., Pinnschmidt, H. O., Oxley, S. J. P. and Newton, A. C. (2008). Resistance, epidemiology and sustainable management of *Rhynchosporium secalis* populations on barley. *Plant Pathol*., 57 (1), 1–14.

Zhang, M., Chen, R., Zhou, X. and Wu, J. (2018). Monoclonal antibody-based serological detection methods for wheat dwarf virus. *Virol. Sin*., 33, 173–180.

Zhang, S., Ravelonandro, M., Russell, P., McOwen, N., Briard, P., Bohannon, S. and Vrient, A. (2014). Rapid diagnostic detection of plum pox virus in Prunus plants by isothermal AmplifyRP® using reverse transcription-recombinase polymerase amplification. *J. Virol. Methods*, 207, 114–120.

Zhang, S., Sun, A., Wan, B., Du, Y., Wu, Y., Zhang, A., Jiang, D., Ji, P., Wei, Z., Zhuang, G. and Zhang, G. (2020a). Development of a directly visualized recombinase polymerase amplification–SYBR Green I method for the rapid detection of african swine fever virus. *Front. Microbiol*., 11, 602709.

Zhang, X., Lowe, S. B. and Gooding, J. J. (2014). Brief review of monitoring methods for loop-mediated isothermal amplification (LAMP). *Biosens. Bioelectron*., 61, 491–499.

Zhang, X., Ovenden, B. and Milgate, A. (2020). Recent insights into barley and *Rhynchosporium commune* interactions. *Mol. Plant Pathol*., 21 (8), 1111–1128.

Zhang, Y., Gao, Y. L., He, W. Q., Wang, Y. Q., Qian, Y. J., Zhou, X. P. and Wu, J. (2020b). Monoclonal antibody-based serological detection of potato virus M in potato plants and tubers. *J. Integr. Agric*., 19 (5), 1283–1291.

Zhang, Y., Wu, L., Gupta, P., Desai, A. A., Smith, M. D., Rabia, L. A., Ludwig, S. D. and Tessier, P. M. (2020c). Physicochemical rules for identifying monoclonal antibodies with drug-like specificity. *Mol. Pharm*., 17 (7), 2555–2569.

Zhao, A., Tohidkia, M. R., Siegel, D. L., Coukos, G. and Omidi, Y. (2016). Phage antibody display libraries: a powerful antibody discovery platform for immunotherapy. *Crit. Rev. Biotechnol*., 36 (2), 276–289.

Zhao, J., Nussinov, R., Wu, W. J. and Ma, B. (2018). *In-silico* methods in antibody design. *Antibodies*, 7 (3), 22.

Zhou, J., Qi, Q., Wang, C., Qian, Y., Liu, G., Wang, Y. and Fu, L. (2019). Surface plasmon resonance (SPR) biosensors for food allergen detection in food matrices. *Biosens. Bioelectron*., 142, 111449.

Zhu, S., Li, Y., Vossen, J. H., Visser, R. G. F. and Jacobsen, E. (2012). Functional stacking of three resistance genes against *Phytophthora infestans* in potato. *Transgenic Res*., 21 (1), 89–99.

Appendices

Appendix A. Sample results of dual-labelled primer RPA optimisation

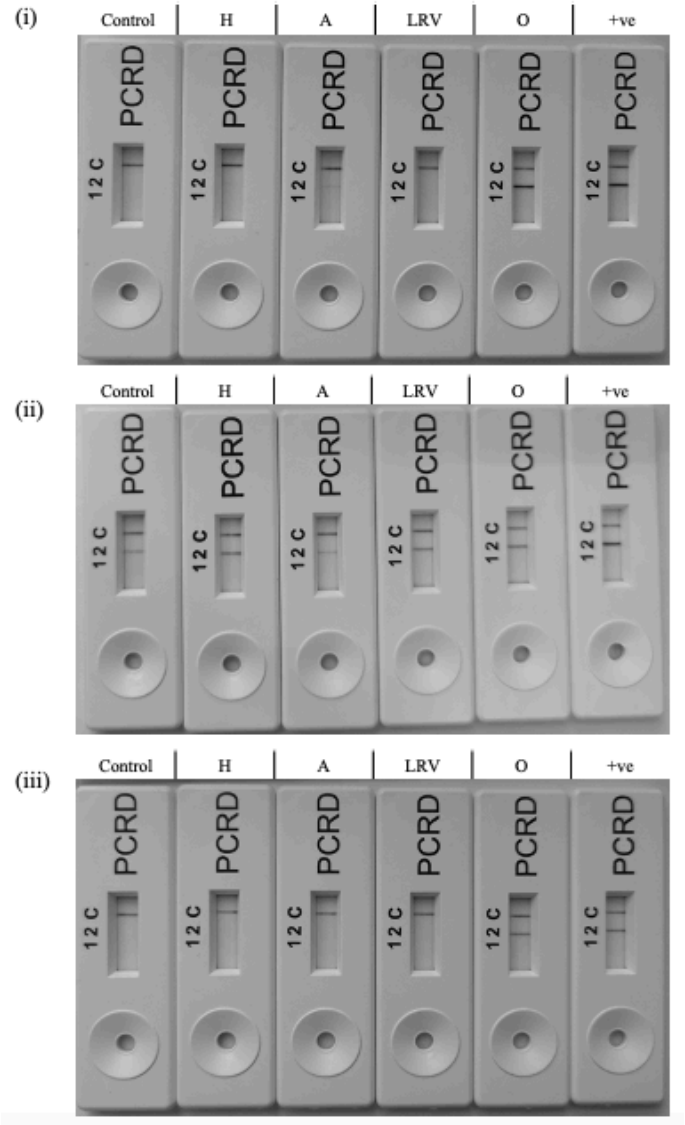

Dual-labelled primer NALFIA optimisation with 180nM primers and betaine

(i) *180nm primer cross reactivity performed with cDNA or the PVY gene fragment.* ***(ii)*** *Addition of betaine at a concentration of 0.8M to the RPA reaction.* ***(iii)*** *Repeat experiment of betaine-RPA reaction (H= healthy plant, A = PVA, L = PLRV, O= PVY^{O}, +ve = 10^{6} copies PVY CP gene, control = NTC).*

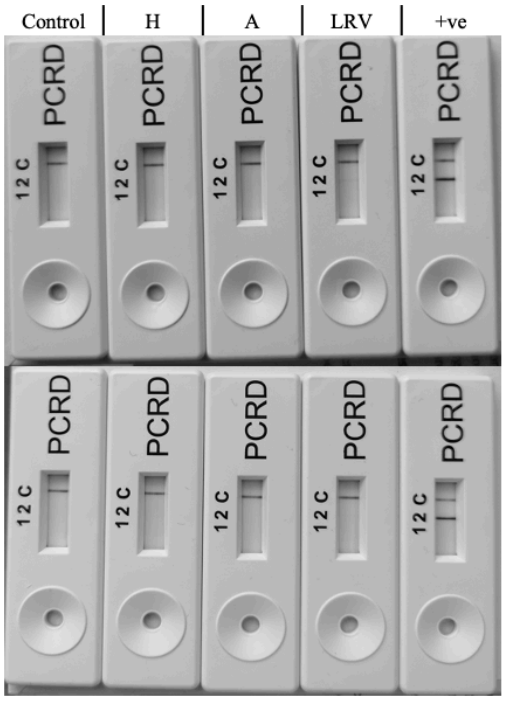

Dual-labelled primer NALFIA optimisation with 120nM primers

Duplicate reactions of 120nM primer cross reactivity performed with cDNA or the PVY gene fragment (H= healthy plant, A = PVA, L = PLRV, O= PVY^{O}, +ve = PVY gene fragment, control = NTC).

Dual-labelled primer NALFIA optimisation with 100nM primers

Duplicate reactions of 120nM primer cross reactivity performed with cDNA or the PVY gene fragment (H = healthy plant, A = PVA, L = PLRV, O= PVY^{O}, +ve = PVY gene fragment, control = no template).

Appendix B. RPA forward primer alignment with PVY genotypes

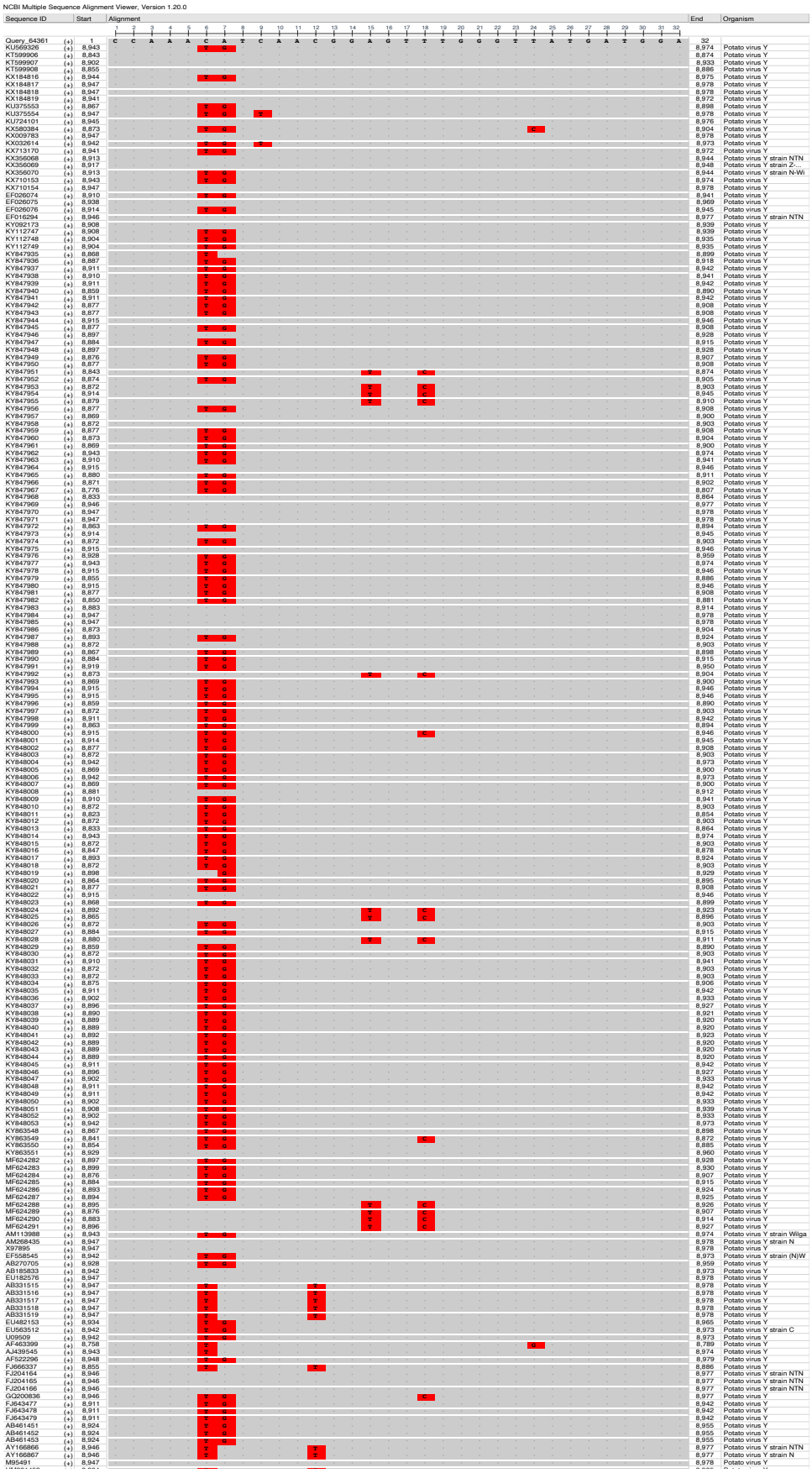

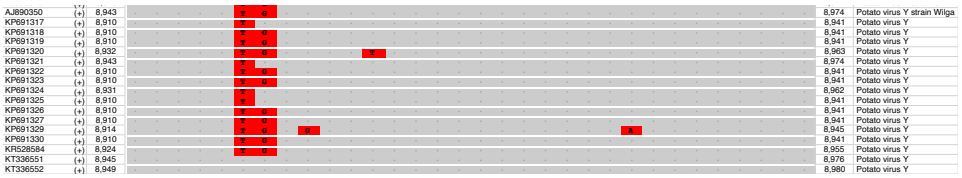

Alignment of RPA3 forward primer with PVY genotypes in Blastn

The RPA3 primer was compared against 401 PVY genotypes The resulting alignment revealed that the primer region was relatively well conserved across genotypes. Bases highlighted in red indicate mismatches between the PVY genotype and the primer.

Appendix C. RPA reverse primer alignment with PVY genotypes

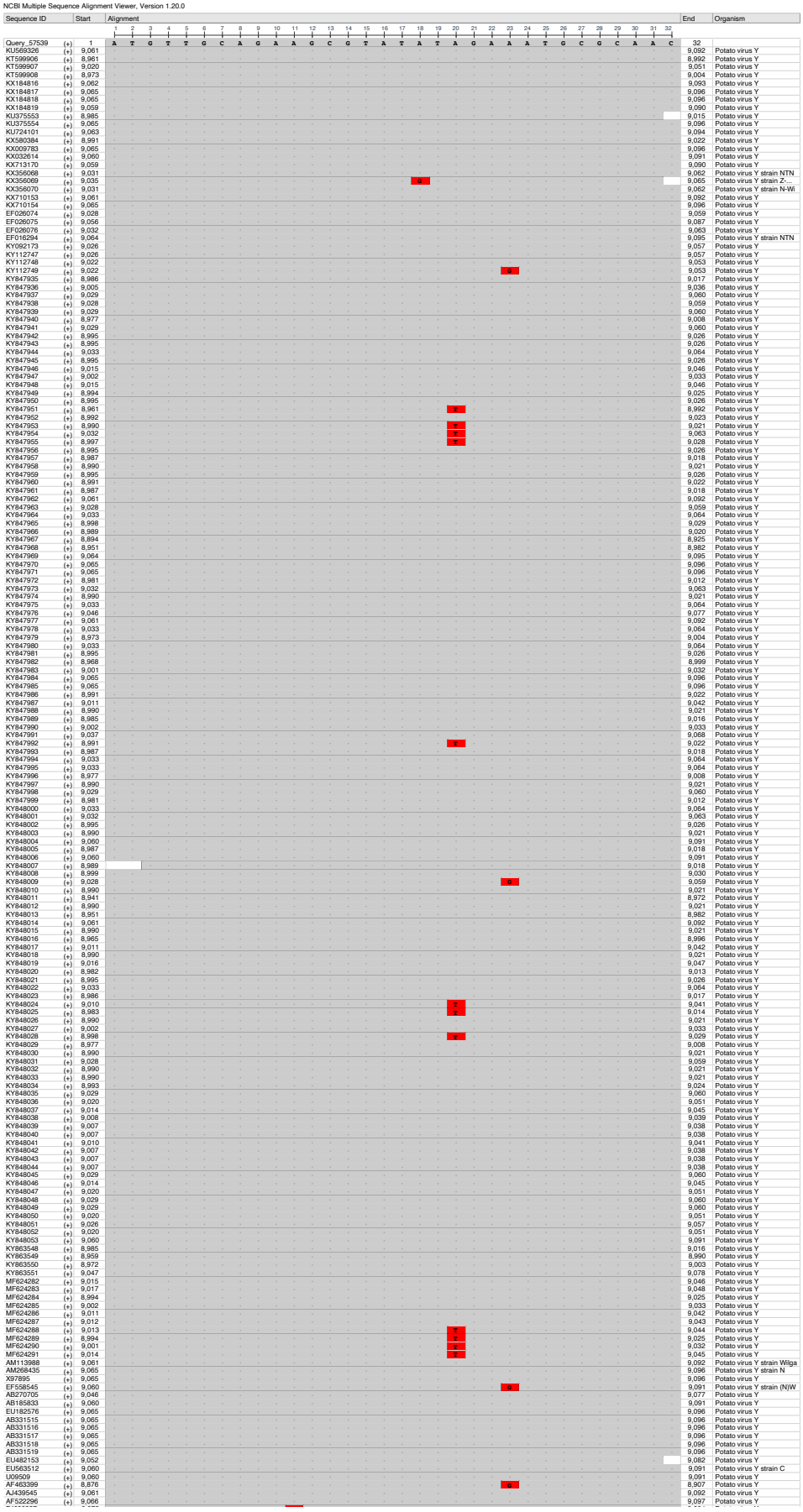

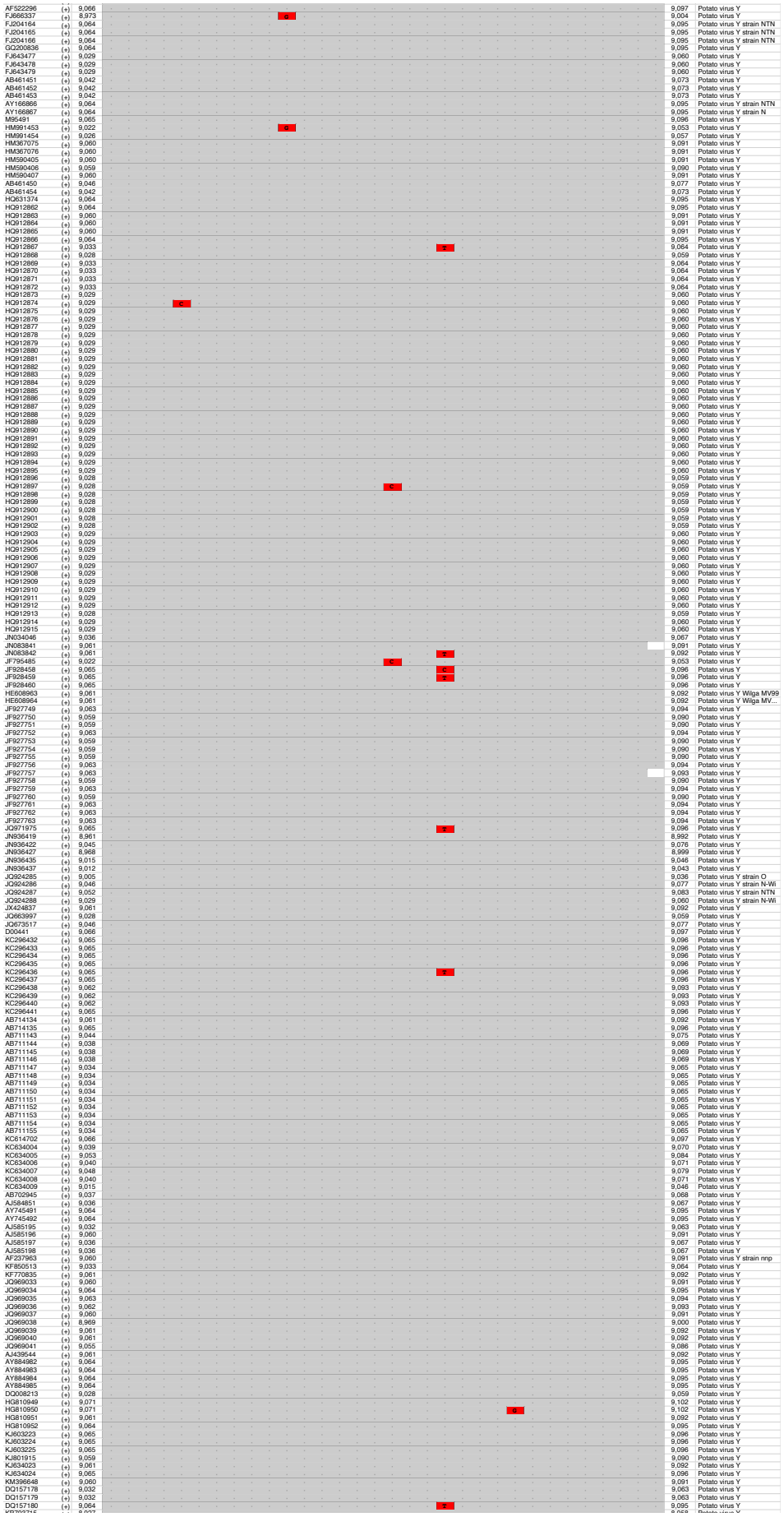

AF522296	(+)	9,066			9,097	Potato virus Y
FJ666337	(+)	8,973	G		9,004	Potato virus Y
FJ204164	(+)	9,064			9,095	Potato virus Y strain NTN
FJ204165	(+)	9,064			9,095	Potato virus Y strain NTN
FJ204166	(+)	9,064			9,095	Potato virus Y strain NTN
GQ200836	(+)	9,064			9,095	Potato virus Y
FJ643477	(+)	9,029			9,060	Potato virus Y
FJ643478	(+)	9,029			9,060	Potato virus Y
FJ643479	(+)	9,029			9,060	Potato virus Y
AB461451	(+)	9,042			9,073	Potato virus Y
AB461452	(+)	9,042			9,073	Potato virus Y
AB461453	(+)	9,042			9,073	Potato virus Y
AY166866	(+)	9,064			9,095	Potato virus Y strain NTN
AY166867	(+)	9,064			9,095	Potato virus Y strain N
M95491	(+)	9,065			9,096	Potato virus Y
HM991453	(+)	9,022	G		9,053	Potato virus Y
HM991454	(+)	9,026			9,057	Potato virus Y
HM367075	(+)	9,060			9,091	Potato virus Y
HM367076	(+)	9,060			9,091	Potato virus Y
HM590405	(+)	9,060			9,091	Potato virus Y
HM590406	(+)	9,059			9,090	Potato virus Y
HM590407	(+)	9,060			9,091	Potato virus Y
AB461450	(+)	9,046			9,077	Potato virus Y
AB461454	(+)	9,042			9,073	Potato virus Y
HQ631374	(+)	9,064			9,095	Potato virus Y
HQ912862	(+)	9,064			9,095	Potato virus Y
HQ912863	(+)	9,060			9,091	Potato virus Y
HQ912864	(+)	9,060			9,091	Potato virus Y
HQ912865	(+)	9,060			9,091	Potato virus Y
HQ912866	(+)	9,064			9,095	Potato virus Y
HQ912867	(+)	9,033		T	9,064	Potato virus Y
HQ912868	(+)	9,028			9,059	Potato virus Y
HQ912869	(+)	9,033			9,064	Potato virus Y
HQ912870	(+)	9,033			9,064	Potato virus Y
HQ912871	(+)	9,033			9,064	Potato virus Y
HQ912872	(+)	9,033			9,064	Potato virus Y
HQ912873	(+)	9,029			9,060	Potato virus Y
HQ912874	(+)	9,029	C		9,060	Potato virus Y
HQ912875	(+)	9,029			9,060	Potato virus Y
HQ912876	(+)	9,029			9,060	Potato virus Y
HQ912877	(+)	9,029			9,060	Potato virus Y
HQ912878	(+)	9,029			9,060	Potato virus Y
HQ912879	(+)	9,029			9,060	Potato virus Y
HQ912880	(+)	9,029			9,060	Potato virus Y
HQ912881	(+)	9,029			9,060	Potato virus Y
HQ912882	(+)	9,029			9,060	Potato virus Y
HQ912883	(+)	9,029			9,060	Potato virus Y
HQ912884	(+)	9,029			9,060	Potato virus Y
HQ912885	(+)	9,029			9,060	Potato virus Y
HQ912886	(+)	9,029			9,060	Potato virus Y
HQ912887	(+)	9,029			9,060	Potato virus Y
HQ912888	(+)	9,029			9,060	Potato virus Y
HQ912889	(+)	9,029			9,060	Potato virus Y
HQ912890	(+)	9,029			9,060	Potato virus Y
HQ912891	(+)	9,029			9,060	Potato virus Y
HQ912892	(+)	9,029			9,060	Potato virus Y
HQ912893	(+)	9,029			9,060	Potato virus Y
HQ912894	(+)	9,029			9,060	Potato virus Y
HQ912895	(+)	9,029			9,060	Potato virus Y
HQ912896	(+)	9,028			9,059	Potato virus Y
HQ912897	(+)	9,028		C	9,059	Potato virus Y
HQ912898	(+)	9,028			9,059	Potato virus Y
HQ912899	(+)	9,028			9,059	Potato virus Y
HQ912900	(+)	9,028			9,059	Potato virus Y
HQ912901	(+)	9,028			9,059	Potato virus Y
HQ912902	(+)	9,028			9,059	Potato virus Y
HQ912903	(+)	9,029			9,060	Potato virus Y
HQ912904	(+)	9,029			9,060	Potato virus Y
HQ912905	(+)	9,029			9,060	Potato virus Y
HQ912906	(+)	9,029			9,060	Potato virus Y
HQ912907	(+)	9,029			9,060	Potato virus Y
HQ912908	(+)	9,029			9,060	Potato virus Y
HQ912909	(+)	9,029			9,060	Potato virus Y
HQ912910	(+)	9,029			9,060	Potato virus Y
HQ912911	(+)	9,029			9,060	Potato virus Y
HQ912912	(+)	9,029			9,060	Potato virus Y
HQ912913	(+)	9,028			9,059	Potato virus Y
HQ912914	(+)	9,029			9,060	Potato virus Y
HQ912915	(+)	9,029			9,060	Potato virus Y
JN034046	(+)	9,036			9,067	Potato virus Y
JN083841	(+)	9,061			9,091	Potato virus Y
JN083842	(+)	9,061		T	9,092	Potato virus Y
JF795485	(+)	9,022		C	9,053	Potato virus Y
JF928458	(+)	9,065		C	9,096	Potato virus Y
JF928459	(+)	9,065		T	9,096	Potato virus Y
JF928460	(+)	9,065			9,096	Potato virus Y
HE608963	(+)	9,061			9,092	Potato virus Y Wilga MV99
HE608964	(+)	9,061			9,092	Potato virus Y Wilga MV...
JF927749	(+)	9,063			9,094	Potato virus Y
JF927750	(+)	9,059			9,090	Potato virus Y
JF927751	(+)	9,059			9,090	Potato virus Y
JF927752	(+)	9,063			9,094	Potato virus Y
JF927753	(+)	9,059			9,090	Potato virus Y
JF927754	(+)	9,059			9,090	Potato virus Y
JF927755	(+)	9,059			9,090	Potato virus Y
JF927756	(+)	9,063			9,094	Potato virus Y
JF927757	(+)	9,063			9,093	Potato virus Y
JF927758	(+)	9,059			9,090	Potato virus Y
JF927759	(+)	9,063			9,094	Potato virus Y
JF927760	(+)	9,059			9,090	Potato virus Y
JF927761	(+)	9,063			9,094	Potato virus Y
JF927762	(+)	9,063			9,094	Potato virus Y
JF927763	(+)	9,063			9,094	Potato virus Y
JQ971975	(+)	9,065		T	9,096	Potato virus Y
JN936419	(+)	8,961			8,992	Potato virus Y
JN936422	(+)	9,045			9,076	Potato virus Y
JN936427	(+)	8,968			8,999	Potato virus Y
JN936435	(+)	9,015			9,046	Potato virus Y
JN936437	(+)	9,012			9,043	Potato virus Y
JQ924285	(+)	9,005			9,036	Potato virus Y strain O
JQ924286	(+)	9,046			9,077	Potato virus Y strain N-Wi
JQ924287	(+)	9,052			9,083	Potato virus Y strain NTN
JQ924288	(+)	9,029			9,060	Potato virus Y strain N-Wi
JX424837	(+)	9,061			9,092	Potato virus Y
JQ663997	(+)	9,028			9,059	Potato virus Y
JQ673517	(+)	9,046			9,077	Potato virus Y
D00441	(+)	9,066			9,097	Potato virus Y
KC296432	(+)	9,065			9,096	Potato virus Y
KC296433	(+)	9,065			9,096	Potato virus Y
KC296434	(+)	9,065			9,096	Potato virus Y
KC296435	(+)	9,065			9,096	Potato virus Y
KC296436	(+)	9,065		T	9,096	Potato virus Y
KC296437	(+)	9,065			9,096	Potato virus Y
KC296438	(+)	9,062			9,093	Potato virus Y
KC296439	(+)	9,062			9,093	Potato virus Y
KC296440	(+)	9,062			9,093	Potato virus Y
KC296441	(+)	9,065			9,096	Potato virus Y
AB714134	(+)	9,061			9,092	Potato virus Y
AB714135	(+)	9,065			9,096	Potato virus Y
AB711143	(+)	9,044			9,075	Potato virus Y
AB711144	(+)	9,038			9,069	Potato virus Y
AB711145	(+)	9,038			9,069	Potato virus Y
AB711146	(+)	9,038			9,069	Potato virus Y
AB711147	(+)	9,034			9,065	Potato virus Y
AB711148	(+)	9,034			9,065	Potato virus Y
AB711149	(+)	9,034			9,065	Potato virus Y
AB711150	(+)	9,034			9,065	Potato virus Y
AB711151	(+)	9,034			9,065	Potato virus Y
AB711152	(+)	9,034			9,065	Potato virus Y
AB711153	(+)	9,034			9,065	Potato virus Y
AB711154	(+)	9,034			9,065	Potato virus Y
AB711155	(+)	9,034			9,065	Potato virus Y
KC614702	(+)	9,066			9,097	Potato virus Y
KC634004	(+)	9,039			9,070	Potato virus Y
KC634005	(+)	9,053			9,084	Potato virus Y
KC634006	(+)	9,040			9,071	Potato virus Y
KC634007	(+)	9,048			9,079	Potato virus Y
KC634008	(+)	9,040			9,071	Potato virus Y
KC634009	(+)	9,015			9,046	Potato virus Y
AB702945	(+)	9,037			9,068	Potato virus Y
AJ584851	(+)	9,036			9,067	Potato virus Y
AY745491	(+)	9,064			9,095	Potato virus Y
AY745492	(+)	9,064			9,095	Potato virus Y
AJ585195	(+)	9,032			9,063	Potato virus Y
AJ585196	(+)	9,060			9,091	Potato virus Y
AJ585197	(+)	9,036			9,067	Potato virus Y
AJ585198	(+)	9,036			9,067	Potato virus Y
AF237963	(+)	9,060			9,091	Potato virus Y strain nnp
KF850513	(+)	9,033			9,064	Potato virus Y
KF770835	(+)	9,061			9,092	Potato virus Y
JQ969033	(+)	9,060			9,091	Potato virus Y
JQ969034	(+)	9,064			9,095	Potato virus Y
JQ969035	(+)	9,063			9,094	Potato virus Y
JQ969036	(+)	9,062			9,093	Potato virus Y
JQ969037	(+)	9,060			9,091	Potato virus Y
JQ969038	(+)	8,969			9,000	Potato virus Y
JQ969039	(+)	9,061			9,092	Potato virus Y
JQ969040	(+)	9,061			9,092	Potato virus Y
JQ969041	(+)	9,055			9,086	Potato virus Y
AJ439544	(+)	9,061			9,092	Potato virus Y
AY884982	(+)	9,064			9,095	Potato virus Y
AY884983	(+)	9,064			9,095	Potato virus Y
AY884984	(+)	9,064			9,095	Potato virus Y
AY884985	(+)	9,064			9,095	Potato virus Y
DQ008213	(+)	9,028			9,059	Potato virus Y
HG810949	(+)	9,071			9,102	Potato virus Y
HG810950	(+)	9,071		G	9,102	Potato virus Y
HG810951	(+)	9,061			9,092	Potato virus Y
HG810952	(+)	9,064			9,095	Potato virus Y
KJ603223	(+)	9,065			9,096	Potato virus Y
KJ603224	(+)	9,065			9,096	Potato virus Y
KJ603225	(+)	9,065			9,096	Potato virus Y
KJ801915	(+)	9,059			9,090	Potato virus Y
KJ634023	(+)	9,061			9,092	Potato virus Y
KJ634024	(+)	9,065			9,096	Potato virus Y
KM396648	(+)	9,060			9,091	Potato virus Y
DQ157178	(+)	9,032			9,063	Potato virus Y
DQ157179	(+)	9,032			9,063	Potato virus Y
DQ157180	(+)	9,064		T	9,095	Potato virus Y

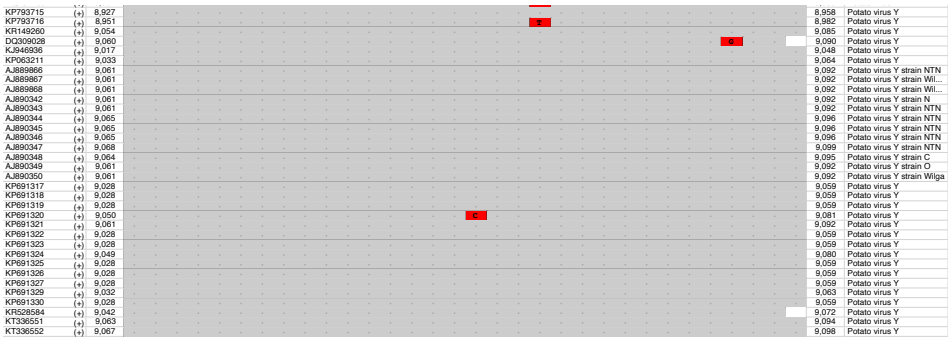

KP793715	(+)	8,927		8,958	Potato virus Y
KP793716	(+)	8,951		8,982	Potato virus Y
KR149260	(+)	9,054		9,085	Potato virus Y
DQ309028	(+)	9,060		9,090	Potato virus Y
KJ946936	(+)	9,017		9,048	Potato virus Y
KP063211	(+)	9,033		9,064	Potato virus Y
AJ889866	(+)	9,061		9,092	Potato virus Y strain NTN
AJ889867	(+)	9,061		9,092	Potato virus Y strain Wi...
AJ889868	(+)	9,061		9,092	Potato virus Y strain Wi...
AJ890342	(+)	9,061		9,092	Potato virus Y strain N
AJ890343	(+)	9,061		9,092	Potato virus Y strain NTN
AJ890344	(+)	9,065		9,096	Potato virus Y strain NTN
AJ890345	(+)	9,065		9,096	Potato virus Y strain NTN
AJ890346	(+)	9,065		9,096	Potato virus Y strain NTN
AJ890347	(+)	9,068		9,099	Potato virus Y strain NTN
AJ890348	(+)	9,064		9,095	Potato virus Y strain C
AJ890349	(+)	9,061		9,092	Potato virus Y strain O
AJ890350	(+)	9,061		9,092	Potato virus Y strain Wilga
KP691317	(+)	9,028		9,059	Potato virus Y
KP691318	(+)	9,028		9,059	Potato virus Y
KP691319	(+)	9,028		9,059	Potato virus Y
KP691320	(+)	9,050		9,081	Potato virus Y
KP691321	(+)	9,061		9,092	Potato virus Y
KP691322	(+)	9,028		9,059	Potato virus Y
KP691323	(+)	9,028		9,059	Potato virus Y
KP691324	(+)	9,049		9,080	Potato virus Y
KP691325	(+)	9,028		9,059	Potato virus Y
KP691326	(+)	9,028		9,059	Potato virus Y
KP691327	(+)	9,028		9,059	Potato virus Y
KP691329	(+)	9,032		9,063	Potato virus Y
KP691330	(+)	9,028		9,059	Potato virus Y
KR528584	(+)	9,042		9,072	Potato virus Y
KT336551	(+)	9,063		9,094	Potato virus Y
KT336552	(+)	9,067		9,098	Potato virus Y

Alignment of RPA3 reverse primer with PVY genotypes

The RPA3 reverse primer sequence was compared to 401 PVY genotypes in Blastn. The resulting alignment revealed mismatches between primer and template were rare. Mismatches between the primer and PVY templates are presenting as bases highlighted in red.

Appendix D. RPA probe alignment with PVY genotypes

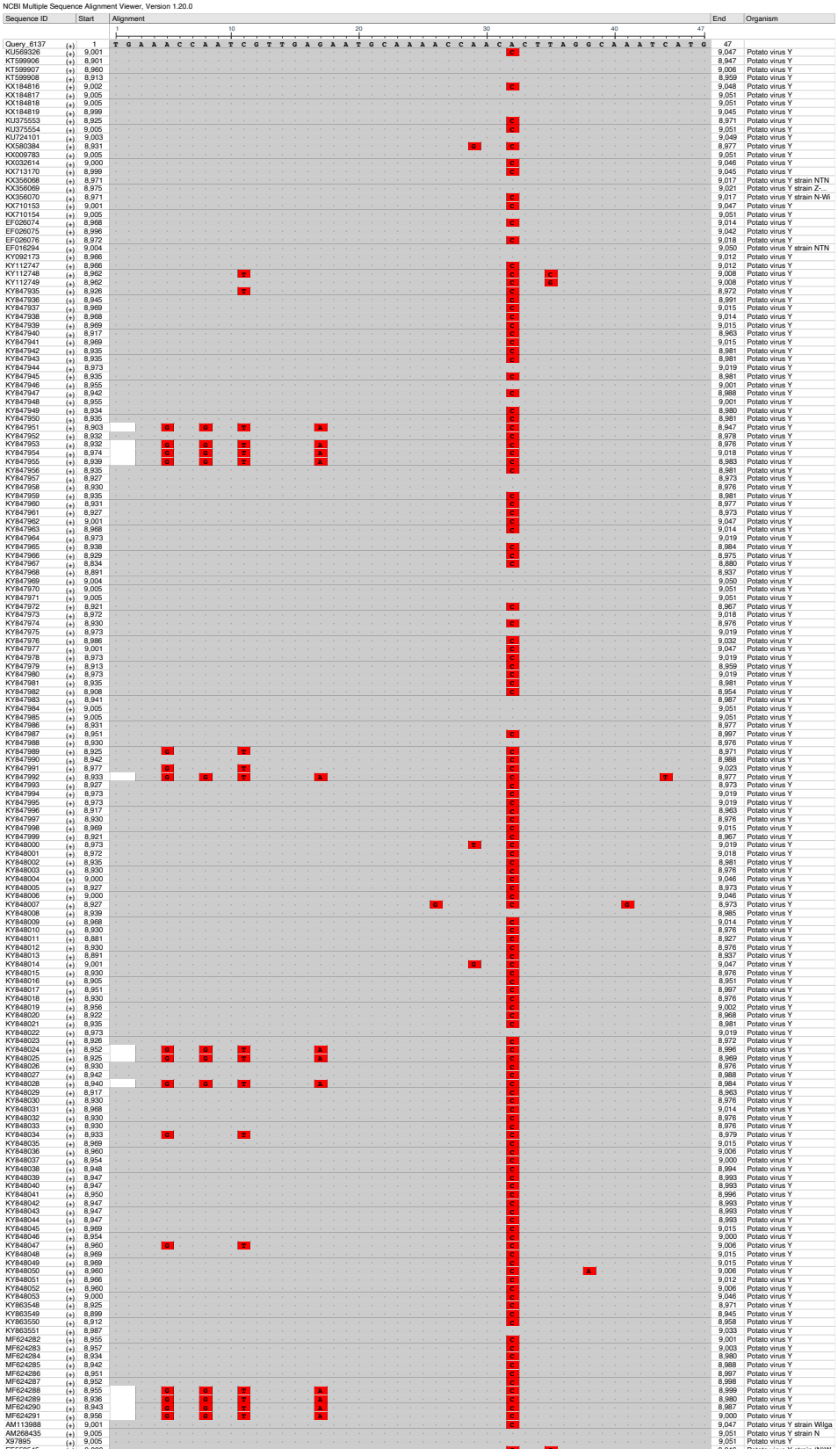

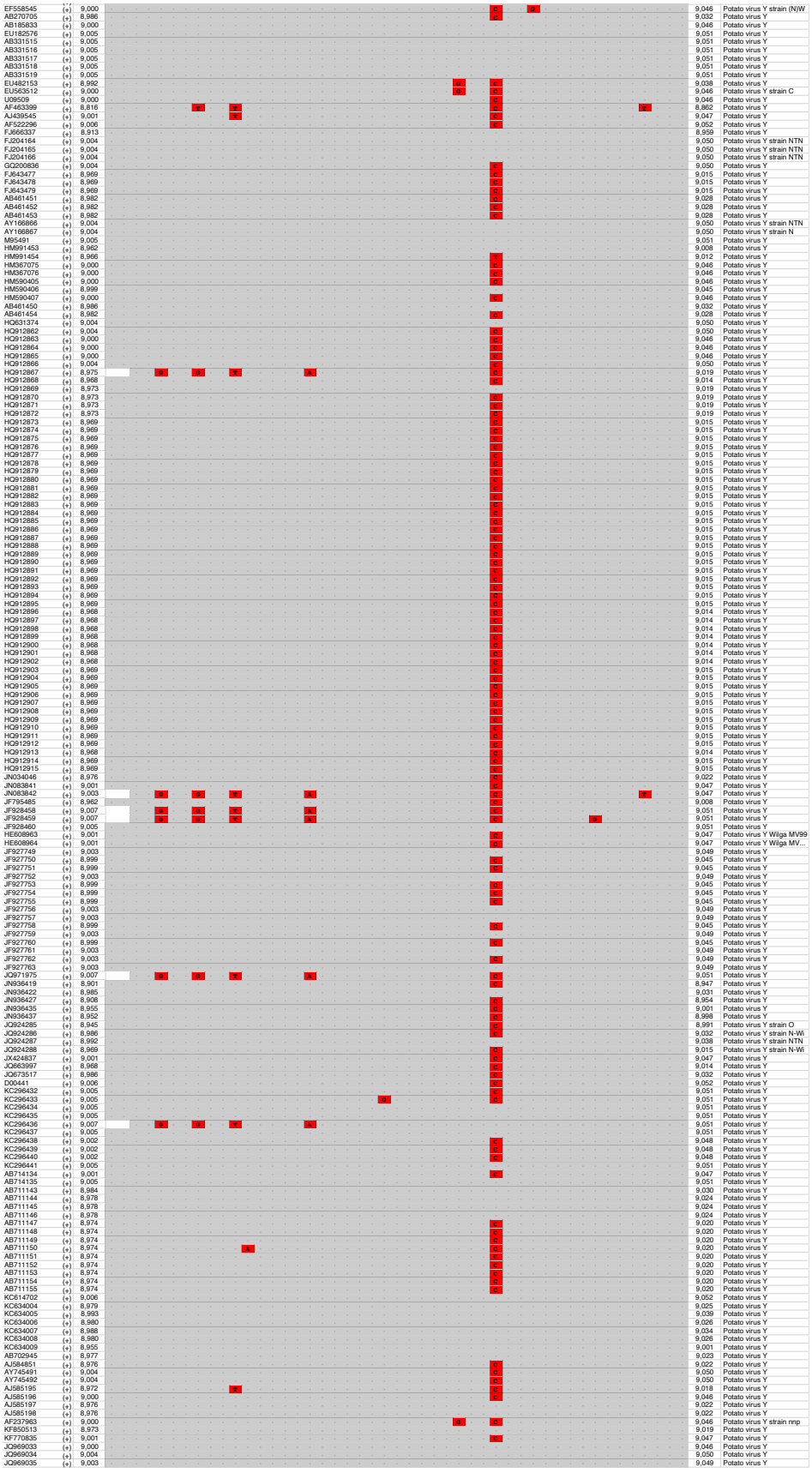

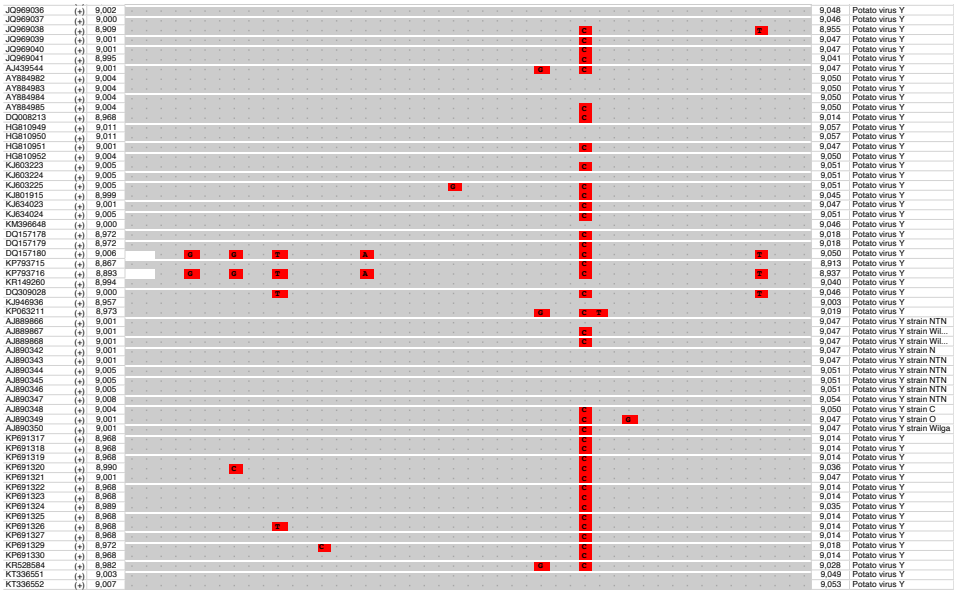

Alignment between the RPA probe and PVY genotypes

The probe was compared against 401 PVY genotypes in Blastn. Red bases in the alignment represent mismatches between the probe and PVY template. To note, the "C" at base number 32 of the probe was included only for this analysis, in practice, it is replaced entirely with a THF residue.